NOTICE

The quality of this microform is heavily dependent upon the quality of the original thesis submitted for microfilming. Every effort has been made to ensure the highest quality of reproduction possible.

If pages are missing, contact the university which granted the degree.

Some pages may have indistinct print especially if the original pages were typed with a poor typewriter ribbon or if the university sent us an inferior photocopy.

Reproduction in full or in part of this microform is governed by the Canadian Copyright Act, R.S.C. 1970, c. C-30, and subsequent amendments.

AVIS

La qualité de cette microforme dépend grandement de la qualité de la thèse soumise au microfilmage. Nous avons tout fait pour assurer une qualité supérieure de reproduction.

S'il manque des pages, veuillez communiquer avec l'université qui a conféré le grade.

La qualité d'impression de certaines pages peut laisser à désirer, surtout si les pages originales ont été dactylographiées à l'aide d'un ruban usé ou si l'université nous a fait parvenir une photocopie de qualité inférieure.

La reproduction, même partielle, de cette microforme est soumise à la Loi canadienne sur le droit d'auteur, SRC 1970, c. C-30, et ses amendements subséquents

ACCIDENTAL ECCENTRICITY AND LIMITING THE EFFECTS OF DESIGN ECCENTRICITY FOR SEISMIC RESPONSE OF BUILDINGS

Richard Guimond

A Thesis

in

The Faculty

of

Engineering

Presented in Partial Fulfillment of the Requirements
for the degree of
Master of Engineering
at
Concordia University
Montreal, Quebec, Canada

May 1989

ISBN 0-315-49120-5

ABSTRACT

ACCIDENTAL ECCENTRICITY AND LIMITING THE EFFECTS OF DESIGN ECCENTRICITY FOR SEISMIC RESPONSE OF BUILDINGS

Richard Guimond

Building codes for earthquake resistant design generally specify the design eccentricity as $e_d = e_{d1} \pm e_{d2}$ where e_{d1} is the dynamic eccentricity and e_{d2} is the additional or accidental eccentricity. Whereas, e_{d1} is defined by the known distribution of mass and the structural layout of the building, the accidental term e_{d2} is intended to account for such factors as unforeseen variation in relative stiffness, uncertainty in the distribution of mass, possible torsional ground motion and the effects of inelastic or plastic actions. In the National Building Code of Canada, the accidental eccentricity e_{d2} was increased in 1985 from $0.05D_n$ to $0.10D_n$, where D_n is the perpendicular dimension of the building.

This thesis examines the adequacy of the above code accidental eccentricities to account for torsion introduced by statistical variation of strengths of otherwise identical structural elements. Thus, the accidental eccentricity examined is that due to inelastic or plastic action. An equation for the maximum permitted deviated strength from the mean is derived from intrinsic requirements of the Code. A parameter λ representing this statistical variation of strength has been introduced and is found to have an expected value $\lambda = 0.3$ for North American construction practice. Torsion arising from different hysteretic behaviour is also investigated. If no allowance is made for other sources of accidental eccentricity, a design value of the latter of $0.10\ D_n$ is found to be adequate for design purposes whereas accidental eccentricity of $0.05D_n$ has a high probability of exceedance due to the statistical variation in structural strength.

Performance of friction bracing devices, which are becoming increasingly popular in aseismic design of buildings, is also studied for the more general case of eccentric building and is found beneficial with substantial reduction in structural response. A three dimensional, inelastic analysis of an eccentric reinforced concrete structure equipped with friction bracing is also presented.

ACKNOWLEDGEMENTS

I wish to thank my supervisor Dr. O. A. Pekau for his guidance in the preparation of this work. I would also like to thank the Concordia University Computer Center for the use of their facilities and Concordia University, in particular, for assistance given to me in terms of a full and part time lab instructorships. The Graduate Fellowship together with the financial support from the National Sciences and Engineering Council of Canada under grant A8258 are also greatfully acknowledged.

Thanks are also extended to my numerous friends for their help and patience. Perhaps the most important inspiration of all was provided by my wife Isabelle, whose encouragement made this work possible.

TABLE OF CONTENTS

TABLE OF CONTENTS

TABLE OF CONTENTS

PAGE

TABLE OF CONTENTS

PAGE

LIST OF FIGURES

LIST OF TABLES

NOMENCLATURE

a	depth of concrete stress block
b	width of a concrete beam
d	effective depth of a concrete beam
D	dead load
f'_c	compressive strength of concrete
f'_{cdes}	nominal or specified compressive strength of concrete
f_y	yield strength of steel
f_{ydes}	nominal or specified yield strength of steel
FDBF	friction damped braced frame
KB	lateral stiffness of the bracing without the influence of the frame
KF	lateral stiffness of the frame without brace
L	live load
MRF	moment resisting frame
P_f	probability of failure
R	resistance of a member
RB	resistance of the brace
RF	resistance of the frame
$\overline{R}$	mean resistance
R_n	nominal resistance
R^*	resistance at design point
S	maximum load in life of structure
$\overline{S}$	mean load
S_d	design load for specified loading
S^*	load at design point

V_R coefficient of variation of the resistance = σ_R/R

V_S coefficient of variation of the load = σ_S/S

Z R - S

ζ factor obtained from the cumulative normal distribution for a given probability of understrength of material

ϕ performance factor

p percentage reinforcement in a concrete beam

λ variation from the mean resistance

σ_R standard deviation of the resistance

σ_S standard deviation of the load

σ_Z $(\sigma_R^2 + \sigma_S^2)^{1/2}$

ρ mass radius of gyration about the center of mass

CHAPTER I

INTRODUCTION

This thesis pertains to torsion in buildings arising from eccentricity. Building codes for aseismic design generally specify the design eccentricity as $e_d = e_{d1} \pm e_{d2}$ where e_{d1} is the dynamic eccentricity and is found from the known distribution of mass and structural layout. Most of the research on torsion to date dealt with the proper assessment of e_{d1} . The accidental eccentricity term e_{d2} accounts for such factors as unforeseen variation in relative stiffness, uncertainty in distribution of mass, possible torsional ground motion and the effects of inelastic or plastic actions.

The work presented herein consists of three phases; the first phase addresses the effects of accidental eccentricity on a one storey model structure, the second phase examines the use of friction devices to limit the effects of eccentricity when these are incorporated into the one storey model . This can be seen as a logical extension of the previous phase. The third phase consists of a case study of a multistorey building equipped with friction devices and can be viewed as an application of the results found in the previous phase.

Phase I examines the adequacy of the code accidental eccentricity provisions to account for torsion introduced by the statistical variation of strength, thus the accidental eccentricity is due to inelastic or plastic actions. To date this author has encountered no research reported for this particular topic. The magnitude of the accidental eccentricity term e_{d2} is assessed; for this study e_{d2} accounts for eccentricity caused by accidental, unintentional, or statistical differences in strength of lateral load resisting systems. Particular attention is drawn to structures depending primarily on two lateral load resisting systems such as two braced bays, two end shear walls, or two primary moment resisting frames.

In Phase II a parametric study of frames with friction devices is conducted to examine the feasibility of eliminating the effects of accidental eccentricity e_{d2}, and reducing the effects of design eccentricity e_d by means of friction damped bracing introduced to a one storey model of a structure. Phase III extends the findings of the previous phase to a multistorey concrete building and presents a case study of the 5 storey Concordia Library Building as it was initially proposed.

Details involved in the above work are presented in the following. It should also be noted that a review of the relevant literature is given individually in the introductory sections of the pertinent Chapters.

1.1 PHASE I - ACCIDENTAL ECCENTRICITY

Structures which possess a centre of rigidity non-coincident with the centre of mass will be subjected to torsion under lateral loading. The National Building Code of Canada [1] accounts for this eccentricity and additionally specifies the accidental eccentricity which may arise due to the presence of torsional ground motion, unforeseen variation in relative stiffness of lateral resisting elements, uncertainities in the distribution of mass, the different arrangement of movable wall panels and partitions, the variation of stiffness with time and inelastic or plastic action.

It is well known that structures built in accordance with code specifications are permitted an inelastic response under severe earthquake loading. Since different structural systems have different hysteretic behaviour a torsional component of loading may evolve. This phenomenon was first mentioned by Newmark [2].

The code also allows a certain variation in properties of structural materials, such as yield strength of steel and the compressive strength of concrete, during the construction process. Consequently the lateral load resisting elements are made of materials that vary in properties due to this inherent random nature of the construction materials or of the

fabrication process which in turn influences their resistance or strength and affect the position of the centre of resistance.

The importance of the variation in properties was recognized early by Freudenthal[3] which led to the formulation of the probability based load and resistance design concept called the 'Limit States Design'. Chapter 2 of this thesis investigates the various factors relevant to the variation in strength of structural elements. It shows that the strength variation in materials is caused mainly by three factors: variability in the material strength, variation due to fabrication errors, and simplified assumptions used by engineers.

Each factor is expressed by the statistical coefficient of variation, as the ratio of the standard deviation to the mean of the random normal variable. Findings of Ellingwood [4], MacGregor [5], Allen [6] and Tso [7] led to an overall estimation of variation of strength of concrete members $V_R = 0.14$. For steel members the findings of Galambos and Ravindra [8,9], Yura [10], Kennedy and Gad Aly [11] and Ellingwood and Ang[4,12] result in the same coefficient of variation $V_R = 0.14$.

The strength variation parameter, λ, is introduced in Chapter 2 as a means to quantify the possible change in strength of lateral resisting elements. This parameter relates the mean strength $\bar{R}$ of the lateral resisting member to the code specified limit of deviated resistance R^* given in CSA S408-1981 [13] as the design point. However, R^* is not readily known because, until now, researchers have avoided its explicit formulation to concentrate on obtaining the performance factors used in Limit States Design. Hence, to obtain λ, a discussion is presented to show how the design point resistance is obtained in Limit States Design. The design point represents the failure combination with the highest probability of occurence and is found by equating the design load S^* to R^* [14]. Using this concept an equation for parameter λ is derived. This equation applies equally well for any material once the level of safety is specified and the coefficient of variation of resistance V_R and the coefficient of variation of load V_S are known.

To investigate the importance of parameter λ, with respect to code provisions for accidental eccentricity for a building subjected to severe earthquake, a structural model consisting of a rigid rectangular deck with dimensions 3ρ by $\sqrt{3}\,\rho$ and total mass m, supported by two lateral resisting elements is shown in Chapter 3, where ρ is the mass radius of gyration. This model represents a one storey, singly asymmetric structure. Even though the model is only one storey its behaviour is indicative of the behaviour of multistorey buildings [15].

For simplicity the model is symmetric about the X-axis and no lateral displacement is allowed in this direction at the center of mass; thus the X and Y displacements are decoupled and the model has only two degrees of freedom, translational displacement in the Y-direction of the center of mass CM relative to the ground and rotation about a vertical axis through the center of mass. To investigate accidental eccentricity the lateral supporting elements with equal stiffness are placed equidistant from the center of mass and response in the elastic range is free of torsion; however, the second element's strength is varied from the first by an amount $\lambda\overline{R}$ and torsion arises when the structure's elastic limit is exceeded.

Hence, within the elastic range the structure is presumed to be symmetric with the center of mass and the center of resistance coincident, but in the inelastic range the structure possesses an inelastic asymmetry. To evaluate the anticipated lateral-torsional dynamic response of the model the concept of static plastic eccentricity e_p is introduced. It represents the eccentricity of the plastic centroid from CR as a function of λ and Ω_0, where the latter parameter defines the uncoupled torsional to lateral frequency ratio.

Based on the previously discussed variation of strength for individual steel and reinforced concrete members, it is assumed that the accidental strength parameter λ varies over the range $0 < \lambda < 0.40$. In terms of probability of occurence, a strength difference between two individual structural members of $\lambda = 0.3$ has a probability of 6.5 percent for $V_R = 0.14$ when a normal distribution of resistance is assumed.

The above structural model is subjected to a parametric study in Chapter 4 consisting of time-history analyses for different earthquake records employing the computer program DRAIN-2D [16]. Damping is assumed to be 5 percent for the two modes of response. The input parameters consist of the following: (1) three earthquake records - El Centro 1940 NS, Olympia 1949 N80E, and Taft 1952 N69W; (2) six translational periods - T = 0.25, 0.50, 0.75, 1.0, 1.5 and 2.0 seconds; and three frequency ratios Ω_0^2 = 0.5, 1.0, 1.5, with λ varying from 0 to 0.40.

To ensure yielding occurs, the maximum induced elastic resistance of an element is limited to a value equal to its elastic symmetric force R_{el} divided by the earthquake severity factor Q. This study generally uses a value of Q = 4.0 although other values were also investigated.

A second method of evaluating eccentricity caused by plastic action is by having the first lateral resisting element with elastoplastic hysteresis while the second element exhibits Takeda degrading stiffness characteristics. For both these methods, responses are compared with the provisions of accidental eccentricity given in the 1980 National Building Code of Canada (NBCC 1980) [17], and in the 1985 National Building Code of Canada (NBCC 1985) [1]. The adequacy of code provisions are examined in terms of average (AVG), average plus one standard deviation (AVG+σ) and extreme values for 54 cases. If no allowance is made for other sources of accidental eccentricity the value e_{d2} = $0.10D_n$ of NBCC 1985 is found adequate for design purposes whereas accidental eccentricity e_{d2} = 0.05Dn of NBCC 1980 has a high probability of exceedance due to the statistical variation in structural strength. Based on the results presented in Chapter 4, the variation in the strength of lateral load resisting elements may result in considerable accidental torsion. Compared to symmetric response, this may result in sizeable amplification factors for maximum edge displacement. Furthermore, the parametric study indicates that torsionally flexible structures are more susceptible to the effects of accidental eccentricity.

In terms of the adequacy of code accidental eccentricity provisions for multi-element systems, minimum eccentricity of $0.05D_n$ becomes inadequate when the static plastic eccentricity $e_p \geq 0.06\rho$, whereas $0.10D_n$ is able to account for $e_p \leq 0.20\rho$.

In terms of different types of hysteresis behavior of lateral resisting elements the NBCC 1980 provisions for accidental eccentricity are again found inadequate, whereas the requirements of the NBCC 1985 code are satisfactory. Furthermore, it is shown that these structures are susceptible to increases in edge displacement when torsionally flexible and when their lateral period is in the range of 0.75 to 1.25 seconds.

1.2 PHASE II - PARAMETRIC STUDY OF FRAMES WITH FRICTION DEVICES

In recent years a novel approach to the aseismic design of frames has been introduced which consists in the incorporation of friction devices patented by Pall[18] in tension cross braces to absorb the detrimental energy input of severe earthquake excitations. An early study [19] found that the seismic energy input of a structure with period T = 1.0 second was 40 times in excess of its elastic capacity when subjected to the El Centro 1940 NS excitation with an earthquake severity factor Q = 2.6. In Chapter 5 these devices are incorporated into a structural model similar to that previously described with the addition of two elements (representing the devices) superimposed, one each, at the location of the lateral resisting elements. The study investigated whether the benefits of the device offset the additional requirements of accidental eccentricity.

Until now, research in the field of friction braces has been limited to the two dimensional case with the inclusion of the device in symmetrical buildings. Results of previous studies [18, 20-25] have claimed dramatic improvements in the behavior of frames when compared to the response of frames without the device. The friction devices

were considered tuned by previous investigators when the slip load that activates the device is such that the dissipation of seismic energy is maximized [24,25].

The process of finding the optimum slip load was heuristic with the main criterion that the device operates before yielding occurs in a frame member. Recently, Baktash [25] proved the device absorb maximum energy when its contribution to carry lateral storey shear equals that of the frame without the brace. In other words, RB = RF, where RB is the lateral resistance of the brace acting alone and RF is the yield strength of the frame without the brace. Other studies have investigated the actual slip load of the friction dampers for a given structure [18,20-24]; Chapter 5, however, investigates the effect of stiffness ratio, KB / KF, and also the strength ratio, RB / RF, which together better describe the characteristics of the device for its influence on the seismic response of any structure. Note that KB represents the lateral stiffness of the friction bracing acting alone and KF represents the lateral stiffness of the frames without the brace.

The study is extended to the more general case of eccentric stuctures to see if the device is equally beneficial. For this purpose, a parametric study employing the first 15 seconds of response to the Newmark - Blume - Kapur artificial earthquake, with time step Δt = 0.01 seconds, was carried out using the computer program DRAIN - 2D [16]. Viscous damping of 5 percent was assumed. The response of the model, whose lateral period is 1.0 seconds and frequency ratio Ω_o^2 = 1.0 is evaluated for strength ratios RB/RF = 0.0, 0.2, 0.4, 0.6, 0.8, and 1.0; for stiffness ratio KB/KF = 0.0, 0.5, 1.0, 2.0 and 3.0; and for eccenticity e* = 0.0, 0.3, 0.75, 0.9, 1.2, and 1.5. The parameter e* denotes the structural eccentricity normalized by the mass radius of gyration ρ. With this parametric study, it is possible to quantify the improvement in response by the incorporation of friction dampers and establish optimum structural parameters with respect to a given frame.

The results corroborate the findings of other investigators [18, 20-25] for symmetrical buildings with very significant improvements of a structure's response when

the device is properly tuned. Until now, tuning of the device has been done with regard to the slip load only; Chapter 5 reveals that it is also important to tune the stiffness ratio KB/KF. The study confirms the work of Baktash [25] that, for symmetrical structures, a slip load corresponding to the strength ratio RB/RF = 1.0 is optimum; although for the cases studied, there is little difference in response in the range RB/RF from 0.4 to 1.0.

For eccentric structures, considerable improvement in response is obtained by the inclusion of friction devices. For these structures, the optimum slip load corresponds to a strength ratio RB/RF ≈ 0.6 with little difference in response for a strength ratio variation of ± 20 percent from optimum. The optimum stiffness ratio is shown to lie above KB/KF = 1.0 with little difference in results for KB/KF ratios exceeding 2.0 .

The inclusion of the device reduced maximum rotations and decreased the ductility demand. Moreover, it is shown that the devices reduce the energy absorbed by inelastic deformation of frame members by 96 percent for symmetric structures and by 90 percent for structures with low eccentricity. For structures with large eccentricity, the reduction is in the order of 70 percent.

1.3 PHASE III - CASE STUDY OF A 5 STOREY CONCRETE BUILDING

Finally, Chapter 6 presents a case study of the three dimensional response of a structure equipped with friction bracing. More specifically, it examines the performance of friction damped bracing which will be installed in the new Concordia University Library Complex by conducting a three dimensional inelastic analysis with the computer program Drain - Tabs [26]. Earlier, a two dimensional study was performed by Pall [24] which showed very substantial benefits when friction devices are incorporated into a 9 storey reinforced concrete moment resisting frame. Chapter 6 reviews the two 5 storey portions which at the time of study were independent from the 9 storey portion but have since been linked.

Unlike the devices mentioned earlier, the friction bracing used in this chapter consists of tension-compression cross-bracing, because the 5 storey portion of the Library Complex is stiffer than the 9 storey part analyzed by Pall. The friction braces employed are similar to those used by Baktash [25]. Moreover, the NBCC code [27] recognizes the better post-elastic behaviour of tension - compression bracing and allows a reduction of 23 percent in imposed seismic loads over tension bracing alone. Therefore, it is more likely that tension-compression bracings will be employed for multistorey buildings. The friction bracing is incorporated into this structure because it is considered an important structure with a code assigned importance factor I = 1.3 for library buildings compared to I = 1.0 and, because of the expensive computer equipment to be located there.

The five storey portion studied in Chapter 6 consists of a reinforced concrete building 36.9 m long and 27.6 m wide, with columns spaced essentially on a 9 m grid. Fire hazards and clear storey height dictated the use of a flat slab structure with drop panels [24]. The first storey is 5.3 m high and there are four storeys of 4.2 m, with two additional storeys below grade.

For X-direction excitation (N-S), bracing is located in a bay near each of the East and West edges of the building which is desirable. However, for Y-direction excitation (W-E) bracing is provided at only one edge of the building and depending on the lateral stiffness of the bracing used, may introduce considerable eccentricity. This sort of arrangement is not favoured by engineers but was imposed by architectural considerations. It is recognized that this is possibly the worst condition imposed on friction bracing. To assess the properties of the building, the lateral stiffness of the structure is defined in Chapter 6 as the ratio of top deflection to base shear when the NBCC 1985 [1] pseudo-static forces act through the center of resistance CR of each floor. However, it should be noted that for multistorey structures, there is no consensus on a definition for CR.

According to Humar [28], the center of rigidity at a floor is defined as the point through which the resultant lateral force of the level acts and causes no rotation for that

floor although other floors may rotate. Cheung and Tso [29] define the center of rigidity of a multistorey building as the locus of points located at each floor level such that when a given distribution of lateral loads passes through them, no rotational movement of the building about a vertical axis occurs.

The definition of CR used in this study is different from other investigators since it utilizes a torque applied by horizontal couples at a floor level to find the point about which rotation occurs for that level. The application of static loads at the CR locations using the above method caused no rotation and indicates that these are indeed the center of resistance of the elastic structure.

The analyses consisted of subjecting the structure to 6 seconds of the Newmark - Blume - Kapur artificial earthquake at 0.18g peak ground acceleration; this represents a 10 percent probability of exceedance in 50 years for Montreal [27]. Zero structural damping is assumed and the time step used is $\Delta t = 0.01$ seconds. The building is further analyzed by assuming a shift in the center of mass in the X direction from the centroid by a distance of $\pm 0.25\ D_n$ thus giving large eccentricity for Y - direction excitations. Optimization of the slip load was first done for Y - direction excitation with a low KB/KF (≈ 0.25) value chosen to reduce the bracing's effect on eccentricity. Similar bracing in the X - direction gave a KB/KF ratio of approximately 0.5.

Results for the structure with the bracing proposed showed reduction of edge displacement response for Y - direction excitation and considerable decrease in peak ductility demand. It is shown that a fictitious structure having similar characteristics as the library building but with a shift in CM of $\pm 0.25\ D_n$ would benefit moderately from the inclusion of friction braces. An increase of the stiffness ratio to KB/KF ≈ 1.0 gave considerable improvement in response.

An investigation of the effects of friction devices in the X - direction for the proposed structure showed reduction in rotation, reduction in peak ductility demand and good absorption of seismic energy, but small reduction in edge displacement. When the

structure is modified with an increase in stiffness ratio to a value KB/KF ≈ 1.5, a significant reduction in edge displacment is also obtained. This implies that the stiffness ratio is also an important parameter to consider in the design of buildings equipped with friction bracings.

CHAPTER II

ACCIDENTAL ECCENTRICITY IN BUILDINGS WITH STRENGTH VARIATION OF LATERAL RESISTING ELEMENTS

2.1 INTRODUCTION

Lateral load resisting elements are made of materials that vary in properties due to the inherent random nature of the construction materials and of the fabrication process. This influences the resistance or strength of the elements.

The importance of the variation in properties, and therefore of strength, was recognized early in the development of the probability based load and resistance design concept called the 'Limit States Design'. In an early paper Freudenthal [3] lists some of the most pertinent factors, such as inaccuracy in the assumed mechanism of resistance, variability of resisting limits of materials, and variation of structural dimensions. Later on Freudenthal and other investigators used probabilistic methods to evaluate the variation in structural properties.

This chapter studies the various factors relevant to the variation in strength of structural elements and introduces the strength variation parameter λ as a means of quantifying the possible change in strength of lateral resisting elements.

2.2 STRENGTH VARIATION IN STRUCTURAL ELEMENTS

The strength of a structural element is dependent on many factors which are best described by using a statistical terminology. The coefficient of variation, denoted by the symbol 'V', is a probabilistic measure which indicates how likely a property varies from the mean and is defined as the ratio of the standard deviation 'σ' to its mean.

The objective of this section is to quantify the variation in strength of structural elements and to investigate the pertinent factors contributing to this variation as they apply firstly to concrete elements and secondly to steel elements.

2.2.1 Strength Variation in Concrete Elements

The strength of a concrete element varies basically for the following three reasons:

a) Variability in material strength, expressed by V_m, which is dependent on the compressive strength of concrete f'_c and the yield strength of reinforcing steel f_y.

b) Variation due to fabrication errors, V_f, occurring as a result of rolling tolerances in the reinforcing steel and deviation in the geometrical dimensions of concrete members or in the placement of the reinforcement.

c) Simplifying assumptions used by engineers give variations, V_p, which affect their solutions.

An acceptable and convenient assumption is that each of the above terms has a variation which follows a normal distribution.

2.2.1.1 Variation Due to Material Strength

Engineers are familiar with variation in compressive strength f'_c of concrete and are aware that the building codes allow for construction tolerances in the fabrication process. Specifically Chapter 4 of the ACI code [30] section 4.3.2 requires that the mean compressive strength $(f'_c)_{mean}$ of 15 tests be greater than the specified compressive strength f'_c by 1.55 standard deviations. The requirement is reduced to 1.34 standard deviations for samples of 30 or more tests.

Unlike the standard deviation, the coefficient of variation, V_c, of concrete strength remains almost constant when the mean is varied by adjusting the proportions of the design mix [31] and therefore provides a more useful method of finding the required mean

compressive strength $(f'_c)_{mean}$ at the mixing plant. For example equation (4-1) of ACI 318 [30]

$$(f'_c)_{mean} = (f'_c)_{des} + 1.34\,\sigma \tag{2.1}$$

which is dependent on the standard deviation σ, can be rewritten as:

$$(f'_c)_{mean} = (f'_c)_{des} / [1 - 1.34V_c] \tag{2.2}$$

and is now dependent on V_c, the coefficient of variation of concrete. These equations provide for a probability against understrength of 1 in 100 that the average of three consecutive tests falls below the specified value of f'_c [75].

Based only on evaluations of standard cylinder tests of concrete, the strength of concrete has a coefficient of variation of 0.12 [4]. However, the resistance of concrete elements can also be affected by shrinkage, creep, strain rate, duration of load, casting direction, on-site curing or lack of curing of the member, and effects of confinement. Taking these factors into account Ellingwood [4] estimates a coefficient of variation of the strength of concrete as 0.16. Furthermore, in-situ concrete strength f_c is different from the strength f'_c of test cylinders and Ellingwood attributes another coefficient of variation of 0.07. Taking all of these effects together, he reports a coefficient of variation of 0.21.

Not only does concrete strength depend on the mix, it also depends on the workmanship or control at the mixing plant. In another paper, MacGregor [5] reports overall coefficients of variation V_c of 0.20, 0.15 and 0.10 for poor, average and good control respectively, whereas Allen [6] reports V_c of 0.18 for minimum acceptable workmanship and 0.15 for good control.

An important consideration in the strength of a reinforced concrete element is the variation in yield strength of the reinforcing steel. Allen [6] recommends a normal distribution (Fig. 2.1) for the high strength 60 ksi bars and reports a coefficient of variation of steel yield strength V_{fy} of 0.09. Ellingwood [4] reports the same basic variation of yield strength, but when consideration is made of bar size effects, commercial testing procedure and rate of testing, V_{fy} is computed as 0.15. MacGregor [5] reports that

the mean yield strength of 60 ksi rebars is relatively constant but decreases for bars of sizes No. 11 U.S. or greater (Fig. 2.2).

The Canadian Standard CSA S408 [13] requires that all these effects be considered in evaluating the variation of an element's resistance together with effects resulting from location of test piece, grading defects and concrete maturing.

2.2.1.2 Variation Due to Fabrication Errors

Another important factor influencing the strength of a reinforced concrete element is the error due to fabrication. Because of the wear in the rolls, deformed reinforcing bars of steel change in area slightly. For bars No. 3, 9.53 mm (3/8") diameter and larger, CSA and ASTM standards allow for up to 6% underweight on any individual bar. MacGregor [5] reports that the mean area should be taken as 0.975 of the nominal area with coefficient of variation of 1.6% (Fig. 2.3).

The geometrical errors in cross sectional dimensions also play an important part in the variation of strength in an element; especially the effective depth of the reinforcing steel in a slab, since the moment capacity is proportional to the square of the depth. Allen [6] reports a coefficient of variation of the depth for a concrete slab as:

$$(V_d)_{slab} = 0.025 + (0.20 / d) \qquad (2.3)$$

where d is the effective depth in inches. MacGregor [5] reports that the effective depth for cast in place slabs has a mean of 0.25 inch (6.35 mm) less than specified, with a standard deviation of 0.3 inch (7.62 mm) at the positive moment region and that the top steel is placed at an average depth of 0.75 inch (19.05 mm) less than specified with a standard deviation of $\sigma = 0.5$ inch (12.7 mm) at the negative moment region.

For beams, Ellingwood [32] suggests that the coefficient of variation of the effective depth in concrete follows the relation:

$$(V_d)_{beams} = 0.68/h_n \qquad (2.4)$$

where h_n is the nominal member dimension in inches and is the dimension given on the engineer's structural drawing.

Furthermore, MacGregor [32] suggests that the coefficient of variation in dimension for a concrete beam or column be given by:

$$V_b = V_h = 0.4 / h_n \qquad (2.5)$$

Two other researchers, Tso and Zelman [7], after investigating 299 columns, found an average error in dimensions of +0.06 inch (1.52 mm) with standard deviation σ = 0.28 inch (7.11 mm) (Fig. 2.4) .

2.2.1.3 Variation Due to Professional Assumptions

Engineers use simplifying assumptions while modeling a structure or predicting the loads imposed on it which affect the estimated variation in an element's property [9]. For example, assuming a rectangular stress block and limiting the strain at which concrete crushes introduce both systematic and random errors. Based on tests performed by Mattock, MacGregor [5] estimates that reinforced concrete beams have a mean strength of 1.01 times greater than based on the rectangular stress block; whereas the mean strength of columns is only 98% of that based on the rectangular stress block.

The use of discrete sizes such as the number of bars in an 18 in. x 18 in. (457 mm x 457 mm) column gives a mean area of steel 1.02 times the reinforcement required by theory with a coefficient of variation of 5% [5].

2.2.1.4 Overall Strength Variation in Concrete Elements

To obtain the overall strength variation V_R of a reinforced concrete element, consideration must be given to all the previous variations. According to MacGregor [33], the overall coefficient of variation of strength V_R in concrete beams depends on the grade and percentage ratio of the reinforcing steel; he also reports a coefficient of variation V_R =

0.11 for grade 60 ksi and $p = 0.5p_b$ and $V_R = 0.14$ for grade 40 ksi and $p = 0.35p_b$, where p is the percentage ratio.

2.2.2 Strength Variation in Steel Elements

The strength of structural steel elements varies essentially for the following three reasons:

a) Variability in material strength denoted by V_m, which is dependent primarily on the yield strength of steel for beams and on the Young's Modulus and moment of inertia for long columns. For beam columns, it is dependent on yield strength, Young's modulus and moment of inertia.

b) Variation due to fabrication errors, V_f, which occurs as a result of rolling tolerances, deviations in geometrical dimensions, and initial out of straightness.

c) Simplifying assumptions made by engineers, such as resistance equations that govern the four classes of sections result in variations, V_p, which affect their solutions.

A brief discussion of these factors is given below.

2.2.2.1 Variation in Material Properties

The most important material property affecting the resistance of a structural steel element is the yield stress of the material [8,11]. The yield stress depends on the chemical composition and on the fabrication process. ASTM specifications, CSA standards G40.20 M1977 and G40.21 M1977, and quality control at the steel mill ensures that the mill yield stress of test coupons is greater than or equal to the specified value required by the designer.

Much data has been collected for the mill yield stress for rolled W shaped beams; however, these must be modified to take into account the rate of loading during the tests. For example, the mean mill yield stress $(f_y)_{mean}$ is reported as 121% of the specified yield

strength by Galambos [8] but when adjustments are made for the strain rate effects this value is considerably reduced. Taking this into account, Galambos lists the following properties:

Flanges in rolled shapes: $(f_y)_{mean} = 1.05\ f_y$, $V_{fy} = 0.10$

Plates and webs in rolled shapes: $(f_y)_{mean} = 1.10\ f_y$, $V_{fy} = 0.11$

Other properties are also important for laterally unbraced beams; for example, the elastic lateral torsional buckling moment M_c as given by:

$$M_c = \frac{C_b \pi}{K_{ly} L_b} \sqrt{EI_y GJ + \frac{\pi^2 E^2 I_y C_w}{(K_{lz} L_b)^2}} \qquad (2.6)$$

where L_b = unbraced length of beam

E = elastic modulus

G = elastic shear modulus

I_y = moment of inertia about minor axis

J = St. Venant torsion constant

C_w = warping moment of inertia

C_b = loading coefficient

K_{ly}, K_{lz} = effective length factors for lateral and torsional end restraints.

M_c does not depend on the yield strength of steel but more importantly on its Young's modulus E and also on its shear modulus G [10]. Galambos [8] reports that the mean modulus of elasticity, E, equals 29,000 ksi with $V_E = 0.06$ and that the mean shear modulus equals 11, 200 ksi with $V_G = 0.06$.

Moreover, the elastic limit of laterally braced class 3 members can be adversely affected by residual stresses since their bending resistance is given by [10]:

$$M_r = S_x (f_y - f_r) \qquad (2.7)$$

Galambos [8] has found that the residual stress has a mean of 10 ksi, a coefficient of variation $V_{fr} = 0.05$, and that the residual stress is independent of the grade of steel for beam shapes; thus its effects are more pronounced for low grades of steel.

In short columns, the critical stress depends primarily on the yield strength f_y. However, for intermediate and long columns the strength variation will also depend on the variation in the Young's modulus because of Euler buckling.

2.2.2.2 Variation Due to Fabrication Errors

The variation in dimensions of structural steel members are specified by ASTM and CSA standards to within a certain tolerance and these provisions can be used to supplement mill data in order to estimate such statistical parameters as standard deviation and coefficient of variation. This was done by Kennedy and Gad Aly [11] who calculated the variations in various section properties. Their results for rolled W shaped sections are presented in Table 2.1 .

Table 2.1 Statistical Parameters of the Variation of Geometric Properties for Rolled W Shapes [11]

Property	Mean/nominal	Coefficient of variation
b	1.005	0.0135
t_f	0.979	0.0417
w	1.017	0.0384
d	1.000	0.0009-0.0030
A	0.99	0.033
I_x	0.99	0.043
I_y	1.00	0.058
S_x	0.99	0.021
S_y	0.99	0.049
Z_x	0.99	0.038
Z_y	0.99	0.048
r	1.00	0.023
J	0.96	0.100
C_w	0.99	0.090

They concluded that the mean to nominal ratio of geometric properties is 0.99 with coefficient of variation V_f ranging from 0.021 to 0.058.

For steel beams, Yura [10] also considered the effect of local flange, local web, and lateral torsional distortions together with out of straightness and reported a coefficient of variation in fabrication, $V_f = 0.05$.

For steel columns, Galambos and Ravindra [34] report that the mean column area is assumed equal to the area listed in the handbook with coefficient of variation of area $V_{Ac} = 0.05$. In another paper and using limits imposed by CSA G40.20, Kennedy and Gad Aly [11] arrive at a ratio of actual to specified area of 1.015 and coefficient of variation of 0.013 which differs a little from Galambos' previous assumptions.

2.2.2.3 Variation Due to Professional Assumptions

Several assumptions made by engineers will also influence their solution. Statistical assumptions such as independence between load and resistance, and assumptions made about the distributions of the statistical parameters will affect the results. It is convenient to assume normal distributions to fit actual distributions, since for parameters influenced by the sum of two or more variables, the mean of the parameter is the sum of the means of the variables [5,13]:

eg. $C = A + B$ (2.8)

then $\overline{C} = \overline{A} + \overline{B}$ and $V_C^2 = V_A^2 + V_B^2$ (2.9) (2.10)

For the multiplicative case $C = AB$ (2.11)

then $\overline{C} = \overline{A}\,\overline{B}$ and $V_C^2 = V_A^2 + V_B^2 + V_A^2 V_B^2$ (2.12) (2.13)

For low coefficients of variations, $V < 0.3$, MacGregor recommends that the last term be dropped, thus:

$$V_C^2 = V_A^2 + V_B^2 \qquad (2.14)$$

According to Dumonteil [12], the actual distribution, whether normal or log normal, does not affect the results because of the low coefficient of variations involved.

For the resistance of steel columns, Galambos and Ravindra [34] based their research on tests performed by Bjorhoude in 1972. The mean resistance is given by the equation:

$$\overline{R} = (A_c)_m \times (f_{cr})_m \tag{2.15}$$

where $(A_c)_m$ is the mean column cross sectional area and the mean critical stress $(f_{cr})_m$ is in this case the mean buckling stress. They give the mean buckling stress as:

$$(f_{cr})_m = \left[\left(\frac{P_u}{P_y} \right)_{theory} \right]_m (f_y)_m (B_{test/theory})_m \tag{2.16}$$

where P_u = ultimate strength predicted by theory

P_y = crushing load $A_c f_y$

$B_{test/theory}$ = "bias" factor comparing test strength with those given by theory.

Galambos and Ravindra [34] also report that Bjorhoude found $B_{test/theory} = 1.03$ with a coefficient of variation of $V_{test} = 0.05$. Moreover, the variation of resistance in a column depends on the professional factor V_p. According to Galambos and Ravindra, both factors $[(P_u/P_y)_{theory}]_m$ and V_p are functions of a slenderness effect factor λ_{sl} given by the AISC as:

$$\lambda_{sl} = L \left(\frac{1}{\pi} \right) \sqrt{\frac{F_y A_c}{EI}} \tag{2.17}$$

As seen from Figure 2.5, the coefficient of variation due to theory, V_p, varies from 0.03 to 0.13 for typical values of λ_{sl}.

Since the coefficient of variation of resistance, V_R, is dependent on V_p, it follows that V_R is also dependent on the slenderness effect. This is shown in Figure 2.6. In another paper, Allen [6] reports a coefficient of variation due to theory $V_p = 0.07$.

2.2.2.4 Overall Strength Variation in Steel Elements

When substituting typical values in the equation for coefficient of variation of resistance:

$$V_R^2 = V_{fy}^2 + V_f^2 + V_{test}^2 + V_p^2 \qquad (2.18)$$
$$= (0.10)^2 + (0.05)^2 + (0.05)^2 + (0.07)^2$$

a value of $V_R = 0.14$ is found. Finally in determining the strength of columns, a mean initial out-of-straightness of 1/1000 of the length is usually assumed [4,12].

However, other important assumptions can be made during the analysis of a structure. Yura [10] reports that the predominant factor in the variation in resistance of steel beams is variations arising from the prediction formula. These prediction formula are very much dependent on whether a beam is simply supported or continuous and whether it is subjected to uniform moment or moment gradient. Moreover, according to Yura, the unbraced length is also an important factor in determining the variation of the prediction formula. In this respect, Kennedy and Gad Aly [11] differ in opinion. According to them, the designer has complete control in determining the unbraced length, and therefore, it should not be a factor subject to statistical variation in the establishment of the performance factor.

Finally, Yura [10] also considers end restraint conditions and reports a coefficient of variation of the ratio of actual predicted critical moment to nominal moment of 0.2, which indicates large variation. It is the predominant factor since $V_m \approx 0.06$ and $V_f \approx 0.05$. With these values the coefficient of variation of resistance in a steel beam becomes $V_R = 0.23$.

2.3 EVALUATION OF STRENGTH VARIATION PARAMETER λ

2.3.1 Derivation of Parameter λ

The objective of this section is to determine the maximum permissible variation of the mean strength, denoted by λ, in a structural element.

The variation of structural properties and resistance is inherently a random process. Arising from this variation in structural properties, engineers expect a deviation in strength from the mean strength $\overline{R}$ of an element. The code accepts a certain amount of variation by attributing performance factors to the nominal resistance R_n and load factors to the specified loads S_d. Thus, for design purposes it is important to quantify the expected variation of resistance in order to obtain performance factors. The parameter λ represents a measure of the variation of resistance and relates the mean resistance $\overline{R}$ of a member to the code specified limit of deviated resistance R^* given in CSA S408 - 1981 as the 'design point' [13].

The design point R^* can be found once the mean resistance $\overline{R}$ is known from the following equation:

$$R^* = (1 - \lambda)\overline{R} \tag{2.19}$$

Where, λ is a unitless quantity given by:

$$\lambda = 1 - (R^*/\overline{R}) \tag{2.20}$$

However, R^* is not readily known because, until now, researchers have avoided its explicit formulation to concentrate on obtaining the performance factors used in Limit States Design. Hence, to obtain λ, it is essential to discuss how the design point resistance is obtained in the Limit States Design process.

In Limit States Design all potential modes of failures are identified and acceptable levels of safety are set which depend on the significance of failure [5]. The Guidelines for the Development of Limit States, CSA S408 - 1981 [13], introduces the concept of equal

levels of failure probability for structures made of different materials. Let R represent the distribution of resistance and S represent the maximum load in 30 years, the mean and standard deviation of each distribution is given by $\overline{R}$, σ_R and $\overline{S}$, σ_S respectively. Failure will obviously occur when S exceeds R or for $Z < 0$ if one lets:

$$Z = R - S \tag{2.21}$$

Since R and S can be considered statistically uncorrelated and having normal distribution it follows that:

$$\overline{Z} = \overline{R} - \overline{S} \tag{2.22}$$

and

$$\sigma_z^2 = \sigma_R^2 + \sigma_S^2 \tag{2.23}$$

with Z also following a normal distribution and

$$\overline{Z} = \beta\sigma_z \tag{2.24}$$

as its mean. Hence, the probability of failure is the area under the curve for Z below zero (Fig. 2.7) and can be found using the cumulative normal distribution function given as:

$$P_f(\beta) = \frac{1}{\sqrt{2\pi}} \int_{\beta}^{\infty} e^{-t^2/2}\, dt \tag{2.25a}$$

for which values are tabulated in most textbooks of probability and statistics. The parameter β is called the reliability index in CSA S408, whereas, most researchers denote this term as the safety index. β equals the number of standard deviation σ_z from zero to $\overline{Z}$ (Fig. 2.7). The probability of failure P_f is related to β by the following equation [5,13]:

$$P_f \approx 460e^{(-4.3\beta)} \tag{2.25b}$$

for $2 < \beta < 6$

From the definition of the safety index and Figure 2.7, one can obtain the following equation for β [13,14]:

$$\beta = \frac{\overline{R} - \overline{S}}{(\sigma_R^2 + \sigma_S^2)^{1/2}} \tag{2.26}$$

Let S^* denote the design load, then the design point $S^* = R^*$ represents the failure combination with the highest probability of occurrence [14] and is found from the following two relations [13,14]:

$$R^* = \overline{R} - \frac{\beta\sigma_R}{\left[1 + \left(\frac{\sigma_S}{\sigma_R}\right)^2\right]^{1/2}} \tag{2.27}$$

$$S^* = \overline{S} + \frac{\beta\sigma_S}{\left[1 + \left(\frac{\sigma_R}{\sigma_S}\right)^2\right]^{1/2}} \tag{2.28}$$

R^* and S^* correspond to the factored resistance and the factored load respectively.

Figure 2.8 shows the design point R^* at a position less than the nominal strength R_n which in turn is less than the mean strength $\overline{R}$. This design point represents the maximum allowable or permissible variation from the mean.

Thus the National Building Code [1,17] intrinsically has a maximum allowable deviated resistance from the mean and this percentage deviation is given by λ. The parameter λ obeys the following equation:

$$\lambda = \frac{\beta V_R}{\left\{1 + \left[\frac{V_S}{V_R} \times \frac{(1 - 0.75\beta V_R)}{(1 + 0.75\beta V_S)}\right]^2\right\}^{1/2}} \tag{2.29}$$

The equation for parameter λ applies equally well for any material once the level of safety is specified by the safety index β and the coefficient of variation of the resistance V_R and the coefficient of variation of the load V_S are known. It should be noted that in equation 2.29 the coefficient of variation of load V_s appears because of the interaction between load

and resistance in the determination of probabilities of failure. This derivation is shown below.

From the Canadian Standard CSA S402, equation A5, the safety index β is given by [13,14]:

$$\beta = \frac{\overline{R} - \overline{S}}{(\sigma_R^2 + \sigma_S^2)^{1/2}} \tag{2.26}$$

But Lind [5,34] proved the following:

$$(A^2 + B^2)^{1/2} \approx \alpha A + \alpha B \tag{2.30}$$

with $\alpha = 0.75$ for ratios of A to B between 1/3 and 3. Since the ratio of standard deviation σ_S to σ_R is within this limit, one can write:

$$\beta = \frac{\overline{R} - \overline{S}}{0.75(\sigma_S + \sigma_R)} \tag{2.31}$$

From the definition of coefficient of variation the following two relations are obtained:

$$\sigma_S = V_S\overline{S} \qquad \sigma_R = V_R\overline{R} \tag{2.32) (2.33}$$

Therefore it follows that:

$$\beta = \frac{\overline{R} - \overline{S}}{0.75(V_S\overline{S} + V_R\overline{R})} \tag{2.34}$$

Hence:

$$\overline{S} = \left[\frac{(1 - 0.75\beta V_R)}{(1 + 0.75\beta V_S)}\right]\overline{R} \tag{2.35}$$

The design point resistance R^* is given by:

$$R^* = \overline{R} - \frac{\beta\sigma_R^2}{[\sigma_R^2 + \sigma_S^2]^{1/2}} \tag{2.36}$$

Therefore,

$$R^* = \overline{R} - \frac{\beta\sigma_R}{[1 + (\frac{\sigma_S}{\sigma_R})^2]^{1/2}} \tag{2.27}$$

Using the definition for coefficient of variation, one obtains:

$$R^* = \overline{R} - \frac{\beta\sigma_R}{\left\{1 + \left[\frac{V_S^2 \overline{S}^2}{V_R^2 \overline{R}^2}\right]\right\}^{1/2}} \tag{2.37}$$

but:

$$\frac{\overline{S}}{\overline{R}} = \frac{1 - 0.75\beta V_R}{1 + 0.75\beta V_S} \tag{2.38}$$

Therefore:

$$R^* = \left[1 - \frac{\beta V_R}{\left[1 + \left(\frac{V_S}{V_R}\right)^2 x \left(\frac{1 - 0.75\beta V_R}{1 + 0.75\beta V_S}\right)^2\right]^{1/2}}\right] \overline{R} \tag{2.39}$$

But from the definition of parameter λ:

$$R^* = (1 - \lambda)\overline{R} \tag{2.19}$$

Thus comparing the above two equations one gets:

$$\lambda = \frac{\beta V_R}{\left\{1 + \left[\frac{V_S}{V_R} \times \frac{(1 - 0.75\beta V_R)}{(1 + 0.75\beta V_S)}\right]^2\right\}^{1/2}} \qquad (2.29)$$

2.3.2 Strength Variation Parameter λ for Steel

According to Galambos and Ravindra [34], the value of the safety index β was established by calibrating the limit states criteria to that of the previous standard (working stress design) for ratios of live to dead load L/D = ∞ and a value of β equal to 3.0 was obtained. For steel beams they reported [34] a coefficient of variation in resistance V_R = 0.13. In another paper, Allen [35] also reports V_R = 0.13. Note however that Yura [10] reports a value of V_R = 0.23 if end constraints are taken into account as previously mentioned in Section 2.2.3. For normal loading, the Canadian Standard CSA S408 [13] recommends a coefficient of variation of loading as V_S = 0.2.

Thus for steel beams, the accidental strength variation parameter λ equals:

$$\lambda = \frac{3.0 \times 0.13}{\left\{1 + \left[\frac{0.2}{0.13} * \frac{(1 - 0.75 \times 3 \times 0.13)}{(1 + 0.75 \times 3 \times 0.2)}\right]^2\right\}^{1/2}} = 0.312$$

According to CSA S408 - 1981 [13], the specified material property should be chosen such that the specified value corresponds to a probability level of between 1% to 10%. Commentaries 'F' of the NBCC Supplement for 1980 and 1985 [27,36] suggest a 5% probability for new materials or new control methods. Table F1 of the NBCC Supplement gives characteristic values for loads and material properties and lists steel yielding in tension as having a probability of understrength of 1% to 2%.

For a set probability of understrength one can use the cumulative standard normal distribution function $F(\zeta)$ to find the strength variation parameter. Most probability texts define $F(\zeta)$ as:

$$F(\zeta) = \frac{1}{\sqrt{2\pi}} \int_{-\infty}^{\zeta} e^{-t^2/2}\, dt \qquad (2.40)$$

where ζ is the value of a random variable having standard normal distribution. The probability of ζ occurring between two limits is given by:

$$P(a \le \zeta \le b) = F(b) - F(a) \qquad (2.41)$$

where: $F(-\infty) = 0$

$F(+\infty) = 1.0$

$F(-\zeta) = 1 - F(\zeta)$

Thus the probability of understrength of normal variable R can be expressed by using the standard normal variable ζ as follows:

$$\zeta = (R - \overline{R}) / \sigma_R \qquad (2.42)$$

Since ζ is a standard normal distribution function, its mean $\overline{\zeta}$ equals zero and its variance equals unity. Hence, the probability of understrength in R is shown in Fig 2.9 as the shaded area and is given by:

$$P[0 \le R \le (1 - \lambda)\overline{R}] \qquad (2.43a)$$

which is approximately equal to:

$$P[-\infty \le \zeta \le \{[(1 - \lambda)\overline{R} - \overline{R}] / \sigma_R\}] \qquad (2.43b)$$

Therefore, the probability of understrength in R is given by:

$$P(\text{understrength}) = 1 - F(\lambda/V_R) \qquad (2.43c)$$

For 1% probability, one gets:

$$0.01 = 1 - F(\lambda/V_R)$$

Hence $F(\zeta) = F(\lambda/V_R) = 0.99$ and from probability tables, $\zeta = 2.327 = (\lambda/V_R)$. Therefore, $\lambda_{steel} = 2.327 \times 0.13 = 0.303$ which is approximately equal with the previous value found.

2.3.3 Strength Variation Parameter λ for Concrete

According to MacGregor [33], the probability of understrength in a reinforced concrete beam is 1 in 1000. This gives a value $\zeta = 3.08 = (\lambda/V_R)$. In another paper, MacGregor [32] gives the coefficient of variation of resistance:

$V_R = 0.11$ for grade 60 ksi and $p = 0.5p_b$ and

$V_R = 0.14$ for grade 40 ksi and $p = 0.35p_b$.

Thus: $\lambda = 3.08 \times 0.11 = 0.339$ or

$\lambda = 3.08 \times 0.14 = 0.431$

depending on the grade of steel.

If one uses equation (2.29) to find λ for a concrete beam, V_S is required:

$$V_S = \frac{\left[V_D^2 + \left(\frac{\bar{L}}{\bar{D}}\right)^2 V_L^2\right]^{1/2}}{1 + \frac{\bar{L}}{\bar{D}}} \qquad [42]\ (2.44)$$

$$\text{Eg.} \quad \begin{matrix} \bar{L} = 50 \text{ psf} \\ \bar{D} = 80 \text{ psf} \end{matrix} \qquad [72]$$

$$V_S = \frac{[(0.106)^2 + (5/8)^2\ (0.36)^2]^{1/2}}{1 + (5/8)} = 0.153$$

Thus, using equation (2.29) with safety index $\beta = 3.5$ [5],

$$\lambda_{60\text{ ksi}} = \frac{3.5 \times 0.11}{\sqrt{1 + \left[\frac{0.15}{0.11} * \frac{(1 - 0.75 \times 3.5 \times 0.11)}{(1 + 0.75 \times 3.5 \times 0.15)}\right]^2}} = 0.316$$

$$\lambda_{40\,ksi} = \frac{3.5 \times 0.14}{\sqrt{1 + \left[\frac{0.15}{0.14} * \frac{(1 - 0.75 \times 3.5 \times 0.14)}{(1 + 0.75 \times 3.5 \times 0.15)}\right]^2}} = 0.398$$

According to Siu et al [37], the safety index value of the ACI code is $\beta = 4.2$. For a heavily reinforced beam, Allen [35] estimates $\beta = 4.0$ for CSA A23.3 - 1973. Taking the latter value, one obtains:

$$\lambda_{60\,ksi} = 0.350$$

$$\lambda_{40\,ksi} = 0.458$$

These values compare well with those found above for a probability of understrength of 1/1000.

The strength variation parameter λ can also be estimated from the code allowable overstrength in steel. More specifically, clause A2.5 of ACI 318 - 83 [30] limits the actual yield strength of reinforcing steel so that it does not exceed 124.1 MPa (18 ksi) above the specified yields of ASTM A615 grade 275.8 MPa (grade 40) and grade 413.7 MPa (grade 60).

This is similar to clause 21.2.5.1 of CSA standard CAN3-A23.3-M84 [38] which limits the actual excess yield stress based on mill tests to less than 125 MPa for steel reinforcement complying with CSA G30.16 and CSA G30.12 grades 300 and 400 when resisting earthquake induced flexural and axial forces.

When the value of the concrete strength or the yield strength differs from the specified, the new ultimate bending capacity is given by (see Appendix 1):

$$M_u = 0.2438\left(\frac{600}{600 + f_{y_{des}}}\right) f'_{c_{des}}\, bd^2 \left(\frac{f_y}{f_{y_{des}}}\right)\left[1 - 0.1594\left(\frac{600}{600 + f_{y_{des}}}\right)\frac{f'_{c_{des}}}{f'_c}\frac{f_y}{f_{y_{des}}}\right] \tag{2.45}$$

It is therefore possible to find a value of λ due to an overstrength of the steel as shown in Fig 2.10 for 300 MPa and 400 MPa steel.

Thus the ACI 1983 code permits a variation of strength

$\lambda = 0.269$ for 275.8 MPa (40 ksi) steel

$\lambda = 0.206$ for 413.7 MPa (60 ksi) steel

to satisfy clause A.2.5, whereas the CSA standard allows for variation of strength

$\lambda = 0.257$ for 300 MPa steel

$\lambda = 0.212$ for 400 MPa steel

to satisfy clause 21.2.5.1 when based solely on steel strength variation. Note that the above λ values do not take into account possible concrete strength variation.

2.3.4 Summary

The parameter λ was evaluated using various approaches. Based on the available literature, values of λ differ slightly:

for steel beams: $\lambda = 0.303 \sim 0.312$ and

for concrete beams: $\lambda = 0.306 \sim 0.458$

It can be concluded that reasonable values of $\lambda_{\text{steel beam}} \approx 0.30$ and $\lambda_{\text{concrete beam}} \approx 0.375$ can be used.

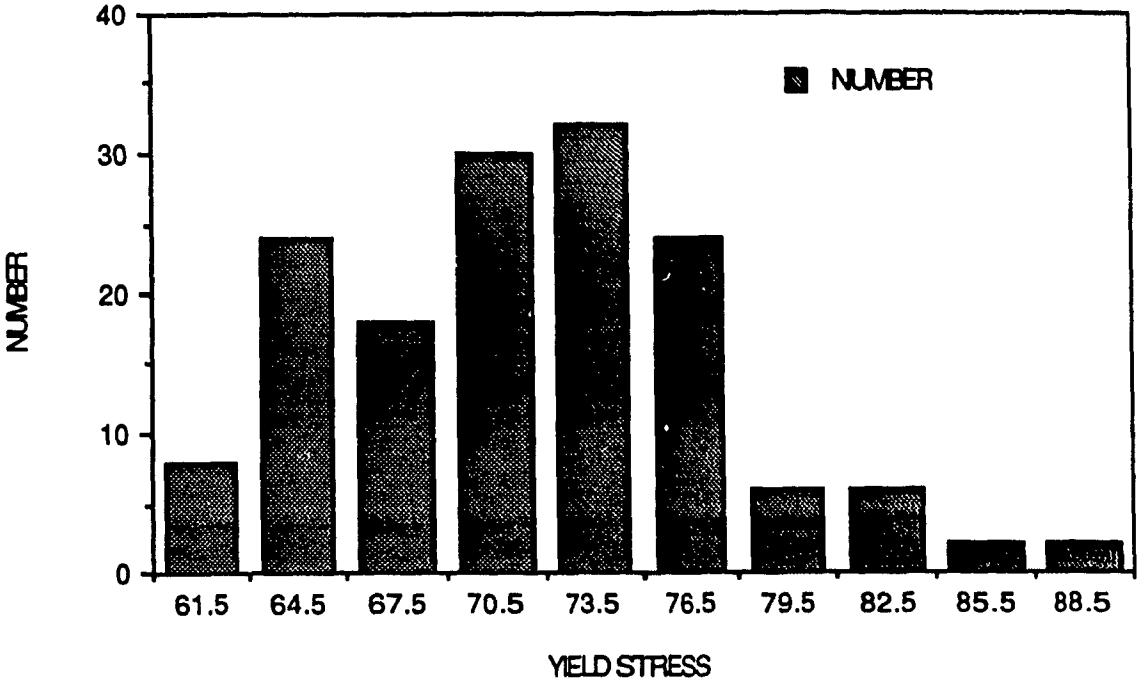

Fig. 2.1 Distribution of Steel Yield Strengths for Grade 60 Reinforcement [5]

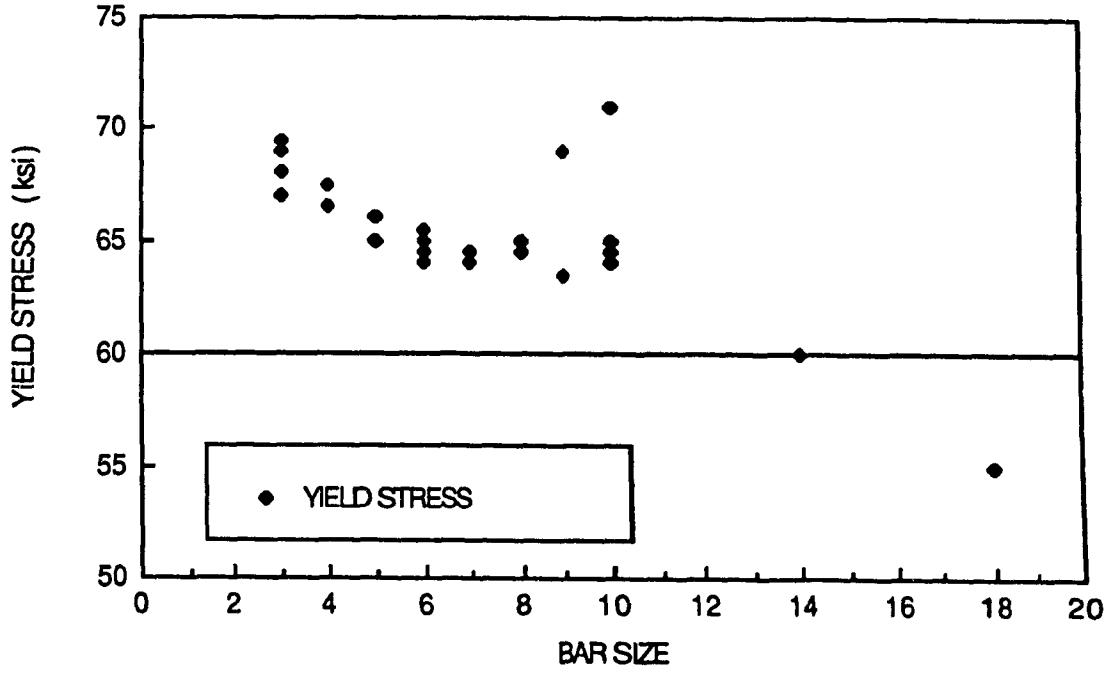

Fig. 2.2 Variation in Mill Test Yield Strength with Bar Size [5]

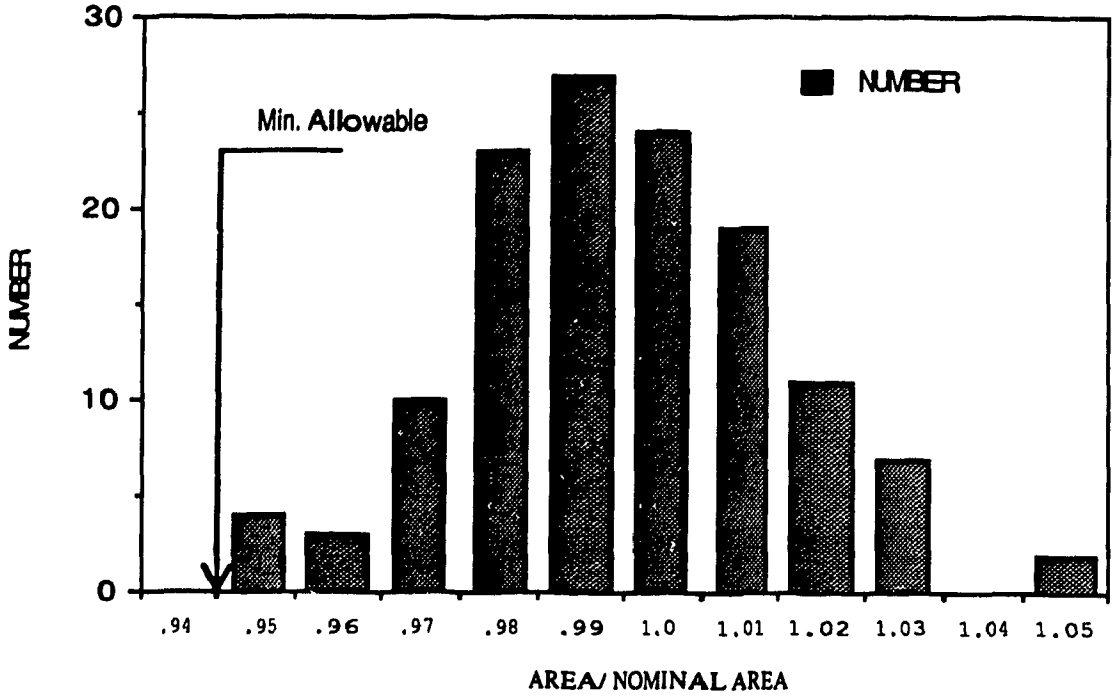

Fig. 2.3 Ratio of Actual Bar Area to Nominal Area [5]

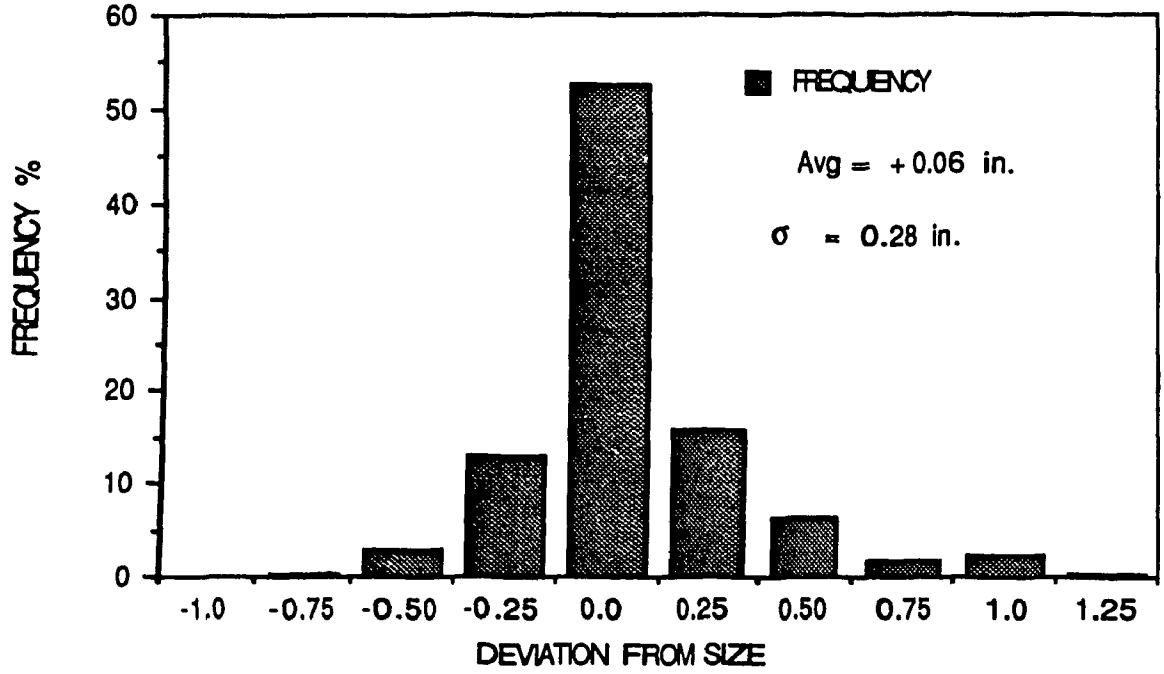

Fig. 2.4 Difference Between Actual and Specified Widths of Columns [5]

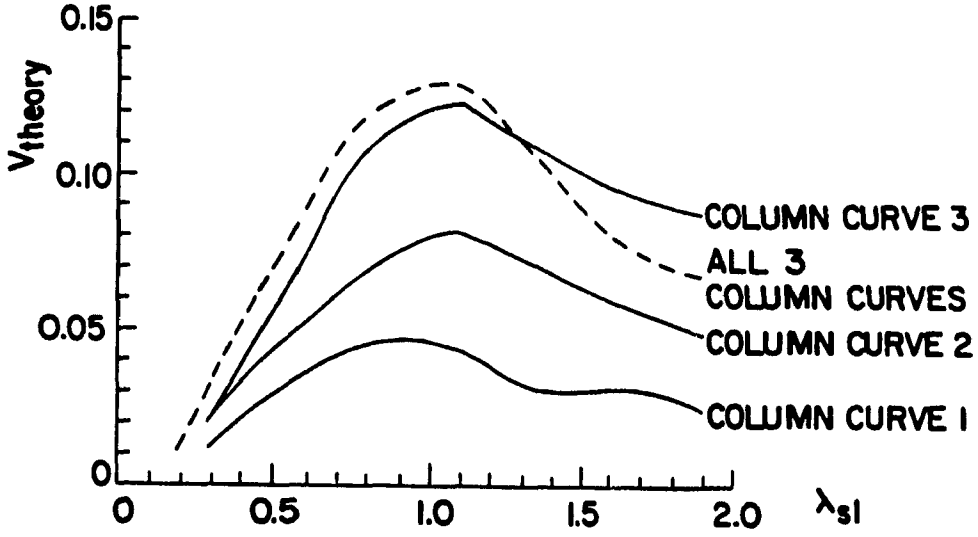

Fig. 2.5 Coefficients of Variation for the Prediction of Column Strength [34]

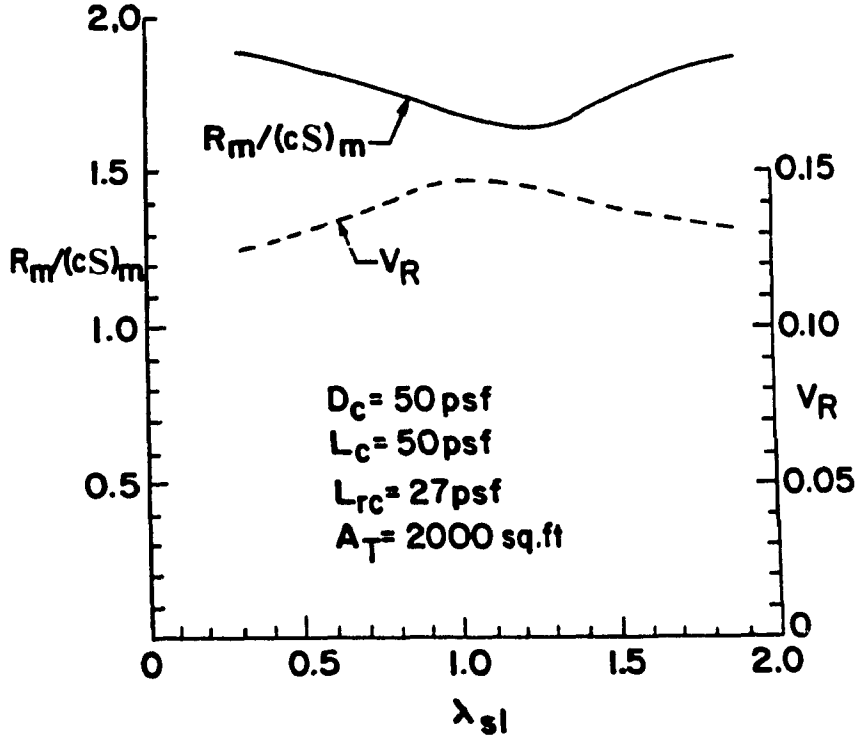

Fig 2.6 Variation of $R_m/(cS)_m$ and V_R with λ_{sl} for Calibration of Columns [34]

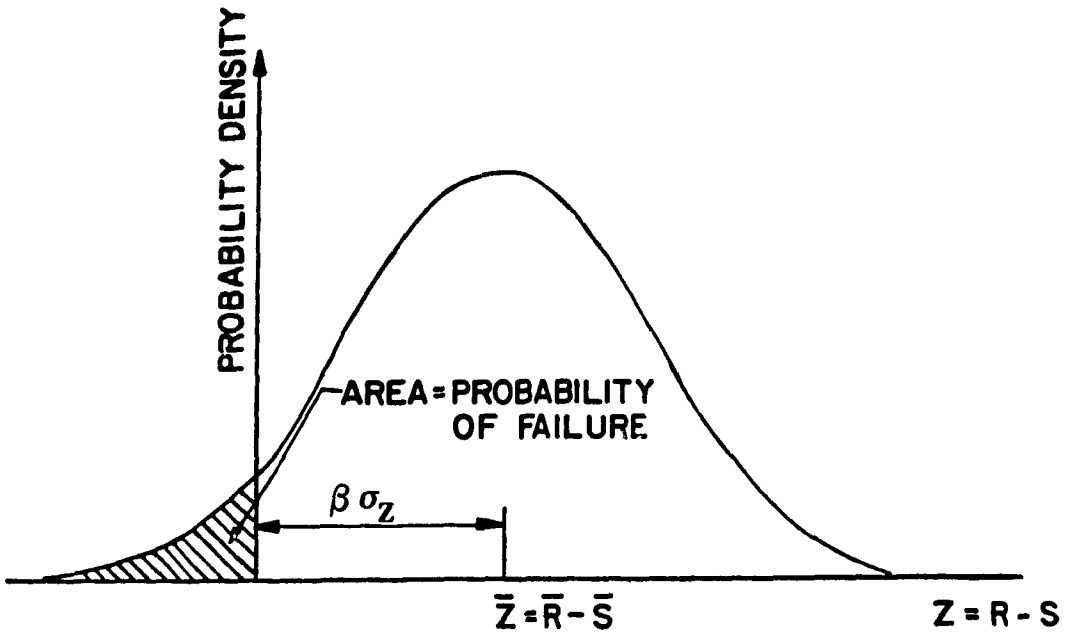

Fig. 2.7 Definition of Reliability Index [13]

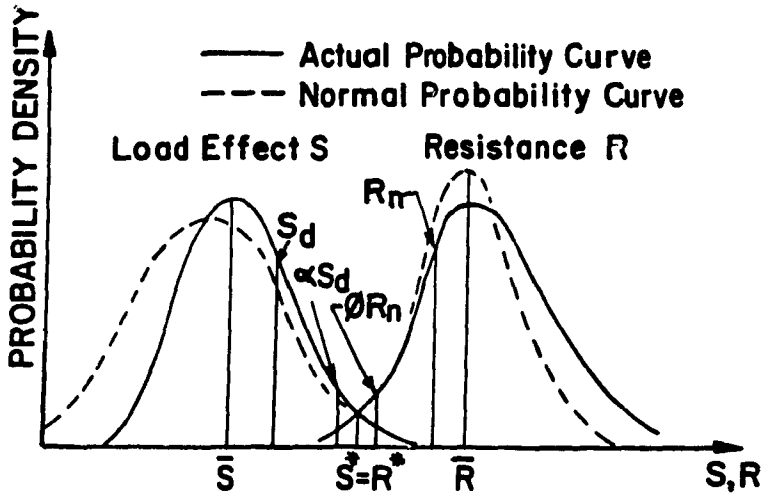

Fig. 2.8 Variation of Loads and Strengths and Definition of Terms [11,13]

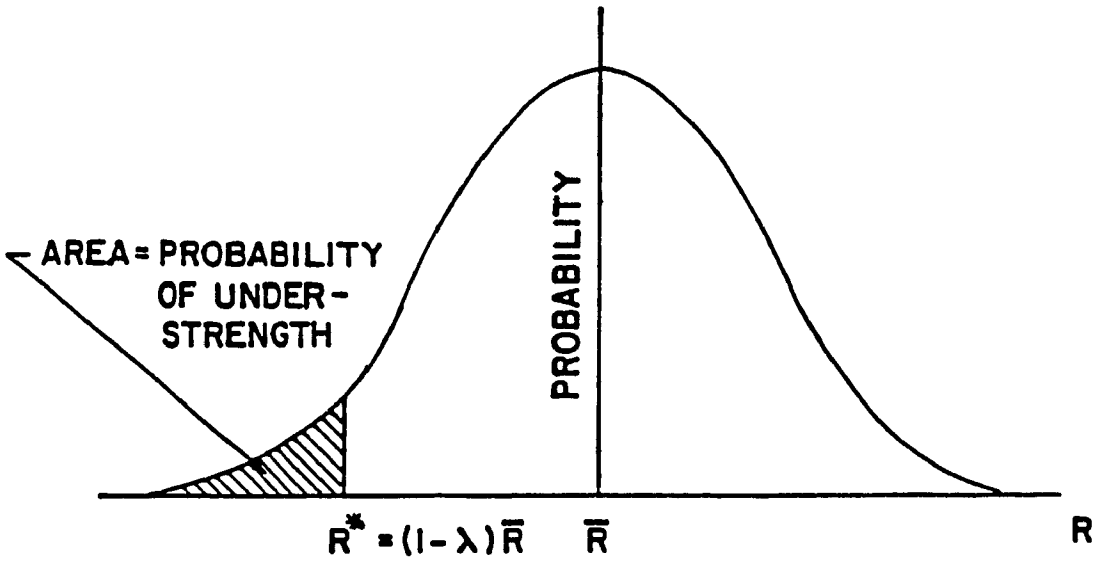

Fig. 2.9 Probability of Understrength

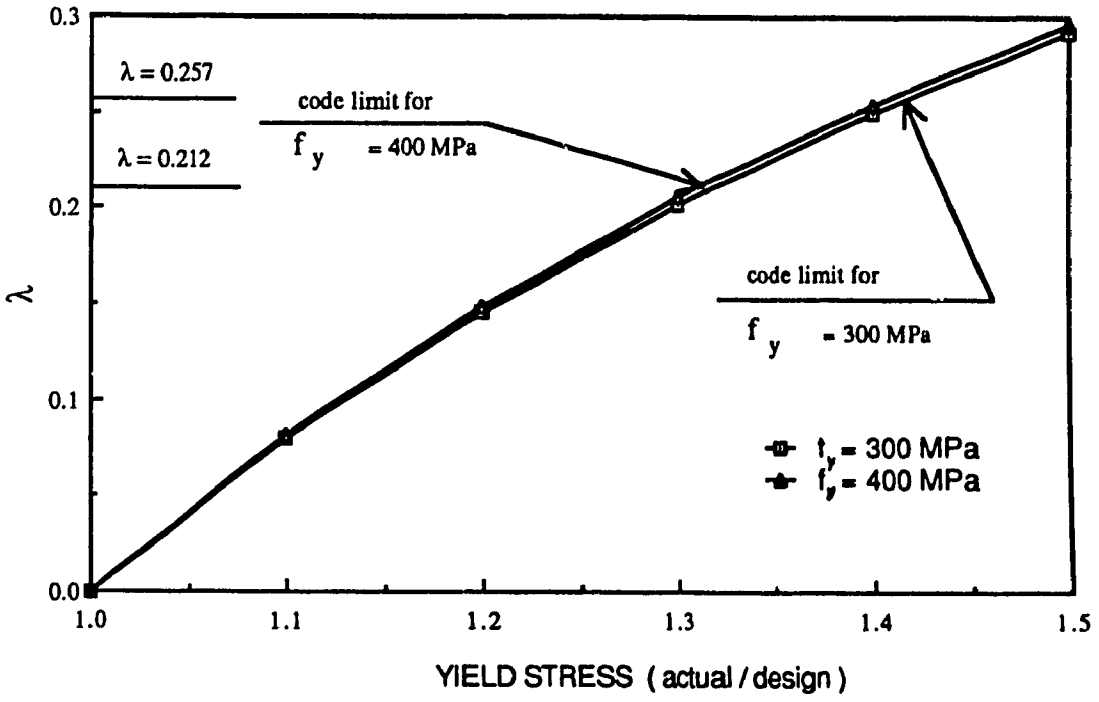

Fig. 2.10 Variation of Strength of Reinforced Concrete Beams Using Ultimate Strength Design.

CHAPTER III

STRUCTURAL MODEL WITH ACCIDENTAL ECCENTRICITY

3.1 INTRODUCTION

This chapter describes the structural model used to investigate the code requirements for accidental eccentricity. Accidental eccentricity is introduced in the model by means of the strength variation parameter λ which affects the resistance of one of the lateral supporting elements. This strength variation λ is an inherent characteristic of any structural element and was derived in the previous chapter from code requirements pertaining to probabilities of failure.

Moreover, this chapter investigates the probabilities associated with the strength variation of lateral resisting elements for the model. Three methods of describing this variation are discussed and each has different probabilities of occurrence for a given strength variation λ.

Finally, a brief review of the pertinent code torsional provisions for Canada and other countries is shown. These are examined with particular regard to their accidental eccentricity requirements.

3.2 DESCRIPTION OF THE STRUCTURAL MODEL

This section describes the structural model used to investigate the code requirements for accidental eccentricity when a structure is subjected to severe earthquake loading. Although the model can be used for representing eccentric structures, it is equally adept at modelling nominally symmetric structures which are symmetric in the elastic range of response but have accidental eccentricity in the inelastic range of response. Thus, the

responses obtained from the model with a set eccentricity can be used in conjunction with building code requirements to evaluate the responses from the model with accidental eccentricity.

The structural model consists of a rigid rectangular deck of total mass m, supported by two lateral resisting elements (Fig. 3.1). This model represents a one storey, singly asymmetric structure. Even though it is only a one storey model, the results are indicative of the behaviour for multi-storey buildings [15]. The deck has dimensions of $D_n = 3\rho$ and $D = (\sqrt{3})\rho$ such that the aspect ratio $(D_n/D) = 1.732$, where ρ is the mass radius of gyration about the center of mass. According to Tso [39], an aspect ratio less than unity gives higher responses but is less likely to occur than the aspect ratio chosen. Moreover it is important that the values chosen for the dimension of the deck follow the mathematical relation for the mass radius of gyration:

$$\rho^2 = 1/12\ (D_n^2 + D^2) \tag{3.1}$$

For simplicity the model is symmetric about the x-axis and no lateral displacemen is allowed in the x-direction at the center of mass; thus the x and y displacements are decoupled and the model has only two degrees of freedom; the translational displacement in the Y- direction of the center of mass (CM on Fig. 3.1) relative to the ground, and rotation θ about a vertical axis through the center of mass. Figure 3.1 shows the lateral resisting element No. 1 positioned at a distance $(e + x_o)$ to the left of the center of mass whereas element No. 2 is positioned at a distance $2x_o$ to the right of element No. 1.

Under seismic excitation $\ddot{u}_g$ acting in the y-direction through the center of mass, the equations of motion for an undamped elastic system can be given in matrix form by [7]:

$$\omega_y^2 \begin{bmatrix} 1 & e^* \\ e^* & \Omega_{CM}^2 \end{bmatrix} * \begin{Bmatrix} y \\ \rho\theta \end{Bmatrix} + \begin{Bmatrix} \ddot{y} \\ \rho\ddot{\theta} \end{Bmatrix} = \begin{Bmatrix} -\ddot{u}_g \\ 0 \end{Bmatrix} \tag{3.2}$$

Lateral and torsional rigidities and the eccentricity of the model are given by:

$$K_y = \sum_i k_{iy} \qquad (3.3)$$

$$K_{\theta_{CM}} = \sum_i k_{iy} x_i^2 + \sum_i k_{ix} y_i^2 + \sum_i k_{i\theta} \qquad (3.4)$$

$$K_{\theta_{CR}} = K_{\theta_{CM}} - K_y e^2 \qquad (3.5)$$

$$e = \left(\frac{1}{K_y}\right) \sum k_{iy} x_i \qquad (3.6)$$

where K_y is the total lateral rigidity in the y-direction and $k_{i\theta}$ is the torsional rigidity of an element about its own axis and can be neglected for planar members. In equation (3.4) for $K_{\theta CM}$, the second term has no value since the only lateral resisting element in the x-direction is placed along the x-axis.

One can now define the uncoupled translational frequency ω_y and the uncoupled torsional frequency about the center of mass as:

$$\omega_y = (K_y/m)^{1/2} \qquad (3.7)$$

$$\omega_{\theta CM} = (K_{\theta CM}/m\rho^2])^{1/2} \qquad (3.8)$$

Other torsional frequencies defined in the literature are [40]:

$$\omega_{\theta CR} = (K_{\theta CR}/[mr^2])^{1/2} \qquad (3.9)$$

where r is the radius of gyration of mass about the center of resistance and

$$\omega_{\partial O} = (K_{\theta CR}/[m\rho^2])^{1/2} \qquad (3.10)$$

For the three torsional frequencies there correspond three uncoupled torsional to lateral frequency ratios, namely:

$$\Omega^2_{CM} = \omega_{\theta CM}^2/\omega_y^2 \qquad (3.11)$$

$$\Omega^2_{CR} = \omega_{\theta CR}^2/\omega_y^2 \qquad (3.12)$$

$$\Omega^2_{O} = \omega_{\theta O}^2/\omega_y^2 \qquad (3.13)$$

The following two equations relate the various definitions of uncoupled torsional to lateral frequency ratios:

$$\Omega_0^2 = \Omega_{CM}^2 - (e^*)^2 \tag{3.14}$$

$$\Omega_0^2 = \Omega_{CR}^2 [1 + (e^*)^2] \tag{3.15}$$

It is preferable to use Ω_0 since it is independent of eccentricity thus simplifying the task of interpreting results [40]. In these equations, the structural eccentricity e when normalized by the mass radius of gyration about the center of mass ρ is defined as e^*; that is

$$e^* = e / \rho \tag{3.16}$$

Moreover, the two coupled natural frequencies of the system can be found from the following relations:

$$(\omega_{1,2})^2 = \left\{ \frac{1 + \Omega_{CM}^2}{2} \pm \sqrt{\frac{[1 - \Omega_{CM}^2]^2}{4} + (e^*)^2} \right\} (\omega_y)^2 \tag{3.17}$$

or

$$\frac{(\omega_{1,2})^2}{(\omega_y)^2} = \frac{[1 + \Omega_{CR}^2 + (e^*)^2]}{2} \pm \sqrt{\frac{[1 - \Omega_{CR}^2 - (e^*)^2]^2}{4} + (e^*)^2} \tag{3.18}$$

The geometry of the model presents an interesting characteristic when the two element rigidities are kept equal; in this instance, the product of the mass radius of gyration ρ and the torsional to lateral frequency ratio Ω_0 equals x_0, where x_0 is the distance between an element and the center of resistance CR, i.e.:

$$\Omega_0 \rho = x_0 \tag{3.19}$$

Another advantage of this model is that the center of mass and the edge positions do not vary for different Ω_0. This is an important characteristic and enables direct comparison of results of the edge displacements for various torsional to lateral frequency ratios, especially since the maximum translational displacements always occur at the edges of the model. The response of the model to seismic excitation was recorded from stations located at the following 6 positions: - 1.5ρ, - 1.0ρ, CR, CM, + 1.0ρ, and + 1.5ρ.

To obtain accidental eccentricity, a value of e = 0 is specified. When the value of e is chosen as zero, torsion will not arise while the lateral resisting elements remain elastic. Even after yielding of the elements torsion will arise only if the lateral resisting elements display non-identical load-displacement characteristics, since this study does not consider the influence of rotational ground motion.

To ensure yielding occurs, the maximum induced elastic resistance of an element is limited to a value of the ratio of its elastic symmetric force (R_{el}) to the earthquake severity factor Q; that is,

$$\overline{R} = R_{el} / Q \tag{3.20}$$

Thus the factor Q reduces the elastic displacement of the sructure. This study generally uses a value of Q = 4.0, although other values were also investigated.

Accidental eccentricity is obtained by using two procedures. The first consists of having element No. 1 at resistance $R = R_{el}/Q$ and element No. 2 at resistance $(1 - \lambda)\overline{R}$ (Fig. 3.2) where λ is the accidental strength variation parameter. Both elements exhibit elastoplastic behavior with a strain hardening ratio $k_2 = 0.00001k$ for numerical stability, where k is the original elastic stiffness of the element.

The second method has the lateral resisting element No. 1 at resistance $R = R_{el}/Q$ with elasto-plastic hysteresis while element No. 2 has an elastic resistance R, but exhibits the Takeda degrading stiffness (Fig. 3.3) after yielding. The Takeda degrading stiffness is formulated to display the properties of reinforced concrete beams when subjected to cyclic loading. It is a well known model and available as part of the Drain - 2D program [16]. Two versions are available: the original Takeda model and the modified Takeda model. In this study the initial stiffness and strain hardening of the Takeda element are kept equivalent to the elasto-plastic element and the parameters α_{tak} and β_{tak} have values of zero to display the original Takeda degrading stiffness. Other typical values of α_{tak} vary from zero to 0.4 and for β_{tak} from, zero to 0.6 [16]. Values of α_{tak} and β_{tak} were chosen

as zero since most of the literature refers to the original Takeda degrading stiffness, thus facilitating comparison with other investigators.

In both of the above methods, torsion arises due to the different post-elastic characteristics of the two elements, even though their initial elastic stiffnesses are specified identically. For this study, damping is mass and stiffness dependent and specified as 5% of critical damping.

To evaluate the anticipated lateral-torsional dynamic response of the model, the concept of static plastic eccentricity is introduced. Consider Figure 3.4: the load P is applied with magnitude such that both element No. 1 and element No. 2 reach their yield strength. The plastic eccentricity e^*_p is then defined as the distance between CR and the point where load P should be applied to cause no rotation of the deck. This point can be defined as the plastic center.

Considering the equations of equilibrium:

$$\sum F_y = 0 \qquad \text{gives } P = (2 - \lambda)R_y \qquad (3.21)$$

$$\sum M_{@2} = 0 \qquad \text{gives } P[\bar{x} + e^*_p] = R_y[2\bar{x}] \qquad (3.22)$$

$$\text{but } \bar{x} = [\Omega_o^2]^{1/2} \qquad \text{so } e^*_p = \lambda\Omega_o / (2 - \lambda) \qquad (3.23)$$

Thus e^*_p represents the normalized static accidental eccentricity resulting from unequal yield strengths of elements 1 and 2. As equation 3.23 indicates, this parameter is a function of strength variation parameter λ and the frequency ratio Ω_o. Figure 3.5 shows the influence of parameters Ω_o and λ on the expected magnitude of e^*_p. For the assumed peak value of $\lambda = 0.4$, the maximum expected $e^*_p = 0.3$.

Since both static accidental eccentricity and accidental eccentricity for structural systems are concerned with eccentricity caused by different yielding levels of the supporting elements, the above equations indicate that λ and Ω_o are pertinent parameters to investigate.

3.3 CODE PROVISIONS FOR ACCIDENTAL ECCENTRICITY

Most building codes provide for the evaluation of torsional effects arising from seismic loads in the earthquake resistant design of structures. The codes generally specify the design eccentricity as:

$$e_d = e_{d1} \pm e_{d2} \tag{3.24a}$$

$$e_{d1} = Ae \tag{3.24b}$$

$$e_{d2} = BD_n \tag{3.24c}$$

where e_d = design eccentricity

e = structural eccentricity defined as the distance between the center of mass and the center of rigidity

D_n = plan dimension of the building in the direction of the computed eccentricity

A = amplification coefficient

B = accidental eccentricity coefficient

e_{d1} = dynamic eccentricity

e_{d2} = additional or accidental eccentricity

The first term, e_{d1}, considers the amplification of structural effects due to the dynamic nature of earthquakes and is defined by the known distribution of mass and the structural layout of the building. The second term, e_{d2}, considers accidental eccentricity and is intended to account for possible additional torsion caused by unforeseen variation in the relative stiffness of lateral resisting elements, uncertainty in the distribution of mass, the different arrangement of movable wall panels and partitions, the variation of stiffness with time, and the inelastic or plastic actions. In addition, the accidental eccentricity term also considers the influence of torsional ground motion. It is the author's perception that accidental eccentricity will arise mainly due to the strength variation when the structures are loaded beyond the elastic limit under a severe earthquake.

3.3.1 National Building Code of Canada Requirements

The National Building Code of Canada (NBCC) 1980 [1] specified the following torsional provisions for the design eccentricity:

$$e_d = 1.5e + 0.05D_n \quad (3.25a)$$

or,

$$e_d = 0.5e - 0.05D_n \quad (3.25b)$$

whichever produces the greater effect on the lateral resisting element. Two equations are necessary since the displacement of a lateral resisting element is generally the sum of a translational component and a torsional component, and the torsional component may be either additive or subtractive depending on the position of the lateral resisting element with respect to the center of rigidity (Fig. 3.6).

After extensive studies [41-43], it was found that the torsional provisions of NBCC 1980 were unconservative for structures having small or zero eccentricity when the torsional frequency is close to the lateral frequency. The NBCC 1980 is, however, too conservative in the case of structures with large eccentricity due to subclause 4.1.9 (23)(b) which required the doubling of the design eccentricity when its value exceeds 0.25 D_n [41-43]. This is shown clearly in Figure 3.7 which was adapted from graphs shown in Reference 34. For eccentricities with e^* less than 0.4 (or $e/D_n \leq 0.133$), the 1980 NBCC underestimated the effective eccentricity, e_e, as defined by Tso [39] as that eccentricity which produces equivalent maximum displacements.

According to Tso [39], for very small eccentricities (i.e. $e^* < 0.075$), the effective eccentricity, e_e, is approximately 3 to 4.5 times the structural eccentricity. The slope of the effective eccentricity curves is about 1.0 for large eccentricities as shown in Figure 3.7. Furthermore, the slope of effective eccentricity is higher at low eccentricities because of modal coupling which may occur.

Several investigators [41,44] report that modal coupling is significant only if a structure has small eccentricity ($e^* < 0.15$ or $e/D_n < 0.05$) and uncoupled lateral to torsional frequency ratio between 0.8 and 1.25. When modal coupling occurs the

translational displacement caused by predominantly lateral modes and the translational displacement caused by the predominantly torsional modes combine to amplify the response.

In the 1985 NBCC, the accidental term, e_{d2}, was increased solely to compensate for the additional torsional effect caused by modal coupling in elastic symmetric buildings or buildings with small eccentricities. Although not explicitly stated in commentary J of the supplement to NBCC 1985, this is the reasoning given by Tso in Reference 39 and by Heidebrecht and Tso in Reference 43.

Thus, the equations for design eccentricity become:

$$e_d = 1.5e + 0.10D_n \tag{3.26a}$$

or,

$$e_d = 0.5e - 0.10D_n \tag{3.26b}$$

Moreover, NBCC 1985 recognizes that the requirement for doubling the design eccentricity when its value exceeds $0.25D_n$ is overly conservative as reported by Tso and others [39,43] and, therefore, this clause was removed.

The requirements of NBCC 1985 are plotted on Figure 3.7. Although these requirements underestimate the effective eccentricity for aspect ratio D_n/D of 0.5 (or lower), the percentage is not significant [39]. Hence, the requirement of NBCC 1985 are deemed satisfactory and one may conclude that the increase in the accidental eccentricity term compensates adequately the effect of modal coupling.

Comparing the requirements of NBCC 1985 with the line $e_d/\rho = 1.5(e/\rho)$, one sees that the increase in accidental eccentricity has little influence for buildings with moderate or large eccentricity [43].

3.3.2 Brief Summary of Other Codes

Most building codes have equations for design eccentricities similar to the NBCC provisions. The design eccentricity for various building codes are listed below [42]:

NBCC 1980:

$$e_d = 1.5e + 0.05D_n \text{ (if } e_d \leq 0.25D_n) \quad (3.27a)$$

$$e_d = 0.5e - 0.05D_n \quad (3.27b)$$

$$e_d = 2[1.5e + 0.05D_n] \text{ (if } e_d > 0.25D_n) \quad (3.27c)$$

NBCC 1985:

$$e_d = 1.5e + 0.10D_n \quad (3.28a)$$

$$e_d = 0.5e - 0.10D_n \quad (3.28b)$$

USA - ATC3 (1978):

$$e_d = e + 0.05D_n \quad (3.29a)$$

$$e_d = e - 0.05D_n \quad (3.29b)$$

Mexico (1976):

$$e_d = 1.5e + 0.10D_n \quad (3.30a)$$

$$e_d = 0.5e - 0.10D_n \quad (3.30b)$$

New Zealand (1976):

$$e_d = 1.7e - (e^2/D_n) + 0.10D_n \quad (3.31a)$$

$$e_d = e - 0.10D_n \quad (3.31b)$$

Each building code gives two alternative equations (except for NBCC 1980); however, designers are mainly concerned with the first of each since it usually governs the requirements due to eccentricity.

The requirements for these five building codes are shown in Figure 3.7; one can immediately observe that the 1985 Canadian Code and the 1976 Mexican Code provisions closely approximate the requirements of effective eccentricity, while the torsional provisions of ATC3 are clearly inadequate. The provisions of the New Zealand code are generally equivalent to the 1985 NBCC except for large eccentricities ($e^* > 1.2$) (or $e/D_n > 0.4$) where the New Zealand code better approximates the effective eccentricity. As stated earlier, the provisions of NBCC 1980 underestimate the effective eccentricity for $e^* < 0.4$ ($e/D_n < 0.133$) and overestimate the effective eccentricity for $e^* \geq 0.4$ ($e/D_n \geq 0.133$).

In the above equations, the first term generally accounts for the increased effect of eccentricity while the second term accounts for the influence of accidental eccentricity (except in the New Zealand code, where it is the third term in equation 3.31a). For each code, the accidental eccentricity term is given below, firstly as a proportion of the building

dimension D_n and secondly as a proportion of the mass radius of gyration of the structural model used in the present study.

NBCC 1980: $e_{d2} = 0.05D_n$ (3.32a)

$e_{d2} = 0.15\rho$ (3.32b)

NBCC 1985: $e_{d2} = 0.10D_n$ (3.33a)

$e_{d2} = 0.30\rho$ (3.33b)

USA ATC 3 (1978): $e_{d2} = 0.05D_n$ (3.34a)

$e_{d2} = 0.15\rho$ (3.34b)

Mexico (1976): $e_{d2} = 0.10D_n$ (3.35a)

$e_{d2} = 0.30\rho$ (3.35b)

New Zealand: $e_{d2} = 0.10D_n$ (3.36a)

$e_{d2} = 0.30\rho$ (3.36b)

In summary, the accidental eccentricity provisions account for possible increase in torsion caused by uncertainty in relative rigidities, loadings, inelastic actions, and the possibility of torsional ground motion. It does not explicitly account for variation in resistance except as implied by the uncertainty in plastic or inelastic action. The 1985 NBCC provisions for accidental eccentricity have been increased from $0.05D_n$ to $0.10D_n$ to compensate for modal coupling that occurs in buildings which are symmetric or with low eccentricity, and have torsional frequency to lateral frequency ratio close to unity. These requirements adequately satisfy the concept of effective eccentricity for elastic structures.

3.4 PROBABILITIES ASSOCIATED WITH STRENGTH VARIATION λ

This section investigates the probabilities associated with a structure whose seismic resistance consists of two lateral resisting elements with varying strength. If the probability is high that a certain strength variation exists, it will indicate the likelihood that

the effects of strength variation should be considered as a major component of the accidental eccentricity provisions.

In Chapter 2, the causes of strength variation were reviewed and a strength variation parameter λ was derived which corresponds to code provisions associated with limit states design. These code requirements implicitly limit the maximum reduction in strength from the mean strength $\overline{R}$ which can be expected for North American construction practice and an acceptable probability of failure. Thus, the minimum strength was found for a member as $(1 - \lambda)\overline{R}$.

The probability associated with a strength variation λ depends on how the deviation in strength is applied to the structural model. Three cases were investigated.

#1 The resistance of element 1, $R_1 = \overline{R}$

while the resistance of element 2, $R_2 = (1 - \lambda)\overline{R}$

#2 The resistance of element 1, $R_1 = (1 + \lambda/2)\overline{R}$

while the resistance of element 2, $R_2 = (1 - \lambda/2)\overline{R}$

#3 The resistance of element 1, $R_1 = R$

while the resistance of element 2, $R_2 = (1 - \lambda)R$, but $R_1 - R_2 = \lambda\overline{R}$.

In the first case, it is assumed that element 1 has the mean strength $\overline{R}$ and the probability of $R_2 \leq (1 - \lambda)\overline{R}$ occurring can be expressed mathematically as:

$$P_1 = P[R_2 \leq (1 - \lambda)\overline{R}]. \tag{3.37a}$$

By using the cumulative standard normal distribution function $F(\zeta)$ (as shown in section 2.3.2), the probability is expressed as:

$$P_1 = 1 - F(\zeta), \text{ where } \zeta = (\lambda/V_R). \tag{3.37b}$$

Figure 3.8 shows that as λ increases, it is less probable that R_2 has a strength $R_2 \leq (1 - \lambda)\overline{R}$ at a given coefficient of variation V_R.

Note that the assumption of element 1 having strength $R_1 = \overline{R}$ is a severe restriction. In probabilistic terms, R is a random normal variable and although it is

possible that an element has strength $\overline{R}$, the probability of one event in the continuous domain is nil.

The second case was investigated after it was found that for an earthquake severity factor Q = 4.0, effects of plus variation (ie. $R_2 = (1 + \lambda)\overline{R}$) gave almost equal results and were of equal probabilities as in the first case. It was thus presumed that responses of the second case associated with $R_1 = (1 + \lambda/2)\overline{R}$ and $R_2 = (1 - \lambda/2)\overline{R}$ gave similar results. The probability of having such a model can be expressed by:

$$P_2 = P[R_1 \geq (1 + \lambda/2)\overline{R} \text{ and } R_2 \leq (1 - \lambda/2)\overline{R}] \tag{3.38a}$$

$$P_2 = [1 - F(\zeta)]\,[1 - F(\zeta)];\ \zeta = \lambda/(2V_R) \tag{3.38b}$$

Figure 3.9 shows the probability of this model occurring.

However it is unrealistically restrictive to demand that element 1 has a positive strength deviation while element 2 has a negative strength deviation. What is of importance is how likely the deviation in strength between the two lateral resisting elements exceeds $\lambda\overline{R}$, given that each element can be thought of as a random variable with mean $\overline{R}$ and standard deviation σ_R. For it is the difference in strength levels of the elements which causes accidental eccentricity. In other words, case 3 examines the likelihood of the structural model occurring for a real structure and the probability associated with this is derived below.

Let R_1 = a random normal variable with mean $(R_1)_{mean} = \overline{R}$ and standard deviation $\sigma_{R1} = \sigma_R$; and let R_2 = a random normal variable with mean $(R_2)_{mean} = \overline{R}$ and standard deviation $\sigma_{R2} = \sigma_R$.

Furthermore, one can define $Z_R = R_1 - R_2$, then by using equation 2.8 and 2.9,

$$\overline{Z}_R = \overline{R}_1 - \overline{R}_2 = \overline{R} - \overline{R} = 0$$

$$\sigma^2_{ZR} = \sigma_{R1}{}^2 + \sigma_{R2}{}^2 = \sigma_R{}^2 + \sigma_R{}^2 = 2\sigma_R{}^2$$

$$\sigma_{ZR} = \sigma_R\sqrt{2}$$

Thus the difference in strength between element 1 and 2 is also a random variable Z_R with mean $\overline{Z}_R$ and standard deviation $\sigma_{ZR} = \sigma_R\sqrt{2}$. The probability that variable $Z_R \leq \lambda\overline{R}$ is

given by the shaded area in Figure 3.10, that is, $P[(R_1 - R_2) \leq \lambda\bar{R}]$ = the shaded area and $P_3 = P[(R_1 - R_2) \geq \lambda\bar{R}] = 1$ - the shaded area.

Using the standard normal variable ζ:

$$P[(R_1 - R_2) \leq \lambda R] = P[-\infty \leq \zeta \leq \{(\lambda R - Z_R)/\sigma_{ZR}\}] \tag{3.39a}$$

Substituting $Z_R = 0$ and $\sigma_{ZR} = \sigma_R\sqrt{2}$ gives:

$$P[(R_1 - R_2) \leq \lambda R] = P[-\infty \leq \zeta \leq \{(\lambda R - 0)/(\sigma_R\sqrt{2})\}] \tag{3.39b}$$

and therefore,

$$P[(R_1 - R_2) \geq \lambda R] = 1 - P[-\infty \leq \zeta \leq \{(\lambda)/(V_R\sqrt{2})\}]. \tag{3.40a}$$

Hence,

$$P_3 = P[(R_1 - R_2) \geq \lambda R] = 1 - F[\lambda/(V_R\sqrt{2})] \tag{3.40b}$$

where $F(\zeta)$ is the cumulative standard normal distribution function.

The probabilities associated with the structural model are given in Figure 3.11 and for the range of strength variation of importance:

$\lambda = 0.3$, $V_R = 0.16$ and $P_3 = 9.25\%$

$\lambda = 0.4$, $V_R = 0.16$ and $P_3 = 3.86\%$.

$\lambda = 0.3$, $V_R = 0.14$ and $P_3 = 6.49\%$

$\lambda = 0.4$, $V_R = 0.14$ and $P_3 = 2.17\%$.

Therefore, there is considerable probability of encountering a variation in structural strength λ between 0.3 and 0.4.

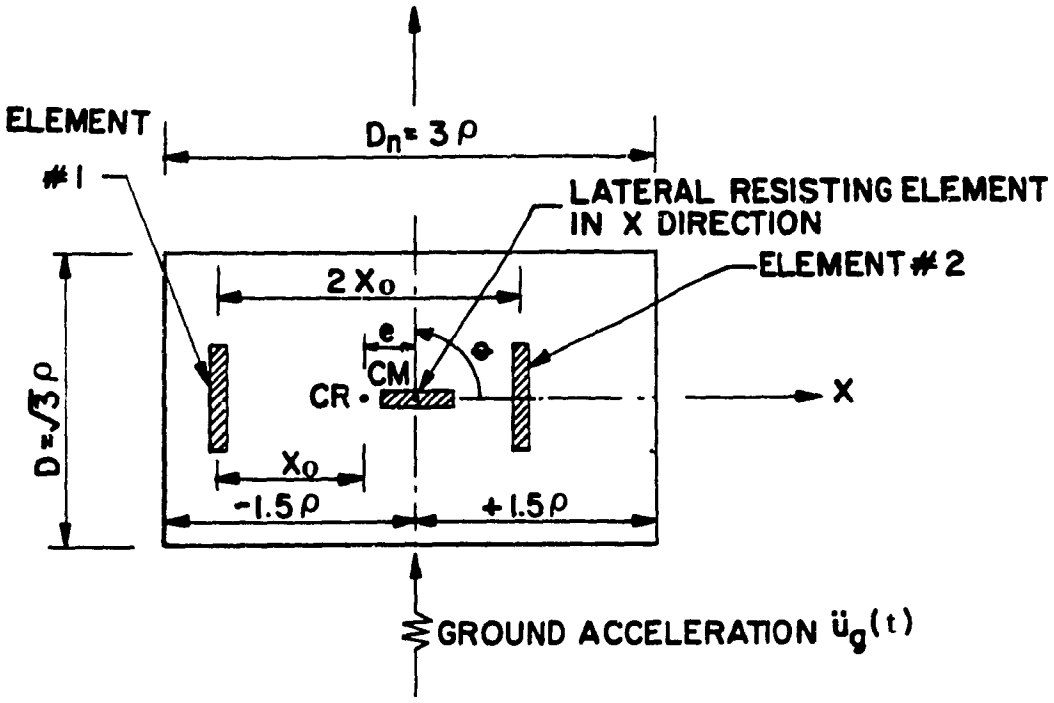

Fig. 3.1 Idealized Model

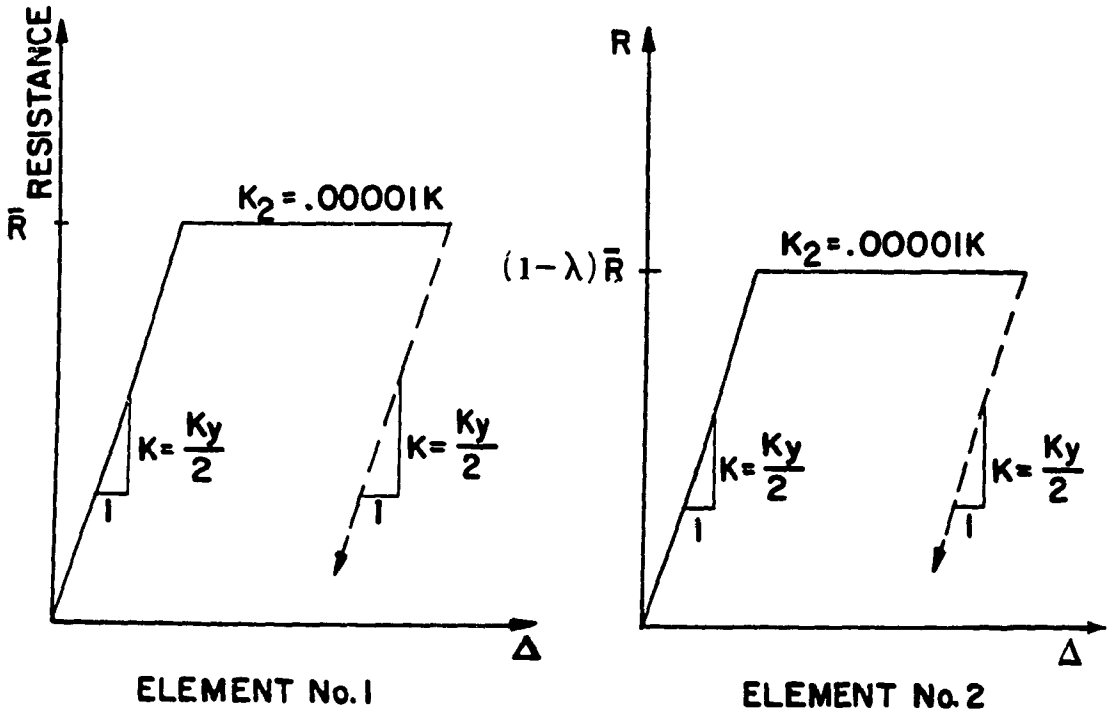

Fig. 3.2 Elastoplastic Hysteresis

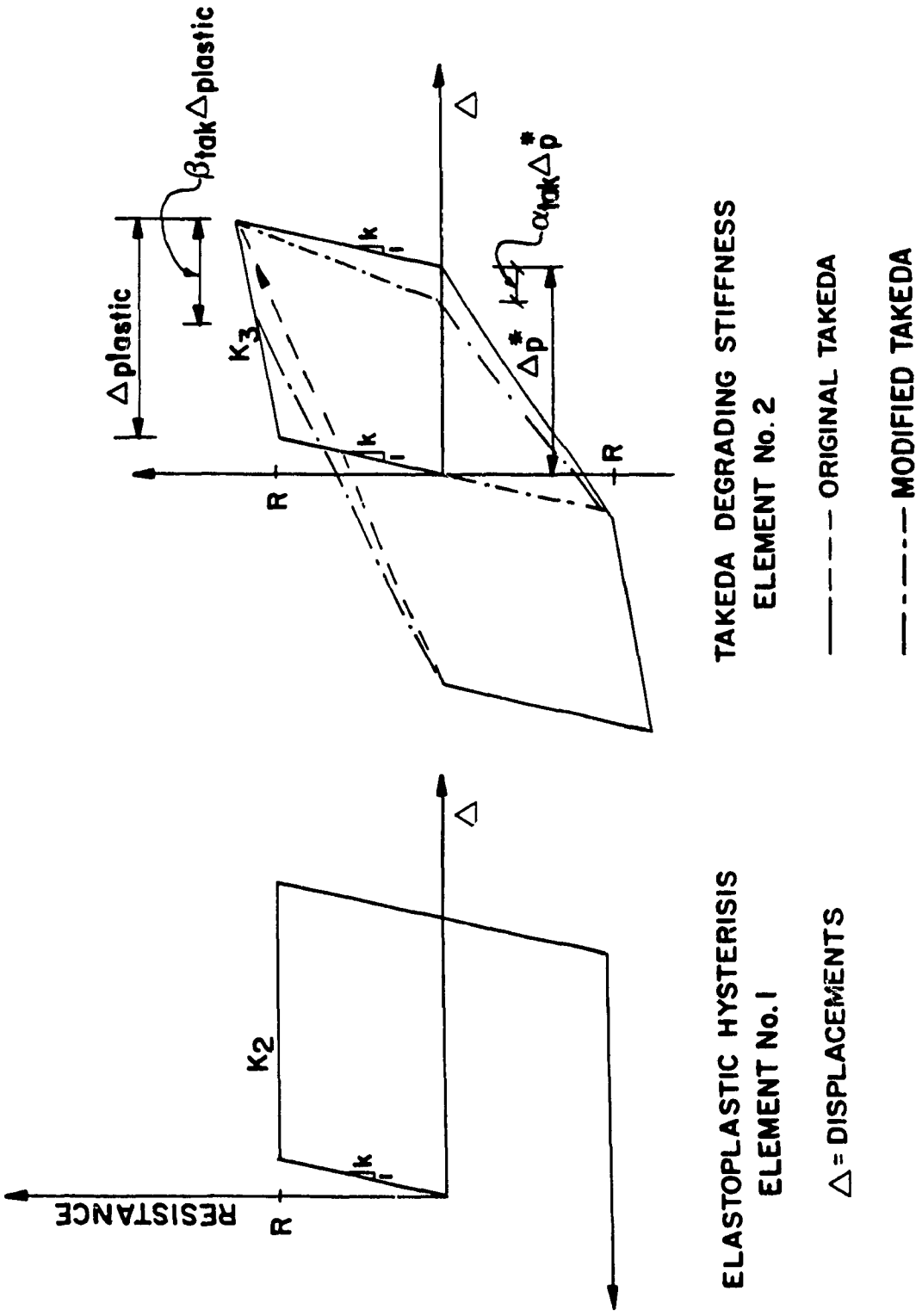

Fig. 3.3 Elastoplastic with Takeda Hysteresis

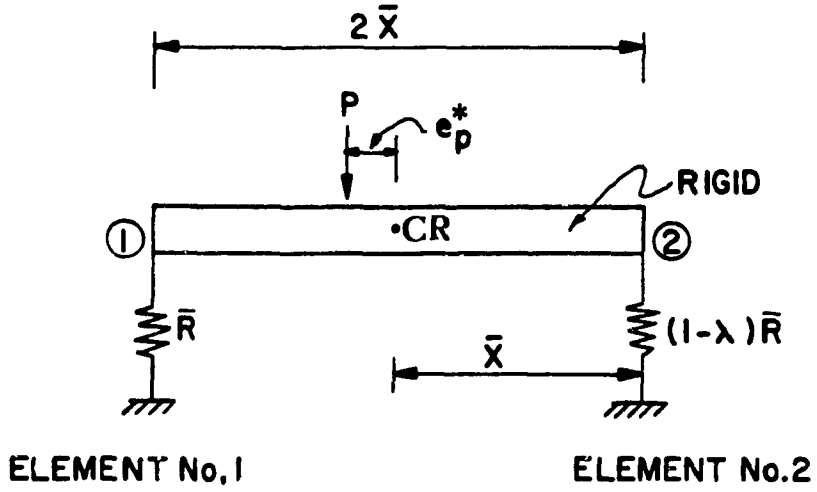

Fig. 3.4 Concept of Plastic Eccentricity

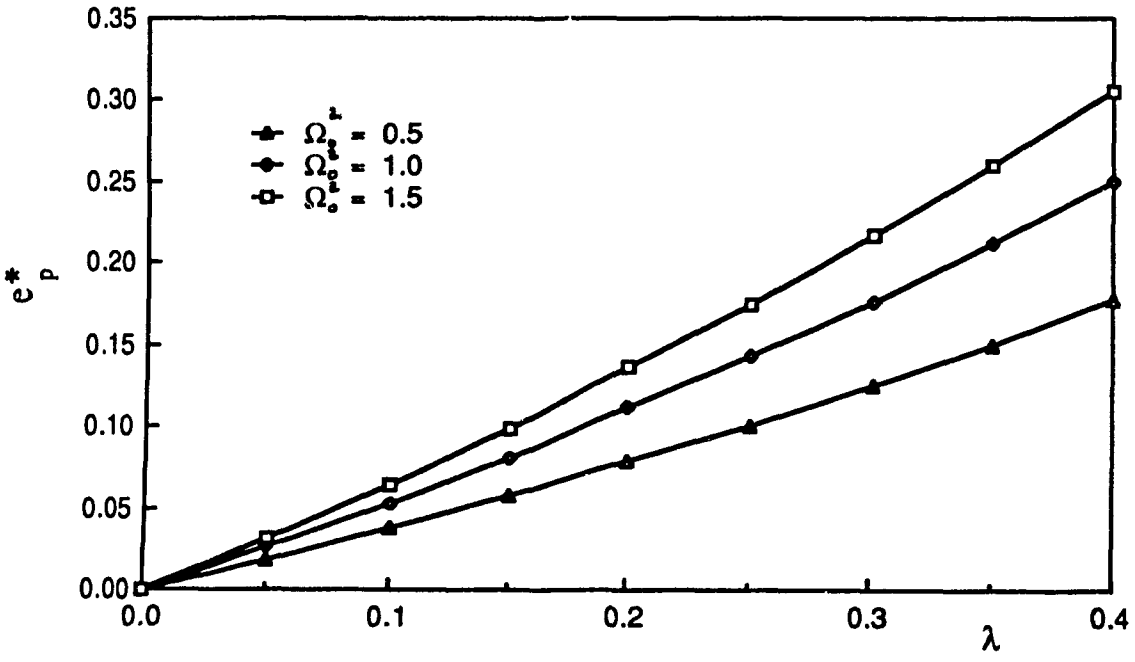

Fig. 3.5 Plastic Eccentricity Versus λ

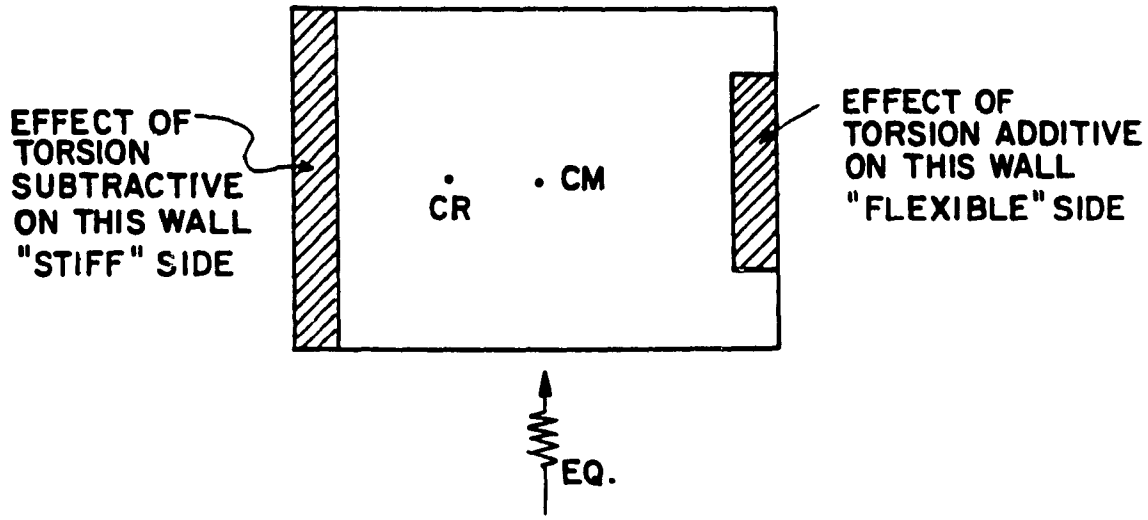

Fig. 3.6 Effect of Torsion on Lateral Resisting Elements.

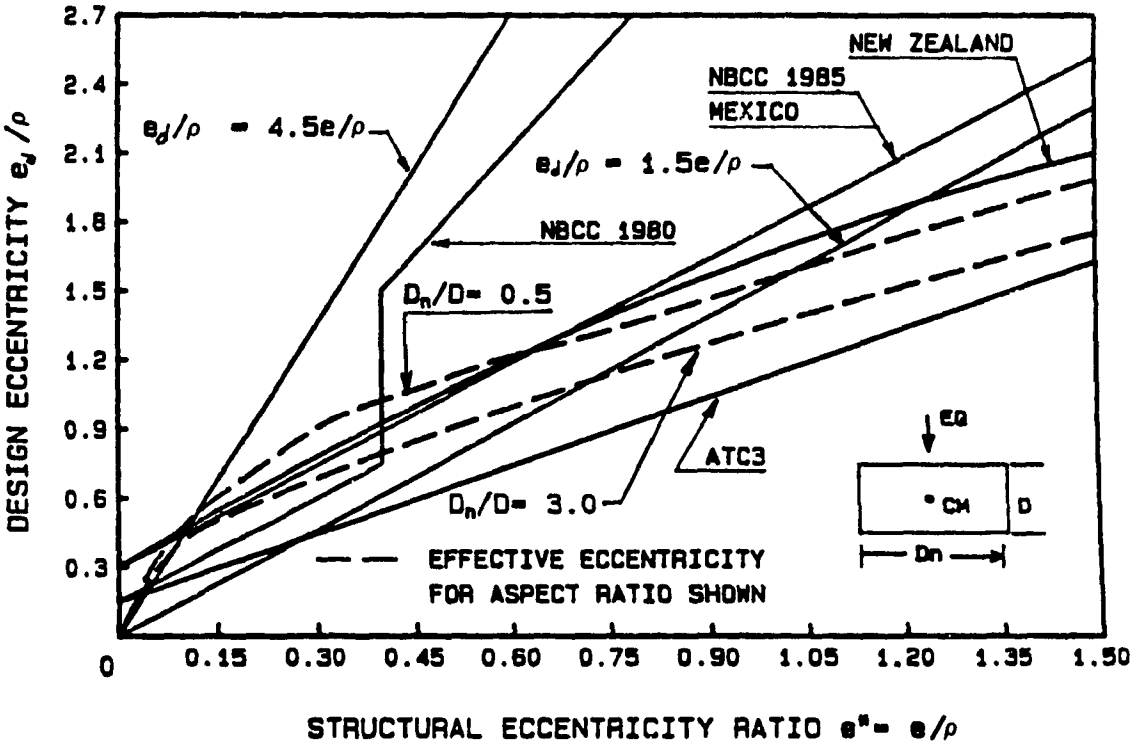

Fig. 3.7. Comparison of Design Eccentricity for Various Codes [derived from 39].

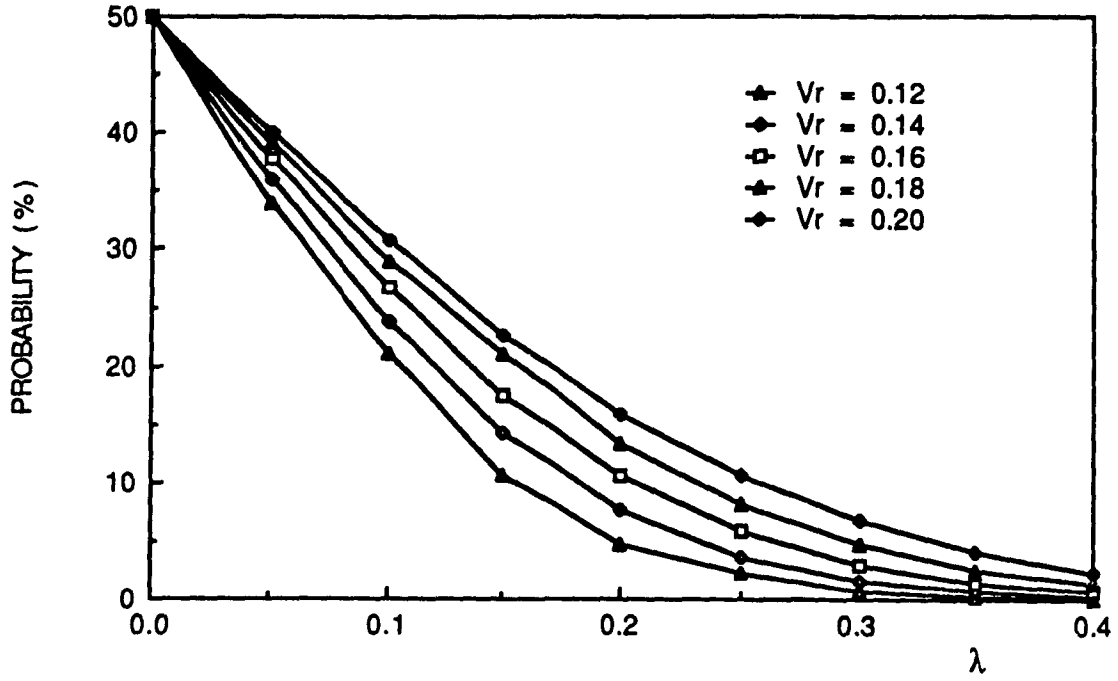

Fig. 3.8. $P_1 = P[R_2 \leq (1 - \lambda)\bar{R}]$.

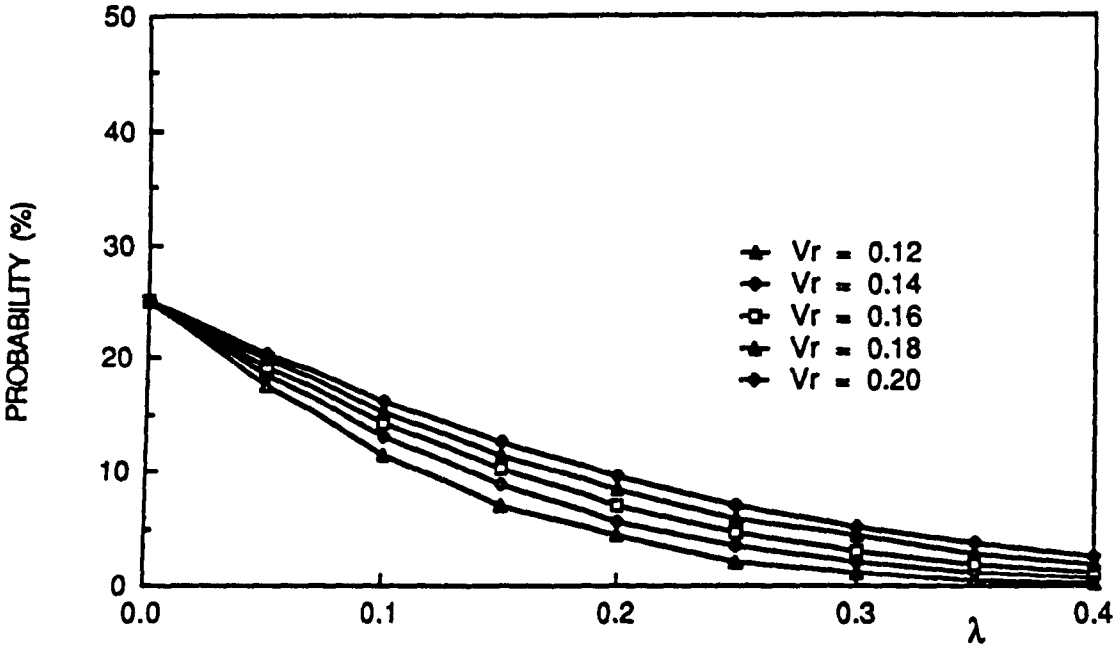

Fig. 3.9. $P_2 = P[R_1 \geq (1 + \lambda/2)\bar{R}$ and $R_2 \leq (1 - \lambda/2)\bar{R}]$.

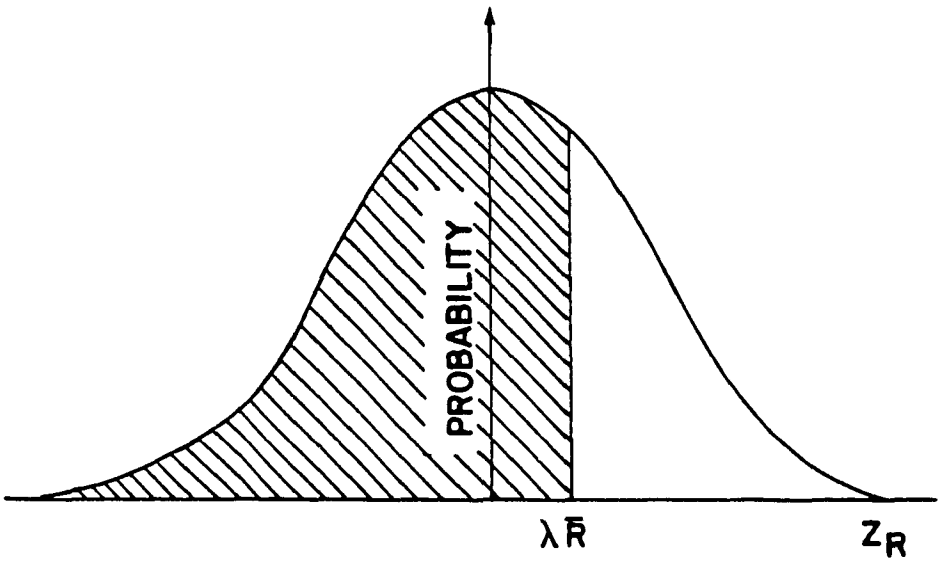

Fig. 3.10. Random Variable $Z_R = R_1 - R_2$.

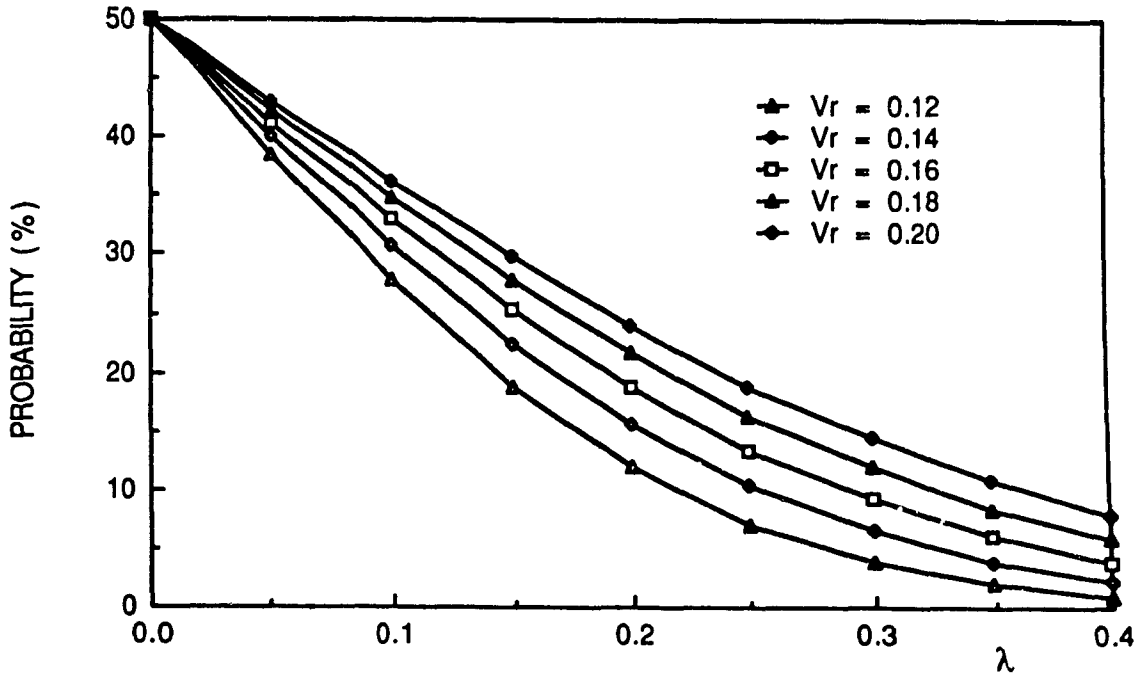

Fig. 3.11. $P_3 = P[R_1 - R_2 \geq \lambda\bar{R}]$.

CHAPTER IV

PARAMETRIC STUDY OF SEISMIC RESPONSE FOR ACCIDENTAL ECCENTRICITY IN BUILDINGS

4.1 INTRODUCTION

Present practice for the aseismic design of buildings requires that designers strive for a structural configuration of mass and elastic stiffness such that the center of mass CM is coincident with the center of rigidity CR. The distance between these two centers is defined as the structural eccentricity e, and when its value is zero, a designer expects the building to respond without torsional motion under seismic loading. However, it has been recognized by several researchers that an ideally symmetric building may have torsional motion due to inelastic action [2] or due to rotational ground motion [42]. This chapter considers accidental eccentricity arising solely from the variation in strength of lateral resisting elements when a structure is subjected to severe ground motion.

The variation in strength is a random process and its effect is to shift the center of resistance when the structure undergoes inelastic deformations. Thus a structure which has no eccentricity in the elastic range of response may possess a plastic eccentricity, e_p, in the inelastic range of response. The accidental eccentricity provisions of the National Building Code of Canada (NBCC) consider these plastic or inelastic actions and also account for the uncertain distribution of mass and stiffness, the possible addition of interior partitions and also the possible torsional ground motion.

In order to ascertain the adequacy of the NBCC specifications, the response of the model described in Chapter 3 consisting of a rigid deck of mass m concentrated at the center of mass CM and supported by two elasto-plastic elements each placed equidistant from the center of resistance CR, is evaluated. Although both lateral resisting elements

have the same elastic stiffness, their plastic strength differs. The first lateral resisting element has a strength:

$$R_1 = \overline{R} = R_{el} / Q \tag{4.1}$$

while the second element has a strength:

$$R_2 = (1 - \lambda)\overline{R} \tag{4.2}$$

where R_{el} is the force of the element for elastic symmetric conditions, Q is the earthquake severity factor and λ is the strength variation parameter.

An earthquake severity factor of Q = 4 is used in the analysis; this ensures inelastic deformation of the lateral resisting elements to a level expected by the NBCC supplement recommendations for response modifications due to plastic behaviour [36]. This reduction is implicit in the pseudo-static provisions of most building codes [36] and therefore allows seismic coefficients which are lower than the elastic spectral accelerations. This is shown in Figure 4.1 where the requirements of NBCC 1980 are compared to a reduced spectral acceleration (x 1/4) of the El Centro 1940 N.S. earthquake. It shows that considerable yielding is expected under seismic loading. The procedure of using an earthquake severity factor is approximately equivalent to those of other investigators [45-49]. It should be emphasized that when Q = 1.0, $e^* = 0$, and $\lambda = 0$, the response is elastic symmetric whereas when Q = 4.0, $e^* = 0$, and $\lambda = 0$ the response is inelastic symmetric. Furthermore, for a single degree of freedom system with perfectly elasto-plastic behaviour the earthquake severity factor equals the structural ductility factor of the NBCC supplement [36], and is similar to the response modification factor of ATC 3 [40].

The second element's strength is varied by using the strength variation parameter, λ, to a level comparable to the statistical permitted deviated strength inherent in the formulation of the Limit States Design Criteria. This level of variation has been found to correspond to a value of λ from 0.3 to 0.4 depending on whether the lateral supporting elements are made of steel or of reinforced concrete acting primarily in bending. Other

values of λ are also used since the lateral supporting elements could be composed of other materials or different structural systems with different levels of ductility.

A value of λ corresponds to a static plastic eccentricity and for this model is given by:

$$e^*_p = \lambda\Omega_o/(2 - \lambda) \tag{4.3}$$

where e^*_p is the plastic eccentricity normalized by the mass radius of gyration about the center of mass ρ.

The model structure was subjected to a parametric study consisting of time history analyses for the first 30 seconds of response with time step of Δt=0.01 second and employing the computer program Drain-2D[16]. The response was evaluated for strength variation parameter λ = 0.1, 0.2, 0.3, 0.35, and 0.4 and five percent damping was assumed for the two response modes. The input parameters consist of three earthquake records, namely: El Centro 1940 NS, Olympia 1949 N80°E, and Taft 1952 N69°W; six uncoupled lateral periods, T = 0.25, 0.50, 0.75, 1.0 ,1.5, and 2.0 seconds; and three uncoupled torsional to lateral frequency ratios, Ω_o^2= 0.5, 1.0, and 1.5.

These were chosen for the following reasons:

1) These earthquakes are often used by other investigators, facilitating comparison.

2) The range of periods (0.25 to 2.0 seconds) covers expected values for most buildings [26] with short periods (T = 0.25 sec.) representing buildings of two or three storeys and long periods (T = 2.0 sec.) representing tall multi-storey buildings.

3) The three torsional to lateral frequency ratios chosen indicate torsionally flexible structures (Ω_o^2 = 0.5), whose main lateral support are at the interior core, to torsionally strong structures (Ω_o^2 = 1.5), which have lateral resistance provided at the perimeter. Particular interest is given to Ω_o^2 = 1.0 since at this torsional to lateral frequency ratio modal coupling drastically increases the response of elastic eccentric structures.

Furthermore, other researchers [39,41] have found that the seismic torque on a building is greatly reduced for $\Omega_0 < 0.75$ and for $\Omega_0 > 1.25$ and consequently this explains the selection of $\Omega_0 = 0.707$ (ie. $\Omega_0^2 = 0.5$) and $\Omega_0 = 1.225$ (ie. $\Omega_0^2 = 1.5$). Note that values of Ω_0 less than 1.0 do not occur often and are expected mainly in central core type structures with no perimeter walls.

For the three earthquakes, six translational periods, and three uncoupled frequency ratios 54 cases are obtained and examined in the form of average (AVG), average plus one standard deviation (AVG + σ) and extreme values (EXTREME), where σ denotes the standard deviation. Note that the extreme value is not an average but an unlikely upperbound. In addition the results were normalized with respect to the response associated with $\lambda = 0$ and specified eccentricity $e^* = 0.0, 0.15, 0.30$. An eccentricity $e^* = 0.0$ corresponds to no eccentricity, that of $e^* = 0.15$ represents the accidental eccentric provisions of NBCC 1980 ($e = 0.05D_n$) and a value of $e^* = 0.30$ denotes the accidental eccentric provisions of NBCC 1985 ($e = 0.10\ D_n$).

To ascertain the importance of the post-elastic behaviour of lateral resisting elements the structural model was further analyzed with the first element having elasto-plastic hysteresis and the second element possessing the Takeda degrading stiffness for an earthquake severity factor $Q = 4.0$.

The responses are investigated to observe the influence of strength variation, period, and frequency ratio and their importance with respect to the accidental eccentricity provisions of the code.

4.2 EFFECT OF ACCIDENTAL ECCENTRICITY ON MAXIMUM DISPLACEMENT FOR ELASTOPLASTIC LATERAL RESISTING SYSTEMS

This section considers the influence of the variation in strength of lateral resisting elements on the response of structures when subjected to severe earthquake excitation (Q = 4.0). The increase in response is compared with the inelastic symmetric response (for e^* = 0.0) and with the inelastic responses at the specified eccentricity ratios e^* = 0.15 and e^* = 0.30 corresponding to the accidental eccentricity code levels of $0.05D_n$ for NBCC 1980 [17] and $0.10D_n$ for NBCC 1985 [1] respectively.

The variation in strength is deemed to cause a direct contribution to accidental eccentricity, and other factors such as stiffness variation and rotational ground motion are not considered. The range of interest for the statistical variation of strength was found in Chapter 2 as lying between $\lambda = 0.3$ and $\lambda = 0.4$.

In particular, this study investigates the maximum edge displacement which is known to have the greatest nonstructural damage potential [48]. This is because it has been shown that displacements at the center of mass and center of rigidity are rather insensitive to eccentricity [46,48], and moreover, since accidental eccentricities are relatively small, their effect is not significant on the displacements of CM and CR.

The analyses found that the maximum lateral displacement occurs at one of the structure's edges, usually but not always, the weaker side (68.5% of the responses) of the model located at $x = +1.5\rho$; this confirms the report of another investigator [46].

4.2.1 Increase in Response from Variation in Strength.

Figures 4.2 , 4.3, and 4.4 show the effect of strength variation parameter λ on the inelastic maximum edge displacement when normalized by the maximum edge displacement for the corresponding structure with $\lambda = 0.0$ and $e^* = 0.0$, 0.15, or 0.30

respectively. This normalization was adopted since it permits evaluation of the adequacy of the code minimum torsional requirements.

The measure for design level response is taken as the (AVG + σ) response and Figure 4.2 shows that the expected statistical maximum variation in strength (λ = 0.4) induces approximately 88 percent increase in response over that of the symmetric behavior. Another aspect noticeable from Figure 4.2 is that strength variation increases the edge displacement response since all the curves show ordinate values greater than unity for λ greater than zero. Furthermore as λ increases the normalized response increases.

Although the curve for extreme value gives an increase in extreme edge displacement of 158 percent (at λ = 0.4) over the symmetric response, this represents an unlikely upperbound. It is therefore not surprising that they fall well above responses associated with the NBCC 1980 code and the NBCC 1985 code requirements as shown in Figure 4.3 and Figure 4.4 respectively. Note that the code requirements are considered satisfied when responses fall below the ordinate value of one; thus in Figure 4.3 a variation of as little as 12 percent gives (AVG + σ) responses equivalent to the accidental eccentricity provisions of the NBCC 1980 code.

An unexpected result shown in Figure 4.3 and Figure 4.4 is that the extreme value at λ = 0 is greater than 1.0, specifically 1.06 in Figure 4.3 and 1.05 in Figure 4.4. This can be explained by the fact that the normalizing eccentricity is small and the time history of actual responses do not correspond to smooth spectra. Even though the shift in fundamental lateral frequency is small it may happen, as it did in this study, that the eccentric response is marginally smaller than the symmetric response; thereby causing the extreme value to be marginally greater than unity.

For the particular range of interest of λ between 0.3 and 0.4, Figure 4.3 shows that the normalized response (AVG + σ) has values from 118% to 136% greater than the NBCC 1980 code provisions of $e^* = 0.15$ (or $e = 0.05D_n$). This indicates that the

accidental eccentric torsion provisions of NBCC 1980 underestimate the edge displacement due to possible variation in strength of materials.

Figure 4.4 reveals that the NBCC 1985 code provisions are met and for a variation in strength $\lambda = 0.3$ the (AVG + σ) response is 95% of the eccentric response ($e^* = 0.3$) whereas for $\lambda = 0.4$ the (AVG + σ) response is 106% of the eccentric response ; thus the proposed (AVG + σ) level of response correlates well with the magnitude of response associated with the NBCC 1985 code eccentricity.

Figure 4.5 summarizes the evaluation of the adequacy of the code provisions and shows that $e^* = 0.15$ of NBCC 1980 adequately represents the torsional effect of strength variation for λ up to 0.12, but underestimates the response by 36 percent for $\lambda = 0.4$. On the other hand, $e^* = 0.30$ predicts normalized responses less than 1.06 for the entire range of λ. Thus, the NBCC 1985 accidental eccentricity provision $e_{d2} = 0.10D_n$ appears to represent well the effective eccentricity required to account for a wide range of unintended variation of lateral element strength.

A similar observation is indicated by Figure 4.6, presented this time in terms of accidental plastic eccentricity e^*_p. This form of denoting strength variation within a structural system is more general in that this parameter can be evaluated for a multi-element system, whereas λ is limited to the two element model of Figure 2.11. Furthermore Figure 4.6 shows that a plastic eccentricity equivalent to 10 percent of the plan dimension of a structure ($e^*_p = 0.30$) results in (AVG + σ) responses 205 percent greater than the symmetric response, therefore the potential for non structural damage at a building's edge can be severe.

Moreover, Figure 4.6 shows that the 1980 NBCC provision $e_{d2} = 0.05D_n$ is adequate for $e^*_p \leq 0.06$, and that the 1985 NBCC provision $e_{d2} = 0.10D_n$ adequately accounts for the effect of accidental plastic eccentricity over the range $0 \leq e^*_p \leq 0.20$.

4.2.2 Influence of the Frequency Ratio

The frequency ratio Ω_o^2 is a parameter that represents the relative torsional stiffness of a structure and has been shown in a previous study [50] of elastic structures to affect the coupled lateral-torsional response when the eccentricity is small. For the inelastic response of this study, Figure 4.7 and Figure 4.8 indicate slight dependence on Ω_o^2 when compared to the inelastic symmetric response.

However, when examining the adequacy of the NBCC 1980 code accidental eccentricity provisions in Figure 4.9 and NBCC 1985 accidental eccentricity requirements in Figure 4.10 one notes that Ω_o^2 also remains unimportant, except for torsionally flexible structures. In particular these figures reveal that there is greater amplification of eccentric response over that of the symmetric response for torsionally flexible structures (Ω_o^2 = 0.5).

A similar amplification occurs when the model is subjected to a static load applied at the center of mass. It is therefore not surprising that amplification exists for the dynamic inelastic case. Figure 4.11 shows this and gives the flexible edge displacement normalized by the symmetric displacement under a given static load. The normalized displacement at CM and at the edge obey the following equations:

$$\frac{u_{CM}}{u_{symm}} = 1 + \frac{(e^*)^2[1 + (e^*)^2]}{\Omega_o^2} \tag{4.4}$$

and

$$\frac{u_{@1.5\rho}}{u_{symm}} = 1 + \frac{(e^*)^2[1 + (e^*)^2]}{\Omega_o^2} + \frac{1.5e^*[1 + (e^*)^2]}{\Omega_o^2} \tag{4.5}$$

Note that the static response is an inverse square function of Ω_0 so that the normalized response is very susceptible for Ω_0 much smaller than one. It should also be noted that the curves of Figures 4.7, 4.8, 4.9, and 4.10 are for the (AVG + σ) responses of 18 values corresponding to the three earthquakes and six periods used in the analyses.

4.2.3 Influence of Period

Investigators [46] have found that the dynamic elastic response to earthquake input motion, when normalized by the center of mass displacement, has weak dependence on the translational periods and explain this by a shift in the natural frequencies induced by the eccentricity. It can easily be observed that the spectra of earthquake ground motions is not smooth and would give different spectral displacements if the natural period shifts slightly.

The weak dependence on translation periods for elastic systems can be expected since the normalized response with respect to the symmetric response of an eccentric system to static load placed at the center of mass does not depend on the translational period as can be seen from equations 3.4 and 3.5. In these equations, the normalized displacement of an eccentric system to static load is dependent only on eccentricity and the torsional to lateral frequency ratio of the system.

However, this study has found pronounced variation in normalized response for inelastic systems depending on the period considered. This is indicated in Figures 4.12, 4.13, and 4.14 which are plots of the (AVG + σ) responses of nine values normalized by the responses associated to $\lambda = 0.0$ and to $e^* = 0.0$, 0.15, and 0.30 respectively. The nine values correspond to the three earthquakes and three torsional to lateral frequency ratio used in the analyses. An examination of the statistical response curves as a function of individual lateral period of vibration T discloses no consistent trend but were included for completeness.

When grouping the six periods into the following three categories the influence of lateral period T is more readily identified: short periods for T = 0.25 and 0.50 second; intermediate period for T = 0.75 and 1.0 seconds; and long period for T = 1.5 and 2.0 seconds. Since each category is a group of two periods, the responses associated with Figures 4.15, 4.16, and 4.17 correspond to the (AVG + σ) response of 18 analyses. Also shown are the extreme responses.

Figure 4.15 shows that long period structures experience greater amplification of response over the symmetric response due to accidental eccentricity. Moreover this figure reveals that for any period, the response increases as λ increases. This is expected since an increase in λ can be considered an increase in accidental eccentricity and it is known that response increases with increasing eccentricity [46].

Figure 4.16 and Figure 4.17 indicate that compared to response associated with minimum code accidental eccentricity, the lateral period of vibration T is not a critical parameter.

Figures 4.18, 4.19, and 4.20 give the normalized response with respect to e^* = 0.0, 0.15 and 0.30 respectively versus period at a given strength variation λ = 0.3. These figures show plots of the average (AVG), the average plus one standard deviation (AVG + σ), and the extreme response for the nine time history analyses performed (corresponding to three earthquakes and three Ω_0). Again one sees large variation in response depending on period. No discernable pattern is apparent and these figures reveal little new about the normalized response except that the mean plus one standard deviation is closer to the extreme values when compared to the other figures, which implies that for a given period and strength variation, the normalized response varies more with earthquakes and frequency ratio.

4.3 EFFECT OF ACCIDENTAL ECCENTRICITY ON MAXIMUM DISPLACEMENT FOR LATERAL RESISTING SYSTEMS OF DIFFERENT HYSTERESIS BEHAVIOUR.

This section investigates the effect of having a structure with two lateral resisting elements with different hysteresis characteristics when subjected to severe ground motion. Element No. 1 has strength $R_1 = R_{el}/Q$ and possesses an elastoplastic hysteresis while element No. 2 has a strength $R_2 = R_{el}/Q$ but the Takeda degrading stiffness as described in Section 2.4.

Such a structure, for example, represents a building whose lateral resistance consist of a concrete shear wall and steel moment resisting frames. Concrete flexural members exhibit degrading stiffness when subjected to severe cyclic loading, whereas properly detailed class 1 and class 2 steel beams retain their elasto-plastic characteristics.

The hysteresis loop is a measure of the energy absorption and with two different elements, the seismic energy input is absorbed more by the elasto-plastic element than by the Takeda degrading element, apart from being dissipitated through damping.

Whereas the structure has symmetric responses in the elastic range, this study found considerable torsional response under seismic ground motion with an earthquake severity factor Q = 4 due to the different level of energy absorption of the two lateral resisting elements.

Figure 4.21 gives the normalized response with respect to $e^* = 0.0$, $e^* = 0.15$, and $e^* = 0.30$ for the average plus one standard deviation (AVG + σ) of nine values corresponding to the three torsional to lateral frequency ratios and the three earthquakes used in the analysis versus the period as the abscissa.

Normalization with respect to the inelastic symmetric response ($e^* = 0$) reveals that structures with different hysteresis characteristics have responses considerably larger. Figure 4.22 shows the normalized response with respect to $e^* = 0.0$ and gives the average

(AVG), the average plus one standard deviation (AVG + σ) and the extreme responses. It also shows that the responses exceed the purely symmetric responses for all periods.

The influence of period again does not show any discernable trend and an extreme response of 213.6% greater than the symmetric response was found for a period of T = 1.5 seconds.

Figure 4.23 shows normalized responses with respect to e* = 0.15 and reveals the inadequacy of the NBCC 1980 accidental torsion provisions since normalized responses at the (AVG + σ) level are approximately 1.25.

Figure 4.24 shows normalized responses with respect to e* = 0.30 and shows the adequacy of the NBCC 1985 accidental torsional provisions to cope with structures possessing lateral resisting elements of different hysteresis characteristics.

Figures 4.25, 4.26 and 4.27 give the normalized responses with respect to e* = 0.0, 0.15 and 0.30 respectively versus period and values represent the average of three earthquakes. Plots are given for Ω_o^2 = 0.5, 1.0 and 1.5. These figures reveal that response is not strongly dependent on the torsional to lateral frequency ratio except in the range of period 0.75 to 1.25 seconds. Moreover, in this range of period, torsionally weak structures (Ω_o^2 = 0.5) are more susceptible to an amplification of response due to different hysteretic behavior than are torsionally strong structures (Ω_o^2 = 1.5).

4.4 SUMMARY

Based on the results presented in this chapter, the variation in the strength of lateral load resisting elements may result in considerable accidental torsion. Compared to symmetric response, this may result in sizeable amplification factors for maximum edge displacement. For a structure relying on two lateral load resisting elements a strength variation given by λ = 0.40 in one of the elements induces an increase in response which at the (AVG + σ) level translate as an amplification factor of 1.88. Furthermore the

parametric study has indicated that torsionally flexible structures are more susceptible to the effects of accidental eccentricity.

In terms of the adequacy of code accidental eccentricity provisions for multi-element systems, minimum eccentricity of $0.05D_n$ becomes inadequate when the static plastic eccentricity $e_p \geq 0.06\rho$, whereas $0.10D_n$ is able to account for $e_p \leq 0.20\rho$ (where ρ is the mass radius of gyration).

In addition to variation in strength, the difference in type of hysteresis behavior of lateral resisting elements may also introduce accidental eccentricity. The NBCC 1980 torsional provisions for accidental eccentricity were again found inadequate in this case, whereas the requirements of the NBCC 1985 code were satisfactory. Furthermore, it was found that these structures are susceptible to increase in edge displacement when torsionally flexible and when their lateral period is in the range of 0.75 to 1.25 seconds.

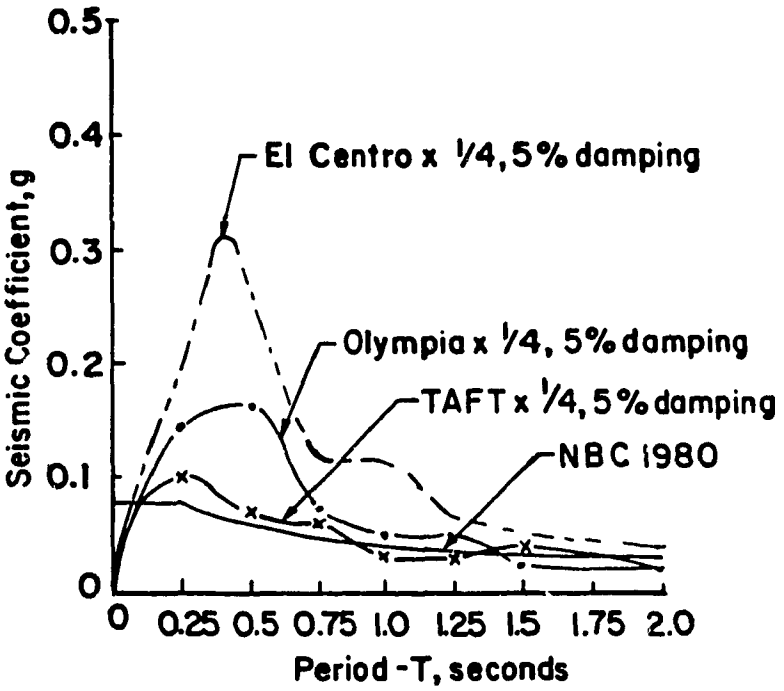

Fig. 4.1 Comparison of NBC Seismic Coefficient with Response Spectra of El Centro 1940 N.S. Earthquake, Olympia 1949 N80°E, and Taft 1952 N69°W

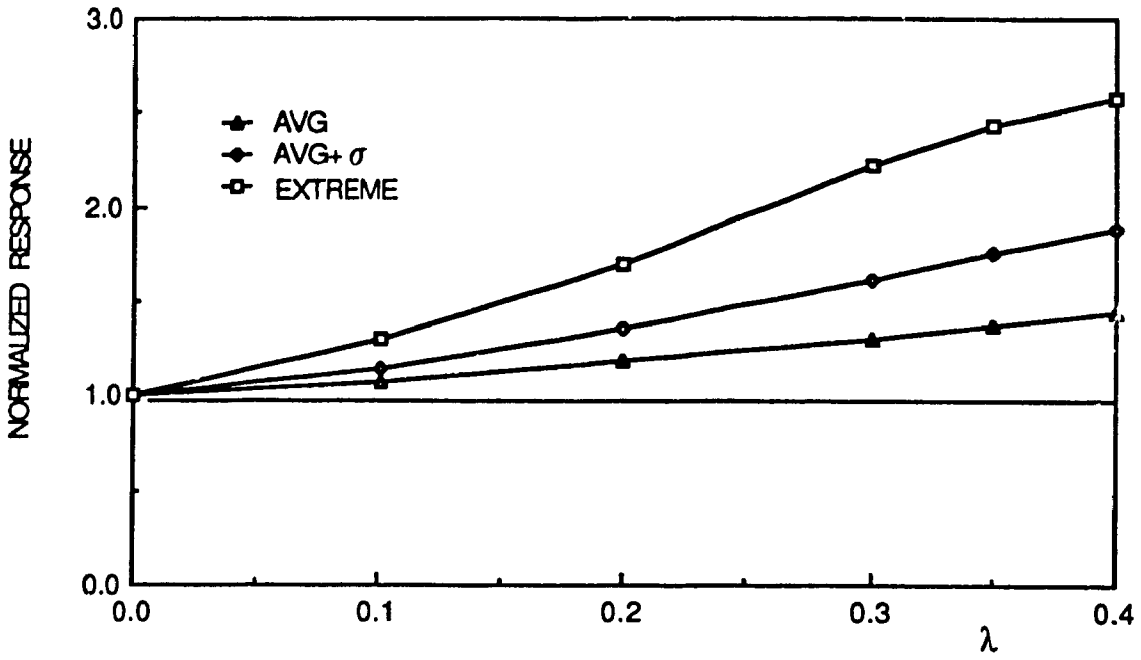

Fig. 4.2 Normalized Response With Respect to e* = 0.0 Versus λ (using 54 values).

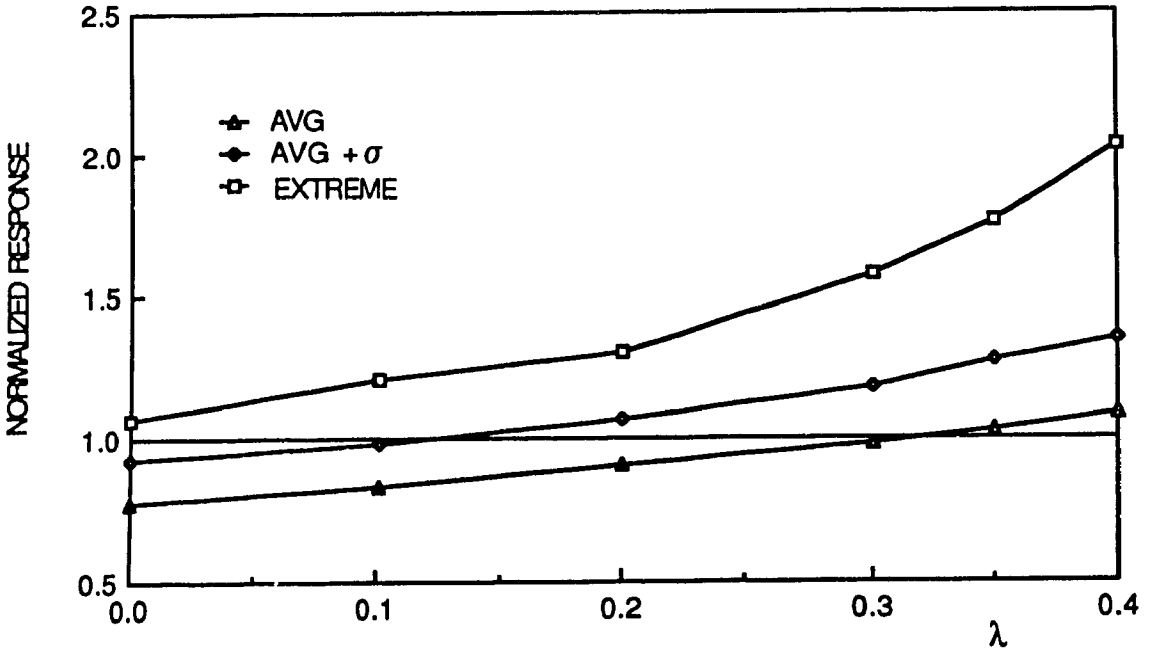

Fig. 4.3 Normalized Response With Respect to e* = 0.15 Versus λ (using 54 values).

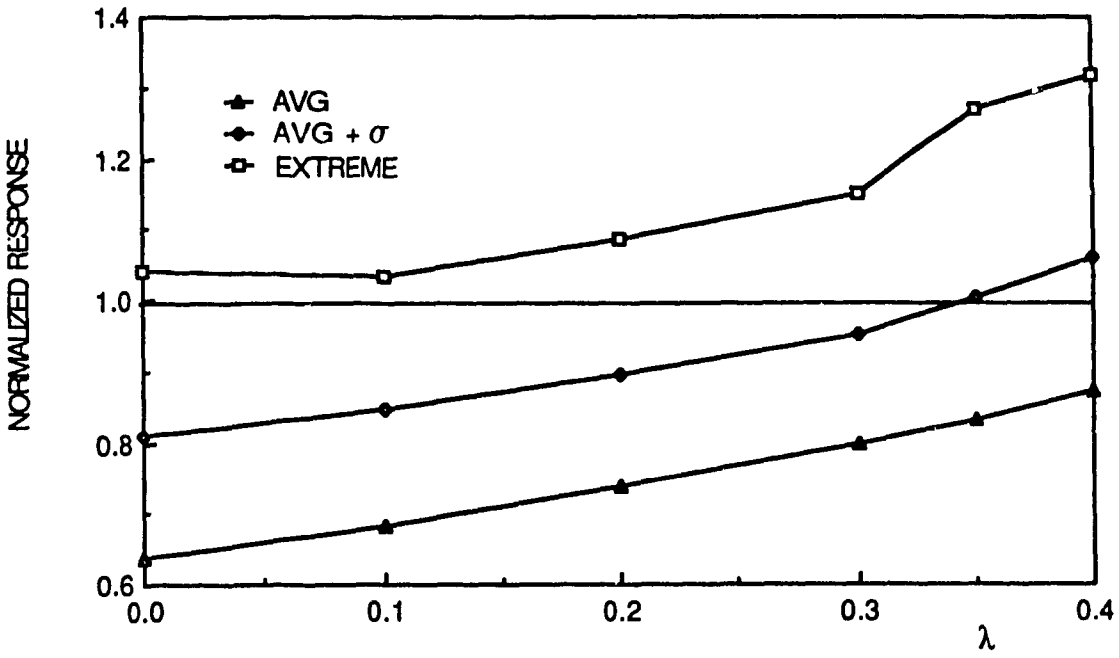

Fig. 4.4 Normalized Response With Respect to $e^* = 0.30$ Versus λ (using 54 values).

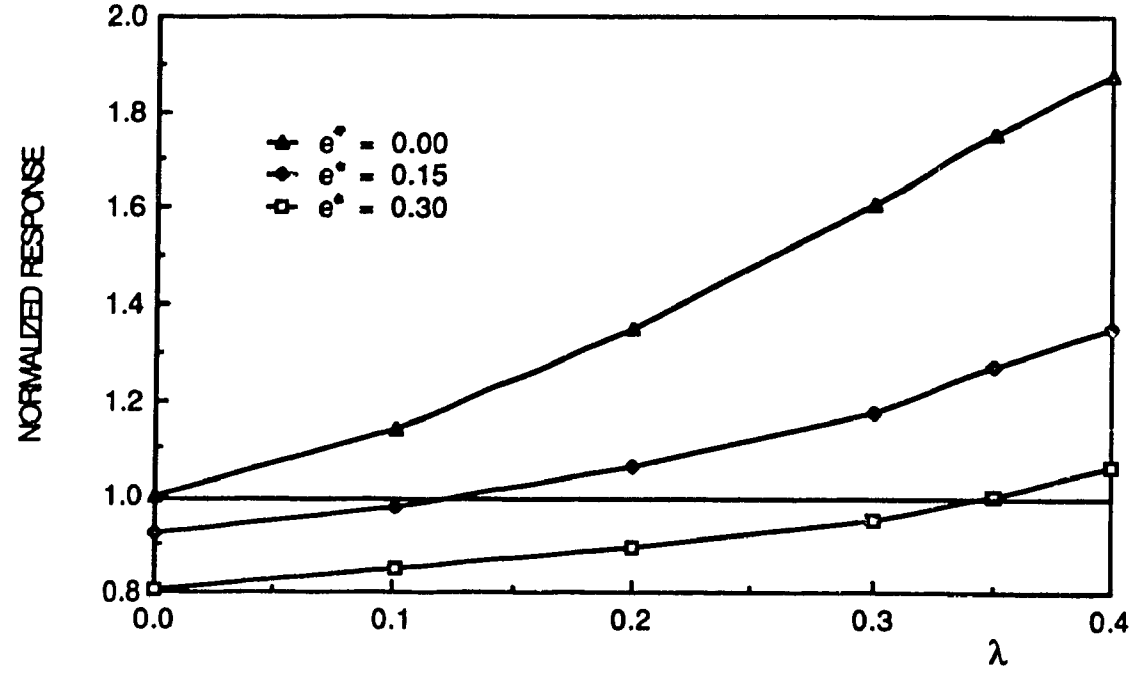

Fig. 4.5 Comparison of Normalized Response (AVG + 1σ) e* = 0.0, 0.15, 0.30.

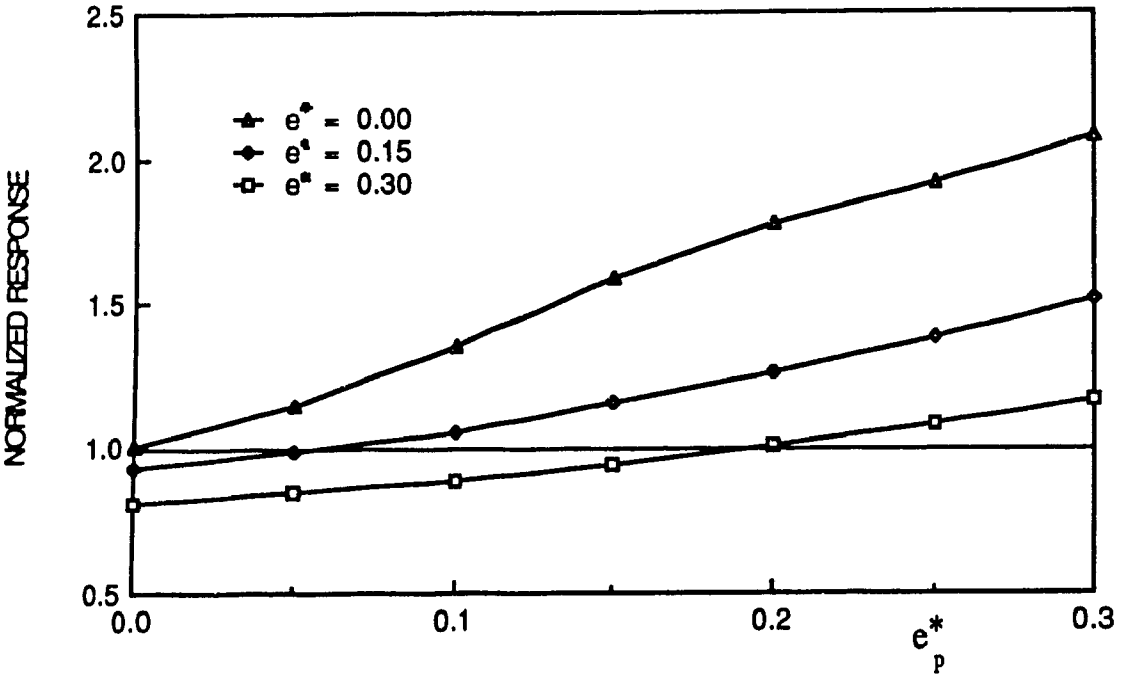

Fig. 4.6 Normalized Response Versus e^*_p.

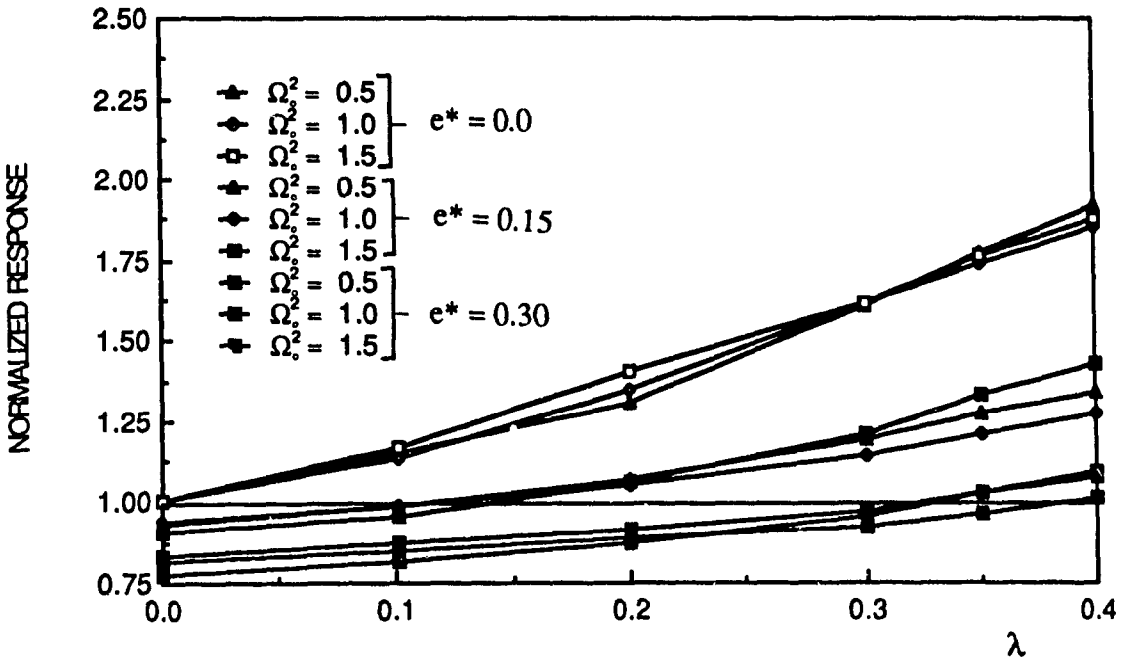

Fig. 4.7 Comparison of Normalized Response (AVG+σ) for Different Frequency Ratios (using 18 values).

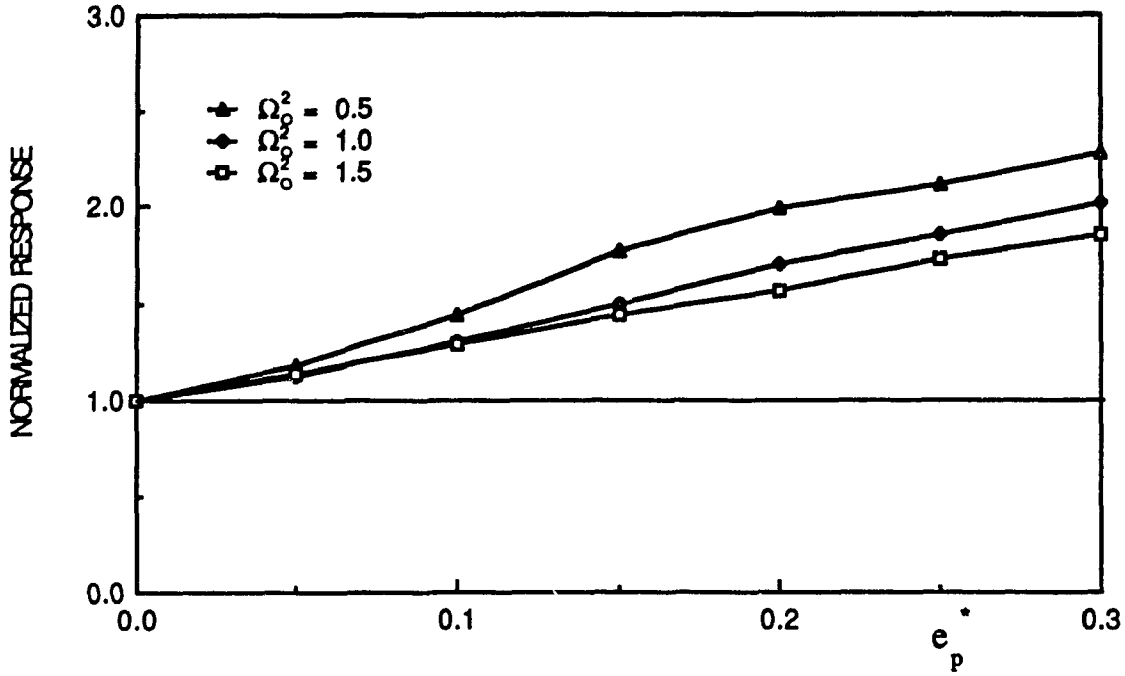

Fig. 4.8 Normalized Response (e* = 0.0) vs Plastic Eccentricity for Various Frequency Ratios (using 18 values).

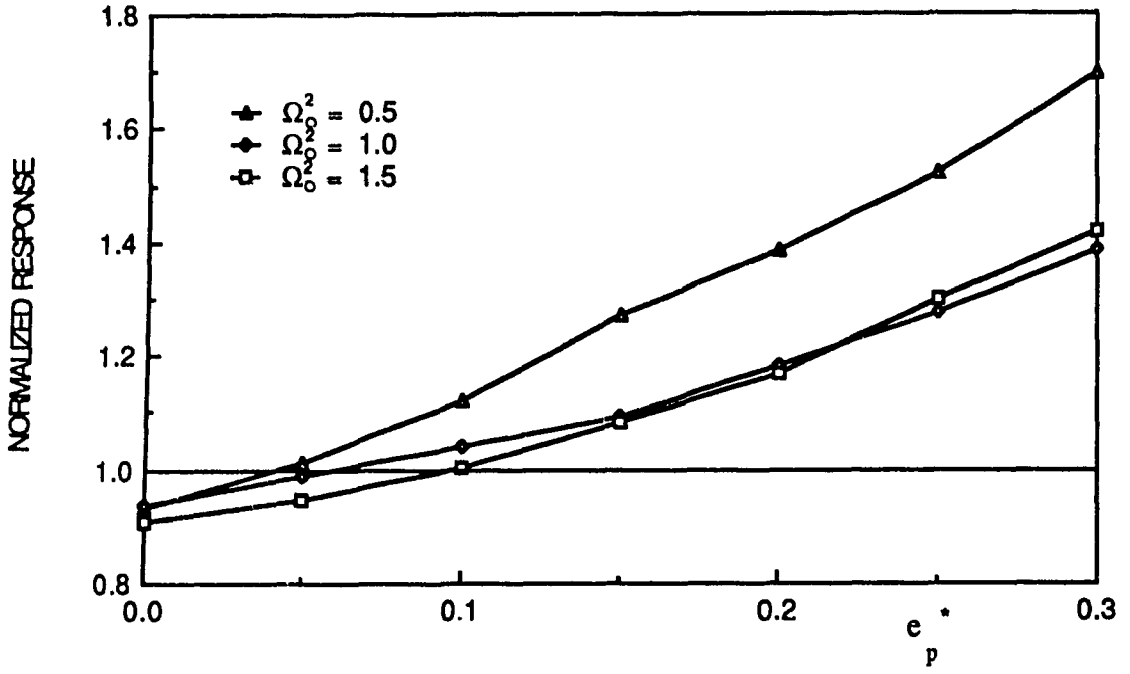

Fig. 4.9 Normalized Response (e* = 0.15) vs Plastic Eccentricity for Various Frequency Ratios (using 18 values).

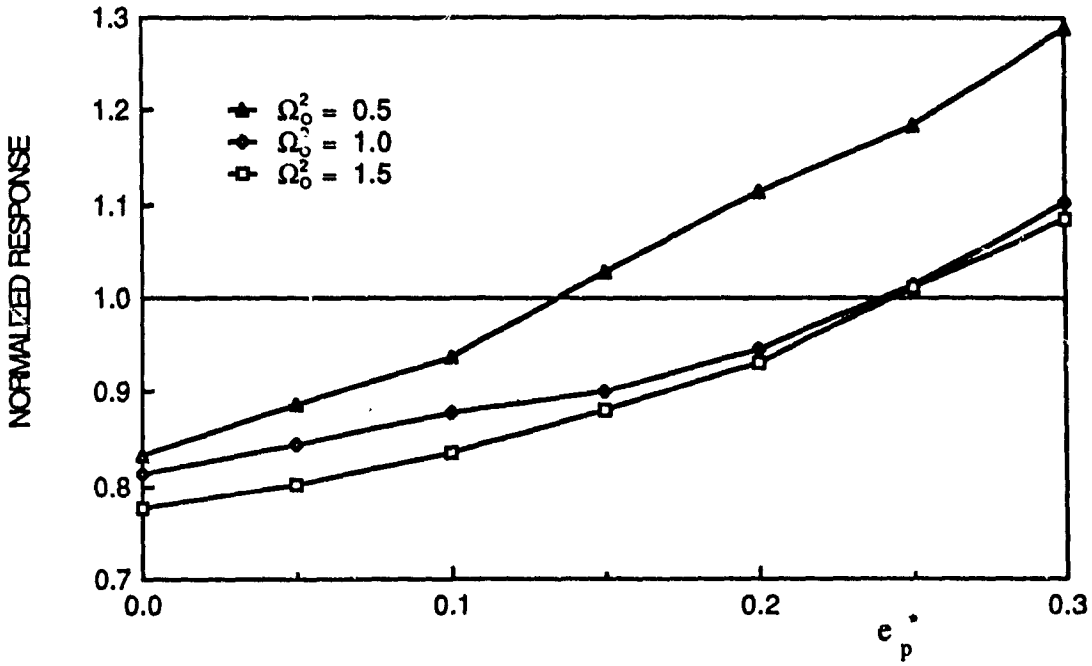

Fig. 4.10 Normalized Response (e* = 0.30) vs Plastic Eccentricity for Various Frequency Ratios (using 18 values).

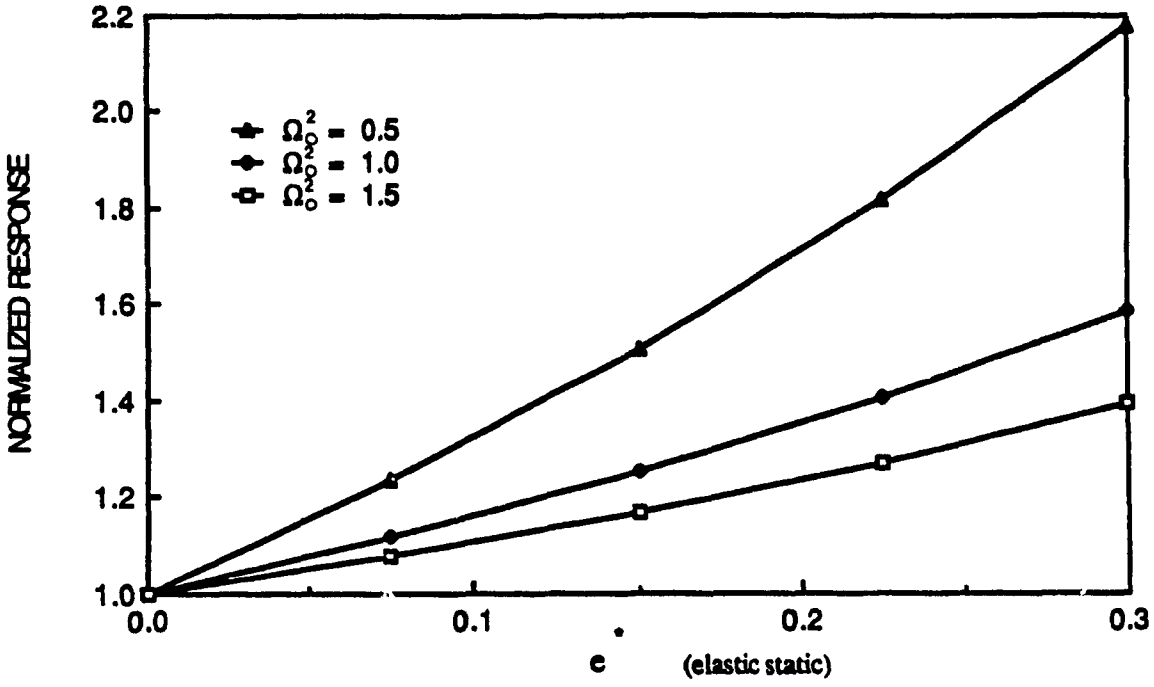

Fig. 4.11 Normalized Static Edge Displacements vs Eccentricity.

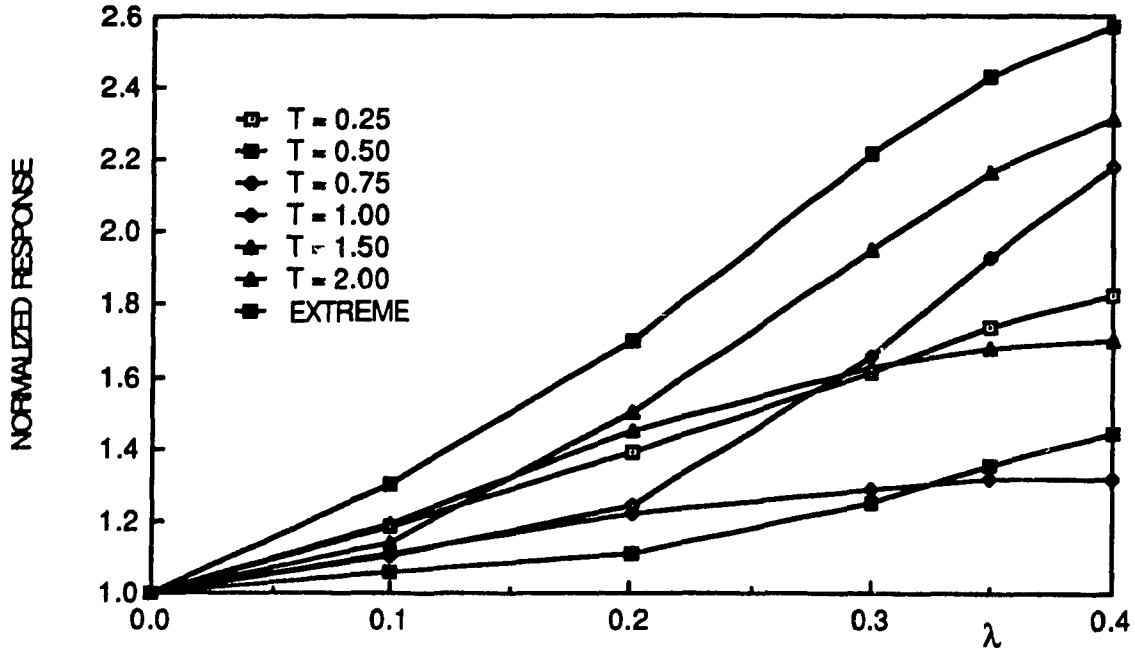

Fig. 4.12 Normalization With Respect to e* = 0.0 vs λ (using 9 values).

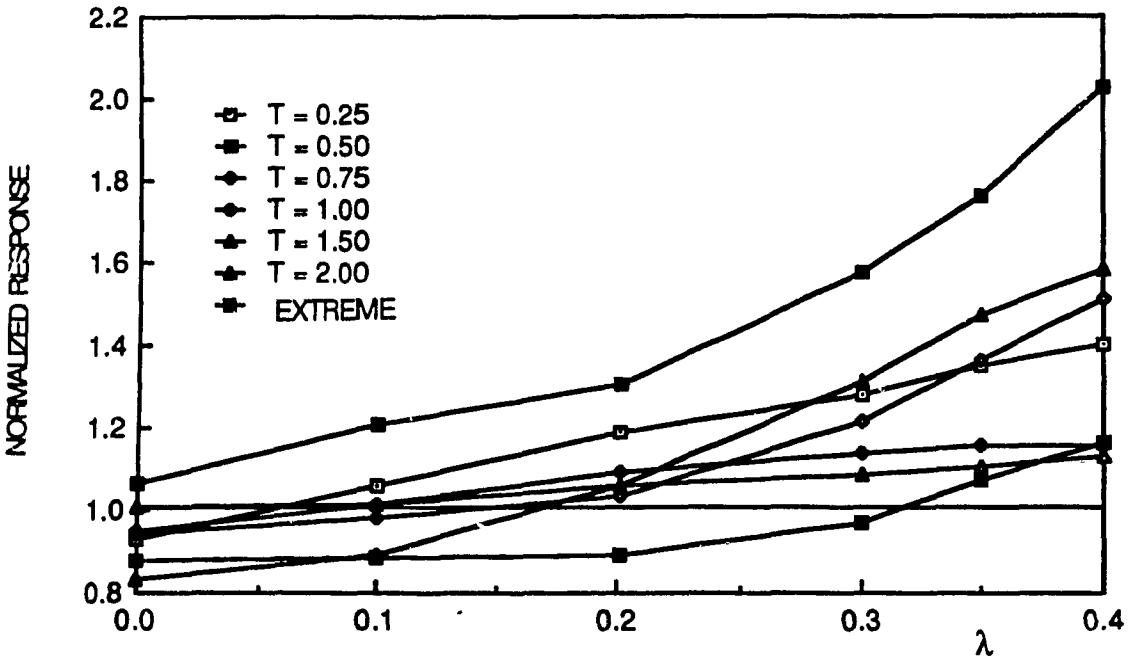

Fig. 4.13 Normalization With Respect to e* = 0.15 vs λ (using 9 values).

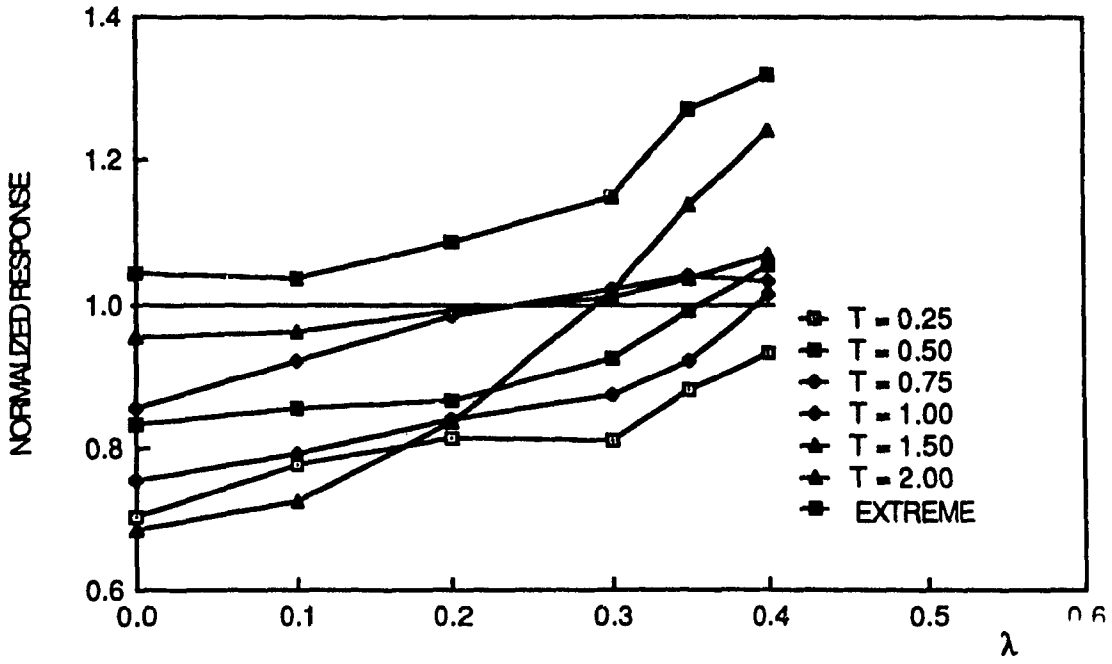

Fig. 4.14 Normalization With Respect to $e^* = 0.30$ vs λ (using 9 values).

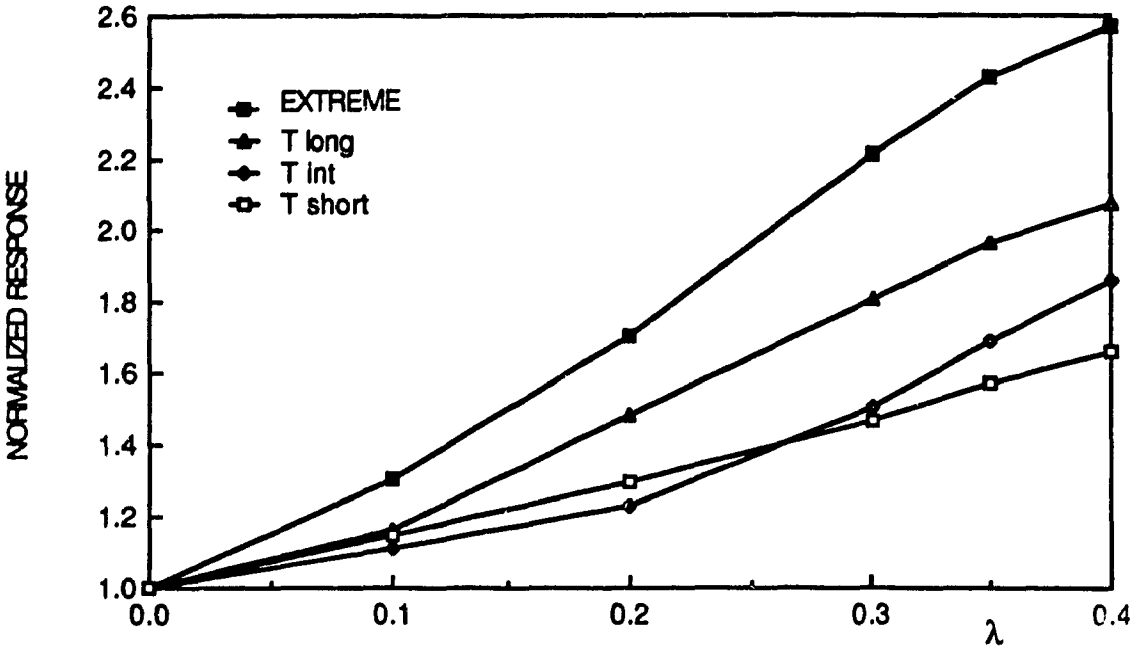

Fig. 4.15 Normalization With Respect to e* = 0.0 vs λ (using 18 values).

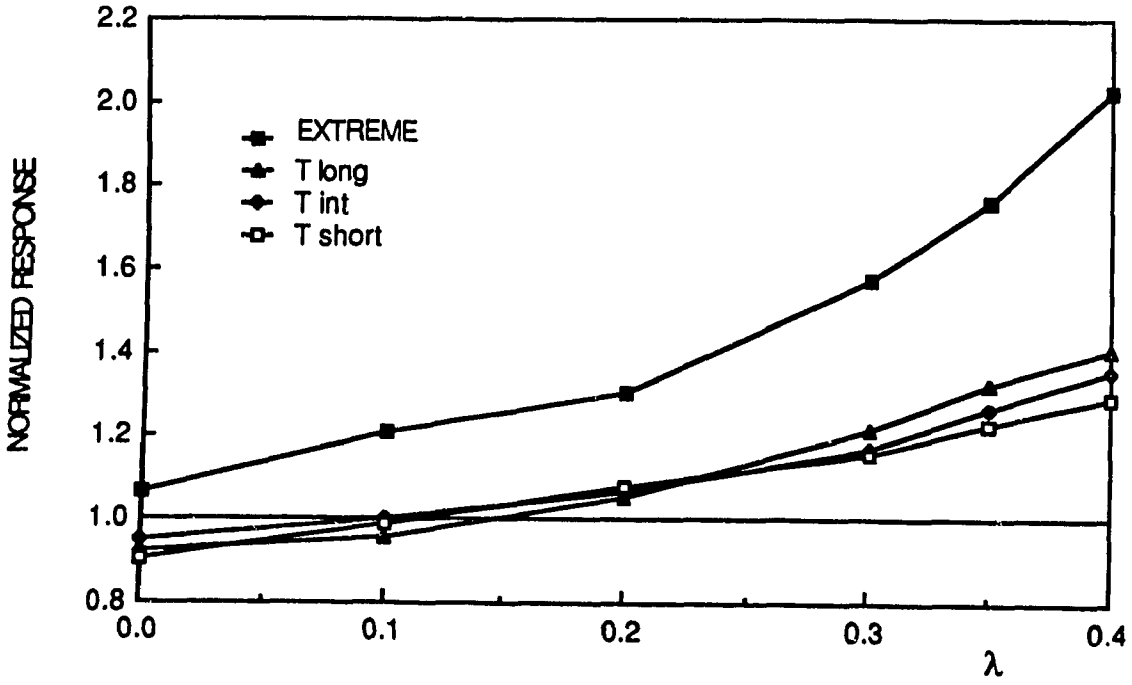

Fig. 4.16 Normalization With Respect to e* = 0.15 vs λ (using 18 values).

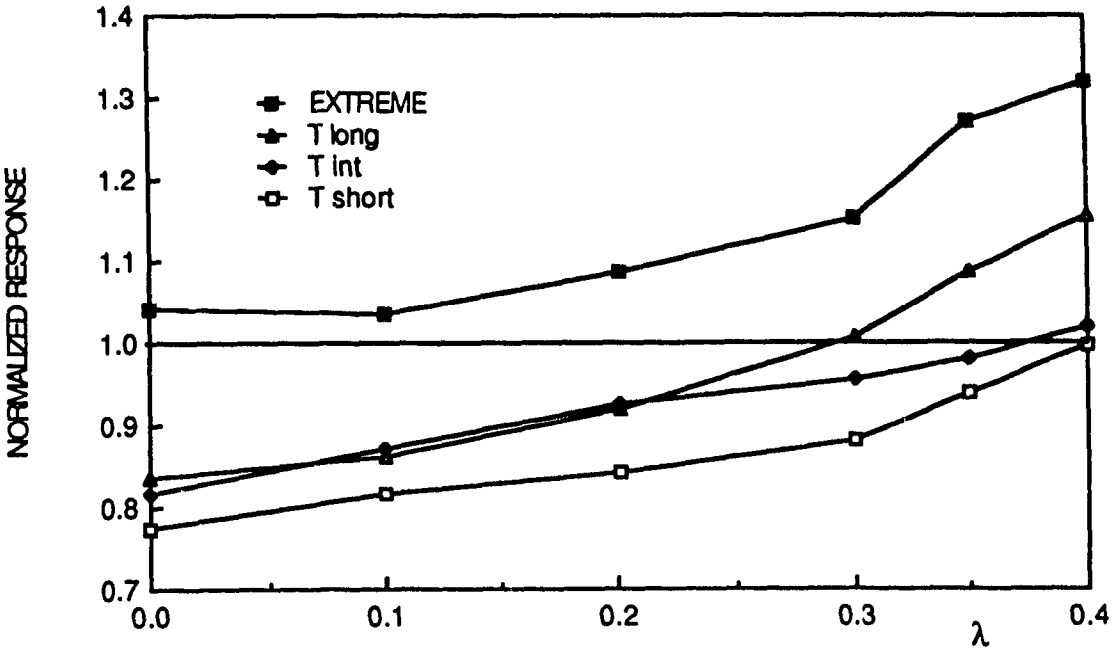

Fig. 4.17 Normalization With Respect to $e^* = 0.30$ vs λ (using 18 values).

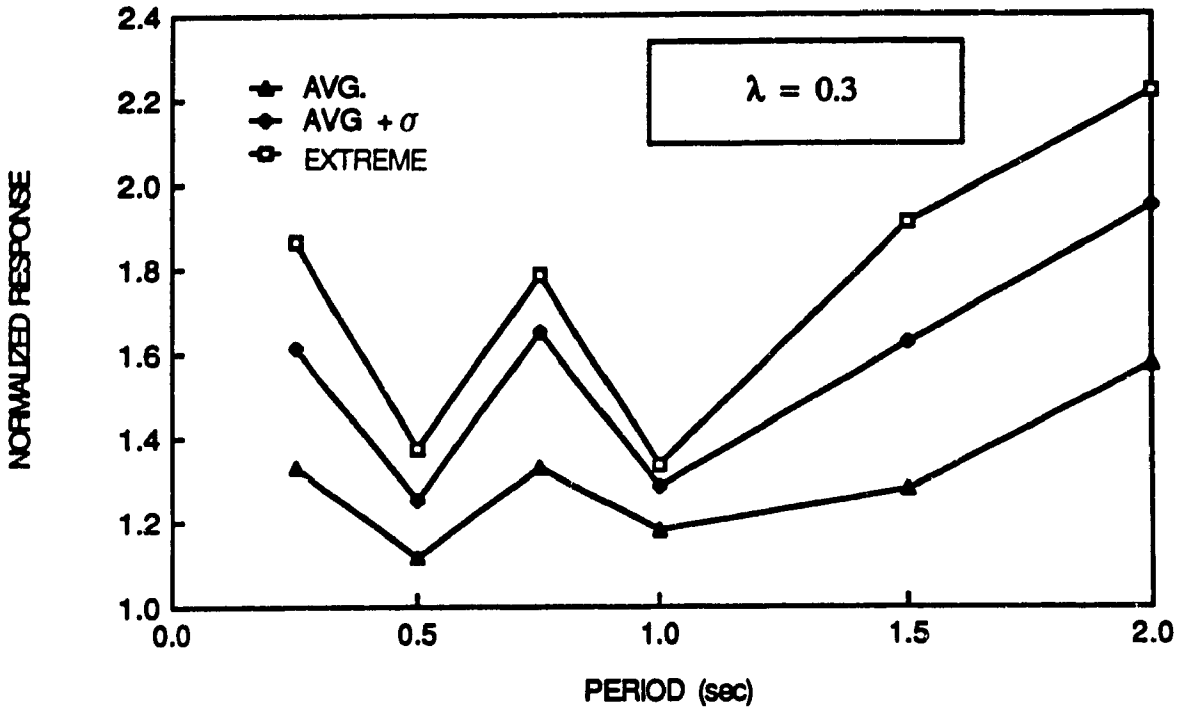

Fig. 4.18 Normalization With Respect to e* = 0.0 vs Period (using 9 values).

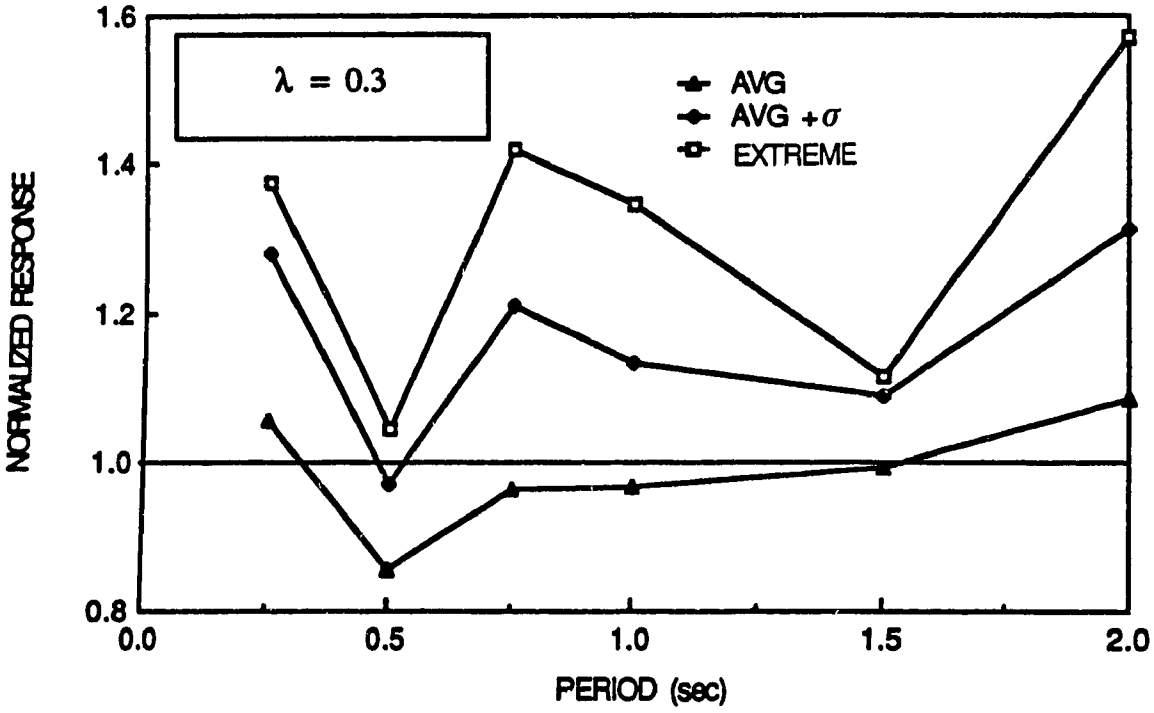

Fig. 4.19 Graph of Normalized Response (e* = 0.15) vs Period (using 9 values).

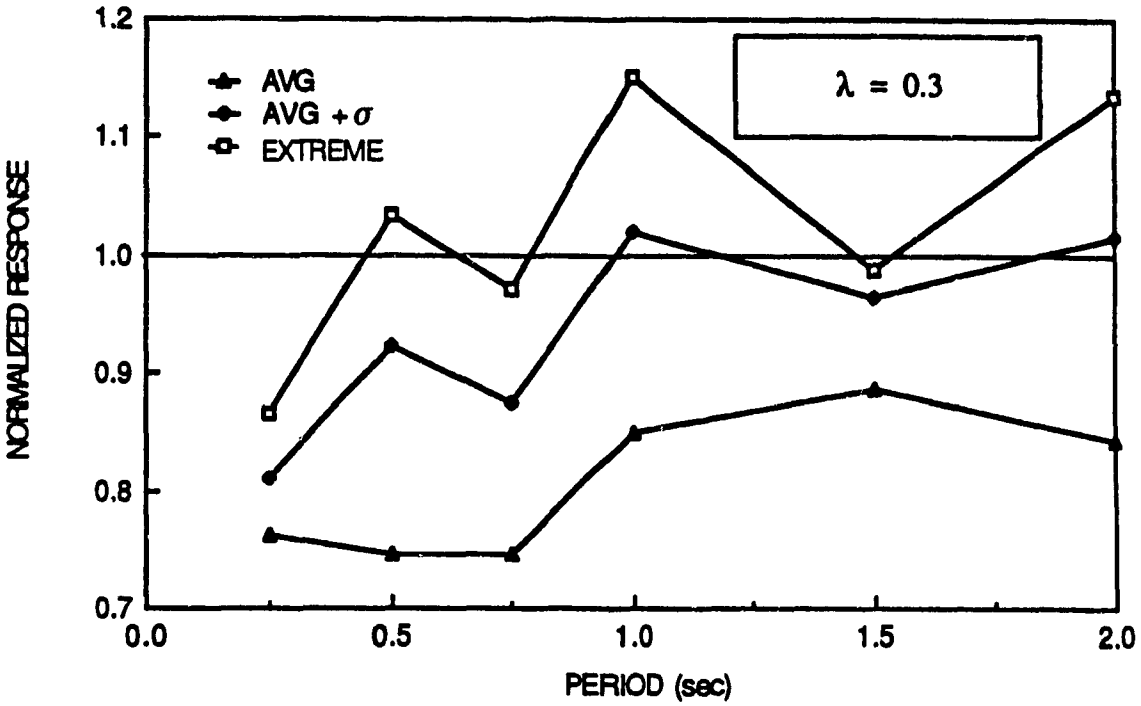

Fig. 4.20 Graph of Normalized Response (e* = 0.30) vs Period (using 9 values).

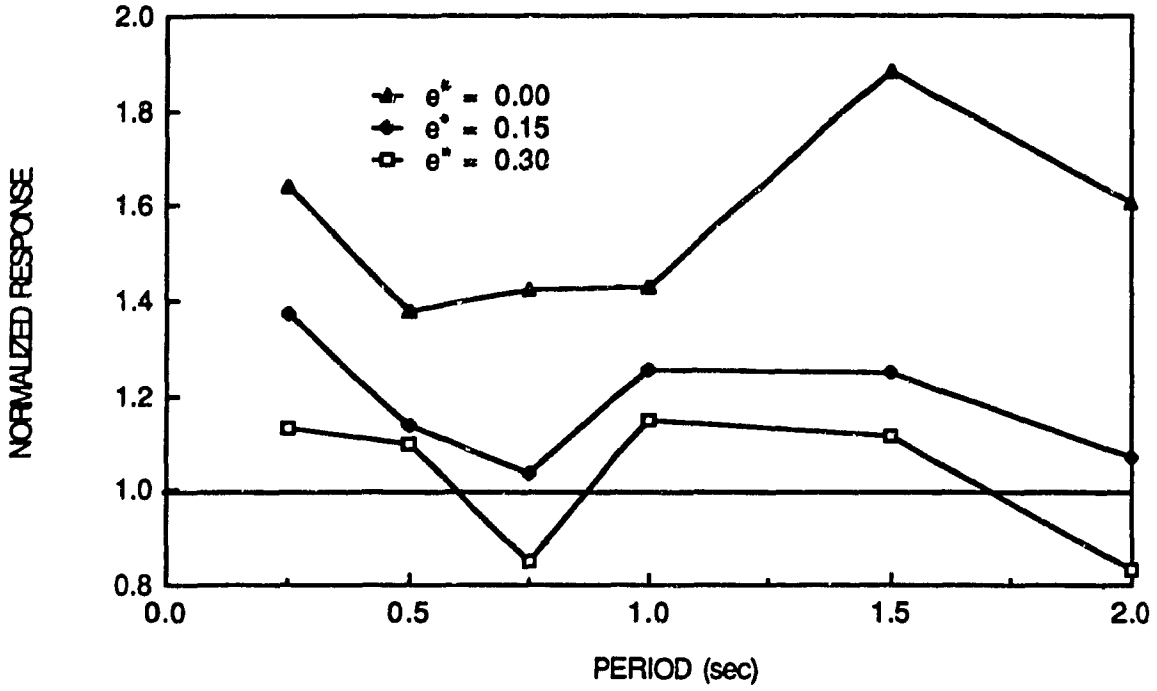

Fig. 4.21 Takeda Responses - Adequacy of Code Provisions for (AVG + 1σ).

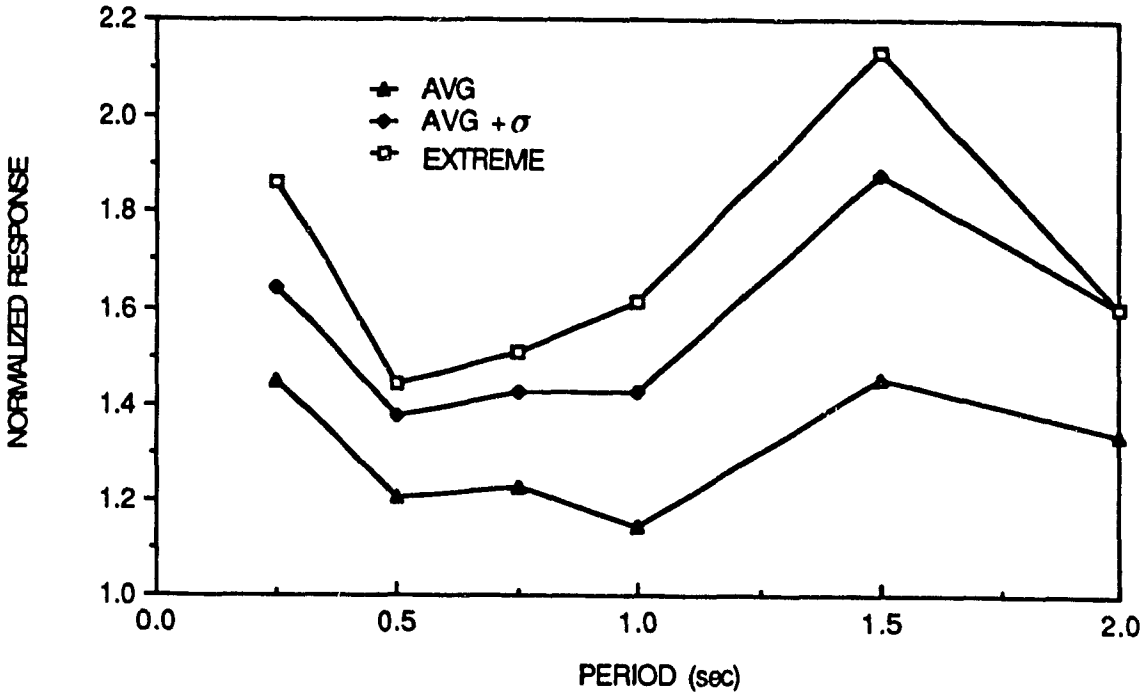

Fig. 4.22 Graph of Normalized Response (e* = 0.0) vs Period - Takeda Model.

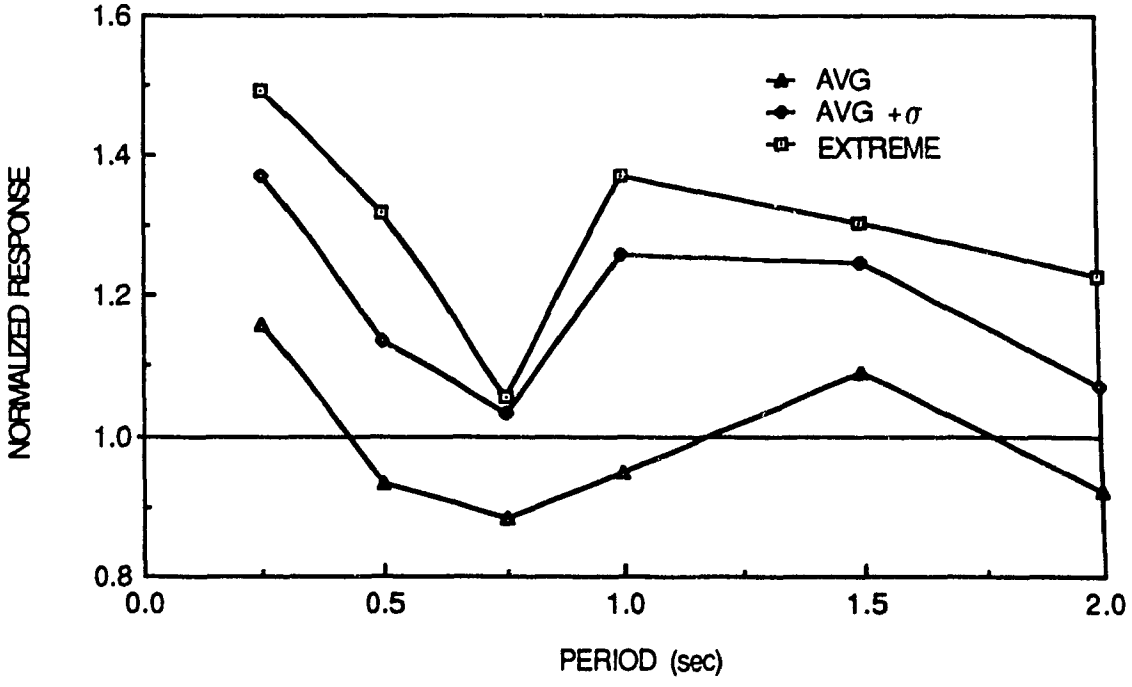

Fig. 4.23 Graph of Normalized Response (e* = 0.15) vs Period - Takeda Model.

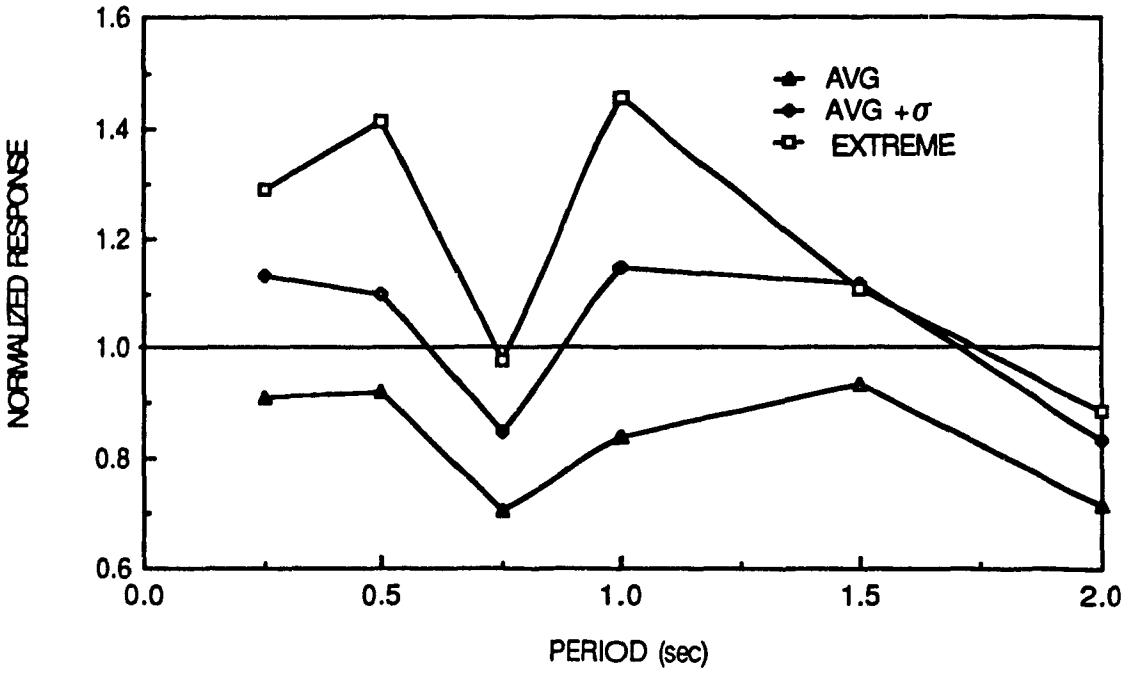

Fig. 4.24 Graph of Normalized Response ($e^* = 0.30$) vs Period - Takeda Model.

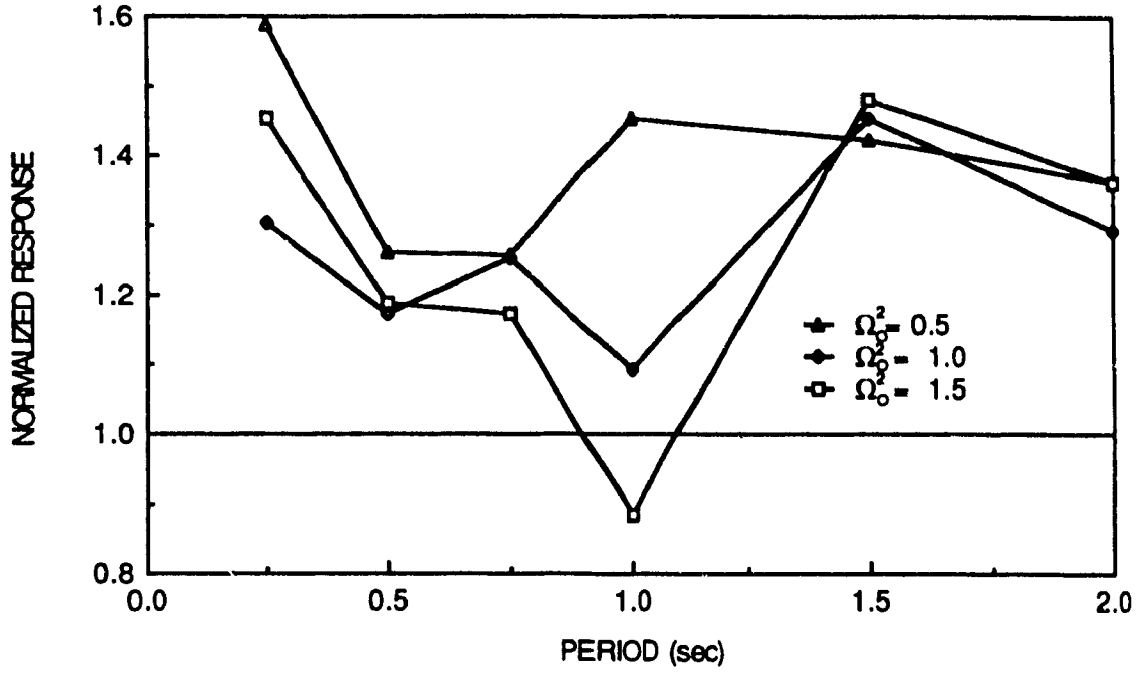

Fig. 4.25 Graph of Takeda Normalized Response (e* = 0.0) vs Period.

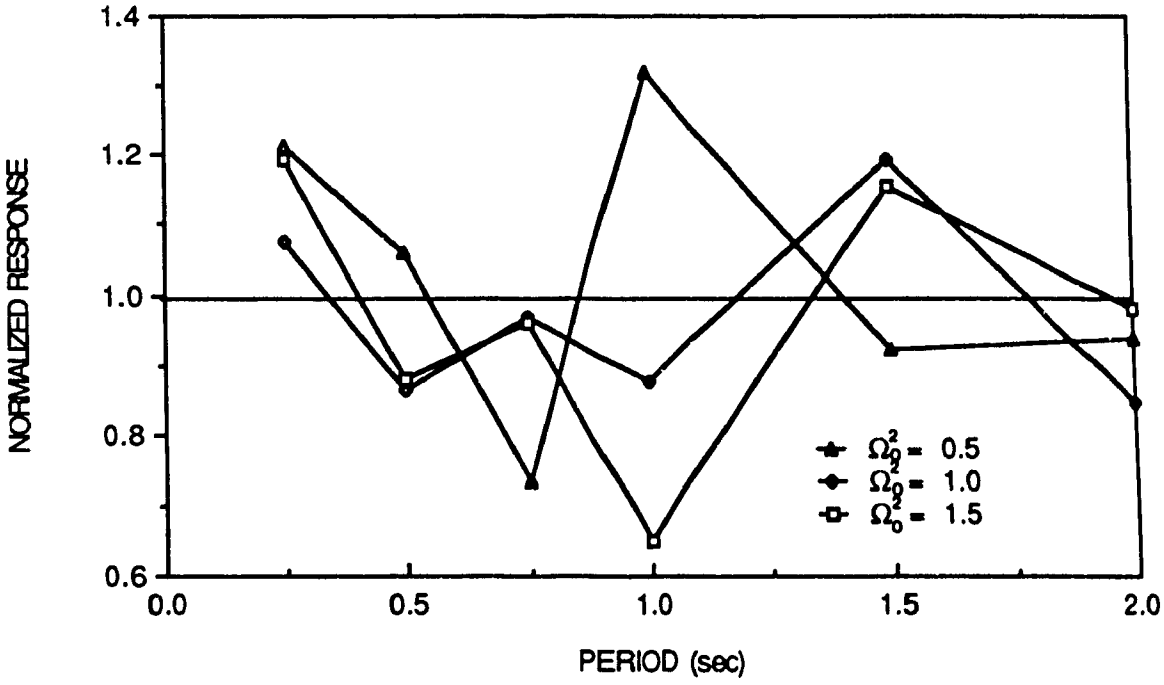

Fig. 4.26 Graph of Takeda Normalized Response (e* = 0.15) vs Period.

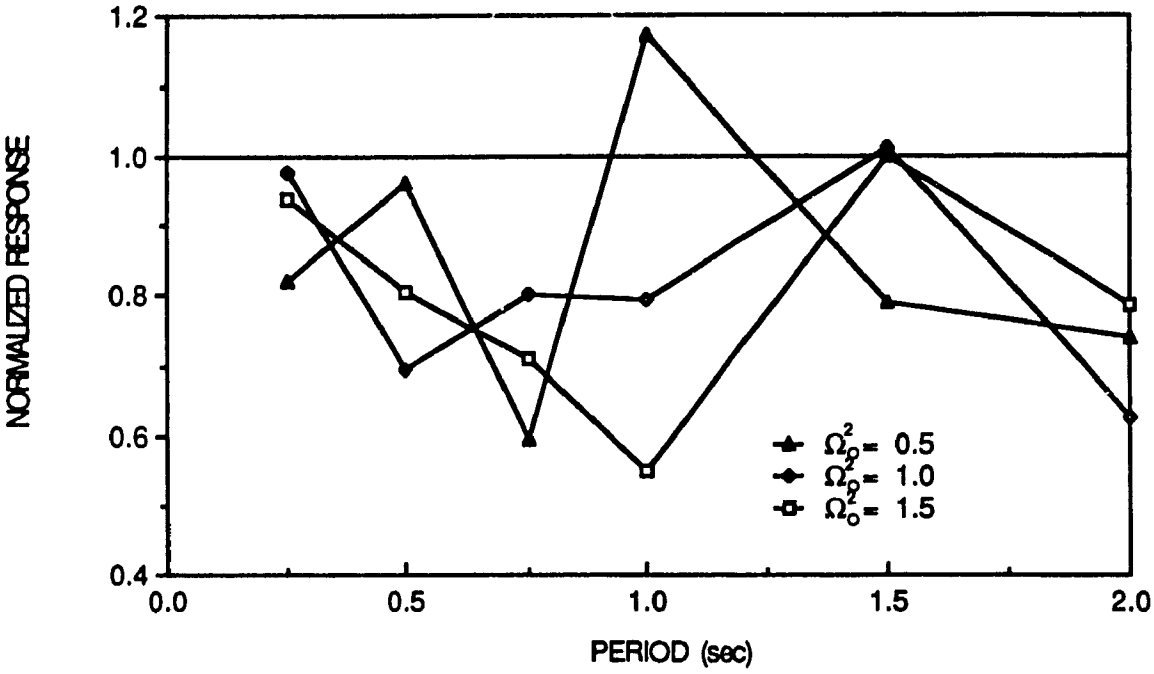

Fig. 4.27 Graph of Takeda Normalized Response (e* = 0.30) vs Period.

CHAPTER V

PARAMETRIC STUDY OF FRICTION DEVICES TO LIMIT SEISMIC RESPONSE IN STRUCTURES

5.1 INTRODUCTION

The previous chapter dealt with accidental eccentricity and its influence on the seismic response of nominally symmetric structures; this chapter, however, investigates a device installed at the periphery of buildings with the purpose of limiting the effects of both accidental eccentricity or specified design eccentricity. In recent years a novel approach for the aseismic design of frames has been introduced which consists in the incorporation of friction devices in tension cross-braces to absorb the detrimental energy input of severe earthquake excitation [18]. This new concept arises from the recognition that the economic costs to replace or repair buildings and their non-structural components in the aftermath of a severe earthquake could be prohibitive.

An early study [19] found the seismic energy input of a structure (with period T = 1.0 sec) 40 times in excess of its elastic capacity when subjected to the El Centro 1940 NS excitation with an earthquake severity factor Q ≈ 2.6. Since it was considered uneconomical to reconcile the design requirements of standard buildings within the elastic limits, except for very important structures such as nuclear power plants, the codes attributed reduced seismic coefficients provided sufficient ductility exists to warrant that there should not be collapse of a structure causing loss of life after a severe earthquake; with minor non-structural damage permitted in the event of a moderate earthquake.

The design of structures possesing good ductile lateral resistance such as moment resisting frames are permitted, by Code, lower seismic coefficients because their stable ductile behavior during repeated reversible loading enables them to deform without failure.

Moment resisting frames have thus been traditionally favored but these structures are very flexible and it is often economically difficult to control their interstorey drift and top deflection for the prevention of non-structural damage [18]. Conventional tension-compression braced frames are stiffer than moment resisting frames but, because of their pinched hysteresis curves, are viewed with suspicion by engineers for aseismic design. Standard tension cross braces exhibit degrading hysteresis and are the least favored. However, by the inclusion of the Pall friction device at the junction of the diagonals in tension cross-bracings, a rectangular stable hysteresis loop is obtained [18,20,22,23].

The friction device is shown in Figure 5.1 and can be placed typically in the central bays of a multistorey frame as shown in Figure 5.2, although many other arrangements are possible [18,23]. Till now the research in this field has been limited to the two dimensional case with the inclusion of the device in symmetrical buildings. Results of previous studies [18,20-22] have shown dramatic improvements in the behavior of frames with the device that were properly tuned when compared to the seismic response of frames without the device. The friction devices were considered tuned when the slip load that activates the device is such that the dissipation of seismic energy is maximized [23,25].

The process of finding the optimum slip load was heuristic with the main criterion that the device operates before yielding occurs in a frame member. Recently a researcher [25] proved that the device provides maximum energy dissipation when its contribution to resisting lateral storey shear equals that of the frame without the brace. In other words for RB = RF, where RB is the lateral resistance of the brace acting alone and RF is the yield strength of the frame without the brace. It should be noted that this study considers the device optimum when the response of the structure is minimum and investigates whether the ratio RB/RF = 1 is indeed optimal.

Other studies have investigated the actual slip load of the friction dampers for a given structure [18,20-24]; this chapter however investigates the stiffness ratio (KB/KF) and the strength ratio (RB/RF) which bettter describe the characteristics of the device for

their influence on the seismic response of any structure. Note that KB represents the stiffness of the brace alone, and that KF represents the stiffness of the frame without the brace. Furthermore the study is extended to the more general case of eccentric structures to see if the device is equally beneficial.

For this purpose a parametric study consisting of time history analyses of the first 15 seconds of response to the Newmark Blume Kapur artificial earthquake, with time step $\Delta t = 0.01$ second, was carried out using the computer package Drain-2D [16]. The response of the model, whose lateral period is 1.0 second and frequency ratio $\Omega_o^2 = 1.0$, was evaluated for strength ratios RB/RF = 0.0, 0.2, 0.4, 0.6, 0.8, and 1.0; for stiffness ratio KB/KF = 0.0, 0.5, 1.0, 2.0, and 3.0; and for eccentricity e^* = 0.0, 0.3, 0.75, 0.9, 1.2, and 1.5 . The parameter e^* denotes the structural eccentricity normalized by the mass radius of gyration ρ. This earthquake was chosen because of its smooth elastic spectrum which does not favor any particular frequency. The period T = 1.0 second was chosen because it is representative of multistorey buildings and it is deemed that the device can have the most significant contribution to aseismic design for this category of structure. The range of stiffness ratio and strength ratio should cover most possible combinations and the reasons for the choice of eccentricity is as follows. The eccentricity $e^* = 0.0$ represents symmetrical conditions and $e^* = 0.3$ is equivalent to the accidental eccentricity provisions of NBCC 1985. The eccentricity $e^* = 0.75$ was chosen because at that level NBCC 1980 required the doubling of the effect of eccentricity. The values $e^* = 0.9$ and $e^* = 1.2$ represent the large eccentricity range whereas $e^* = 1.5$ is the maximum physical limit since for this value the center of mass would be located at the extreme edge of the building. Using this parametric study it should be possible to quantify the improvement resulting from the incorporation of the friction dampers and establish optimum structural parameters with respect to a given frame.

5.2 THE STRUCTURAL MODEL AND THE COMPUTER MODEL

The structural model used for this chapter consists of a one storey asymmetric structure and is similar to the one used in Chapter 3 with the inclusion of two tension cross-braces each equipped with a friction device as patented by Pall. The first friction damped brace (called element #3) is located with lateral resisting element #1, while the second friction damped brace (called element #4) is located with lateral resisting element #2 as shown in Figure 5.3. For simplicity, both friction damped braces have identical properties assigned to them although this is not a necessity. The characteristics of the brace follow the assumption given by Pall [18] that the compression diagonal buckles at a very small load but the device is activated and keeps this member taut. This assumption was verified by Filiatrault and Cherry [20,23] and was found adequate. Because of this assumption the effect of a tension cross-brace equipped with the device is essentially the same as having a single tension- compression diagonal brace with a friction damper. In both instances the hysteresis loop is rectangular [18,20,22]. A typical hysteresis loop of the device is shown in Figure 5.4.

Figure 5.5 shows the definition of stiffness, KB for the brace, and of KF, the stiffness of the frame without the brace. It should be emphasized that the stiffness of the diagonal K_{diag} is not the stiffness of the brace KB but can easily be found by geometry as:

$$K_{diag} = KB / (\cos \alpha_{brace})^2 \qquad (5.1)$$

where α_{brace} is the angle the diagonal makes with the horizontal. However , it is more useful to use the storey drift for the definition of stiffness since this is the one used in the design office. The resistance of the frame is defined as that force which produces the onset of yielding in one of the members of the frame, whereas for the brace its resistance is that force which causes the friction damper to activate and slip at a constant load called

the "slip load". An equivalent computer model for the studied structure is shown in Figure 4.6 where truss elements are used to represent the frames and the friction braces. It should be noted that when either KB or RB is zero, the frame is without the device and the model becomes identical to that of Chapter 3 with $\lambda = 0.0$.

Results were obtained for the maximum responses from stations located at $\pm$ 1.5 ρ and $\pm$ 1.0 ρ from the center of mass CM, as well as at $\pm$ x_0 from the center of resistance CR, together with CM and CR displacements. As in Chapter 3, $x_0 = \Omega_0 \rho$ is a property of this model.

5.3 RESULTS OF THE PARAMETRIC STUDY

5.3.1 Effect of the Stiffness Ratio (KB/KF)

In this section the influence of the friction device on the response of three classes of structures with $e^* = 0.0$, 0.3, and 0.75 respectively is investigated with regard to the effect of the stiffness ratio. Figure 5.7 shows the effect of the stiffness ratio KB/KF of the device on symmetric structures for strength ratios RB/RF = 0.8, 0.6, and 0.4 . These values were chosen because they usually gave the best results and the literature indicates that a plus-minus variation of the slip load by 20 percent gives approximately the same results [18,22]. Note that even though the range chosen implies a variation in the slip load by 33 percent, the response is almost equal. Plotted in Figure 5.7 are the maximum displacements normalized with respect to the displacements without the device. One immediately notes the significant improvement of the response for frames with the device for the whole range of stiffness ratio considered, with more pronounced reductions in response as the stiffness ratio increases. For example at KB/KF = 3.0 and RB/RF = 0.8 the normalized response is only 0.277 that of the symmetric response without the device.

Figure 5.8 shows the effect of the stiffness ratio KB/KF for a structure with small eccentricity, $e^* = 0.3$, which is equivalent to 10 percent of the building dimension

perpendicular to the earthquake. The response shown has been normalized by the symmetric response and values less than one indicate that the device takes care of the eccentricity. In this case one notes a small increase in response for the structure with the device when KB/KF = 0.5 which can be explained by the fact that at that value of stiffness ratio and for the strength ratio utilized, the device is not effective. It can be shown that it is desirable for the device to satisfy the relation:

$$(KB/KF) / (RB/RF) > 1.0 \qquad (5.2)$$

otherwise the frame will yield before the device is activated. The proof is as follows:

$$\Delta_{\text{yield brace}} < \Delta_{\text{yield frame}} \qquad (5.3)$$

at $\Delta = \Delta_{\text{yield brace}}$, the force in the brace is :

$$F_{\text{brace}} = (KB)\ \Delta_{\text{yield brace}} = RB \qquad (5.4)$$

multiplying Equation (5.3) by KB gives:

$$RB < (KB)\ \Delta_{\text{yield frame}} \qquad (5.5)$$

but

$$\Delta_{\text{yield frame}} = RF / KF \qquad (5.6)$$

substituting Equation 5.6 into Equation 5.5 :

$$RB < (KB)\ (RF/KF) \qquad (5.7)$$

Rearranging terms of Equation 5.7 leads to Equation 5.2. Note that braced frames are much stiffer than moment resisting frames and there is no difficulty in achieving a KB/KF value of one or more.

According to Pall [18] the device is designed not to slip under normal wind loads and moderate earthquakes while during severe earthquakes the device activates at a predetermined slip load prior to the occurence of yielding in the diagonal and the other structural elements of the frame. Thus an upper bound for RB/RF exists. Moreover if the slip load is too low the device dissipates little energy. When the device is properly tuned as in the case for KB/KF greater than one in Figure 5.8, there is considerable reduction in response as compared to the response of the symmetric structure without the device.

Figure 5.9 shows the influence of the device for a structure with an eccentricity equivalent to 25 percent of the building dimension. The responses shown are normalized with respect to the symmetric unbraced response and indicate that the device with a stiffness ratio KB/KF of 2.0 or more adequately takes care of the additional effects of eccentricity.

5.3.2 Effect of the Strength Ratio (RB/RF)

Figures 5.10a and 5.10b show the influence of the device for structures with very low stiffness ratio (KB/KF = 0.5). This ratio limits the range of RB/RF values desirable for the device since for RB/RF < 0.2 the energy absorbed by the device is minimal and for RB/RF > 0.5 the frame yields before the device is activated. Note that the energy absorbed by the device equals the slip load multiplied by the slip displacement.

For ease in evaluating results, Figures 5.10b, 5.11, 5.12, and 5.13 regroup the eccentricities into averages of two values as follows: large eccentricity $e^* = 1.2$ and $e^* = 0.9$, moderate eccentricity $e^* = 0.75$ and $e^* = 0.3$; together with the results of the symmetric case $e^* = 0$. Figure 5.11 gives the responses normalized by the symmetric response for a stiffness ratio KB/KF = 1.0 . For this ratio considerable reduction is obtained in structures having no eccentricity and large eccentricity when the device has a strength ratio RB/RF > 0.2, whereas structures with moderate eccentricity benefit from only a small reduction in response. Figures 5.12 and 5.13 are similar to the previous two figures and give the normalized response for KB/KF of 2.0 and 3.0 respectively.

5.3.3 Tuning the Device With Respect to (KB/KF)

From Figures 5.10b, 5.11, 5.12, and 5.13 one sees, in particular, that responses at a given eccentricity are similar in the range of strength ratio 0.4 to 1.0 , with best results for RB/RF around 0.6 . This suggest that the response of structures equipped with the device are not sensitive to the setting of the slip load ± 30 percent, and this was previously

reported by other researchers [18,21,22] in their search for the optimum slip load. This process is called 'tuning' by them. For the pupose of this study tuning with respect to slip load is done by taking the least among the 6 responses correspondng to RB/RF = 0.0,0.2,0.4,0.6,0.8,1.0. Figure 5.14 shows the influence of the stiffness ratio for a structure with a tuned device; responses shown are normalized with respect to the eccentric response of the structure without the device. In particular this figure indicates that response decreases with increasing KB/KF values. Moreover for symmetric conditions as well as with structures possessing large eccentricity the response is significantly lower, only 40 percent as high as the response without the device for KB/KF ratios between 1.0 and 2.0 . For structures with moderate eccentricity the response decreases almost linearly to approximately 60 percent at KB/KF=3.0. This figure indicates that a KB/KF ratio above 1.0 should be used with the optimum being the largest economically feasible, although there is not much benefit in increasing KB/KF from 2.0 to 3.0 .

5.3.4 Tuning the Device With Respect to (RB/RF)

In the previous section, a tuned device with respect to the slip load was further tuned with respect to the stiffness ratio, in order to find the best KB/KF value. This section reverses the process; a tuned structure with respect to the stiffness ratio is further tuned with respect to the strength ratio RB/RF . Figure 5.15 show normalized responses for the least among the 5 cases studied (corresponding to KB = 0.0, 0.5, 1.0, 2.0, 3.0). This figure reveals that the optimum slip load is for a strength ratio RB/RF of approximatively 0.6 which appears to differ with the findings of Baktash [25] which gave the optimum at RB/RF = 1.0 for maximum energy dissipation in symmetrical structures. In fact this study found that for symmetrical structures the optimum slip load was indeed RB/RF = 1.0 for all stiffness ratios except KB/KF = 3.0, where the response at RB/RF = 1.0 is 4.3 percent larger than the response at RB/RF = 0.8 . This difference is not significant, and can be attributed to a multitude of factors; therefore this study can be

considered to corroborate the findings of Baktash for symmetrical structures. However, for asymmetric structures the optimum slip load should be reduced to correspond to the strength ratio RB/RF = 0.6 .

5.3.5 Influence of Eccentricity on Edge Displacement of Tuned Structures

From the previous discussion it appears that tuning should be carried out with respect to the stiffness ratio as well as to the strength ratio. This was done in Figure 5.16 and results show the influence of eccentricity for structures with tuned friction devices compared to the same structure without the device. This figure reveals that the device is almost equally effective in reducing the effects of eccentricity with an average reduction of 60 percent and a standard deviation of 10 percent.

It is known that eccentricity increases the response of structures whereas the device reduces the response. Thus it may be of interest to know for what value of eccentricity could the device account for and still give an equivalent response as a symmetric structure without the device. Figure 5.17 shows the effect of eccentricity and plots the response of a structure with a tuned device normalized by the symmetric response without the device. This figure reveals that by incorporating the device, eccentricity could be adequately accounted for up to $e^* = 1.2$ $(=0.4D_n)$.

5.3.6 Influence of Eccentricity on Maximum Rotation of Tuned Structures

Figure 5.18 shows the maximum rotation obtained from the time history analyses for structures equipped with braces having tuned devices, and for the same structure without the brace and device. This figure indicates that structures with a tuned device have considerable less rotations due to eccentricity. Note that symmetrical structures with devices still have no rotations because each lateral resisting element is equipped with identical devices.

5.3.7 Effect of Friction Devices on Ductility Demand

Figures 5.19 and 5.20 investigate the ductility demand on the lateral resisting elements for the range of eccentricity considered. The ductility demand is defined here as the ratio of total deformation to the deformation at yield, and is a measure of the amount of damage sustained by a structure subjected to severe seismic excitation. Figures 5.19 and 5.20 are for the lateral resisting elements on the "stiff" and the "flexible" sides respectively, and values less than one indicate that the element remains elastic. Plots are given for the structure with and without the braces equipped with the fully tuned devices, and in both figures one notes large reduction in ductility demand. Moreover the reduction is such that the frame on the stiff side essentially remains elastic for any eccentricity even though the earthquake severity factor Q = 4.0 represents a severe earthquake.

5.3.8 Effect of Friction Devices on Energy Absorption by Inelastic Deformation

The energy consumed through yielding of a structural element having elasto-plastic properties is the product of the yield strength and the plastic displacement. Figure 5.21 plots the accumulated plastic energy dissipated by yielding of the moment resisting frames equipped with the device normalized by the accumulated plastic energy dissipated by lateral resisting frames without the device for the range of eccentricity considered. Structures having cross-braces equipped with the device have dramatically less energy consumed by inelastic yielding. For symmetrical structures the energy absorbed in the frames with devices represent only 4 percent of the energy consumed by frames without devices, whereas for a small eccentricity equal to 10 percent of the building dimension the energy absorbed by the frame with device is only 10 percent of that without the device. At other eccentricity the reduction is approximately 70 percent in accumulated inelastic energy. Note that when the device is activated at the slip load the displacement of the friction joint is repeatable and the diagonal members remain elastic.

5.4 SUMMARY

This chapter investigated the ability of a friction device patented by Pall [18] to reduce the response of structures when these are incorporated in simple moment resisting frames. Results corroborate the findings of other investigators [18,20-25] for symmetrical buildings with dramatic improvements of their response when the device is properly tuned. Until now tuning of the device has been done with regard to the slip load only; however this study has found that it is also important to 'tune' the stiffness ratio KB/KF. Furthermore, this study confirms the finding of Baktash [25] that for symmetrical structures a slip load corresponding to the strength ratio RB/RF = 1.0 is optimum, although there is little difference in response in the range RB/RF from 0.4 to 1.0 .

The study was extended to the more general case of eccentric structures and here also considerable improvement in the response was obtained by the inclusion of the friction devices. For these structures it was found that the optimum slip load corresponds to a strength ratio of RB/RF = 0.6 with little difference in response for a strength ratio variation of ± 20 from optimum. The optimum stiffness ratio was found to lie above KB/KF = 1.0 with little difference in results for KB/KF ratios between 2.0 and 3.0 . The inclusion of the device reduced the maximum rotation of the structure with greater benefit as the eccentricity is increased, and the device also had great influence in reducing the ductility demand. In particular the frames on the stiff side stayed essentially elastic when the structure possessed the device, even though it was subjected to the Newmark Blume Kapur excitation with an earthquake severity factor of Q = 4.0 which can be considered severe. Finally it was shown that the device reduces the energy absorbed by inelastic deformation of the frames by 96 percent for symmetric structures and by 90 percent for structures with low eccentricity; for structures with large eccentricity the reduction is in the order of 70 percent.

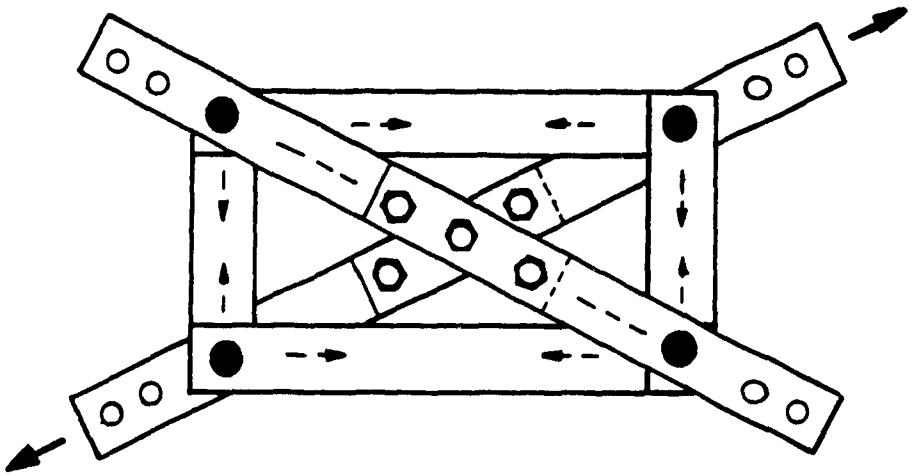

Fig. 5.1 Friction Damping Device

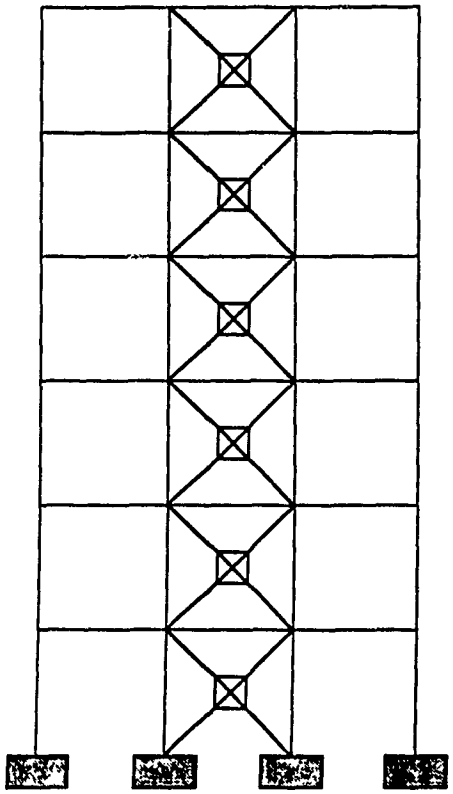

Fig. 5.2 Typical Frame with Friction Device

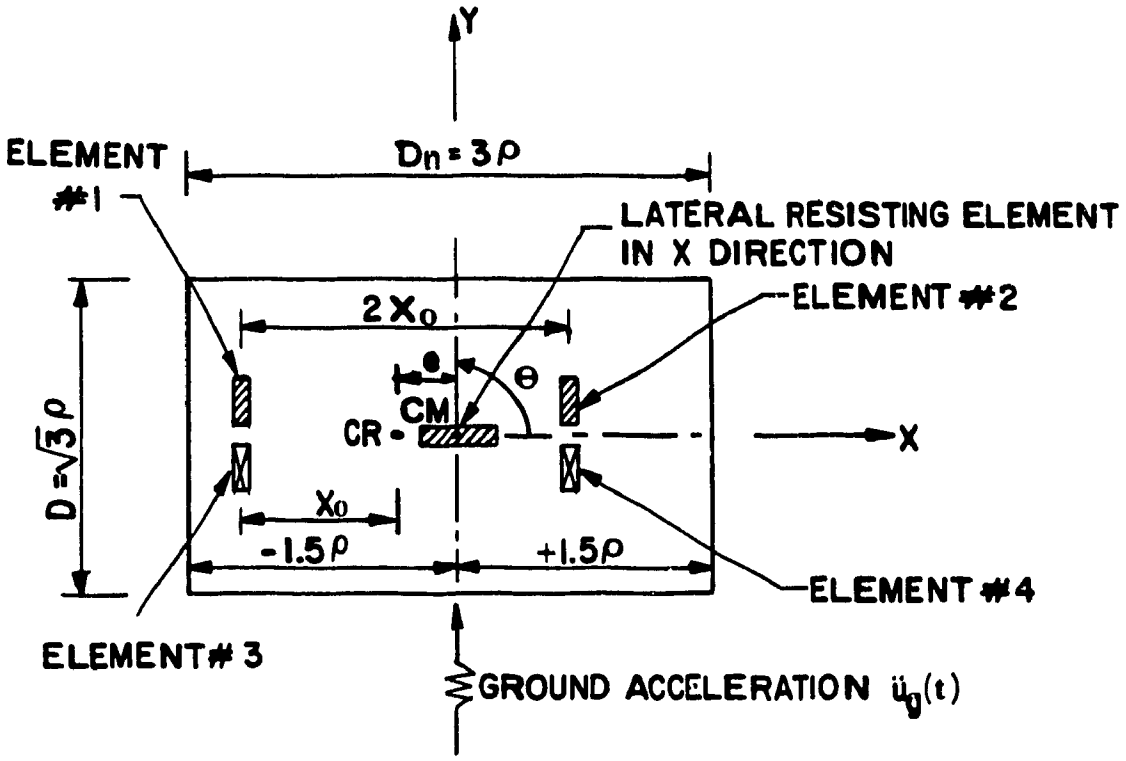

Fig. 5.3 Idealized Model with Friction Device

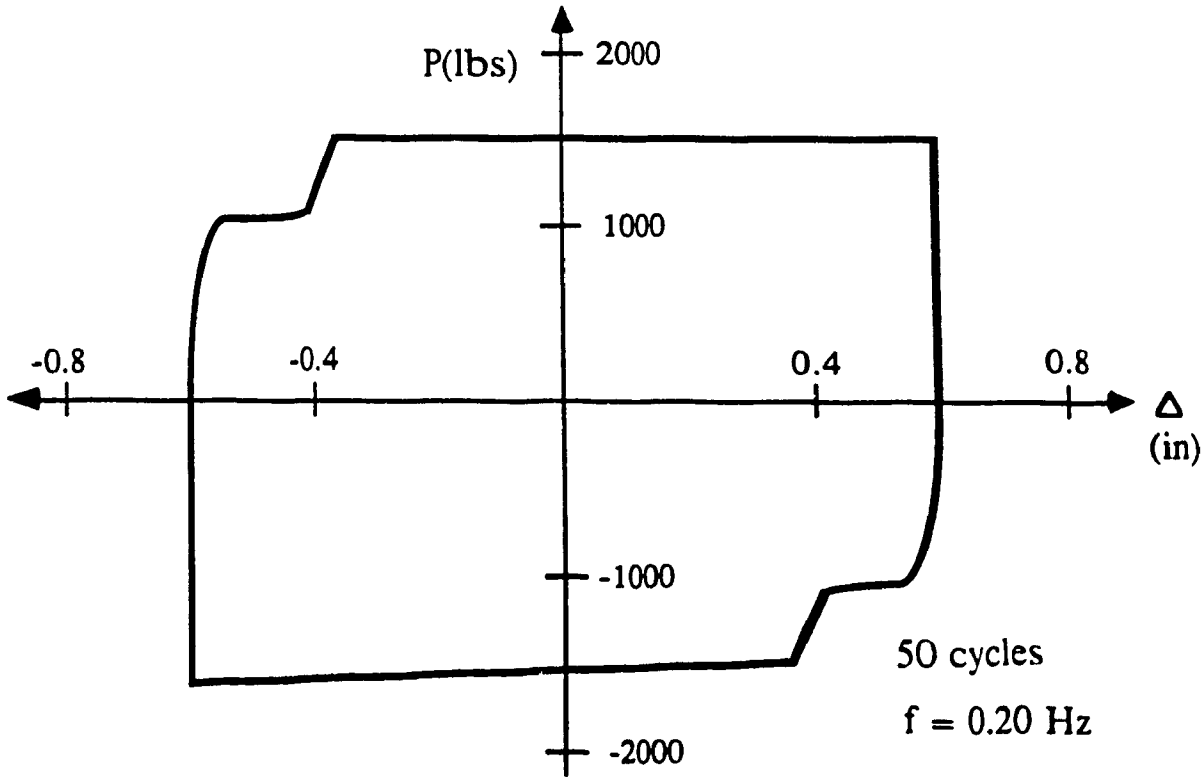

Fig. 5.4 Hysteresis Loop of a Typical Friction Device [20]

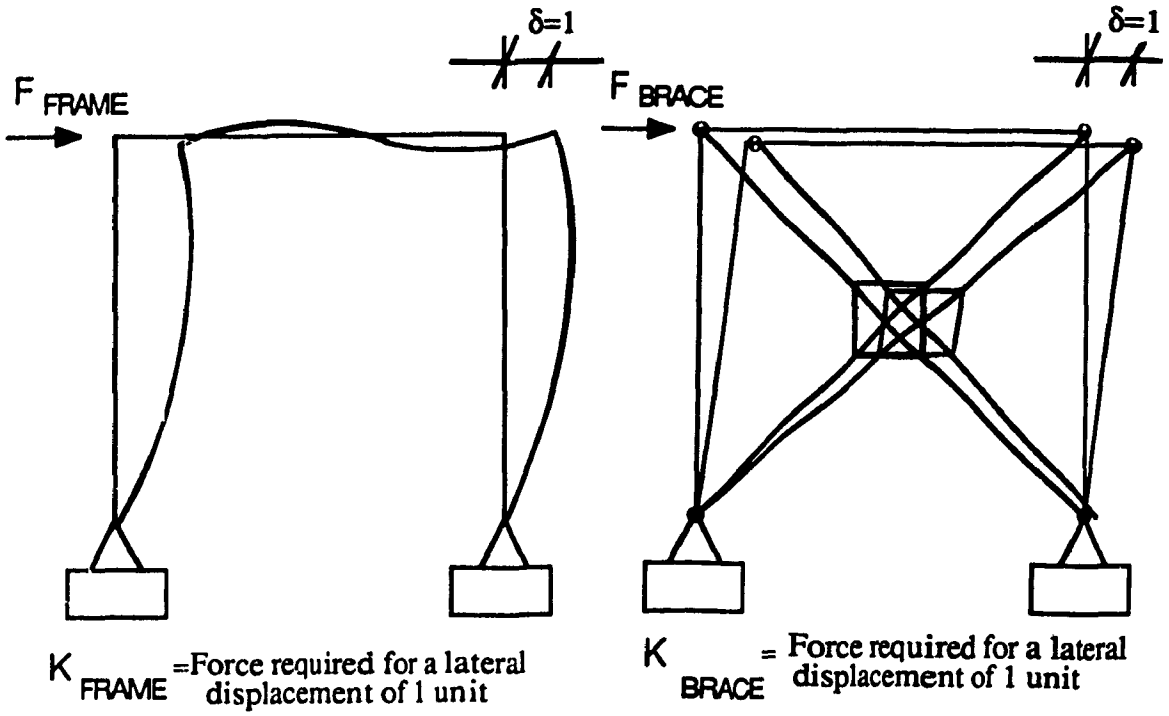

Fig. 5.5 Definition of Stiffness

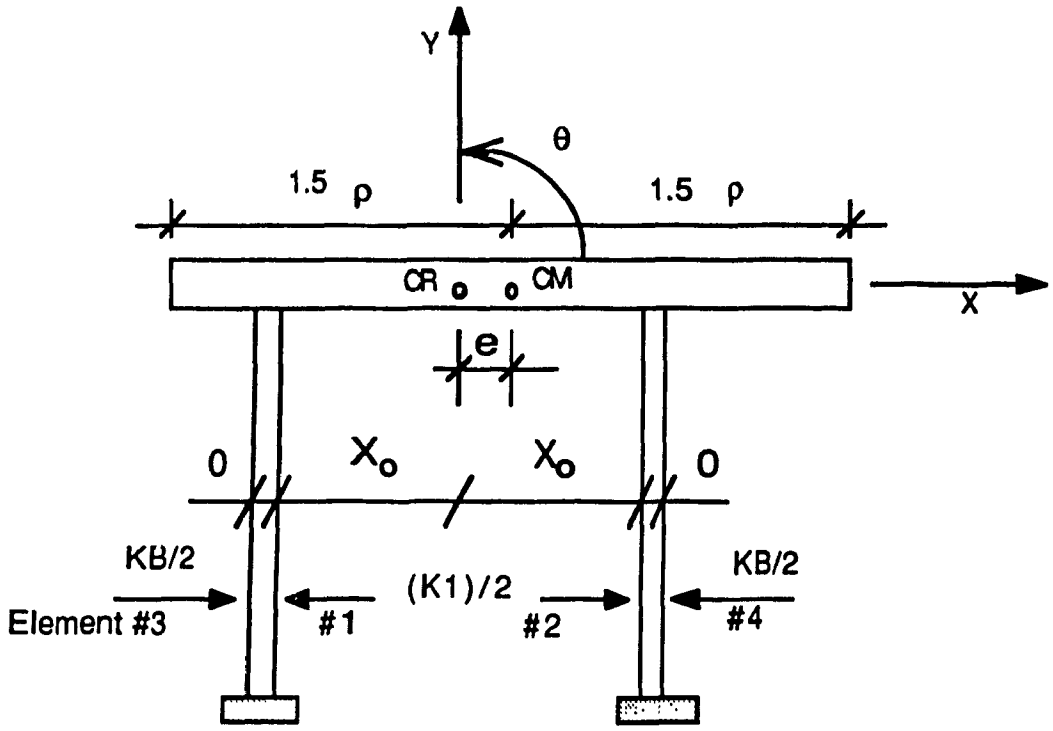

Fig. 5.6 Equivalent Computer Model

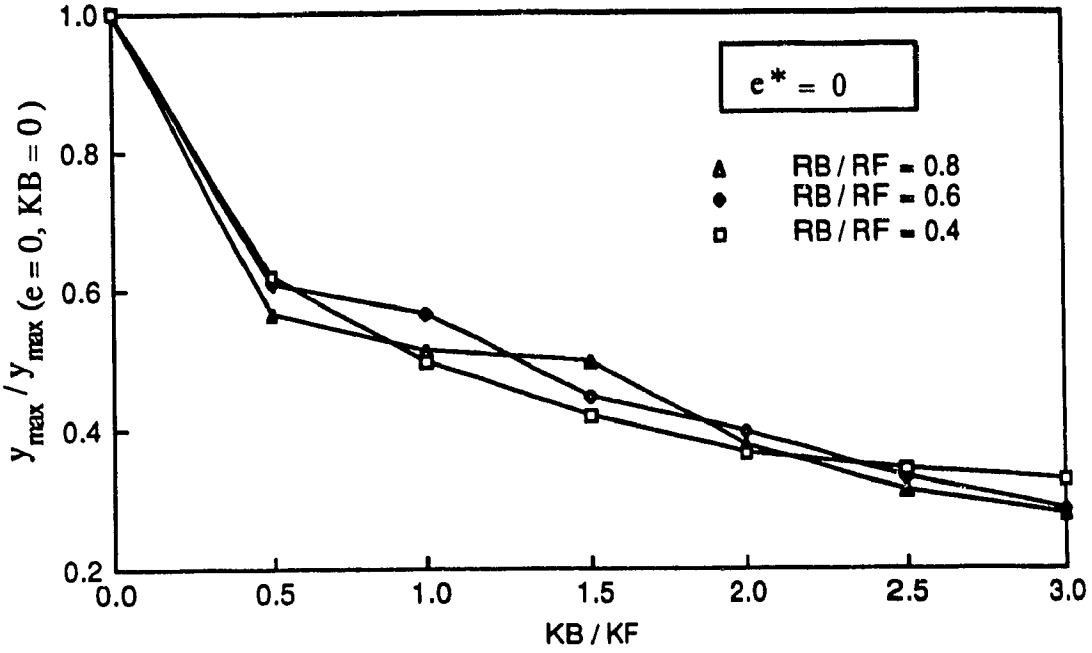

Fig. 5.7 Influence of Stiffness Ratio (KB/KF) - $e^* = 0.0$

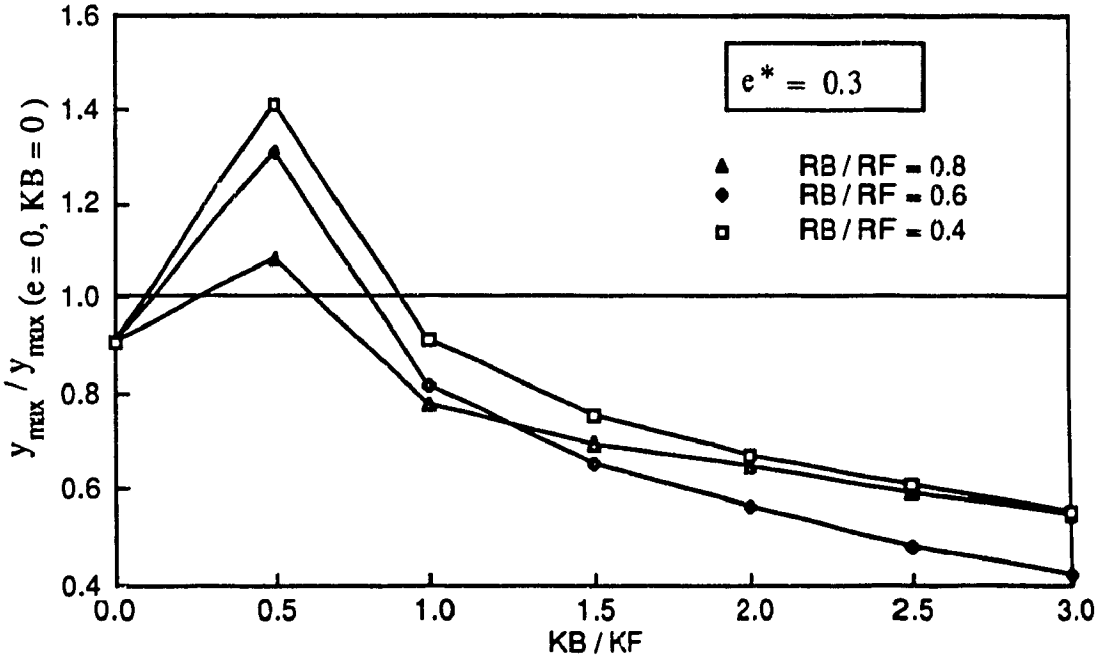

Fig. 5.8 Influence of Stiffness Ratio (KB/KF) - $e^* = 0.3$

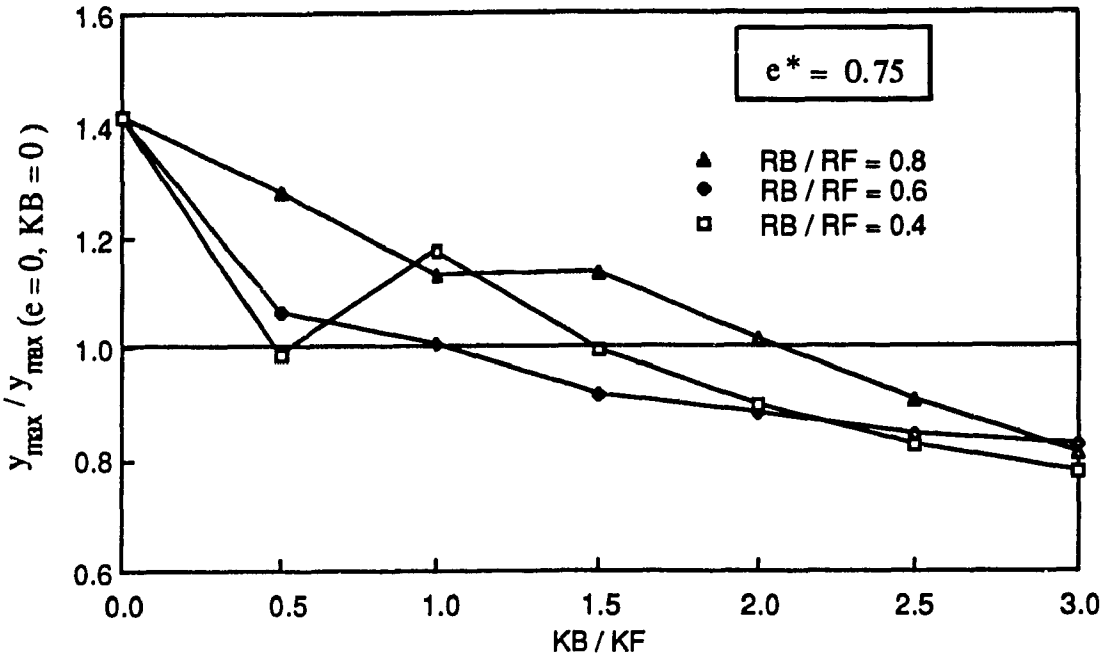

Fig. 5.9a Influence of Stiffness Ratio (KB/KF) - $e^* = 0.75$

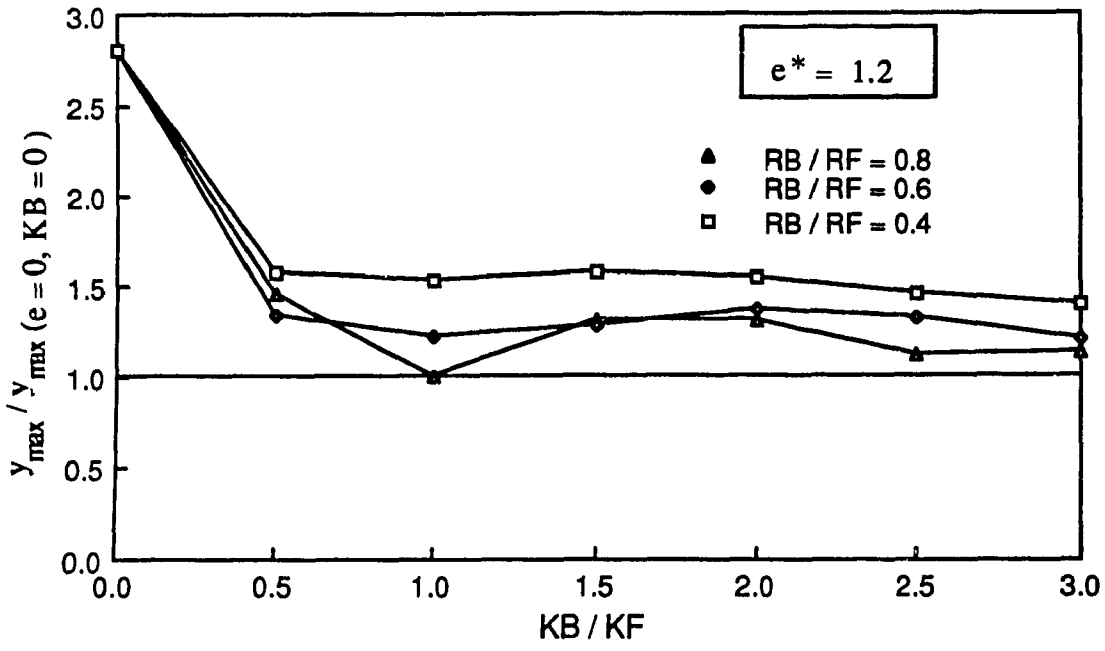

Fig. 5.9b Influence of Stiffness Ratio (KB/KF) - $e^* = 1.20$

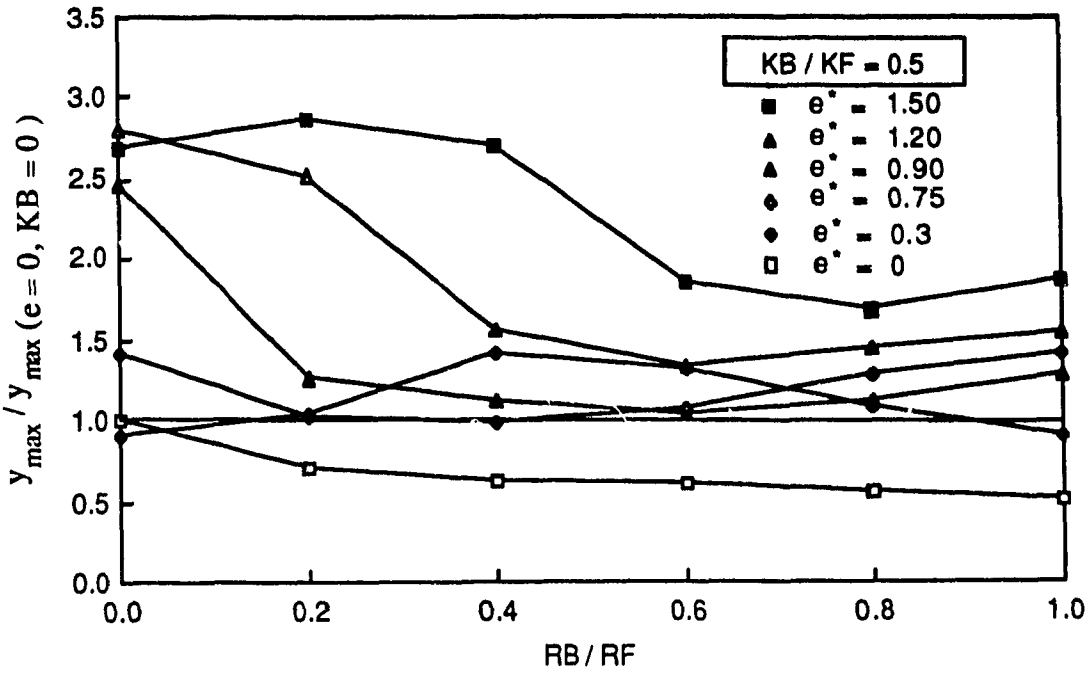

Fig. 5.10a Influence of Strength Ratio (RB/RF) - KB/KF = 0.5

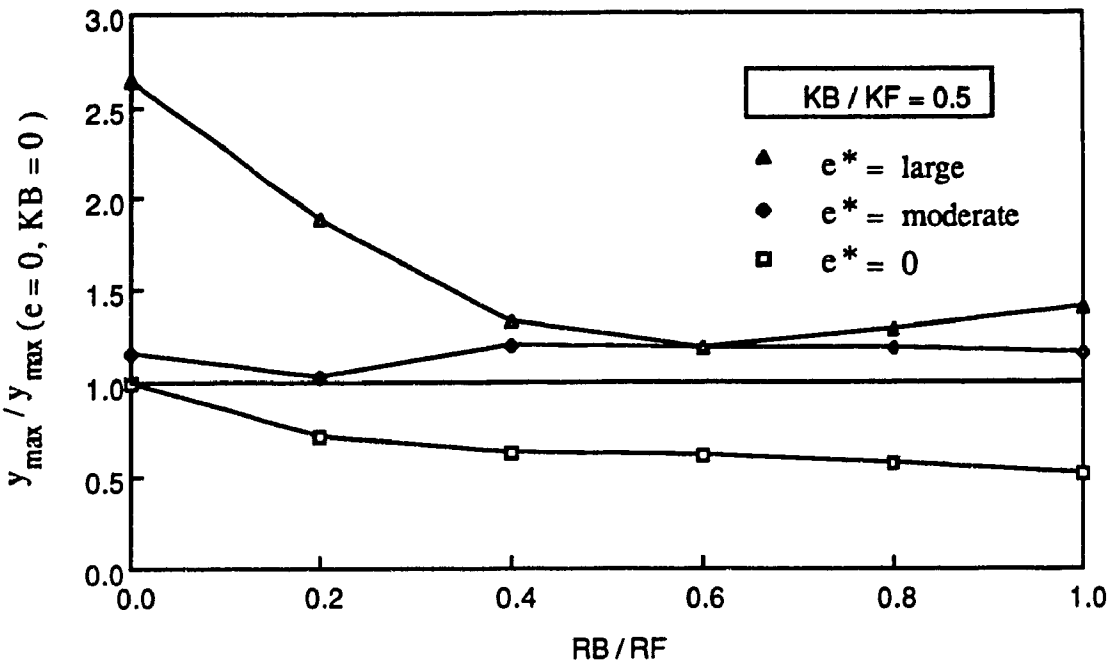

Fig. 5.10b Influence of Strength Ratio (RB/RF) - KB/KF = 0.5

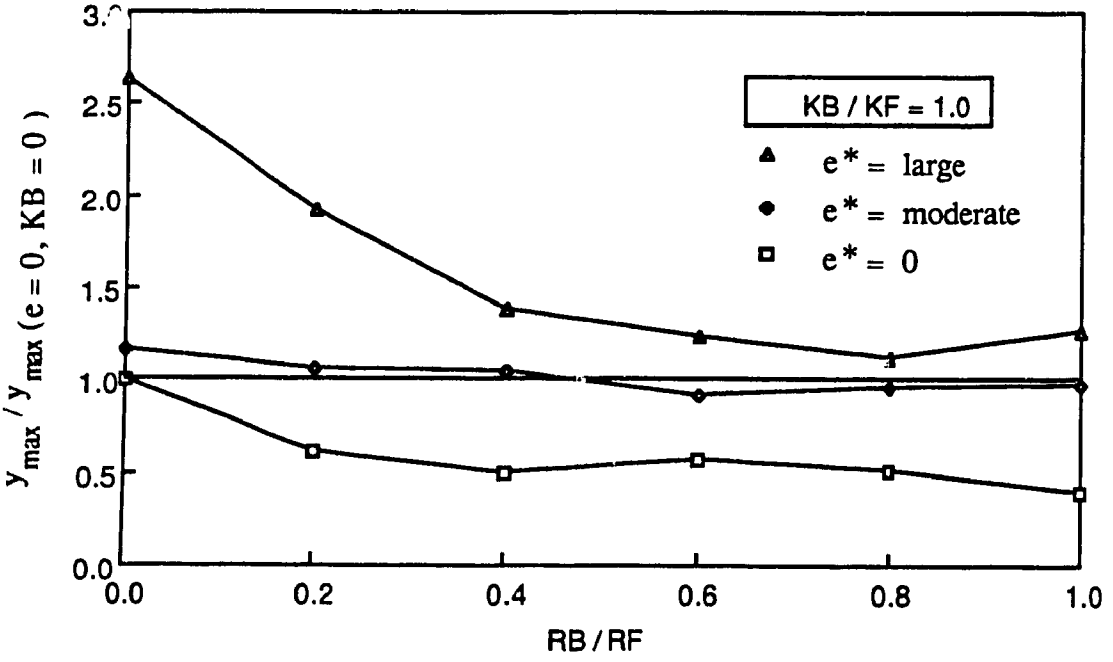

Fig. 5.11 Influence of Strength Ratio (RB/RF) - KB/KF = 1.0

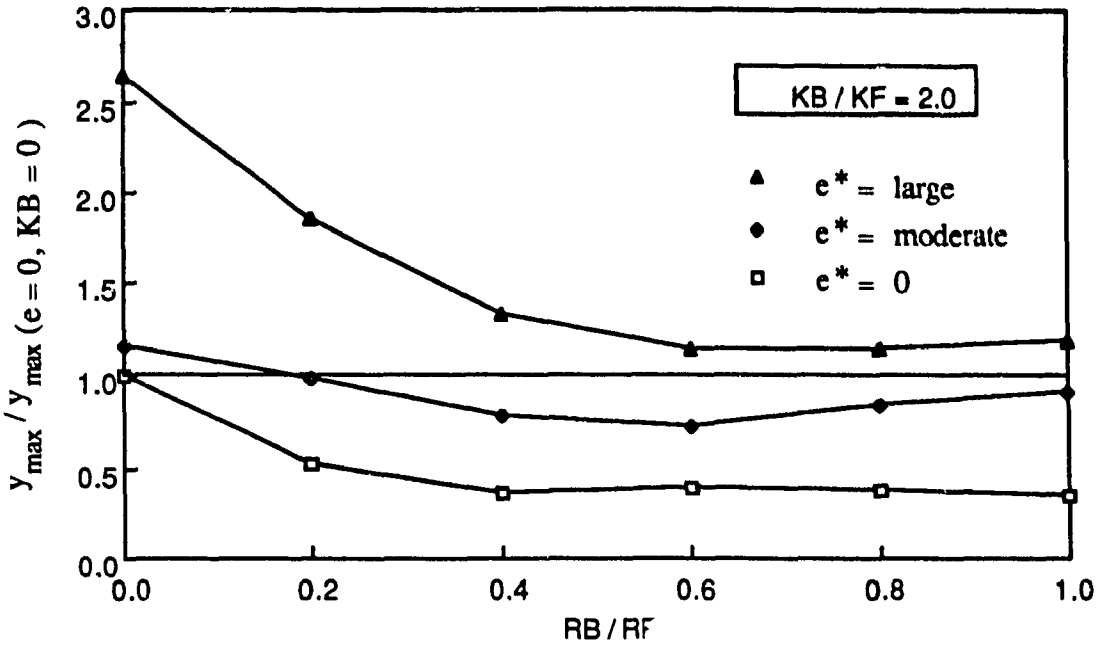

Fig. 5.12 Influence of Strength Ratio (RB/RF) - KB/KF = 2.0

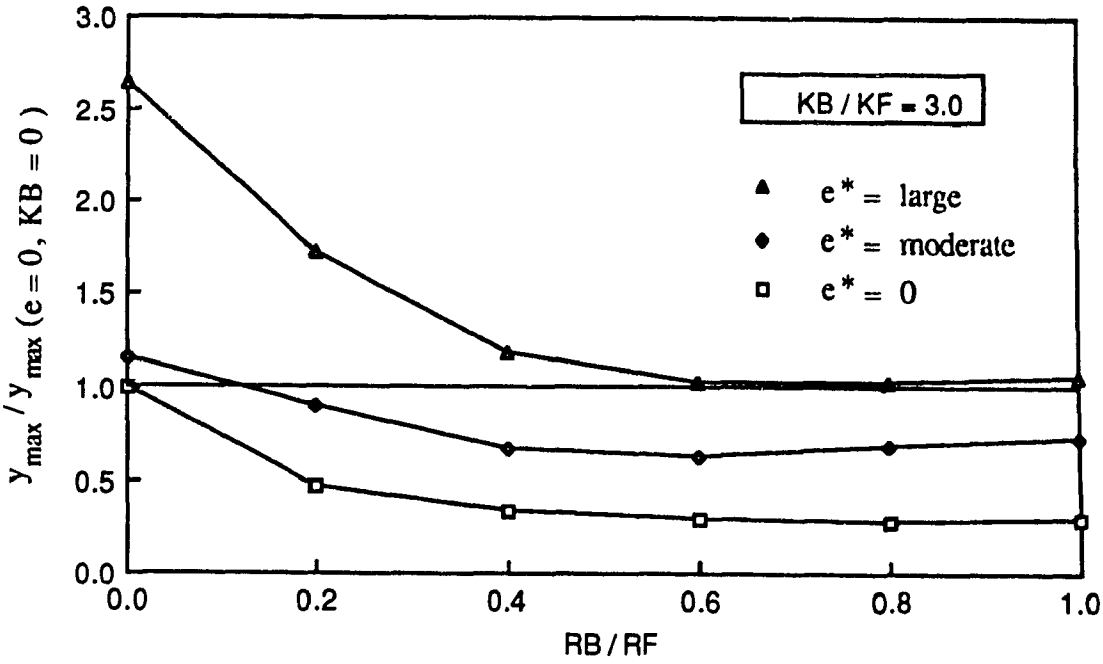

Fig. 5.13 Influence of Strength Ratio (RB/RF) - KB/KF = 3.0

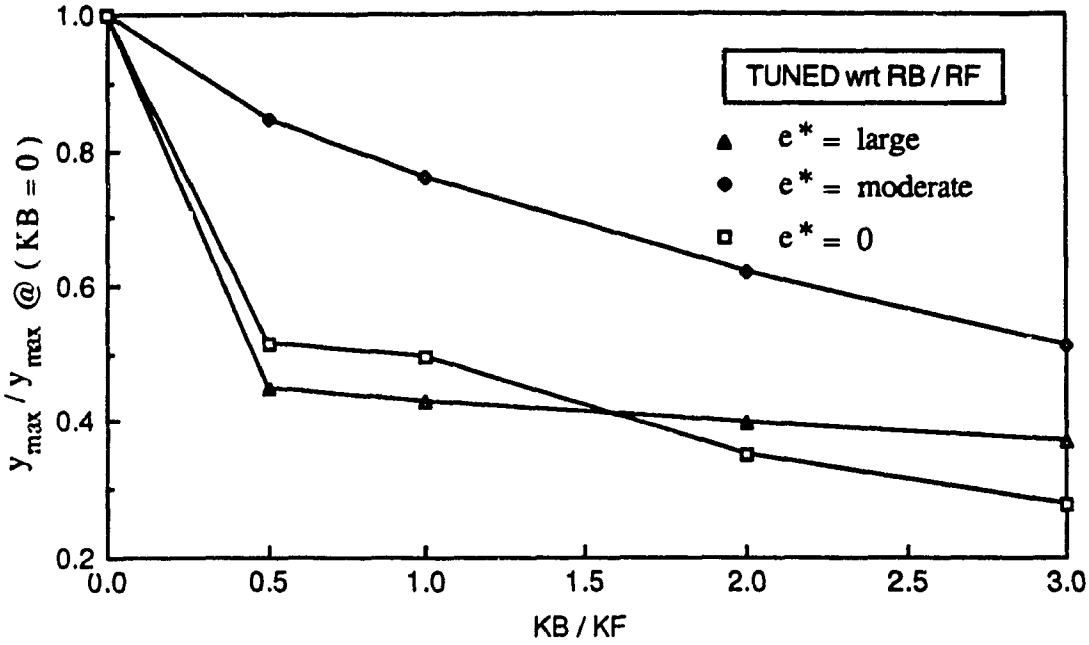

Fig. 5.14 Influence of (KB/KF) for Structures Tuned With Respect To RB/RF

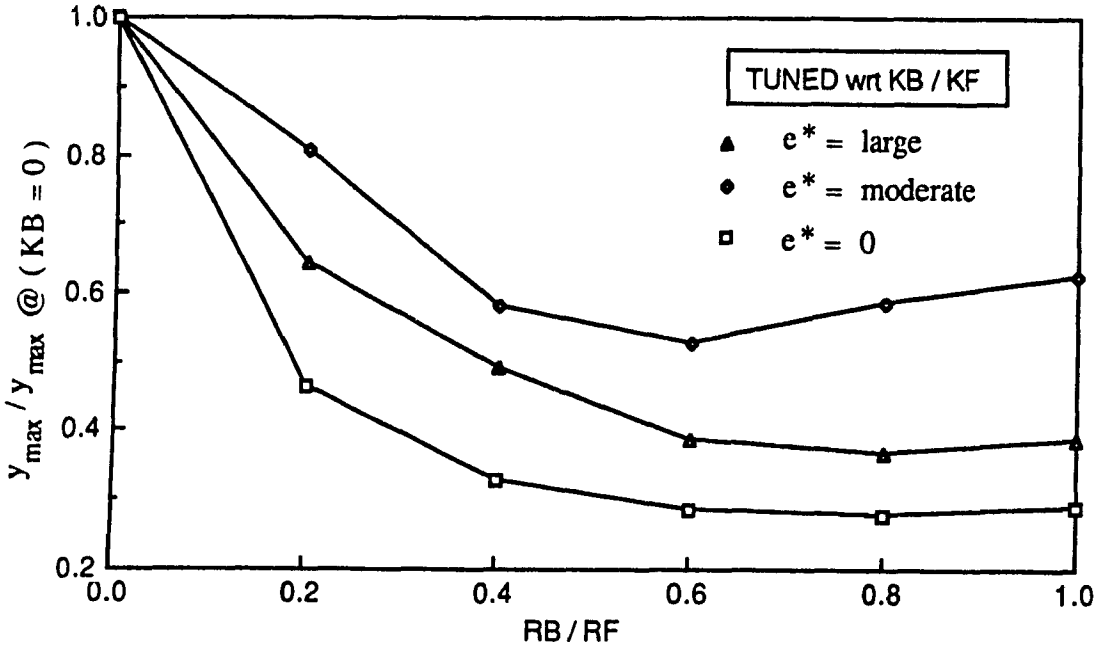

Fig. 5.15 Influence of (RB/RF) for Structures Tuned With Respect To KB/KF

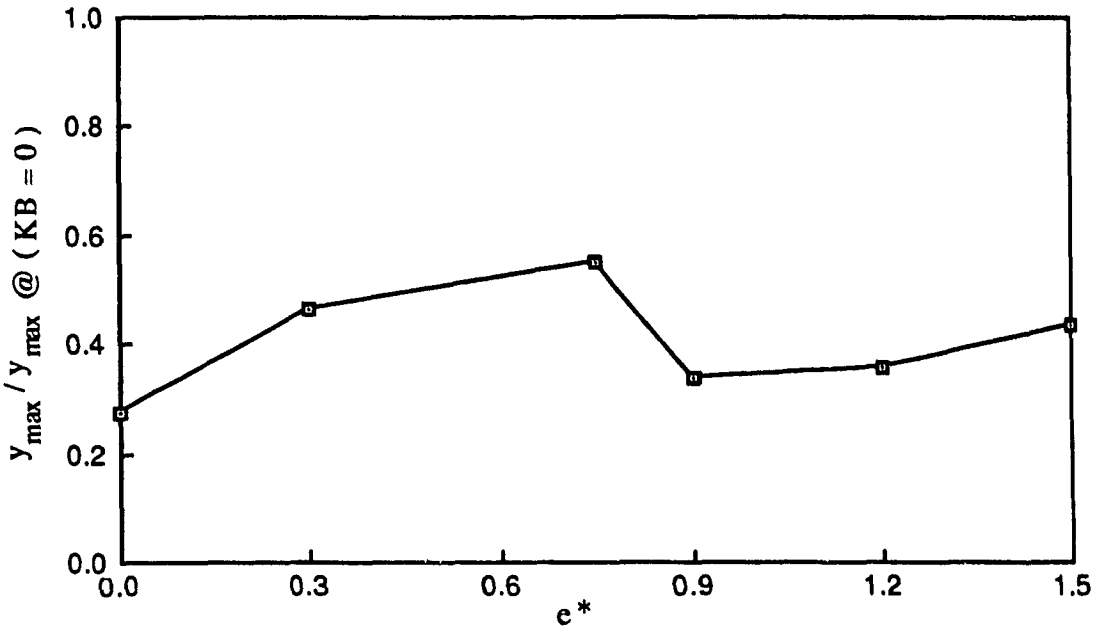

Fig. 5.16 Influence of Friction Devices on the Response of Tuned Eccentric Structures

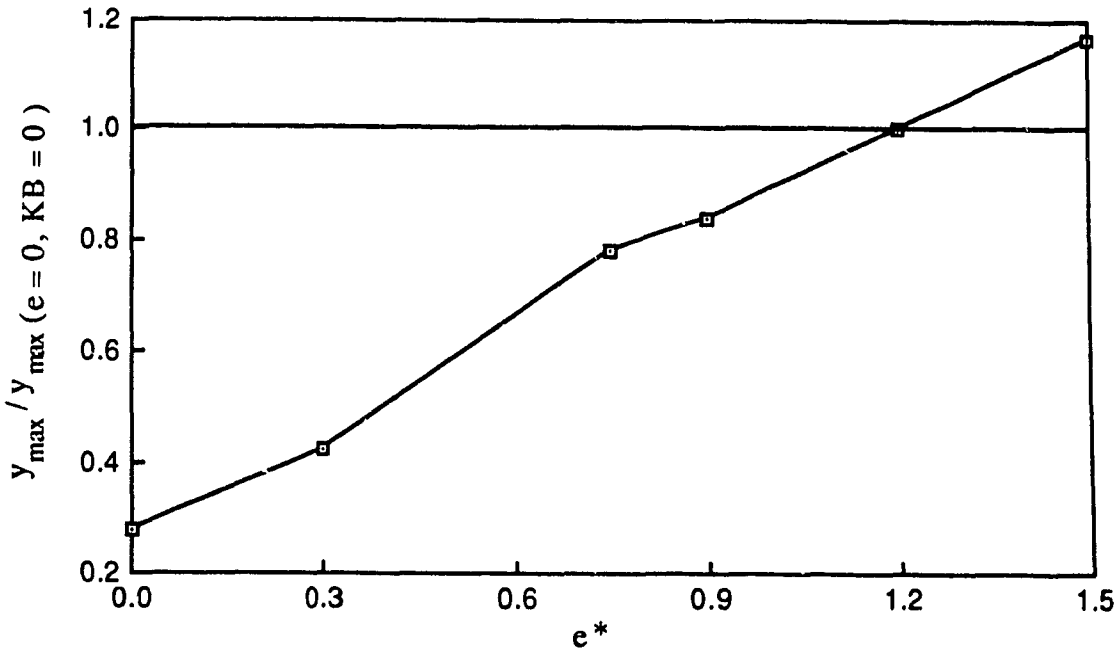

Fig. 5.17 Comparison of Response of a Tuned Structure with the Untuned Symmetric Response

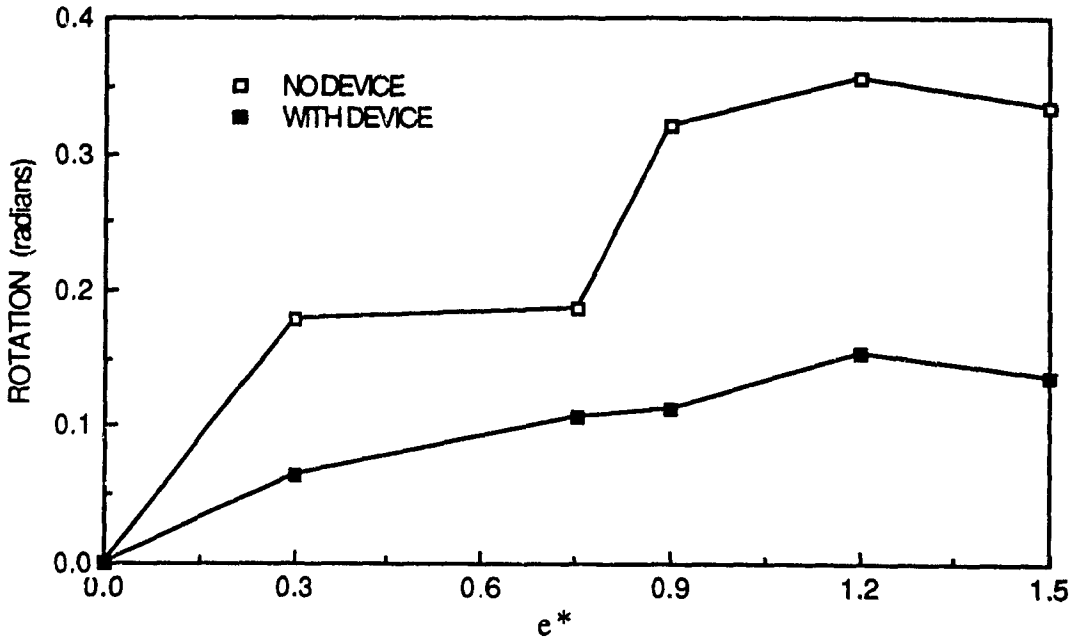

Fig. 5.18 Comparison of Maximum Rotations

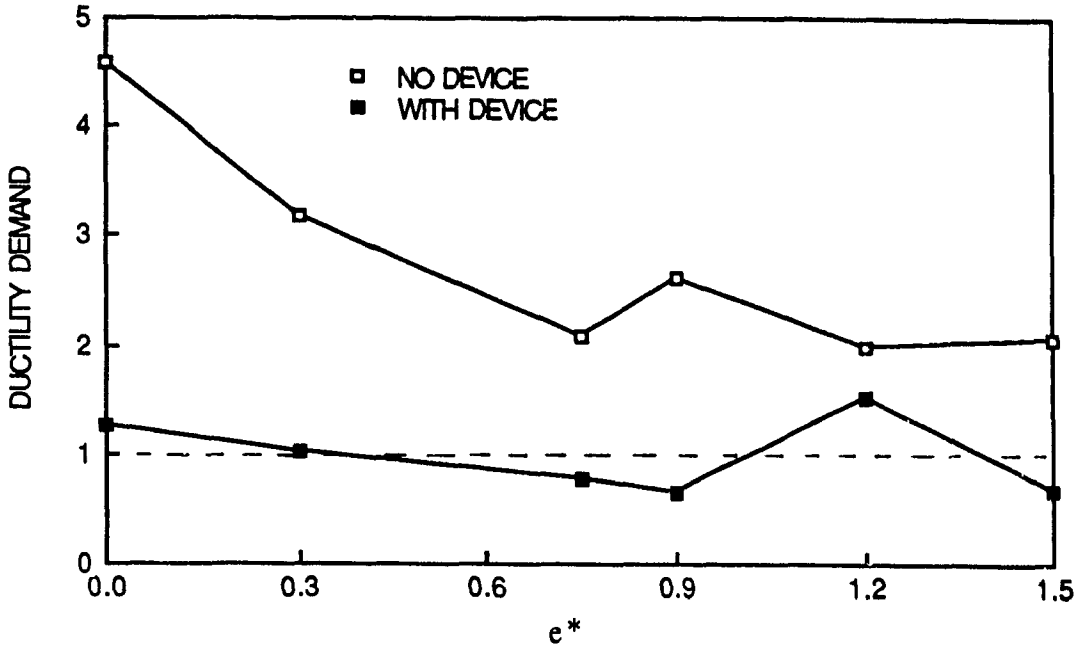

Fig. 5.19 Effect of Eccentricity on Ductility Demand of Frame Elements Located on the "Stiff Side"

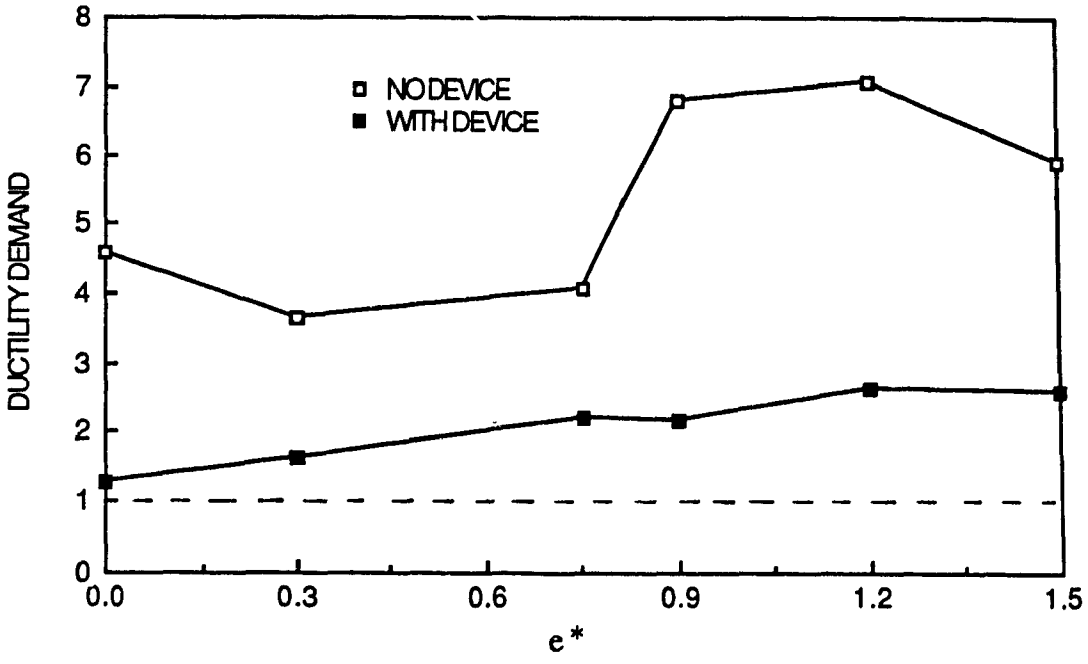

Fig. 5.20 Effect of Eccentricity on Ductility Demand of Frame Elements Located on the "Flexible Side"

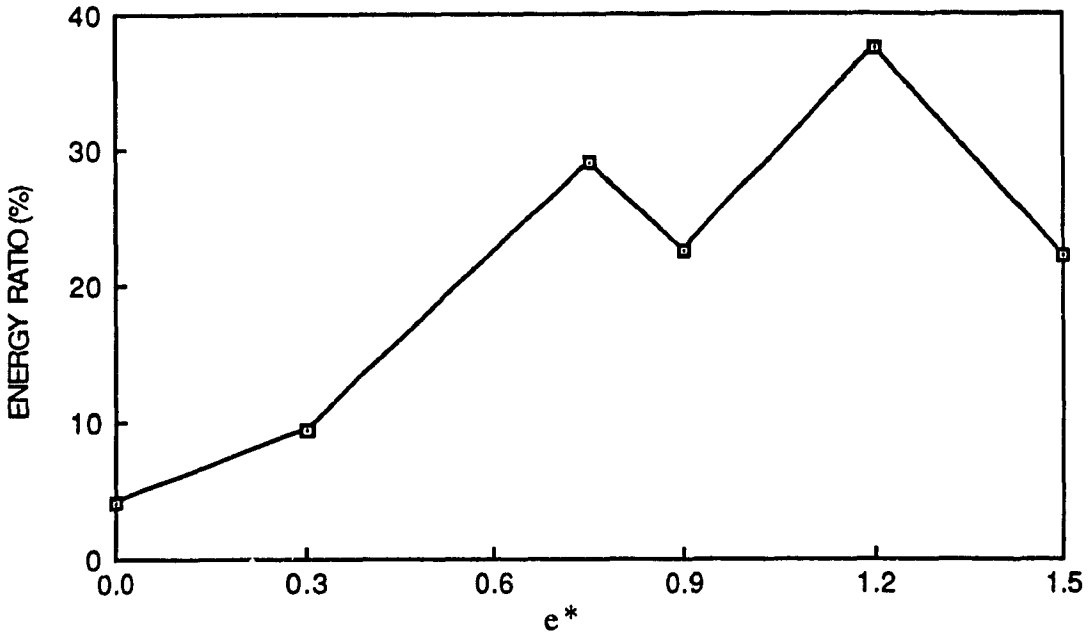

Fig. 5.21 Energy Absorbed By Inelastic Deformation of Frame Elements

CHAPTER VI

THREE DIMENSIONAL RESPONSES OF A STRUCTURE EQUIPPED WITH FRICTION BRACING

6.1 INTRODUCTION

This chapter evaluates the performance of friction damped braces which are being installed in the new Concordia University Library Complex by using a three dimensional dynamic inelastic analysis with the computer package Drain-Tabs [26]. Earlier a two dimensional study was performed by Pall [24] which showed substantial benefits when friction damped bracing devices were incorporated into a reinforced concrete moment resisting frame. In the present analysis a different device also patented by Pall is considered in which the compression brace is designed to sustain the slip load and therefore is not allowed to buckle. Thus the energy absorbed in each cycle is twice as much as bracing used in Chapter 5 and is similar to the friction bracing used by another investigator [25]. This modification is preferred because the 5 storey portion of the Library Complex, which is being analysed here, is considerably stiffer than the 9 storey part analysed by Pall, and will therefore attract larger seismic forces and energy input. To dissipate this energy, it was felt that a tension-compression brace is more suitable. Moreover, the NBCC also allows for a reduction in imposed seismic load of 23 percent when tension-compression diagonal bracing is used compared to tension bracing only [commentary J, NBCC 1985], because the tension-compression brace exhibits better post-elastic behavior. In Pall's design procedure [24] the braced frame must be designed to meet all the statutory requirements of the NBC in order for the structural engineer to fulfill his legal obligations; since friction bracing is not specifically mentioned, all provisions of the present code must apply.

The friction device is incorporated into this structure because it is considered an important structure (the code assigns an importance factor of I = 1.3 for a library building compared to I = 1.0 for a normal structure) and because expensive computer equipment will be stored there. It was recognized that the present code philosophy of designing structures with avoidance of collapse when subjected to severe earthquake excitation is not sufficient and that a novel approach to limit secondary damage is required.

According to NBCC 1985 (Table J2), the probability of a severe earthquake in Montreal is 10 percent in 50 years with a peak horizontal ground acceleration of 0.18g. Without friction bracing, considerable yielding could occur and large demands can be placed on the ductility of the standard moment resisting frame. Moreover it is also essential for the safety of the occupants that the demands placed on the ductility of the structure should not exceed the available ductility [26]

6.2 DESCRIPTION OF THE BUILDING

A plan view of the new library complex as initially proposed is shown in Figure 6.1, with east and west elevations shown in Figure 6.2 and Figure 6.3 respectively. The complex consists of three blocks separated by a galleria and an existing 8 storey building. The main 9 storey building was analyzed by Pall [24] using the two dimensional program Drain 2D [16] and his results showed considerable improvement in the building's seismic behavior when friction dampers were introduced into the moment resisting frame.

Note that the introduction of bracing induces eccentricity in the two 5 storey buildings when seismic forces act in the Y-direction. Since the two 5 storey buildings are essentially mirror images of each other, it is sufficient to analyze one of them.

The 5 storey portion is shown in Figure 6.4 and consists of the first storey at 5.3 m and four storeys at 4.2 m in height; the building is 36.9 m long by 27.6 m wide with columns spaced essentially on a 9 m grid. It also has an additional two levels of

basement. Fire hazards and clear storey height dictated the use of a flat slab reinforced concrete structure with drop panels [24]. Without bracing, lateral loads would be sustained by 6 frames in the X-direction, numbered I through VI and by 5 frames in the Y-direction, numbered VII through XI as shown on Figure 6.4. Note that without the braces, the structure is basically symmetric for X-direction excitation and has small eccentricity for Y-direction excitation.

The addition of friction bracing introduces very small eccentricity for X-direction excitation but potentially large eccentricity for Y-direction excitation depending on the stiffness of the brace compared to that of the frame. This sort of arrangement is not favoured by engineers but was imposed by architectural considerations. To circumvent this to some degree, the bracings were first designed using the minimum area of steel possible.

6.3 STRUCTURAL PROPERTIES OF THE BUILDING

The structural configuration of the 5 storey library building is given by Figure 6.4 for the floor plan with Figures 6.5 and 6.6 showing typical elevations of frames VI and XI respectively. Three types of elements are used; the first type labelled E1.# on the figures are truss elements to represent the braces; the second type labelled E5.# are beam elements to represent the flat slab; and the third type labelled E2.# are beam-column elements to represent the columns. The mass of the structure used for the analysis is 984,000 kg for floors 1 to 4 and account for superimposed dead loads whereas it is 719,000 kg at the roof and accounts for 25 percent snow load, note that in the calculation of structural mass a specific gravity of concrete of 2400 kg/m^3 is considered.

The moment capacities of the beam elements are approximately equal to the tributary width of the slab multiplied by 144 kN·m per meter of width and has elasto-plastic characteristics. This was assumed to ease calculations of inelastic energy

absorption. The slab is assumed 33 cm thick. The effective moment of inertia of beam elements are 15.5 x 10^{-4} m^4 per meter multiplied by the tributary width. Note that this effective moment of inertia in slabs is assumed 50% of the gross moment of inertia. The columns have the following structural properties:

Table 6.1 Properties of a Five Storey Reinforced Concrete Building

	Storeys	Effective Inertia	Moment Capacity	Axial Capacity
Rectangular	3-4-5	14.3×10^{-4} m^4	295 kN·m	6800 kN
weak direction	2	14.3×10^{-4} m^4	395 kN·m	7500 kN
	1	14.3×10^{-4} m^4	505 kN·m	7650 kN
strong direction	5	115×10^{-4} m^4	665 kN·m	7050 kN
	3-4	115×10^{-4} m^4	905 kN·m	8450 kN
	2	115×10^{-4} m^4	1115 kN·m	8750 kN
	1	115×10^{-4} m^4	1500 kN·m	9300 kN
Circular	5	47.7×10^{-4} m^4	525 kN·m	6800 kN
	2-3-4	47.7×10^{-4} m^4	655 kN·m	7500 kN
	1	47.7×10^{-4} m^4	725 kN·m	7650 kN

Note that the effective moment of inertia of the columns is 75% of the gross moment of inertia. A load moment interaction for these columns was assumed where the interaction diagram is bilinear with the change in slope occuring at a point $M_{max}=1.2\,M_0$ and $P = 0.6P_0$ where P_0 is the crushing load of a column without moment and M_0 is the maximum moment without axial load. The structural material properties of the building are as follows: f'_c = 40 MPa, E_c = 31600 MPa, ν_c = 0.15, f_y = 300 MPa, E_s = 200,000 MPa, and ν_s = 0.30; in which ν_c denotes Poisson's ratio for concrete and ν_s denotes Poisson's ratio for steel. The steel areas in the braces oriented parallel to the Y-axis are 4125, 2750, 1650, 1100, and 550 mm^2 for storeys 1 to 5 respectively; whereas for braces

oriented parallel to the X-axis their areas are 3850, 2750, 1650, 825, and 412.5 mm^2 for storeys 1 to 5 respectively.

The period of the structure in the Y-direction according to NBCC 1985 is given by $T = 0.09\ h_n/\sqrt{D_s}$ for a braced structure where h_n is the height of the building in meters and D_s is the width of the lateral supporting element in meters. Thus for a braced bay of 9 m the period is $T_{FDBF} = 0.663$. For a moment resisting frame the code gives the period as : $T = 0.1\ N$ and for a 5 storey building this gives $T_{MRF} = 0.5$ sec.

Figure 6.7 gives the pseudo-static displacements for Y-direction excitation ,and provides the means for a more refined analysis by simply using the Rayleigh approximation given in the 1980 NBCC supplement commentary J :

$$T = 2\pi \{(\sum_{i=1}^{n} W_i \ (\delta_i)^2)/(g\ [\ (\sum_{i=1}^{n-1} F_i \ (\delta_i)) + (F_t + F_n) * (\delta_n)\ ])\}^{0.5} \qquad (6.1)$$

where F_i is the applied force and δ_i is the corresponding deflection at floor " i " .
When this is done for Y- direction excitation: $T_{FDBF} = 1.115$ sec. and $T_{MRF} = 1.261$ sec. For X- direction excitation the periods are: $T_{FDBF} = 0.998$ sec. and $T_{MRF} = 1.227$ sec., as discussed later in section 6.6.2.

According to Pall [24], the braces carry constant load while slipping and additional loads imposed to the inter-storey shear are carried by the moment resisting frame, with a resulting redistribution of forces between successive storeys which compels all the braces to slip and participate. Pall's optimum slip load for the 9 storey building was approximately double the force developed in the bracing using the pseudo-static procedure and was relatively constant at a value between 500 - 700 kN. This study for the 5 storey building found the optimum slip load of the bottom brace in each direction to be approximately triple the force developed in the brace due to quasi-static earthquake loads,

which differs a little from Pall's observations. The optimum slip load was found by trial and error with load increments of 50kN. Another significant feature observed during the present study is that it is necessary to reduce the slip load in the braces used at higher storeys of the building. Thus the slip loads per brace being used in the present study for Y- direction excitation are as follows: 1st storey - 750 kN, 2nd storey - 500 kN, 3rd storey - 300kN, 4th storey - 200kN and 5th storey - 100 kN. This is reasonable because earthquake inter-storey shears are relatively small at the top and large at the bottom of high rise buildings. Since the stiffness of the brace is small compared to the frame, the structural interaction may be small which explains the discrepancy with Pall's findings. Moreover it should be noted that for Y- direction excitation the slip loads of the braces located on the first floor correspond to 2 braces of 750 kN for 5 lateral resisting frames whereas Pall's study [24] gave 4 braces of 700 kN for 9 lateral resisting frames which suggest a similar proportion.

6.4 DEFINING THE STIFFNESS OF A STRUCTURE

For the one storey structure considered in Chapter 5, it was relatively easy to find the stiffness of the brace as the ratio of its force to its displacement. However, in multi-storey buildings, there are many interstorey shears and several important storey deflections such as edge displacements, center of mass displacements, and center of resistance displacements.

This section defines the stiffness of a structure as the ratio of the base shear to the displacement of the center of resistance at the top of the structure, when the pseudo-static seismic loads of NBCC1985 [17] are applied at the center of resistance of each floor. For the 9 storey portion Pall [24] gives top deflections of 53 mm and 27 mm for the MRF and the FDBF respectively when subjected to the pseudo-static forces of NBCC 1985. This implies a stiffness ratio of (KB/KF) ≈ 1.0. For the 5 storey building of this study, the top

displacements under pseudo-static forces acting in the Y-direction through the centers of resistance of the structure was found to be 20.4 mm for the MRF and 16.5 mm for the FDBF which gives (KB/KF) ≈ 0.25. The code static base shear is 1464 kN and was distributed along the height as per the NBC code.

Using the period of the structure, the ratio of stiffness of the FDBF to the MRF can be found by:

$$(K_{FDBF} / K_{MRF}) = (T_{MRF} / T_{FDBF})^2 \qquad (6.2)$$

Thus $K_{FDBF} / K_{MRF} = 1.279$ which implies KB/KF ≈ 0.28 for Y-direction excitation, and $K_{FDBF}/K_{MRF} = 1.51$ which implies KB/KF ≈ 0.51 for X-direction excitation.

These KB/KF ratios are rather low, but it is important to emphasize that the low stiffness of the bracing was dictated from the need to reduce the eccentricity due to the poor placement of the lone braced bay as imposed by the architectural limitations. Also note that the ratio of KB/KF gives the ratio of lateral stiffness of bracing acting alone to that of the frames without braces. Results of the parametric study of Chapter 5 indicate that although of benefit, the reduction in response at (KB/KF) ≈ 0.25 will be less beneficial than that at (KB/KF) ≈ 1.0.

6.5 DEFINING THE CENTER OF RESISTANCE

The eccentricity in a one storey structure is easily found, and obtained from the distance between the center of mass CM and the center of resistance CR; as discussed in Chapter 3. To assess the eccentricity in a multistorey building the process involves finding CM at every level, which is simple once the distribution of mass is known, and determining the center of resistance, which is more difficult since there is no consensus on its definition. According to Humar [28] the centre of rigidity at a floor is defined as the point through which the resultant lateral force of that level acts and causes no rotation of

that floor although other floors may rotate. Cheung and Tso [29] define the center of rigidity of a multistorey building as the locus of points located at each floor level such that when a given distribution of lateral loads passes through them, no rotational movement of the building about a vertical axis occurs. It was recognized by these researchers that a building with identical floor plans may have different centers of rigidity depending on the level considered, especially for wall-frame structures due to the wall-frame interaction. Since a similar interaction exists between moment resisting frames linked to a braced frame, it is expected in this study that the centre of resistance will vary with height.

The definition of centre of resistance used in this study is different from that employed by other researchers [28, 29] since it makes use of a torque applied by horizontal couples at a floor level to find the point about which rotation occurs for that floor. Hence the present study requires the use of three-dimensional computer elastic analysis for this purpose. This procedure is simple and gives eccentricity simultaneously in each direction. Thus to find CR along the height of the 5 storey library building requires only 5 computer runs for each of the two cases considered (MRF and FDBF). This process is believed simpler than the approach proposed by Cheung and Tso which required the two dimensional analysis of every frame, and to that proposed by Humar which required the trial and error placement of loads. Using the torque procedure the centers of resistance for the Y-direction excitation along the height of the building were found and results are shown in Figure 6.8. Note that as expected the center of resistance in each case does not lie on a vertical line. Since the application of static loads at the CR locations shown in Figure 6.8 caused no rotation, it indicates that these are indeed the center of resistance of the elastic structure.

6.6 DISCUSSION OF RESULTS

The analyses consisted of subjecting the structure to 6 seconds of the Newmark-Blume-Kapur artificial earthquake first in the Y-direction and then the X-direction using the computer program DRAIN-TABS [26]. This time limit was imposed to reduce the computer costs. Each run took 3000 sec of CPU time on the 835 CYBER from Control Data Corporation. Figure 6.9 shows the earthquake time history for 15 seconds; since several acceleration peaks of large magnitude occur between the time span of 2 and 5 seconds it suggests that results are still valid. In addition zero structural damping was assumed to enable easy energy calculations. The time step used for the analyses was 0.01 sec. although a verification at time steps 0.0075 and 0.005 seconds gave almost identical responses.

The building was further analysed by assuming a shift in the center of mass in the X-direction from the centroid by a distance of $\pm$ 0.25 D_n thus giving large eccentricity for Y-direction excitation. This enables comparison of the structural behavior with and without friction bracing at large eccentricity. Optimization of the slip load was first done in the Y-direction with the low KB/KF value chosen. Similar cross-section of truss elements were used in the X-direction, thus giving a KB/KF value of approximately 0.5. The results are compared with those for KB/KF of approximately 1.5 , this latter value was achieved by a fourfold increase in the cross-sectional area of the braces.

6.6.1 Earthquake in the Y-Direction

6.6.1.1 Edge Displacement Response

The floor plan of the building indicates that should an earthquake act through the center of mass located at the centroid of the structure torsional motion would arise since the building layout is not symmetrical. Figure 6.4 shows that eccentricity exists in both

the MRF and the FDBF. For the Y-direction excitation it is very low, $e \approx 0.02\ D_n$ for the MRF case; to low, $e \approx 0.10\ D_n$ for the FDBF. The eccentricity for FDBF is approximately equal to the accidental eccentricity provisions of NBCC 1985 and this suggests that results can be compared to those found for the calibration eccentricity of $e^* = 0.30$ ($e = 0.10\ D_n$) as used in Chapter 4 and to the parametric study with value of $e^* = 0.30$ used in Chapter 5.

It is known that eccentricity causes an increase in edge displacement and so it would seem that the placement of a device which increases eccentricity would result in an increase in response. However, friction damped braces absorb seismic energy input by friction which reduces the response. It is therefore expected that for this structural layout the device may not be as efficient as that of Chapter 5. Figure 6.10a and Figure 6.10b present the displacements at the flexible side and stiff side of the building respectively, for KB/KF≈0.25 whereas Figures 6.11a and 6.11b are for KB/KF≈1.0. Figures 6.11c and 6.11d compare the edge response for different stiffness ratio used for frame VII and XI respectively. In the case of KB/KF≈0.25 the reduction in response caused by the lone friction braced bay is only 15.2 percent for frame VII whereas it is 38.3 percent for frame XI. Note that this is achieved even though the rotation of the deck increased by 458 percent to 0.00095 radians (0.054 degrees) as shown in Figure 6.12. The rotation is relatively small for FDBF due to the presence of a braced bay near each edge of the building in the X-direction. Note that for Y-direction excitation the brace in the X-direction are present but do not slip as the maximum force induced in them is approximately 1/4 of the slip load.

Stacks of books in library buildings are usually placed in one area, whereas study rooms are in another area. This could impose a non-uniform distribution of mass on the structure and create an eccentricity of almost $0.08\ D_n$ if the live load ($7.2\ kN/m^2$) is placed on half of the floor plan. Should other accidental eccentricity occur, say due to variation of strength, of $0.10\ D_n$ a total accidental eccentricity of $0.18\ D_n$ is conceivable. For this

study an analysis of eccentricity effects was done for e = ± 0.25 D_n which represents an extreme case in such a structure.

Figure 6.13a and Figure 6.13b reveal the influence of large eccentricity for this structure. Figure 6.13 considers that the mass center is placed 0.25 D_n to the left of the centroid along the X- axis thus inducing an eccentricity when seismic excitation acts in the Y-direction. The eccentricity between CR and CM is approximately 0.23 D_n for the MRF whereas it is almost 0.35 D_n for the FDBF. Figure 6.13a shows considerable improvement in response of the flexible edge when friction braces are used and the response of frame VII is 106 mm for the MRF and 768 mm for the FDBF which represents a reduction of 27.7 percent. The stiff side (frame XI) has also some improvement and Figure 6.13b shows a reduction in edge response of 13.9 percent, from 46.7 mm in the MRF case to 40.2 mm in the FDBF case. When the cross sectional area of steel used for the brace is increased 4 times the improvement in the structure's response by the inclusion of the braces is even more significant. Figure 6.14a and 6.14b show the comparision in response between FDBF and MRF for the flexible side (frame VII) and stiff side (frame XI) respectively when the area of steel is increased, whereas Figure 6.14c and 6.14d show the comparision of response in frame VII and XI respectively between the FDBF with KB/KF ≈ 0.25 and FDBF with KB/KF ≈ 1.0.

Figure 6.15a and Figure 6.15b give the edge displacement of frame VII and frame XI respectively when the structure's center of mass, CM, is located at + 0.25 D_n from the centroid on the X- axis. This shift in CM gives rise to an eccentricity between CR and CM, for Y-direction excitation of e ≈ 0.27 D_n for the MRF and e ≈ 0.15 D_n for the FDBF. Thus frame VII becomes the "stiff" edge, and Figure 6.15a indicates a reduction in response from 48.3 mm for the MRF to 34.1 mm for the FDBF. Figure 6.15b presents the displacement of frame XI which for this eccentricity is on the "flexible" side. Again the reduction in edge displacement due to the device is impressive, from 104 mm for the MRF to 66 mm for the FDBF; a decrease in response of 36.3 percent.

When the cross sectional area of steel is increased 4 times again the improvement in the structure's response by the inclusion of braces is increasingly significant. Figures 6.16a and 6.16b show the benefits in case of frame VII and XI respectively, whereas Figure 6.16c and 6.16d compare the edge displacement response of frame VII and XI respectively for the different stiffness ratios used.

6.6.1.2 Peak Ductility Demand

Ductility in a structure subjected to severe earthquakes is a desirable feature since it allows the structure to deform inelastically without collapse. Because each structural element has a ductility limit it is important to investigate the peak ductility demand requested by an earthquake. Figure 6.17 shows the ductility demand of the library building when it is assumed that the center of mass distribution lies at the centroid of the floor deck. This figure reveals that the friction damped braces reduce the ductility demand on frame elements by as much as 36.6 percent and that all frame elements are within the elastic limit when tuned friction braces are used. This is not the case for the MRF which is without friction bracing.

Since for frames VII - XI the peak ductility demand for the MRF case lies above the ordinate 1.0, yielding occurs in each frame. The level of damage in frames VII through XI imposed by 6 seconds of the Newmark-Blume-Kapur artificial earthquake at 0.18 g is shown by black circles indicating yielding of the member at that location in Figure 6.18 for the MRF case and in Figure 6.19 for the FDBF case. Figure 6.18 shows that the damage is more severe in frames X and XI which can be explained by the fact that these are on the "flexible side" of the structure for the MRF case. Figure 6.19 shows no black circles since none of its members yielded. Note the letter "A" on the brace diagonal indicates that the device was activated and the actual diagonal member did not yield.

Figures 6.20 shows the peak ductility demand for the case of the center of mass located at $-0.25D_n$ on the X- axis. Note that the decrease in ductility demand is minimal

and can be explained by the fact that for a left shift in CM the eccentricity is larger for the FDBF than for the MRF. Figures 6.21 and 6.22a show the damage in the MRF and the FDBF respectively for this condition. Note that only a few members of the FDBF yielded slightly in this case. Figure 6.22b presents the damage for the braces with increased steel area and shows that now no yielding occured.

Figure 6.23 shows the peak ductility demand for the case of CM located at $+0.25D_n$ on the X- axis, and indicates that the friction braced device is effective in reducing the ductility demand for the flexible side of the building with a reduction of 32.3 percent in frame X and 38.9 percent in frame XI. This reduction in response or in ductility demand of the flexible side of the structure is more desirable than on the stiff side since most of the damage is expected for the flexible side of the building. Figures 6.24 and 6.25 present the damage in the MRF and FDBF for this condition. It can again be seen that the friction devices improve the behaviour of the structure considerably when it is subjected to Y-direction excitation. Figure 6.25b shows that for the case of the brace with increased steel again there is no yielding.

6.6.1.3 Energy Absorption

Standard practice for the aseismic design of structures allows for large inelastic deformation, provided proper detailing is done to assure sufficient ductility. An early study by Jennings [19] showed that most of the seismic energy input into a normal structure is consumed by plastic displacement with the elastic strain energy small in magnitude by comparison. The advantage of the friction braced device, when it is properly tuned to a structure, is that it protects the building by absorbing the excess energy input.

Figure 6.26 shows both the inelastic energy absorbed in the moment resisting frame acting alone and the energy dissipated by the friction braces when subjected to Y-direction excitation with the center of mass located at the structure's centroid. The

inelastic energy shown for the moment resisting frame is given by the summation of the product of the moment capacity and the accumulated plastic rotations of each member. This is valid because of the simplification of elasto-plastic behavior for the beams and for the columns. The energy absorbed by the friction braces is the summation of the product of the slip load and the slip displacement for each brace. Since none of the members of the moment resisting frame in the FDBF case yielded, this summation represents the total energy absorbed. Note that, as shown in Figure 6.26, the energy consumed by the bottom brace is many times greater than that of the other braces, and special care should be placed in designing its members. The total energy consumed in the FDBF is 70.9 kN·m whereas it is 22.0 kN·m for the MRF.

Figure 6.27 shows the inelastic energy absorption when center of mass is shifted by $-0.25D_n$ on the X-axis; and indicates that the friction device is not as effective in absorbing energy. The energy absorbed by the friction braces is 11.8 kN·m, and some yielding occurred in the moment resisting frame equivalent to 4.15 kN·m (not shown in Fig. 6.27) for a total of 16 kN-m for the FDBF, whereas the energy absorbed by the MRF alone is 22.6 kN·m.

Figure 6.28 shows the inelastic energy absorption for the case of CM located at $+0.25D_n$ and indicates large energy consumption by the MRF and also large dissipation of friction energy in the FDBF. The total energy absorbed by the MRF is 56.6 kN·m whereas it is 67.3 kN·m for the FDBF. It can therefore be concluded that the effects of positive eccentricity are less deletrious for the FDBF then negative eccentricity since its braces are able to absorb more energy, which is its prime function. Thus if there is a choice as to the location of the book stacks, they should be placed on the edge of the lone brace if not at the center of the structure.

6.6.2 Earthquake in the X-Direction

The direction of the earthquake excitation is not known to the designer, and he must assume that it can be directed in the worst possible orientation; however, it is usually sufficient to analyse a building in two orthogonal directions which match the structure's grid lines. This section considers the effects of earthquake excitation oriented in the X-direction on the structure. The structural properties of the frames were discussed in a previous section. The braces were designed with the same yield stress and the slip load optimization gave 1st storey - 700 kN, 2nd storey -500 kN, 3rd storey - 300 kN, 4th storey - 150 kN, and 5th storey - 75 kN which differs a little from the Y- direction. The analysis of the structure under code pseudo-static forces gives a top deflection of 19.15 mm. for the MRF and 13.42 mm. for the FDBF as shown in Figure 6.29. The eccentricity for X-direction excitation, as mentioned earlier, is small; Figure 6.30 shows that it does not exceed 1.15 percent for the MRF and 1.70 percent for the FDBF. For X-direction excitation, the Rayleigh approximation given by Equation 6.1 leads to a period T=1.227 seconds for the MRF and T=0.998 second for the FDBF. Thus using Equation 6.2 gives a stiffness ratio KB/KF≈0.5.

Figure 6.31 and Figure 6.32 show the maximum edge displacement with the friction damped bracing (FDBF) and without (MRF) . A small improvement is found in the top displacement of frame VI with a reduction in response of 17.1 percent. Figure 6.33 shows that the use of two braces reduces the rotation of the deck by 33 percent which is much better than the 458 percent increase when one brace was used in the Y- direction.

Figure 6.34 shows the peak ductility demand in frames I to VI. The reduction in demand caused by the inclusion of friction braces is considerable; it is 31.7 percent for frame I and 43.2 percent for frame VI. Moreover the reduction occurs where designers expect the largest ductility demand and so the results are evenmore meaningful. Furthermore, Figure 6.34 shows that the peak ductility demand of the FDBF is less than one for all frames and implies that no member has yielded for this case.

Figure 6.35 indicates the large energy dissipation by the friction braces which totals 275.1 kN·m whereas the seismic energy input absorbed by inelastic deformation totals 20.8 kN·m for the MRF case. Thus it can be seen that the braces are effective in absorbing seismic energy. Figure 6.36a shows the yielding that occured in frames I to VI of the MRF and Figure 6.36b shows that the bracing effectively protected the frames from inelastic deformation when the structure is subjected to X-direction excitation with peak acceleration of 0.18g. Since the edge responses are large, even though large energy absorption occurred, it suggests that energy optimization via the slip load is not sufficient.

To investigate the above suggestion a trial run was done in the X- direction with a threefold increase in stiffness ratio to KB/KF ≈ 1.5 and achieved by increasing the area of each brace four times. This was done because it was concluded in Chapter 5 that tuning with respect to KB/KF can be as beneficial as tuning with respect to the slip load. For this situation the period of FDBF is T=0.76 second using the Rayleigh approximation. Results are shown in Figure 6.37a and Figure 6.37b for frame I and frame VI respectively. Note the very significant reduction in response for the FDBF compared to the MRF; it is 45.9 percent for frame I and 53.9 percent for frame VI. Figures 6.38 and 6.39 present the comparison in response for the FDBF for stiffness ratios KB/KF ≈ 1.5 and KB/KF ≈ 0.5 and shows the considerably superior performance of the braces with the higher stiffness ratio. This corroborates the findings of Chapter 5 and suggest that tuning with respect to the stiffness ratio is as important as with the slip load. Figure 6.40 shows that increasing the stiffness ratio does not introduce any yielding of frame elements and moreover the top floor braces are now activated, which suggests stronger frame-brace interaction.

Further, additional analyses were performed which involved subjecting the same structure (with KB/KF ≈ 1.5) to an X - direction earthquake of 0.315g. For this earthquake the displacements of frames I and VI are shown in Figures 6.41a and 6.41b respectively; in which it can be observed that the response for the FDBF are only 64.6

percent of the MRF response for frame I and 56.1 percent for frame VI. Figures 6.42a and 6.42b show the impressive reduction in member yielding when friction bracing with a good stiffness ratio is introduced to the structure should it sustain 0.315g peak acceleration. Note that even though the earthquake acceleration is increased by 75 percent all the members of the FDBF remain elastic.

6.7 SUMMARY

The benefit of incorporating friction braces in the library building as initially proposed was evaluated. For this case study, it was found that the use of friction bracing reduces the response of the structure in the Y- direction with the proposed location of bracing; and also decreases the peak ductility demand considerably. It was found that the response of a fictitious structure having similar characteristics as the library building but with a shift in CM by $\pm 0.25\ D_n$ would benefit moderately from the inclusion of friction braces. This was explained by the poor placement of the lone braced bay located at the edge of the structure.

An investigation of the effects of friction bracing in the X- direction for the proposed structure showed reduction in rotation, reduction in peak ductility demand, and good absorption of seismic energy, but small reduction in edge displacement. When the structure was modified with an increase in stiffness ratio to a value of $KB/KF \approx 1.5$ a significant reduction in edge displacement was also obtained. This implies that the stiffness ratio is an important parameter to consider in the design of friction bracing. Note that only one run was done at the higher stiffness ratio. Computer costs are such that they prohibit a parametric study with three-dimensional analyses of the inelastic behavior of a multistorey building .

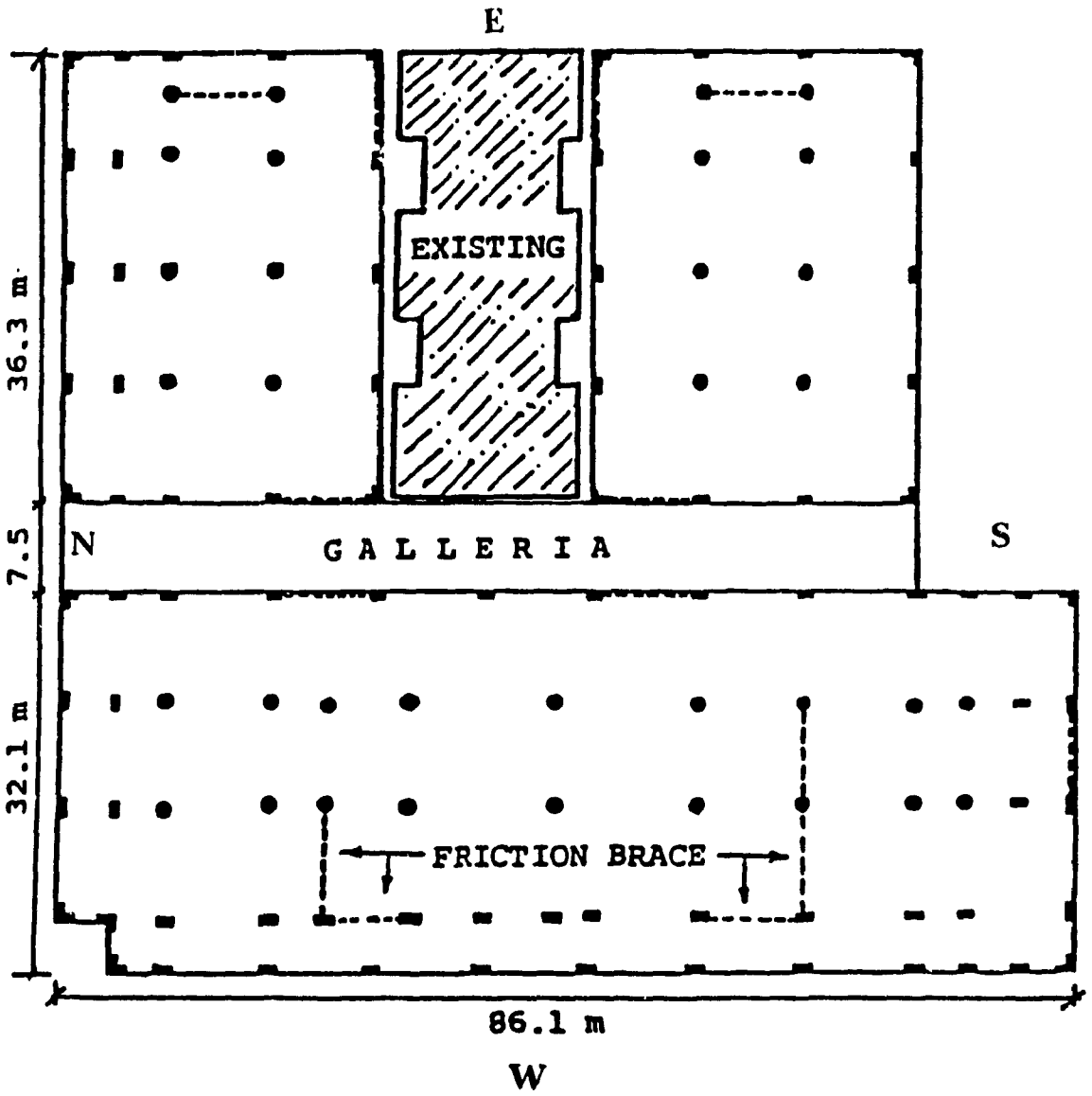

Fig. 6.1 Plan View of the New Concordia Library Building Complex[24]

Fig. 6.2 View from McKay Street [24]

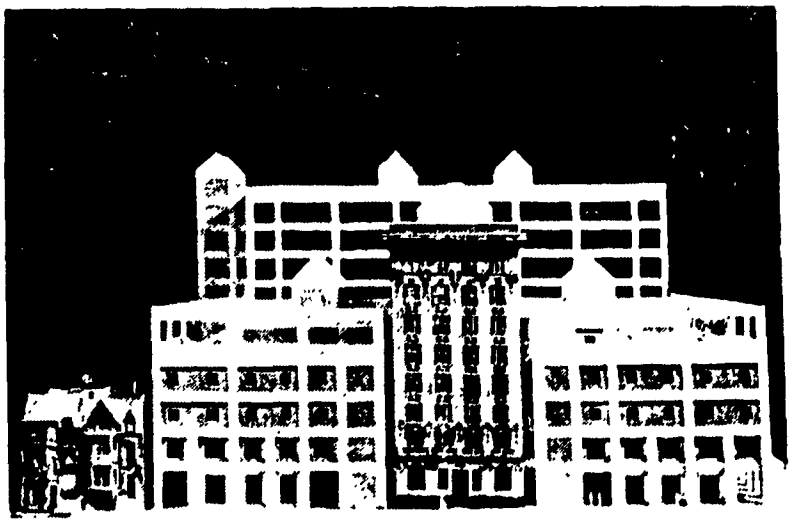

Fig. 6.3 View from Bishop Street [24]

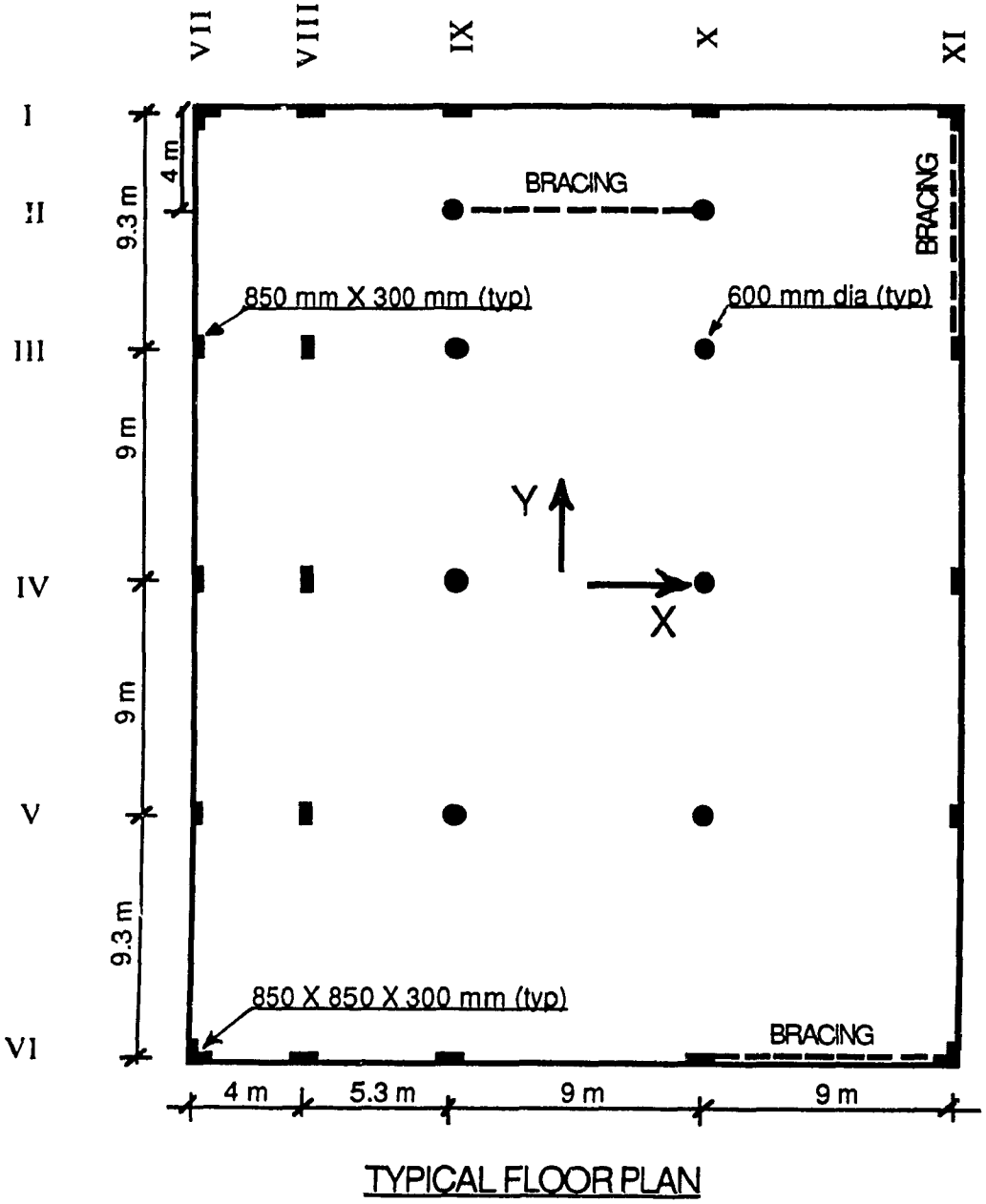

Fig. 6.4 Floor Plan of the 5 Storey Library Building

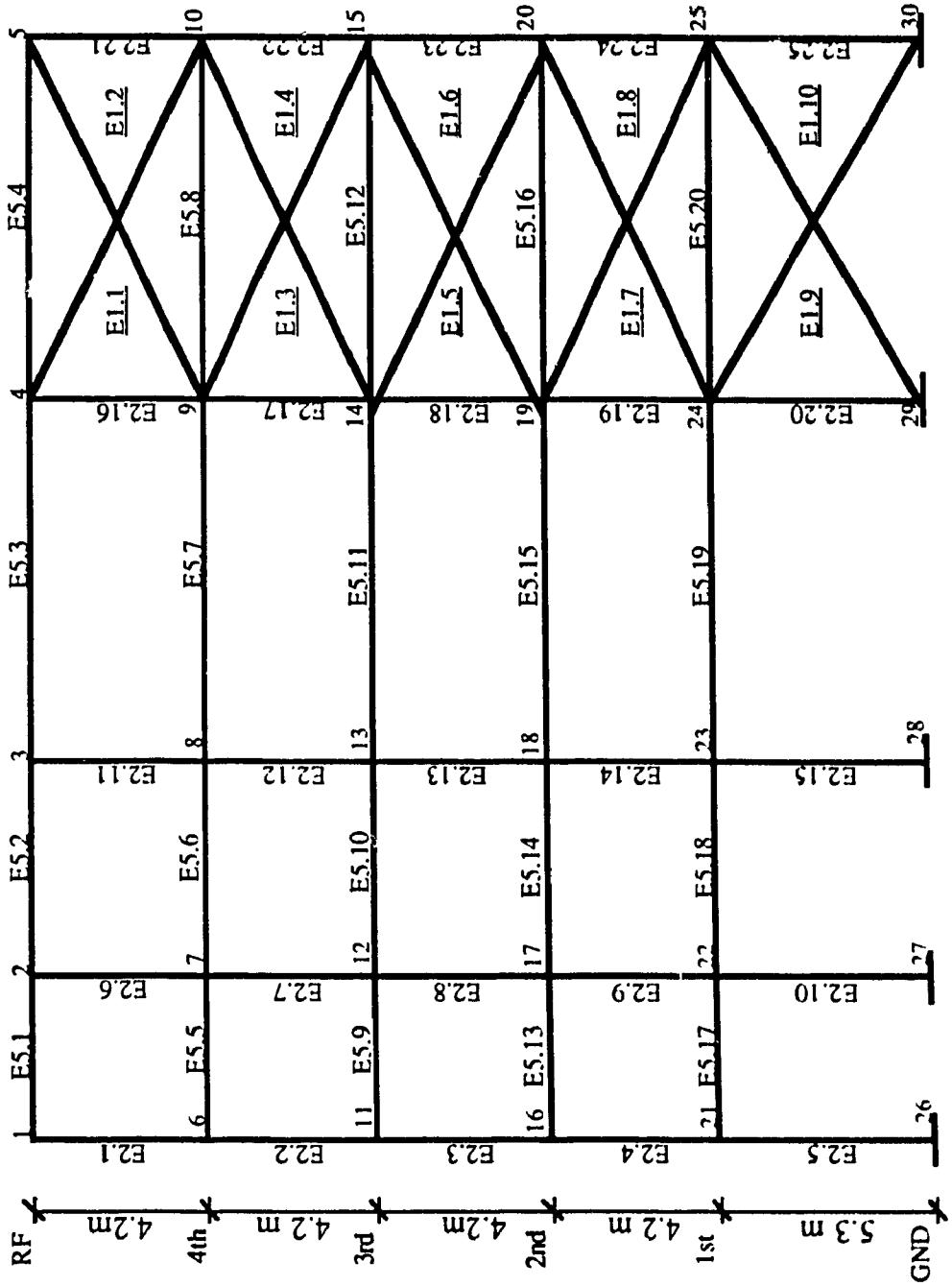

Fig. 6.5 Elevation of Frame VI

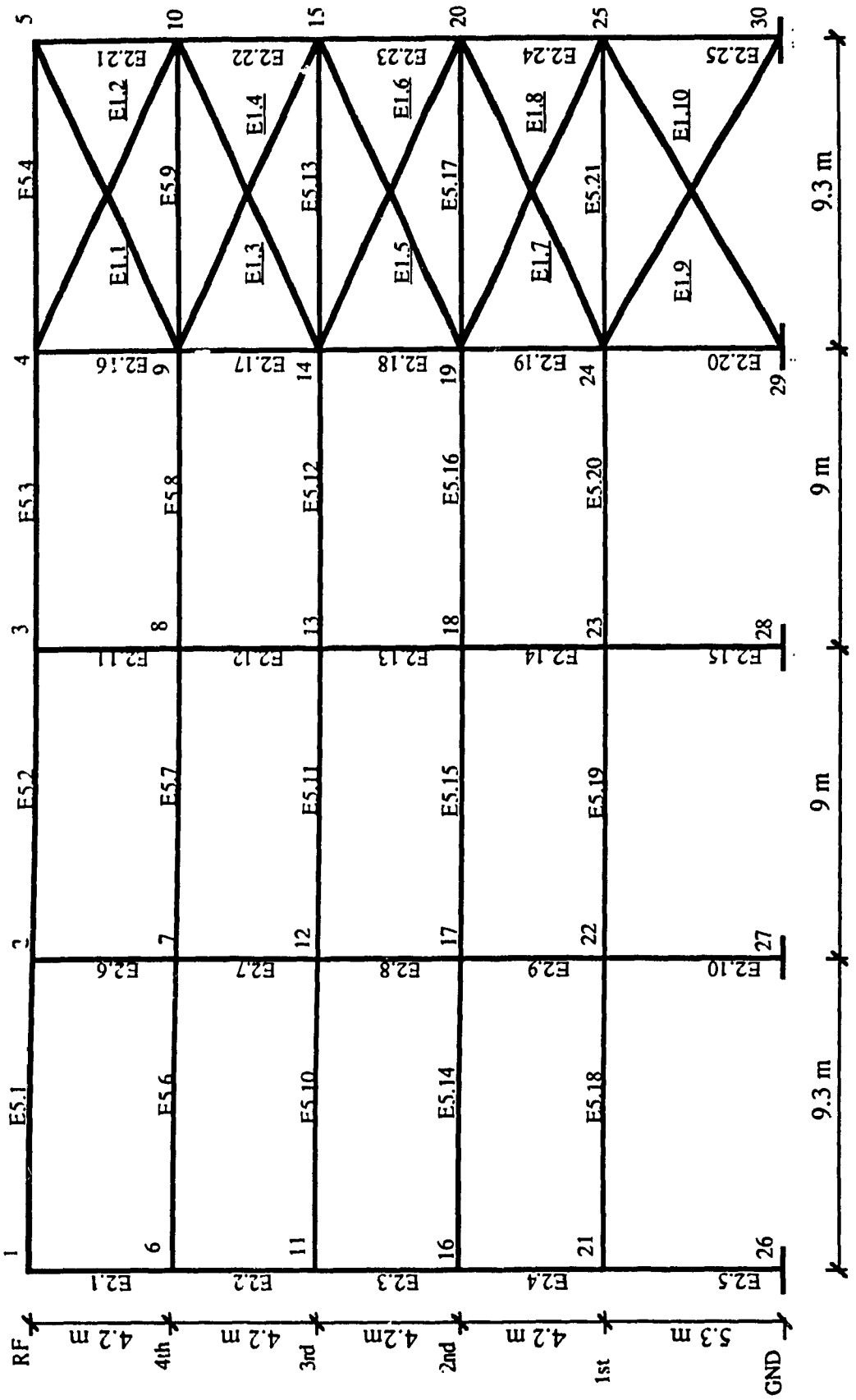

Fig. 6.6 Elevation of Frame XI

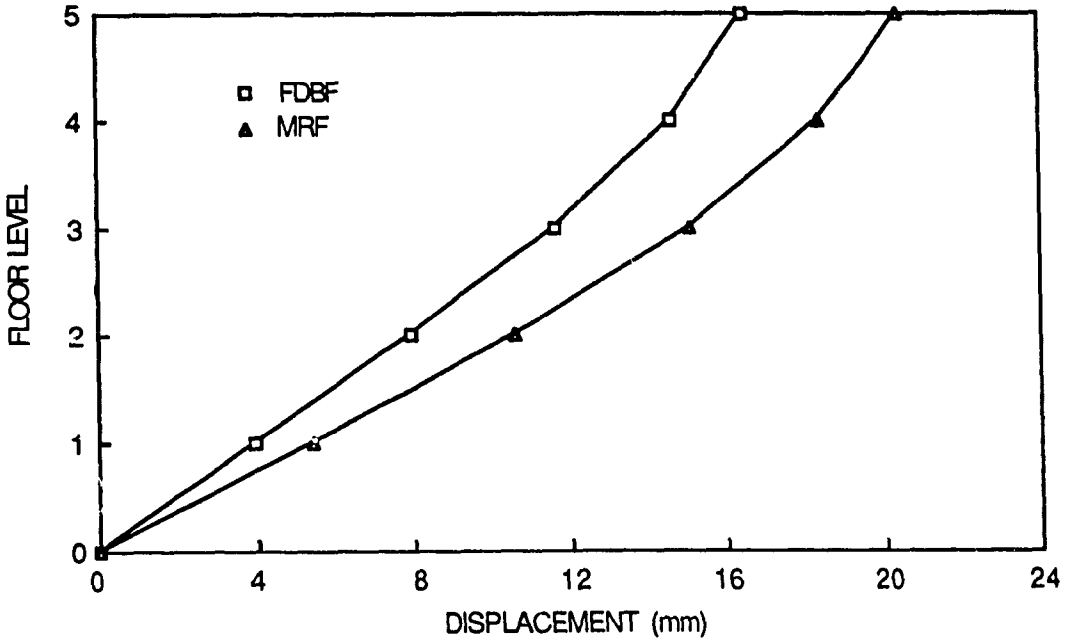

Fig. 6.7 Displacement under Pseudo-Static Forces Acting at CR in the Y-Direction

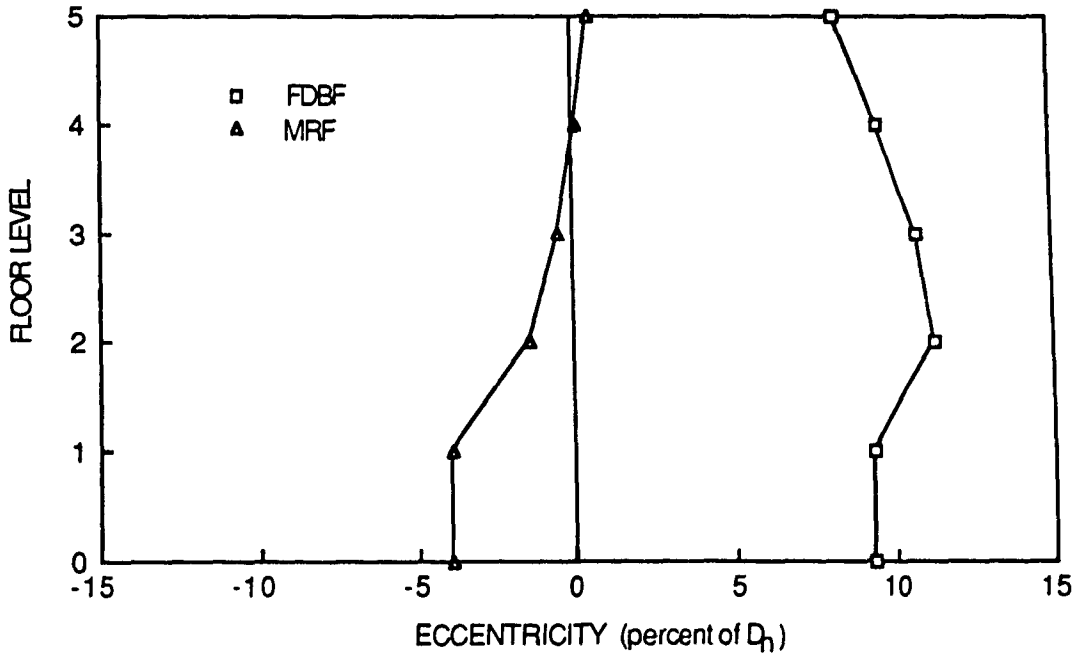

Fig. 6.8 Eccentricity with Height of Building for Seismic Forces in the Y-Direction

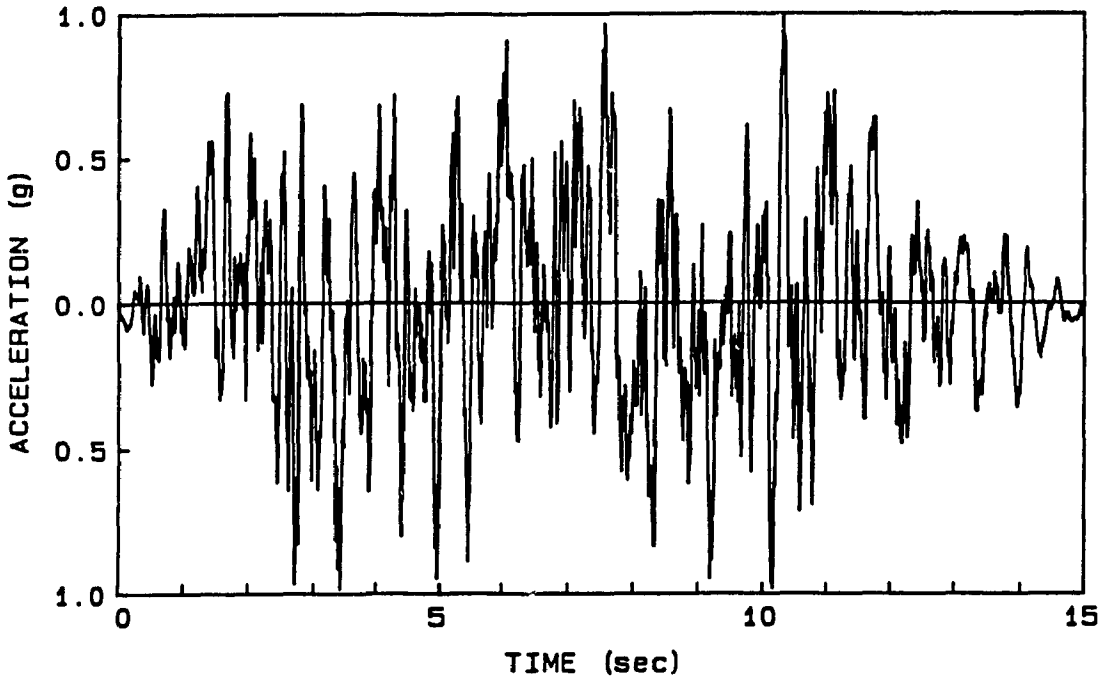

Fig. 6.9 Time History of Acceleration for the Newmark-Blume-Kapur Artificial Earthquake

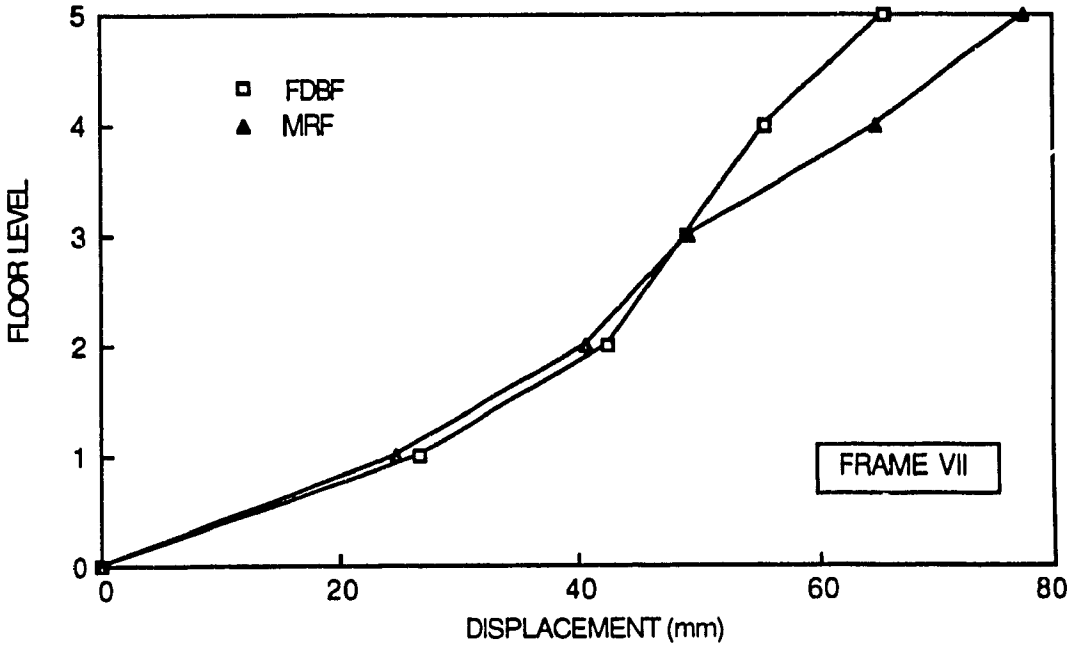

Fig. 6.10a Displacement of Frame VII , Earthquake Y-Direction

(CM @ Centroid)

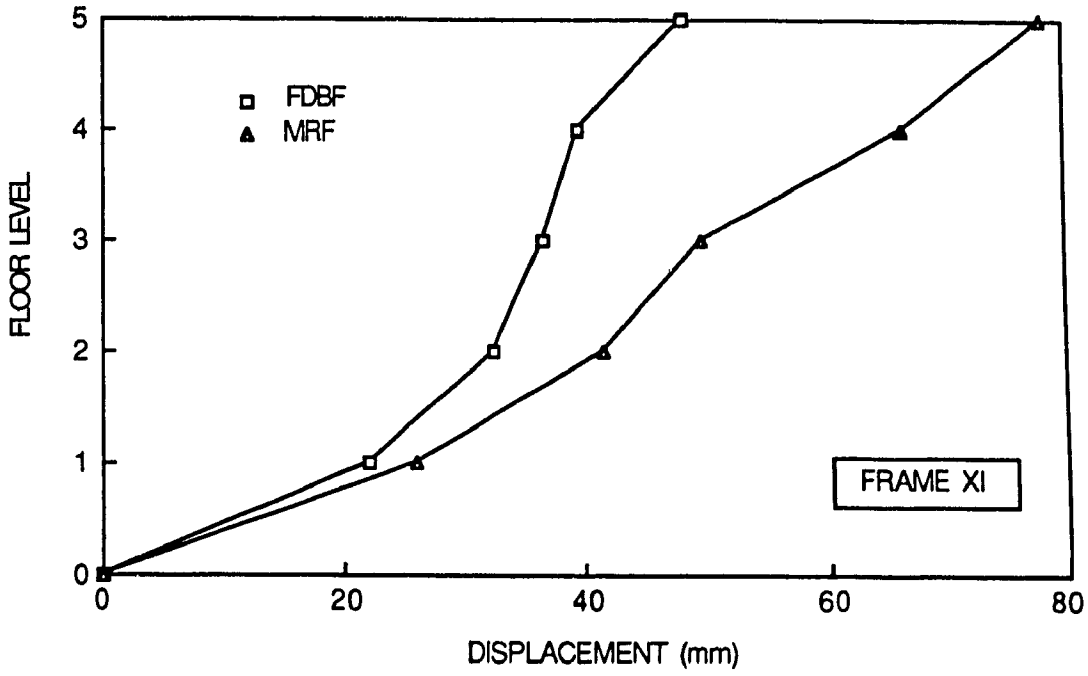

Fig. 6.10b Displacement of Frame XI , Earthquake Y-Direction

(CM @ Centroid)

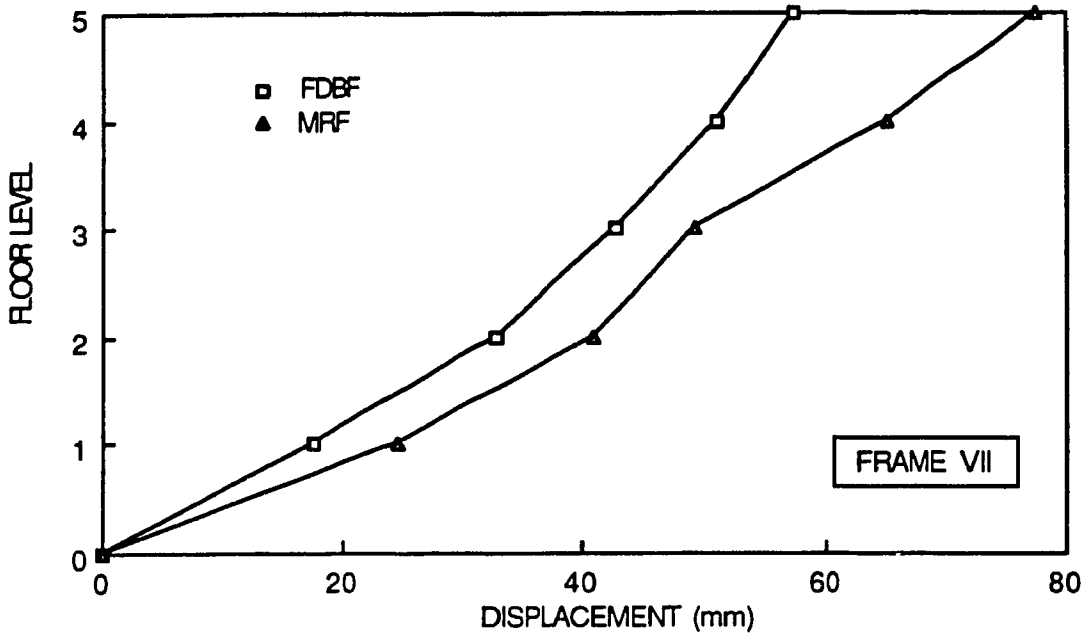

Fig. 6.11a Displacement of Frame VII , Earthquake Y-Direction

KB / KF≈1.0(CM @ Centroid)

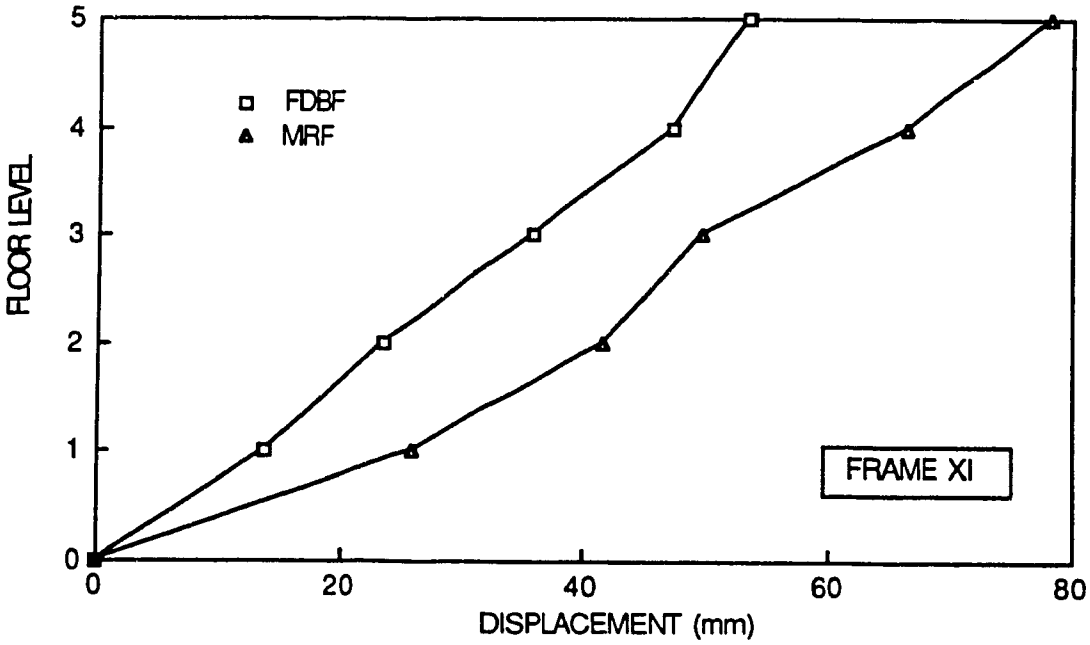

Fig. 6.11b Displacement of Frame XI , Earthquake Y-Direction

KB / KF≈1.0(CM @ Centroid)

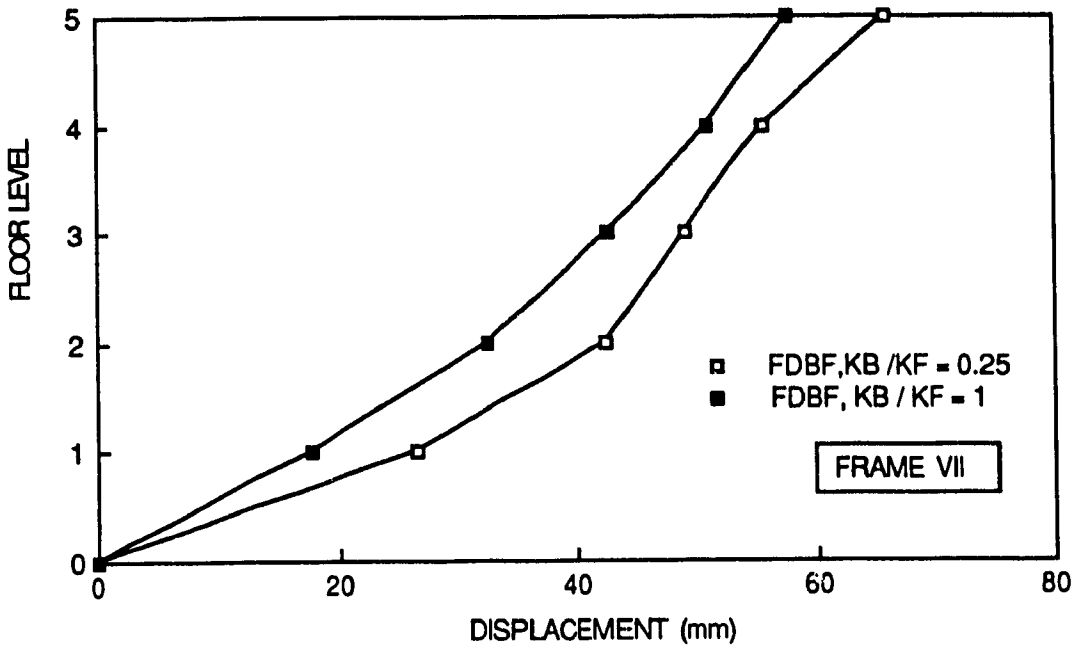

Fig. 6.11c Displacement of Frame VII , Earthquake Y-Direction

Comparision between 2 Stiffness ratios(CM @ Centroid)

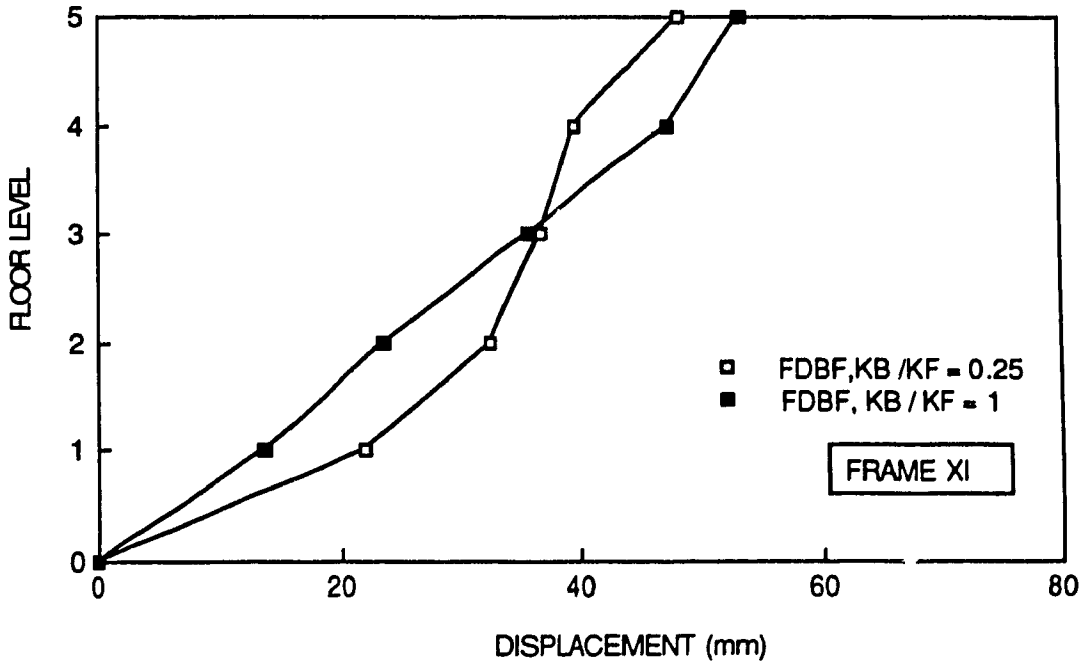

Fig. 6.11d Displacement of Frame XI , Earthquake Y-Direction

Comparision between 2 Stiffness ratios(CM @ Centroid)

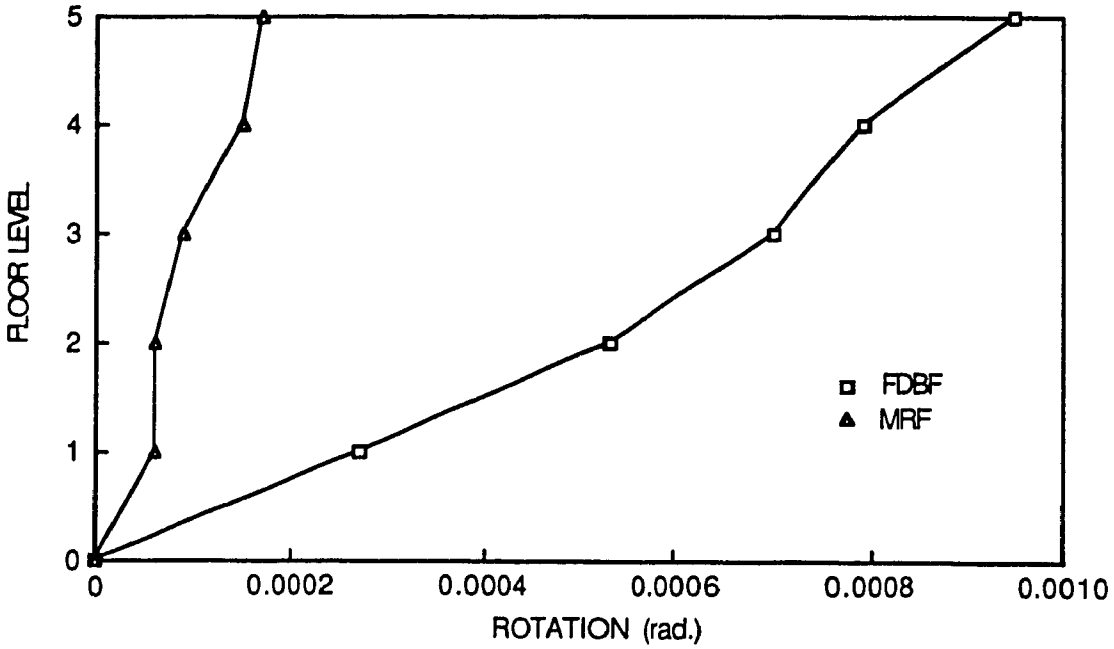

Fig. 6.12 Rotation of Floor Decks, Earthquake in Y-Direction

(CM @ Centroid)

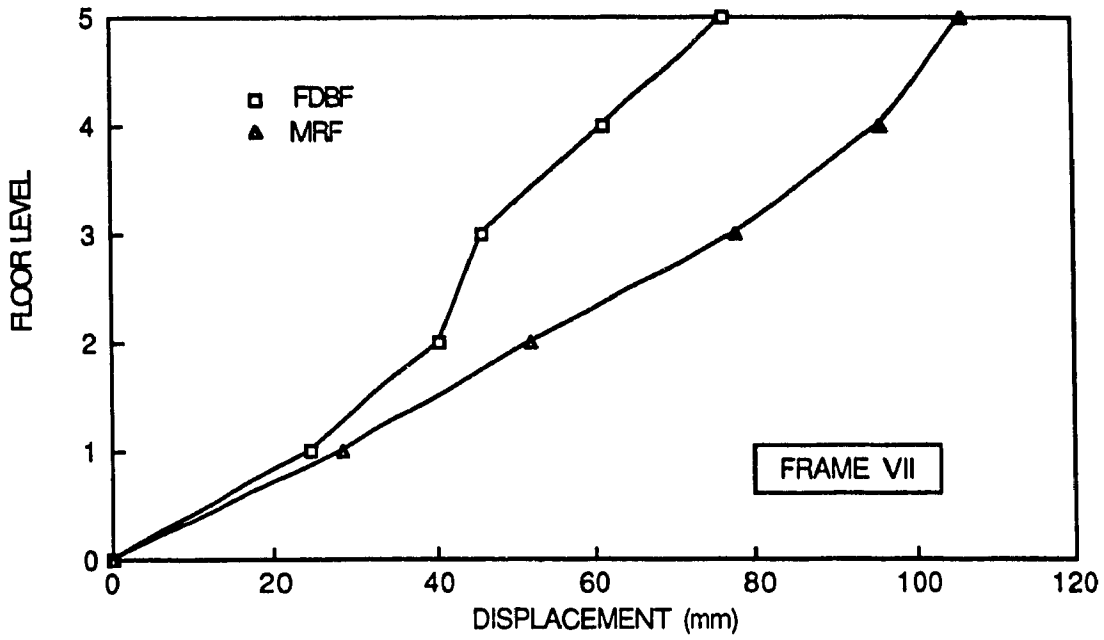

Fig. 6.13a Displacement of Frame VII , Earthquake Y-Direction

KB / KF ≈ 0.25 (CM @ -0.25 D_n)

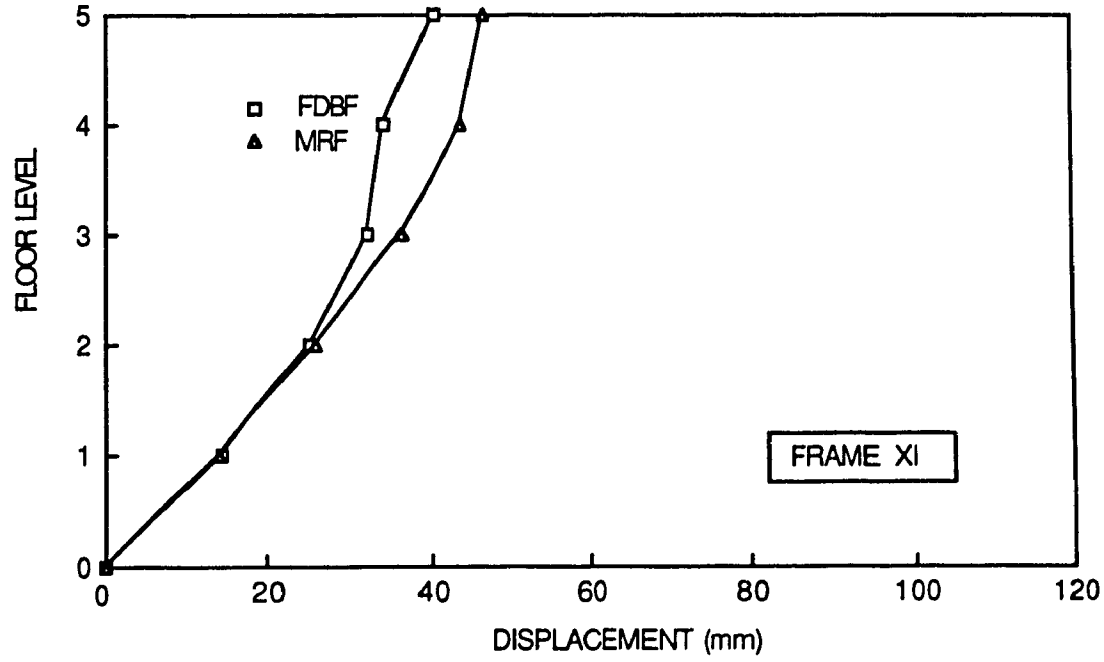

Fig. 6.13b Displacement of Frame XI , Earthquake Y-Direction

KB / KF ≈ 0.25 (CM @ -0.25 D_n)

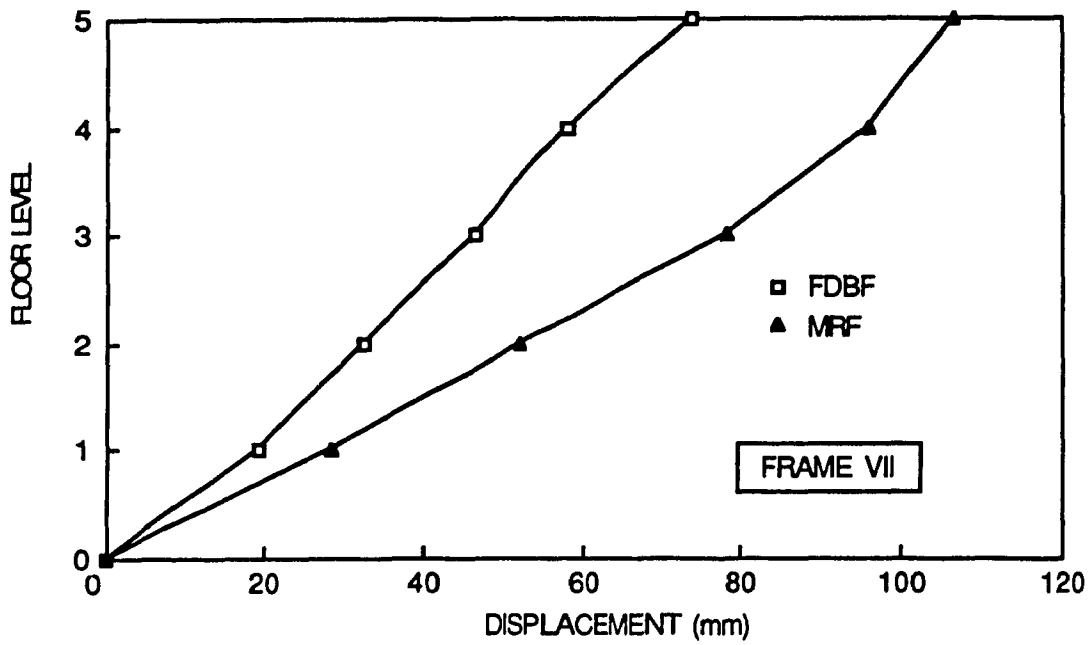

Fig. 6.14a Displacement of Frame VII , Earthquake Y-Direction

KB / KF ≈ 1.0 (CM @ -0.25 D_n)

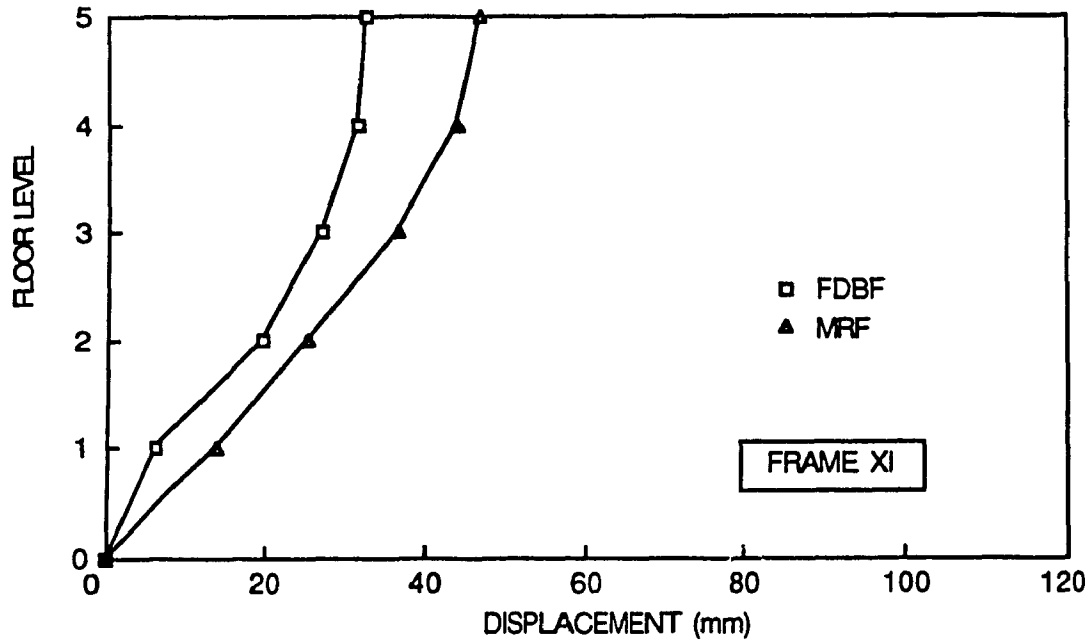

Fig. 6.14b Displacement of Frame XI , Earthquake Y-Direction

KB / KF ≈ 1.0 (CM @ -0.25 D_n)

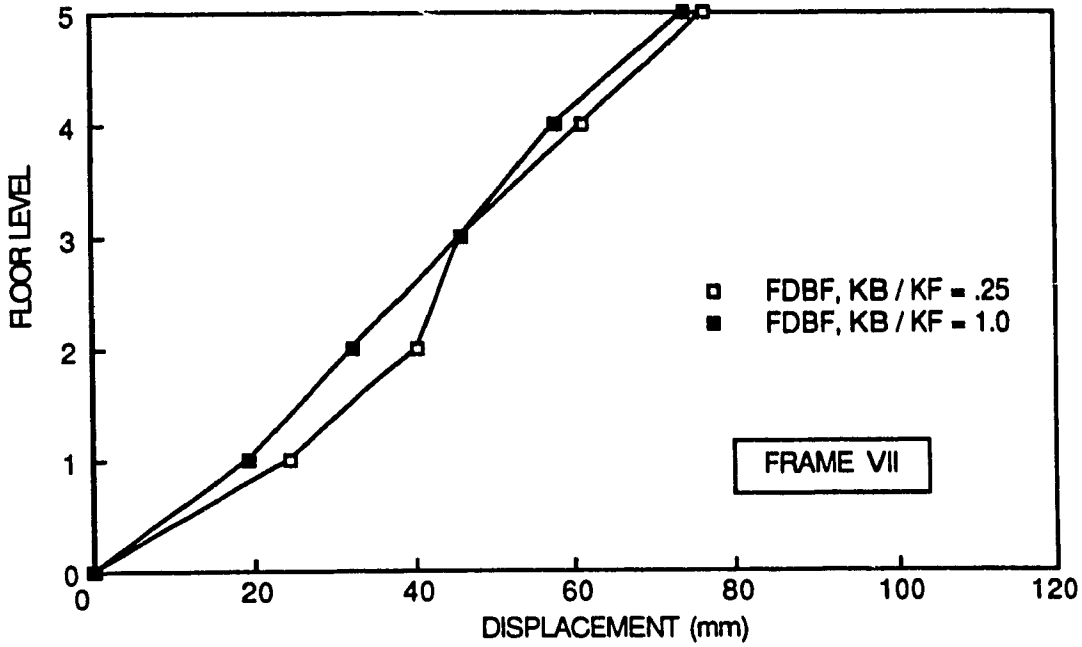

Fig. 6.14c Displacement of Frame VII , Earthquake Y-Direction

Comparision between 2 Stiffness ratios (CM @ -0.25 D_n)

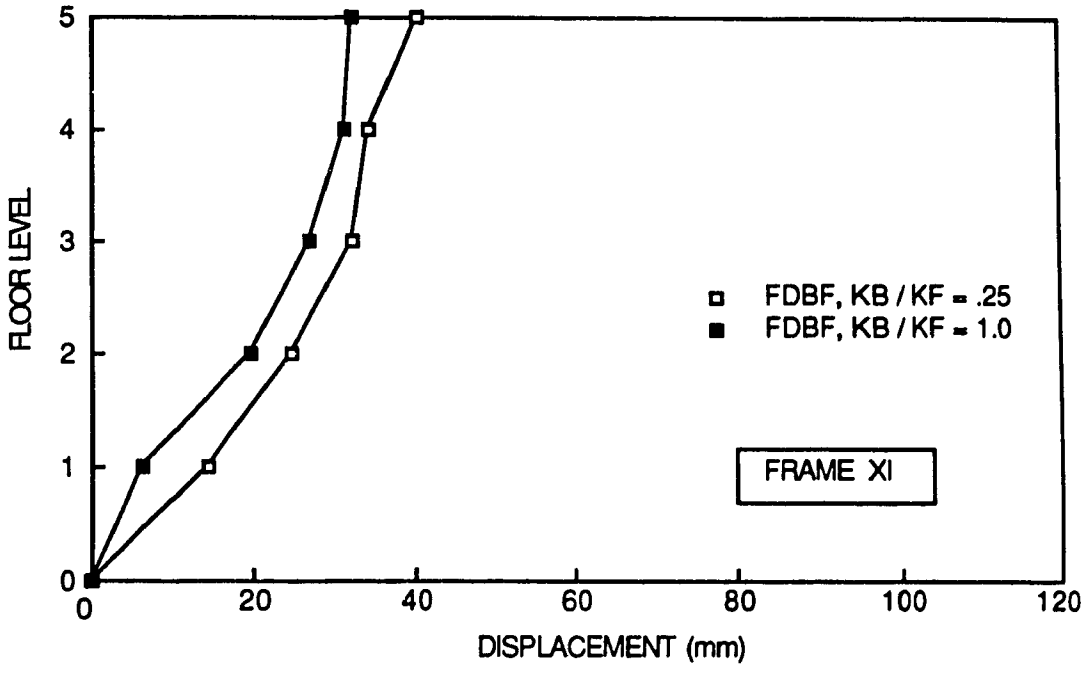

Fig. 6.14d Displacement of Frame XI , Earthquake Y-Direction

Comparision between 2 Stiffness ratios (CM @ -0.25 D_n)

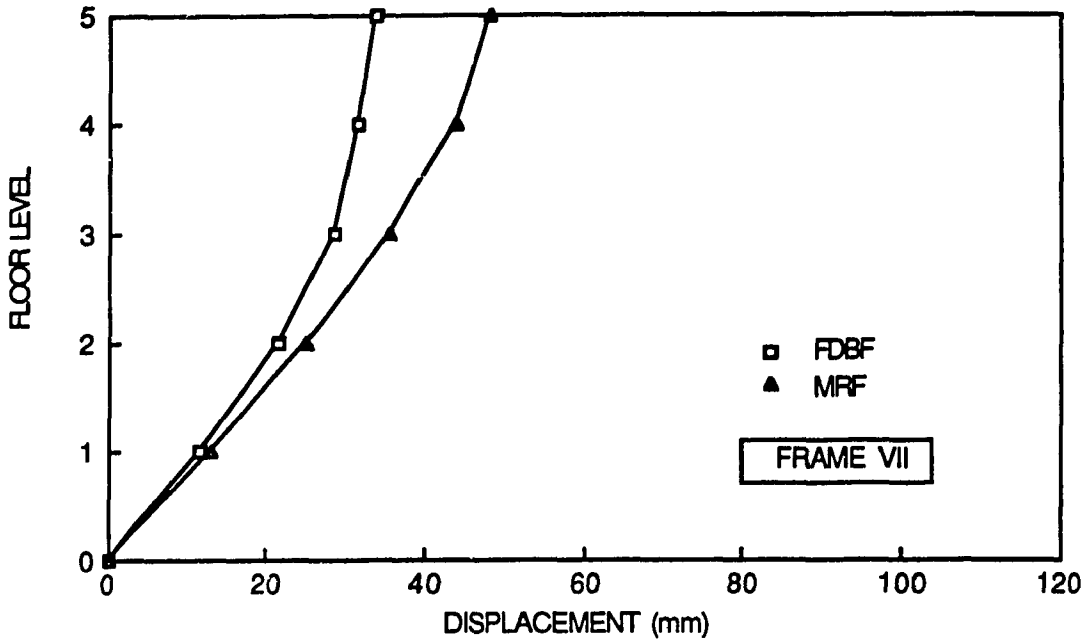

Fig. 6.15a Displacement of Frame VII , Earthquake Y-Direction

(CM @ +0.25 D_n)

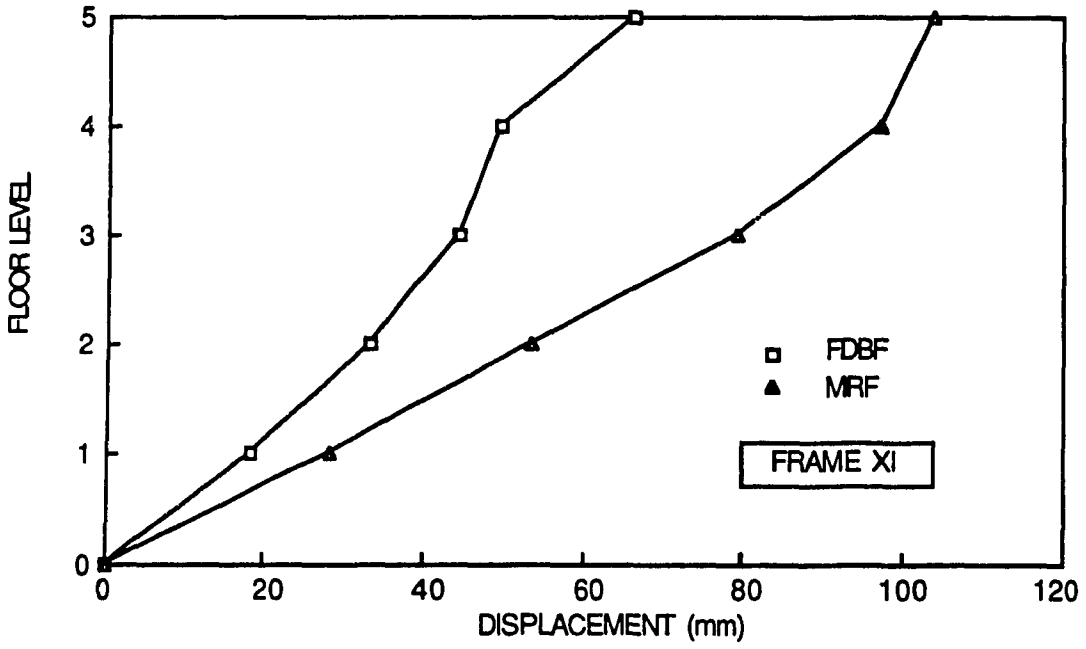

Fig. 6.15b Displacement of Frame XI , Earthquake Y-Direction

(CM @ +0.25 D_n)

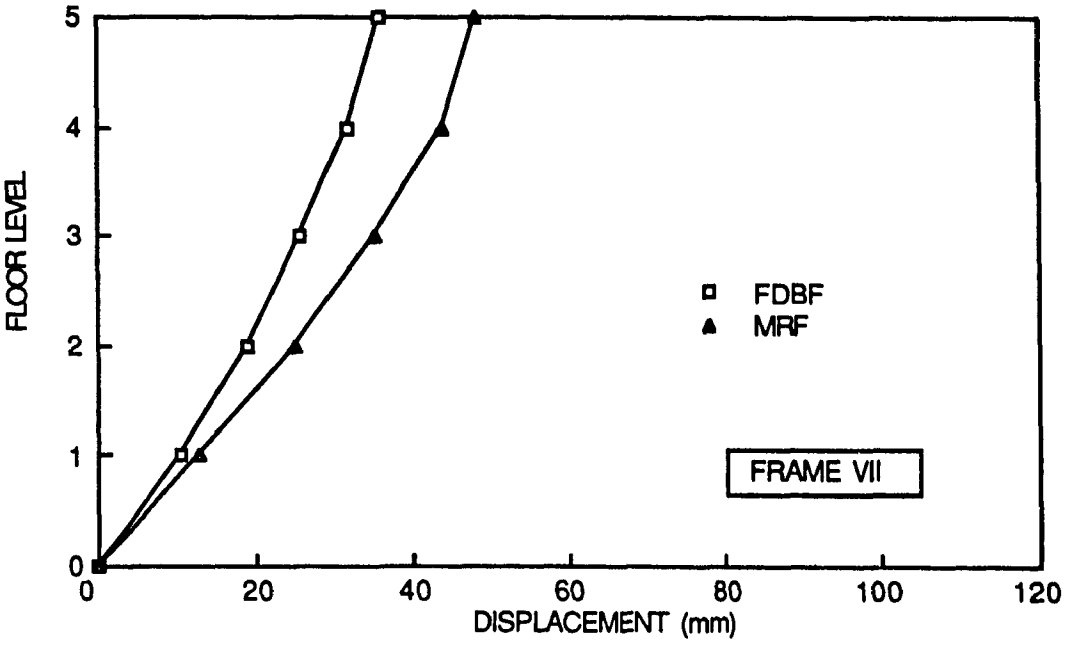

Fig. 6.16a Displacement of Frame VII , Earthquake Y-Direction

KB/KF ≈ 1.0 (CM @ +0.25 D_n)

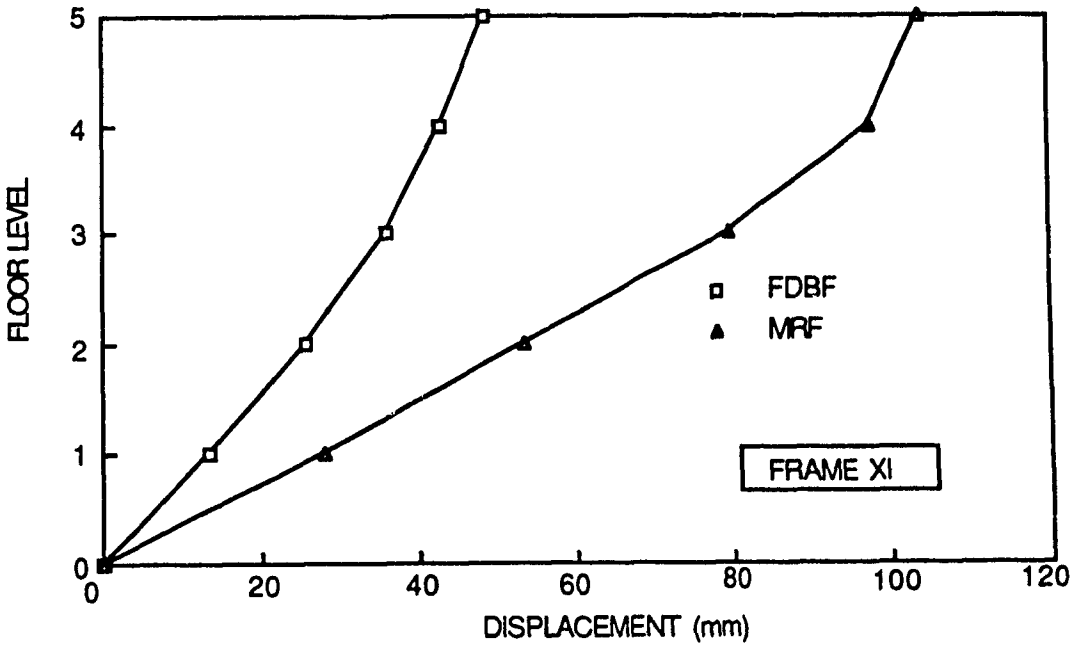

Fig. 6.16b Displacement of Frame XI , Earthquake Y-Direction

KB/KF ≈ 1.0 (CM @ +0.25 D_n)

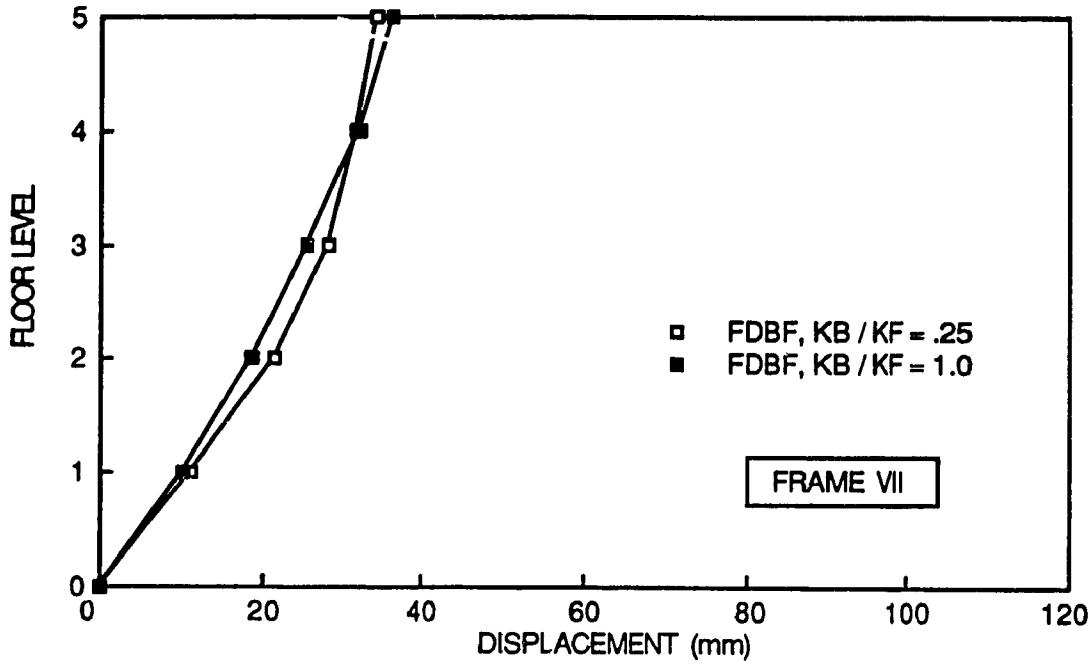

Fig. 6.16c Displacement of Frame VII , Earthquake Y-Direction

Comparision between 2 Stiffness ratios(CM @ +0.25 D_n)

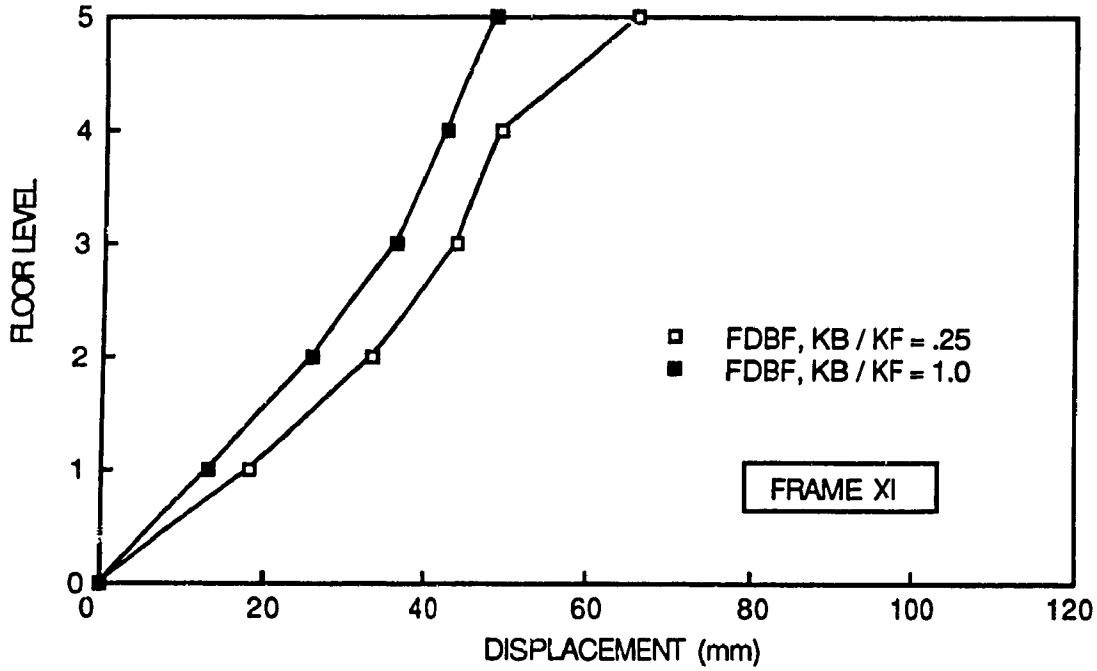

Fig. 6.16d Displacement of Frame XI , Earthquake Y-Direction

Comparision between 2 Stiffness ratios(CM @ +0.25 D_n)

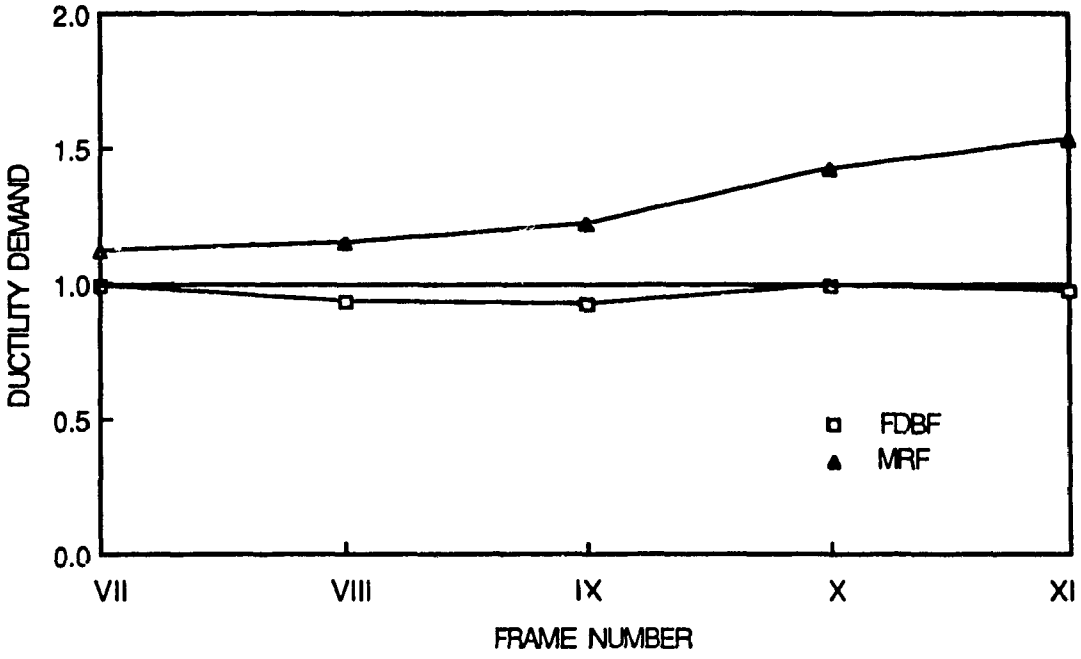

Fig. 6.17 Ductility Demand, Earthquake Y-Direction

(CM @ Centroid)

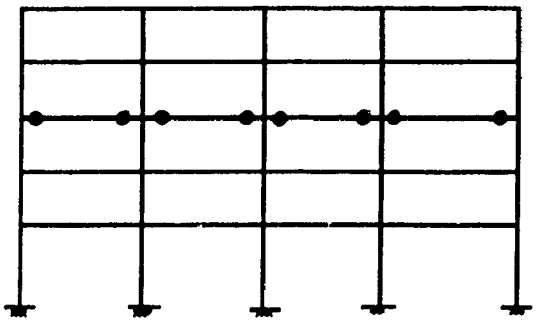

Frame VII

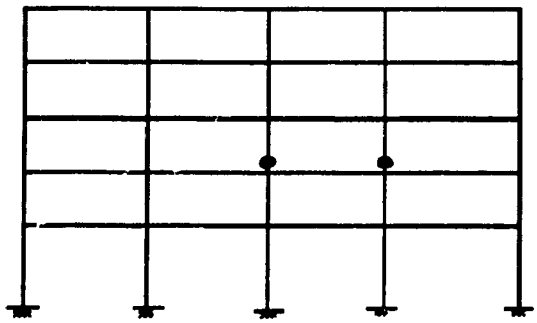

Frame VIII

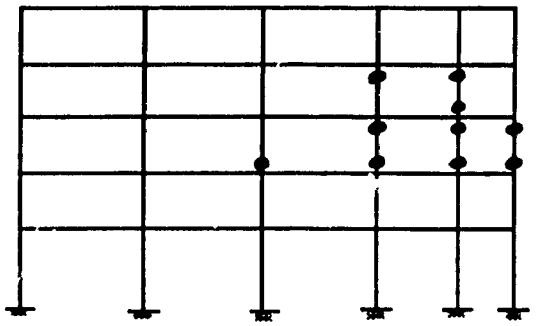

Frame IX

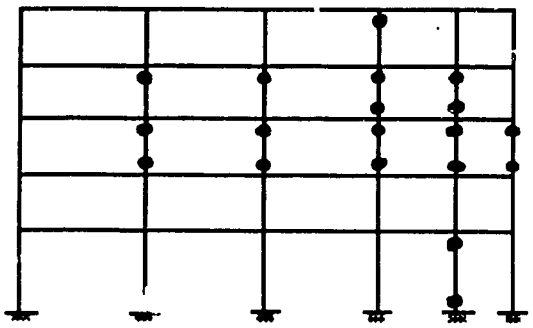

Frame X

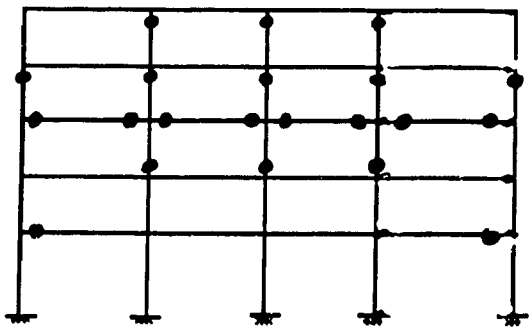

Frame XI

Fig. 6.18 Damage in Frame VII to XI, Earthquake in Y-Direction, MRF

(CM @ Centroid)

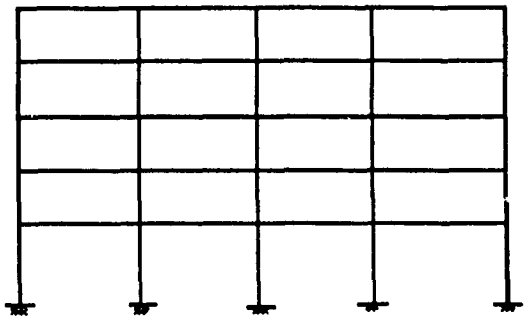

Frame VII

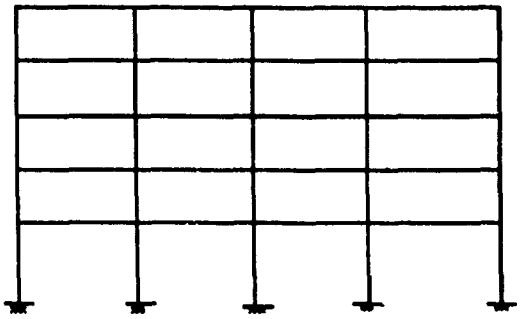

Frame VIII

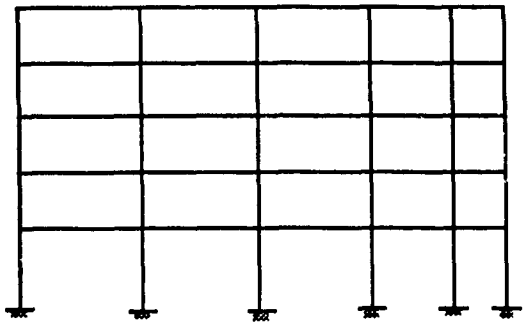

Frame IX

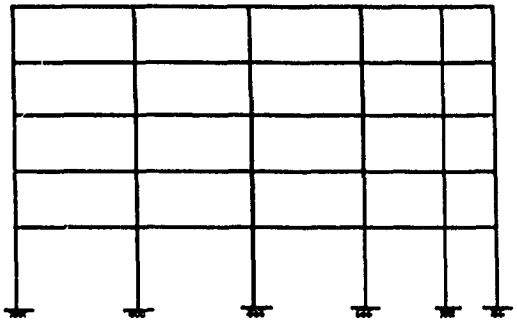

Frame X

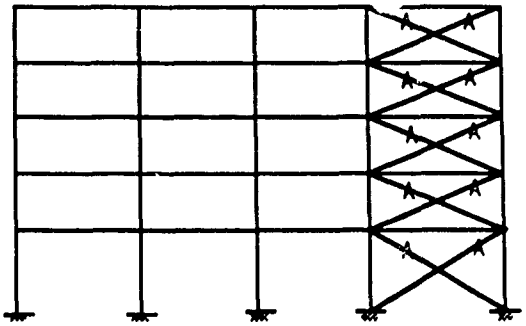

Frame XI

Fig. 6.19 Damage in Frame VII to XI , Earthquake in Y-Direction, FDBF

(CM @ Centroid)

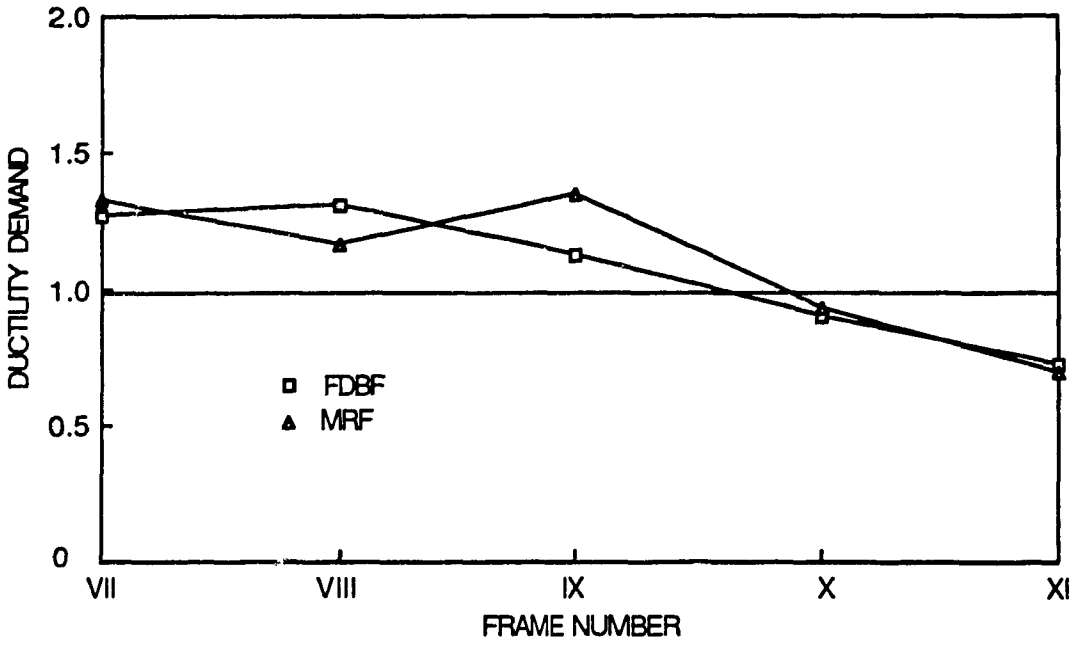

Fig. 6.20 Ductility Demand, Earthquake Y-Direction

(CM @ -0.25 D_n)

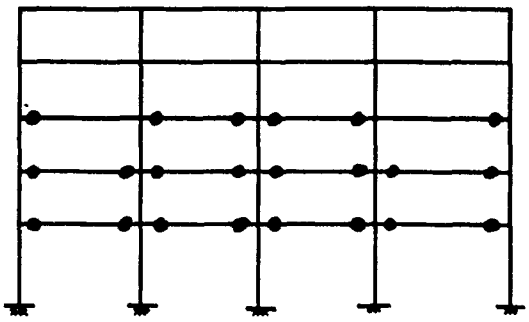

Frame VII

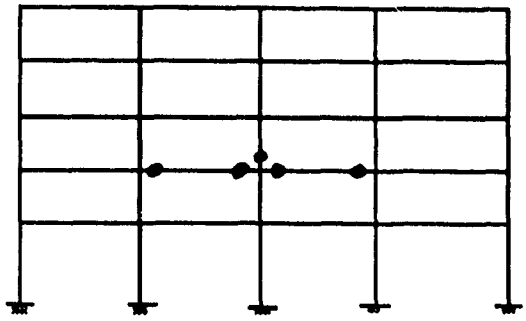

Frame VIII

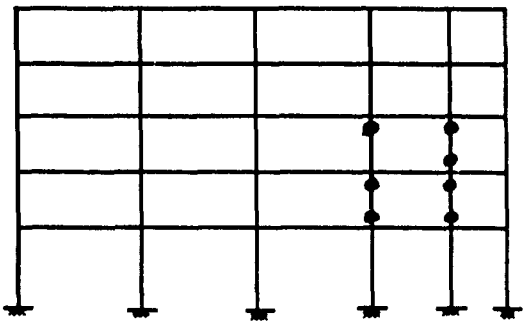

Frame IX

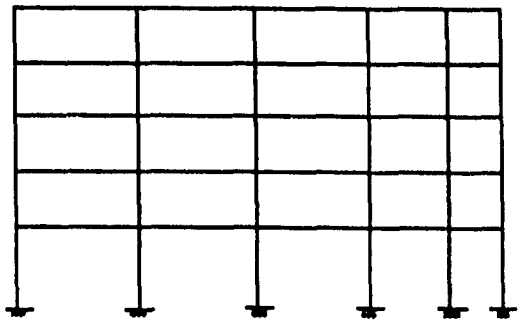

Frame X

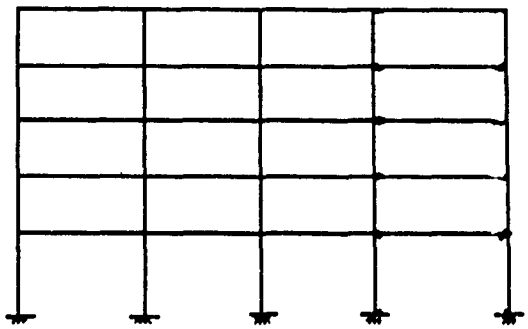

Frame XI

Fig. 6.21 Damage in Frame VII to XI , Earthquake in Y-Direction, MRF

(CM @ -0.25 Dn)

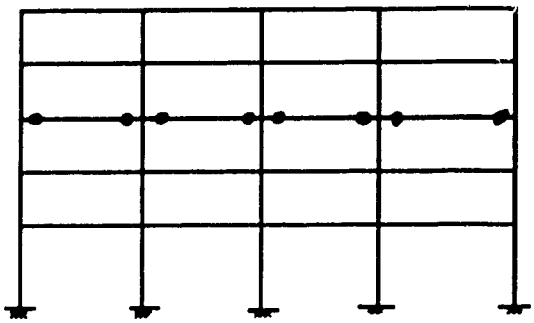

Frame VII

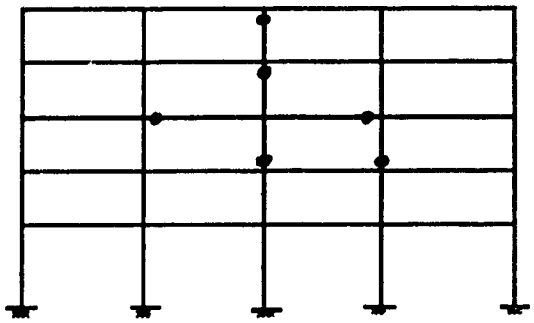

Frame VIII

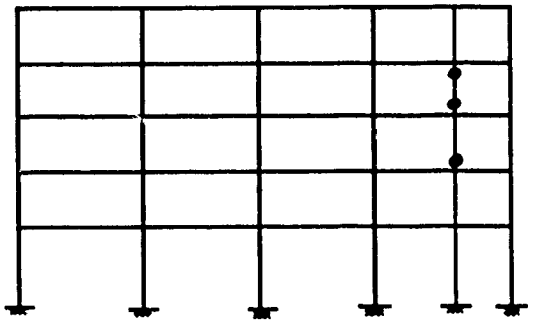

Frame IX

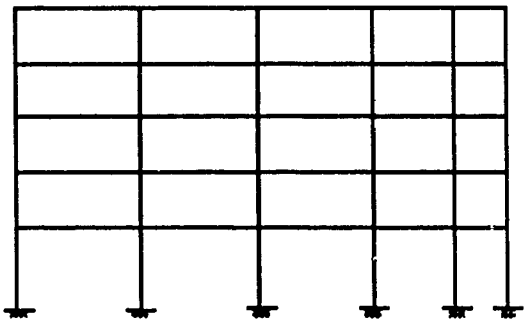

Frame X

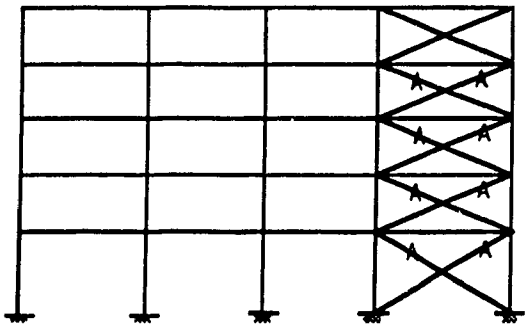

Frame XI

Fig. 6.22a Damage in Frame VII to XI , Earthquake in Y-Direction, FDBF

KB / KF ≈ 0.25 (CM @ -0.25 Dn)

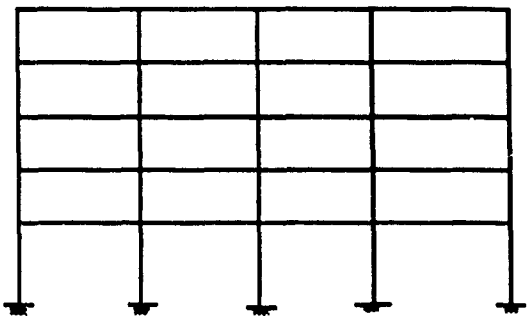

Frame VII

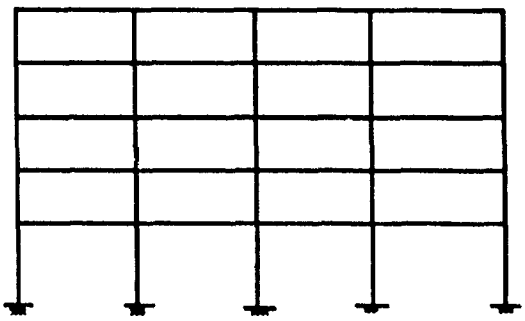

Frame VIII

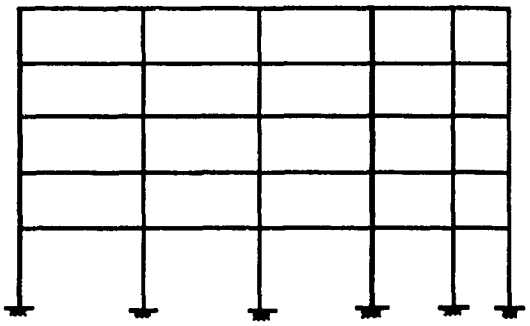

Frame IX

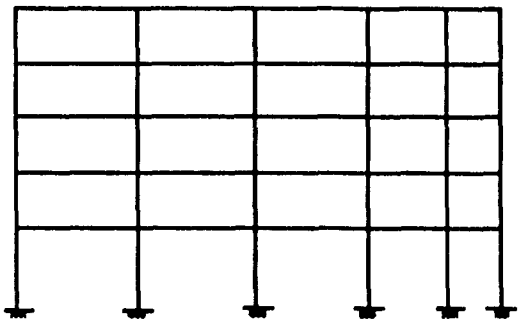

Frame X

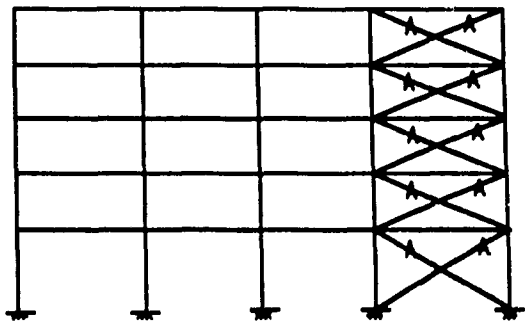

Frame XI

Fig. 6.22b Damage in Frame VII to XI , Earthquake in Y-Direction, FDBF

KB / KF ≈ 1.0 (CM @ -0.25 Dn)

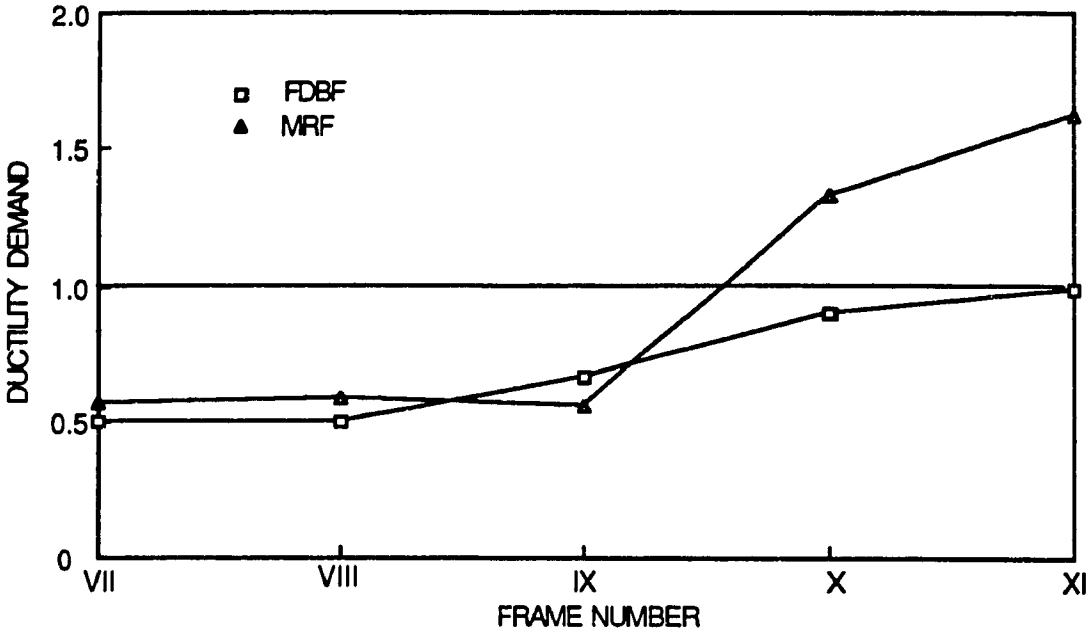

Fig. 6.23 Ductility Demand, Earthquake Y-Direction

(CM @ +0.25 D_n)

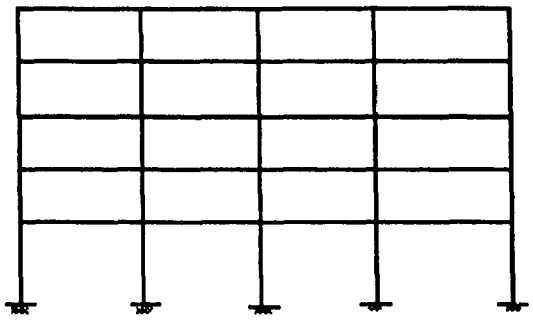

Frame VII

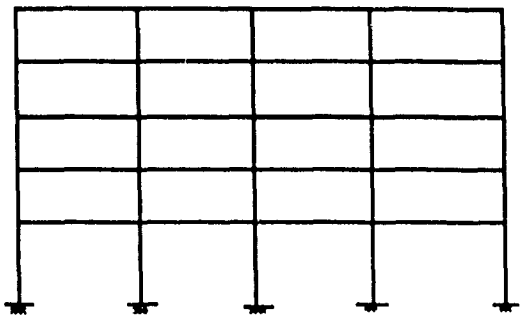

Frame VIII

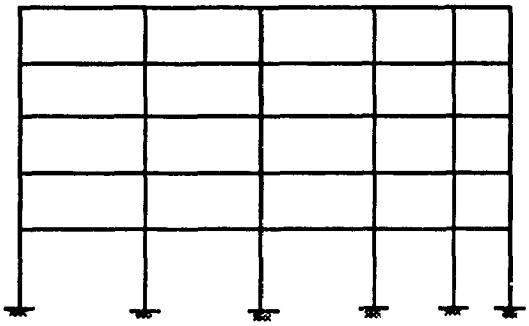

Frame IX

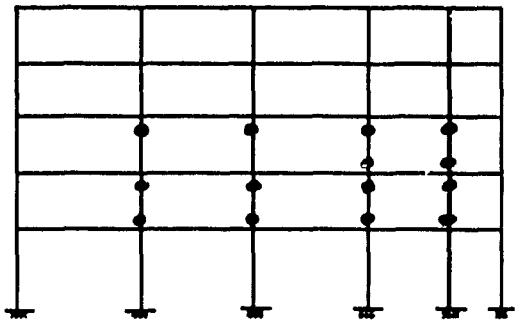

Frame X

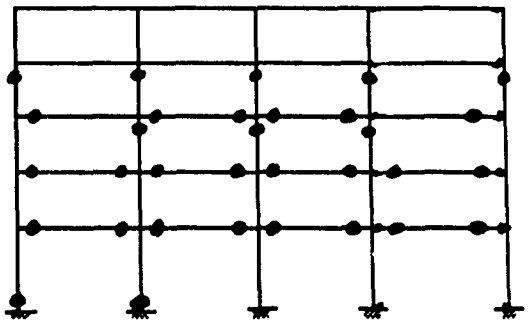

Frame XI

Fig. 6.24 Damage in Frame VII to XI , Earthquake in Y-Direction, MRF

(CM @ +0.25 Dn)

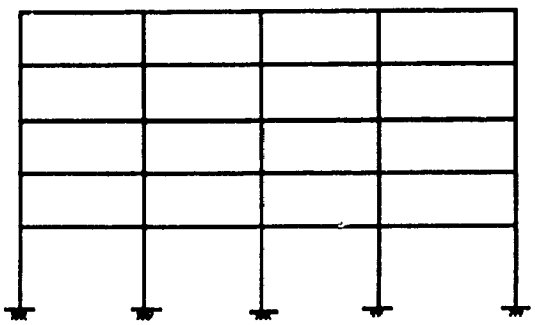

Frame VII

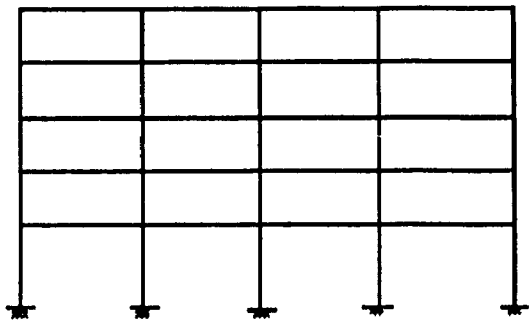

Frame VIII

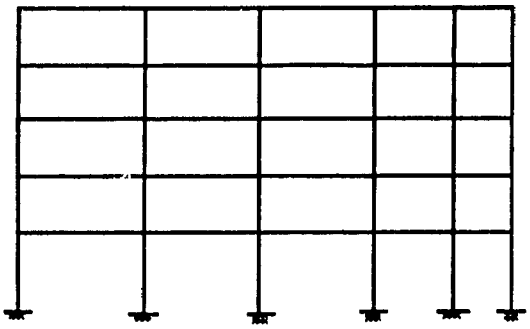

Frame IX

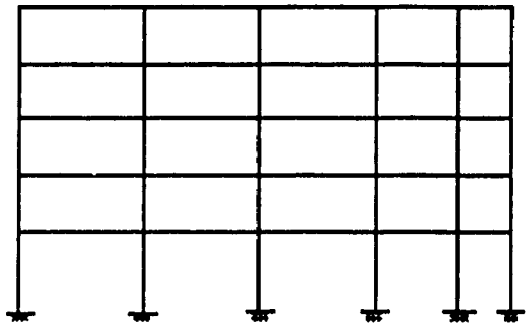

Frame X

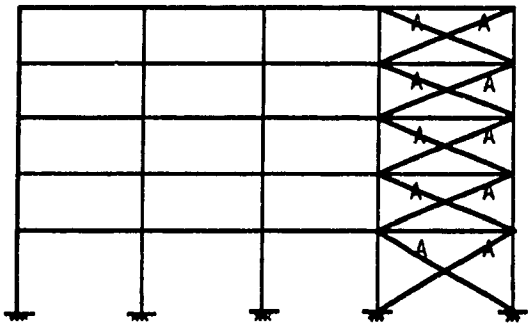

Frame XI

Fig. 6.25a Damage in Frame VII to XI , Earthquake in Y-Direction, FDBF

KB / KF ≈ 0.25 (CM @ +0.25 Dn)

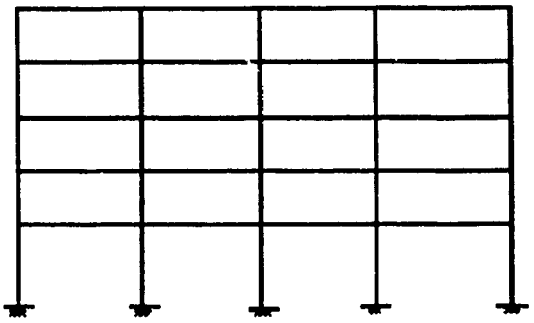

Frame VII

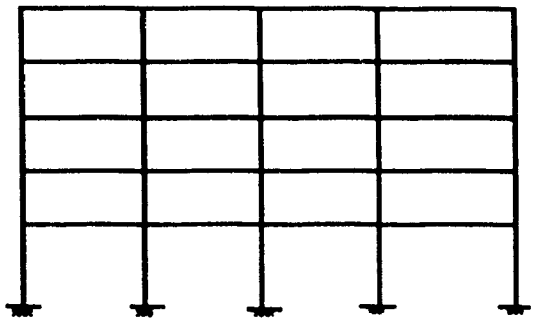

Frame VIII

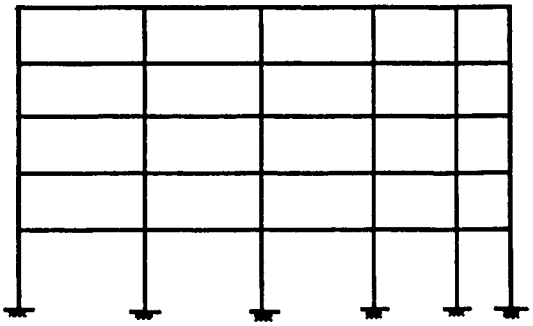

Frame IX

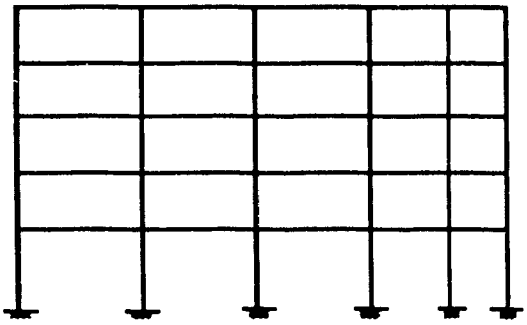

Frame X

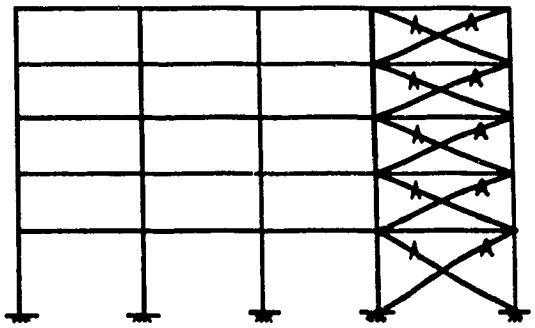

Frame XI

Fig. 6.25b Damage in Frame VII to XI , Earthquake in Y-Direction, FDBF

KB / KF ≈ 1.0 (CM @ +0.25 Dn)

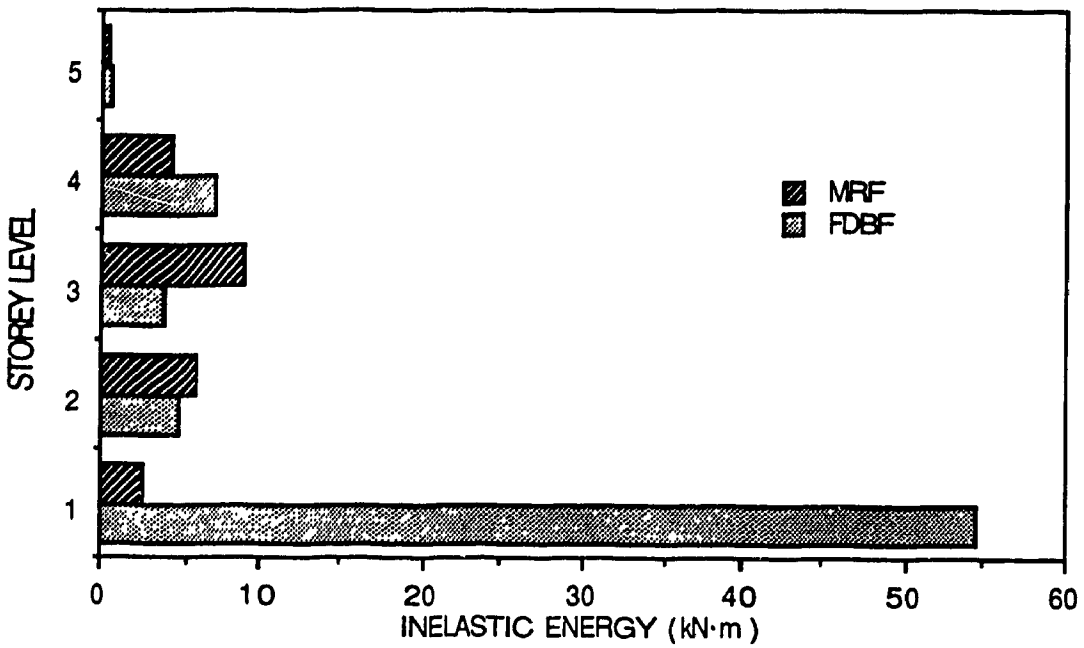

Fig. 6.26 Energy Absorption, Earthquake Y-Direction

(CM @ Centroid)

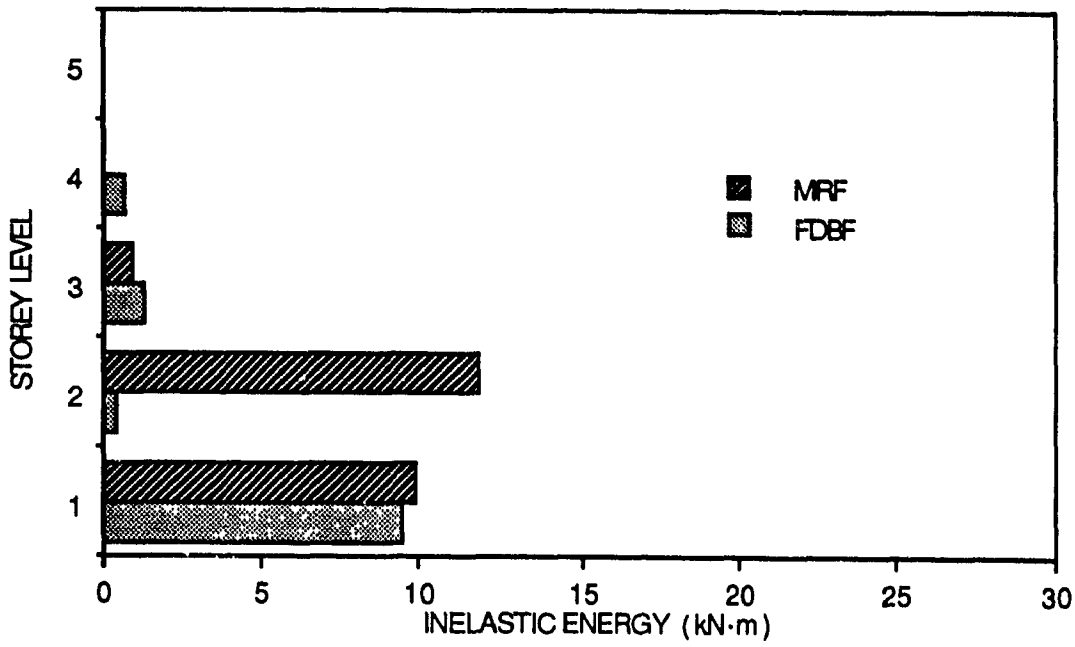

Fig. 6.27 Energy Absorption, Earthquake in Y-Direction

(CM @ -0.25D_n)

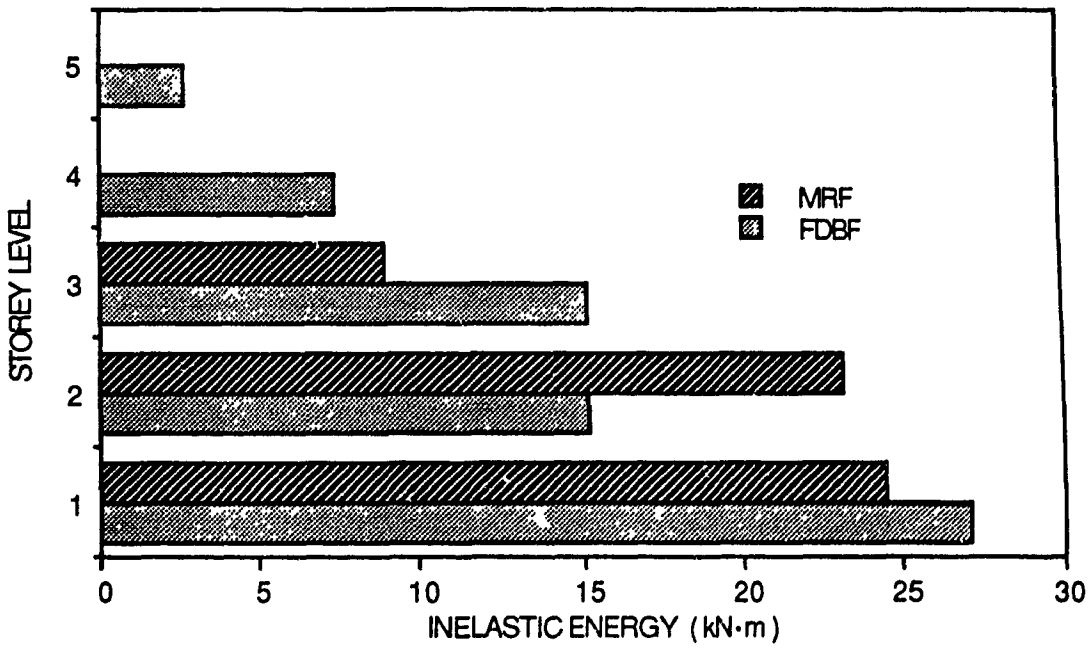

Fig. 6.28 Energy Absorption, Earthquake in Y-Direction

(CM @ +0.25D_n)

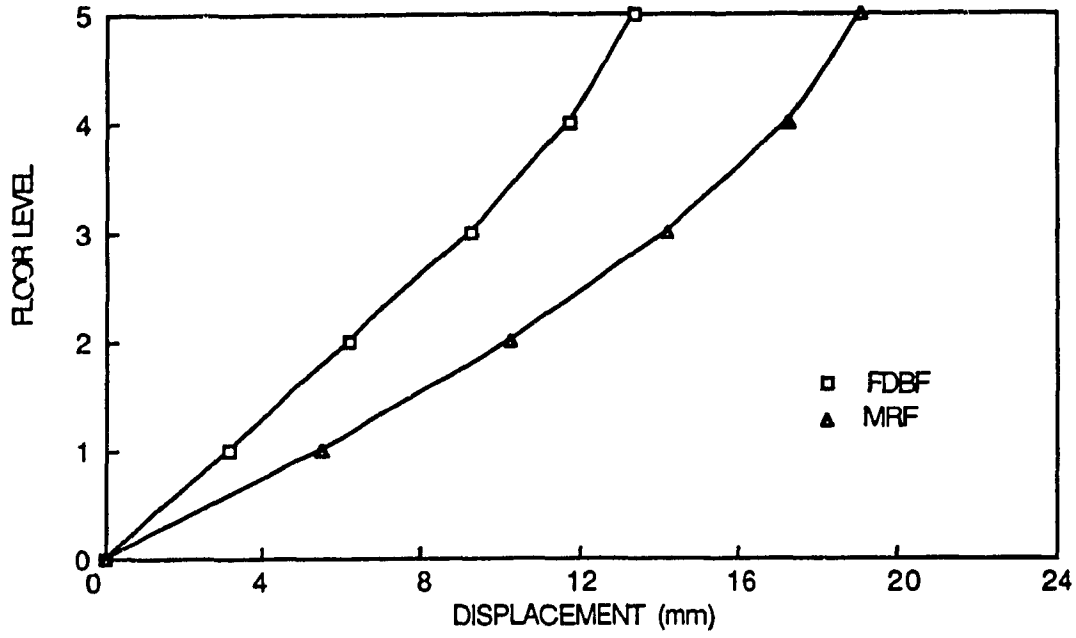

Fig. 6.29 Displacement under Pseudo-Static Forces Acting @ CR in the X-Direction

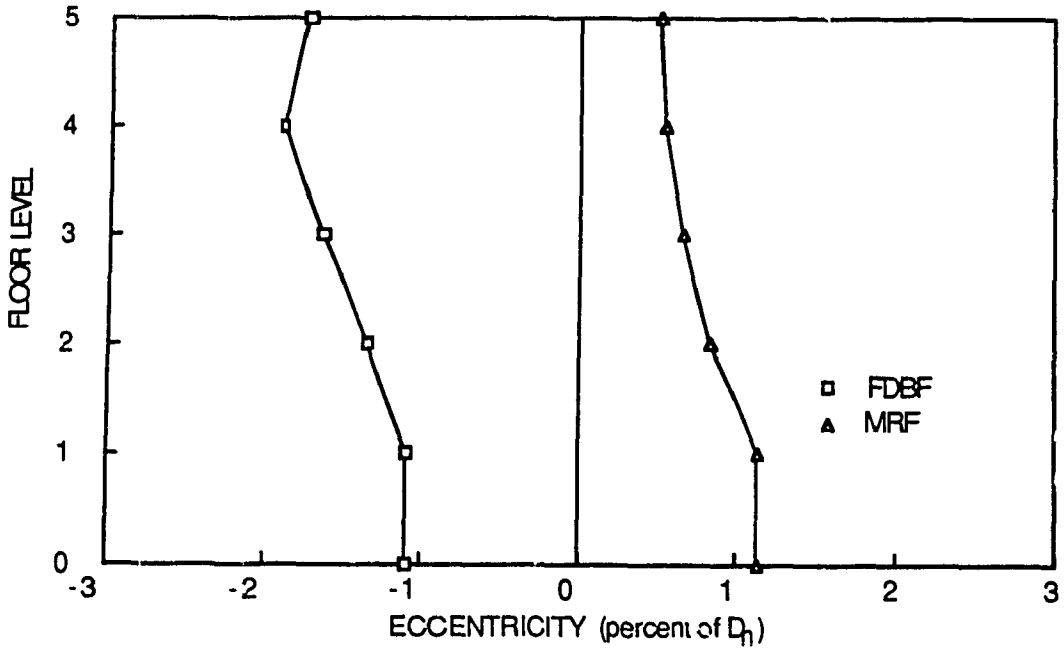

Fig. 6.30 Eccentricity with Height of Building for Seismic Forces in X-Direction

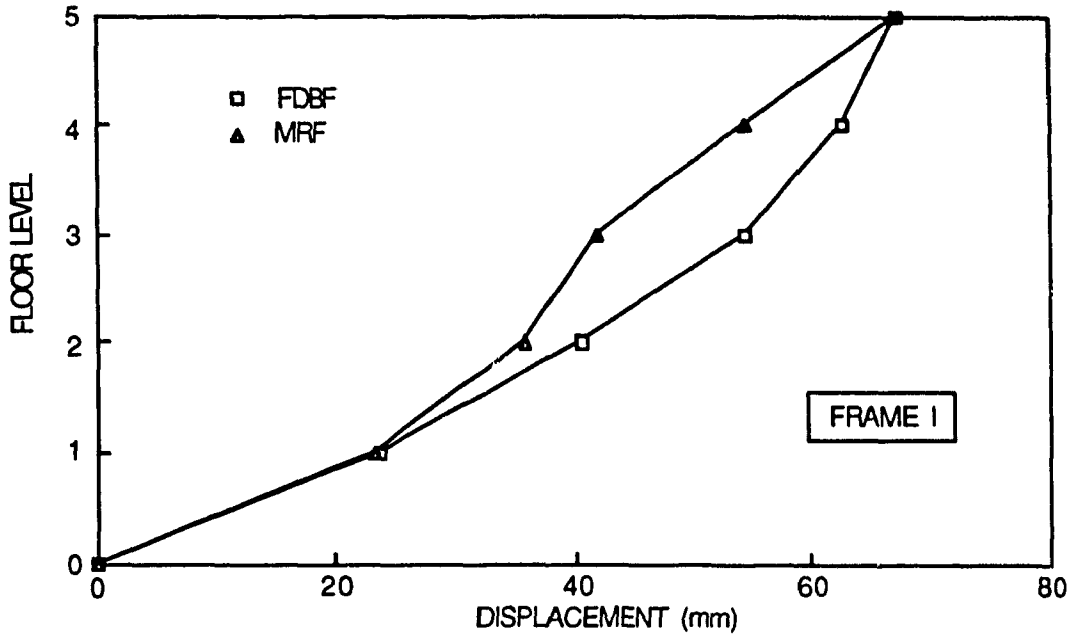

Fig. 6.31 Displacement of Frame I , Earthquake X-Direction

(CM @ Centroid)

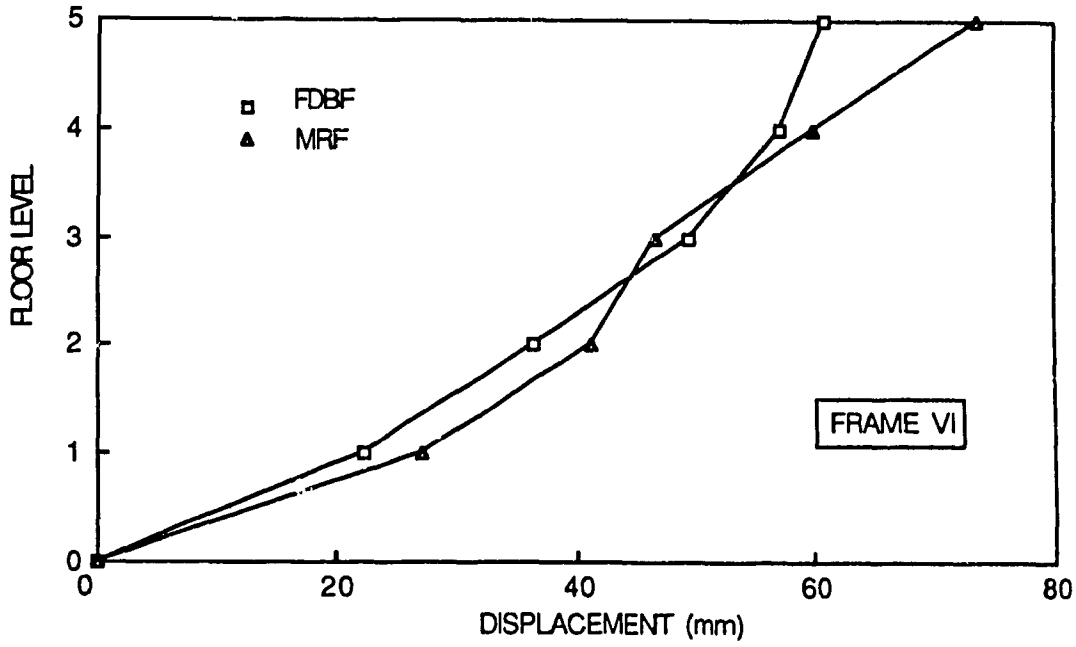

Fig. 6.32 Displacement of Frame VI, Earthquake Y-Direction

(CM @ Centroid)

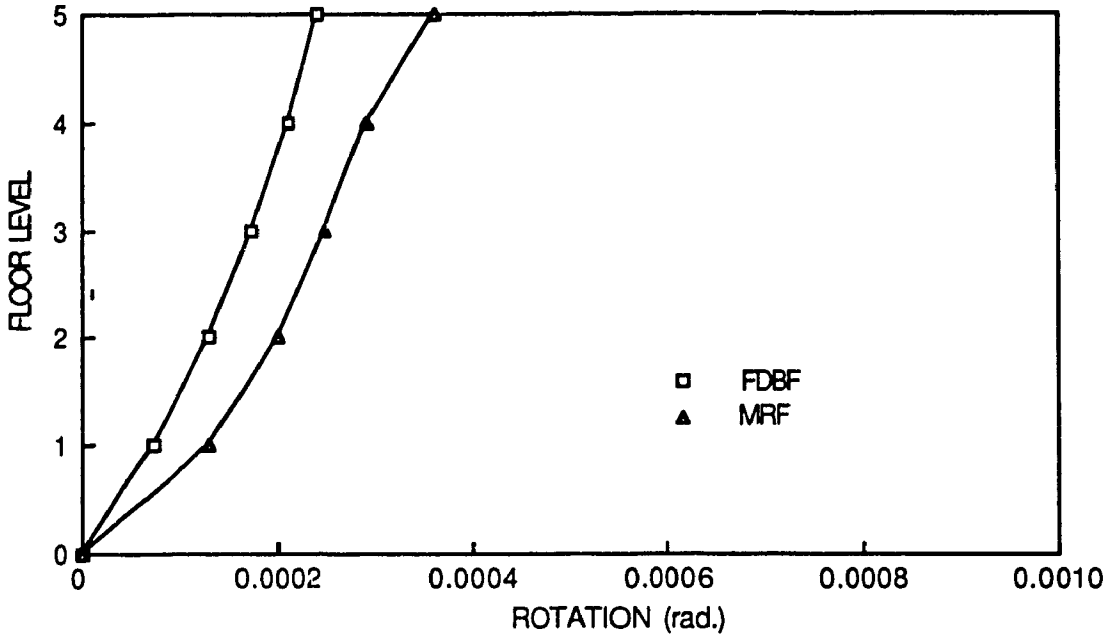

Fig. 6.33 Rotation of Floor Decks, Earthquake in X-Direction

(CM @ Centroid)

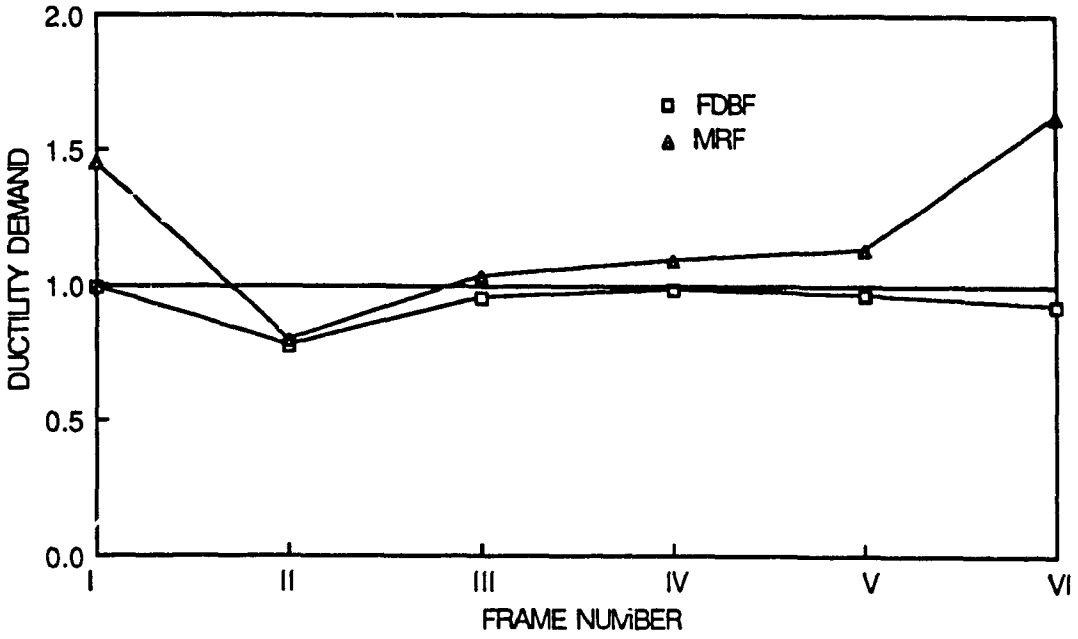

Fig. 6.34 Ductility Demand, Earthquake in X-Direction

(CM @ Centroid)

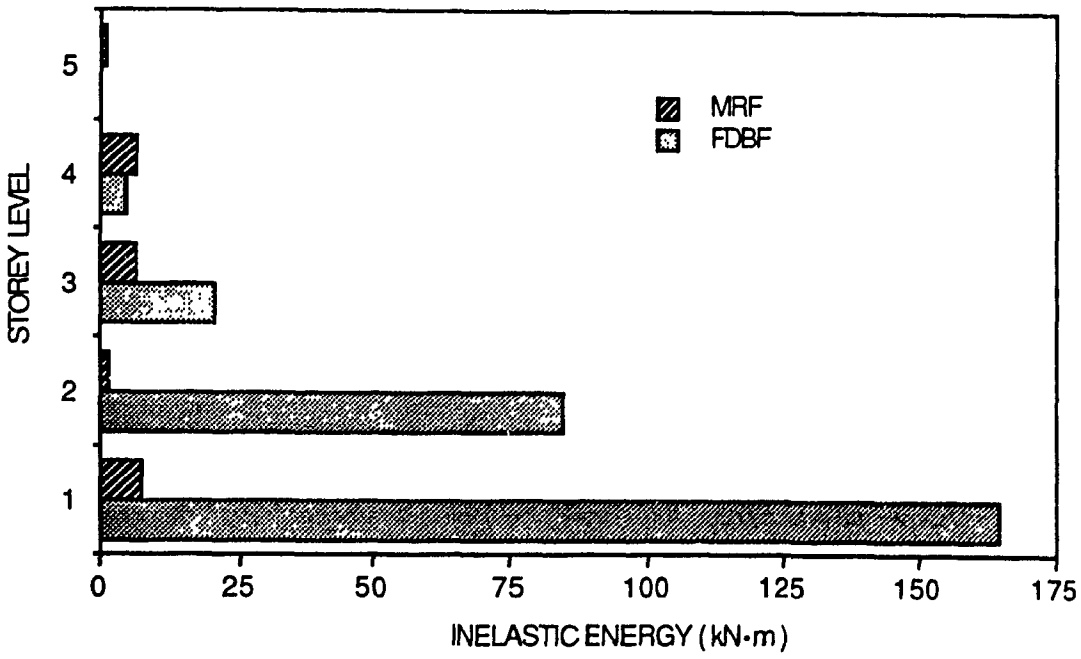

Fig. 6.35 Energy Absorption, Earthquake X-Direction

(CM @ Centroid)

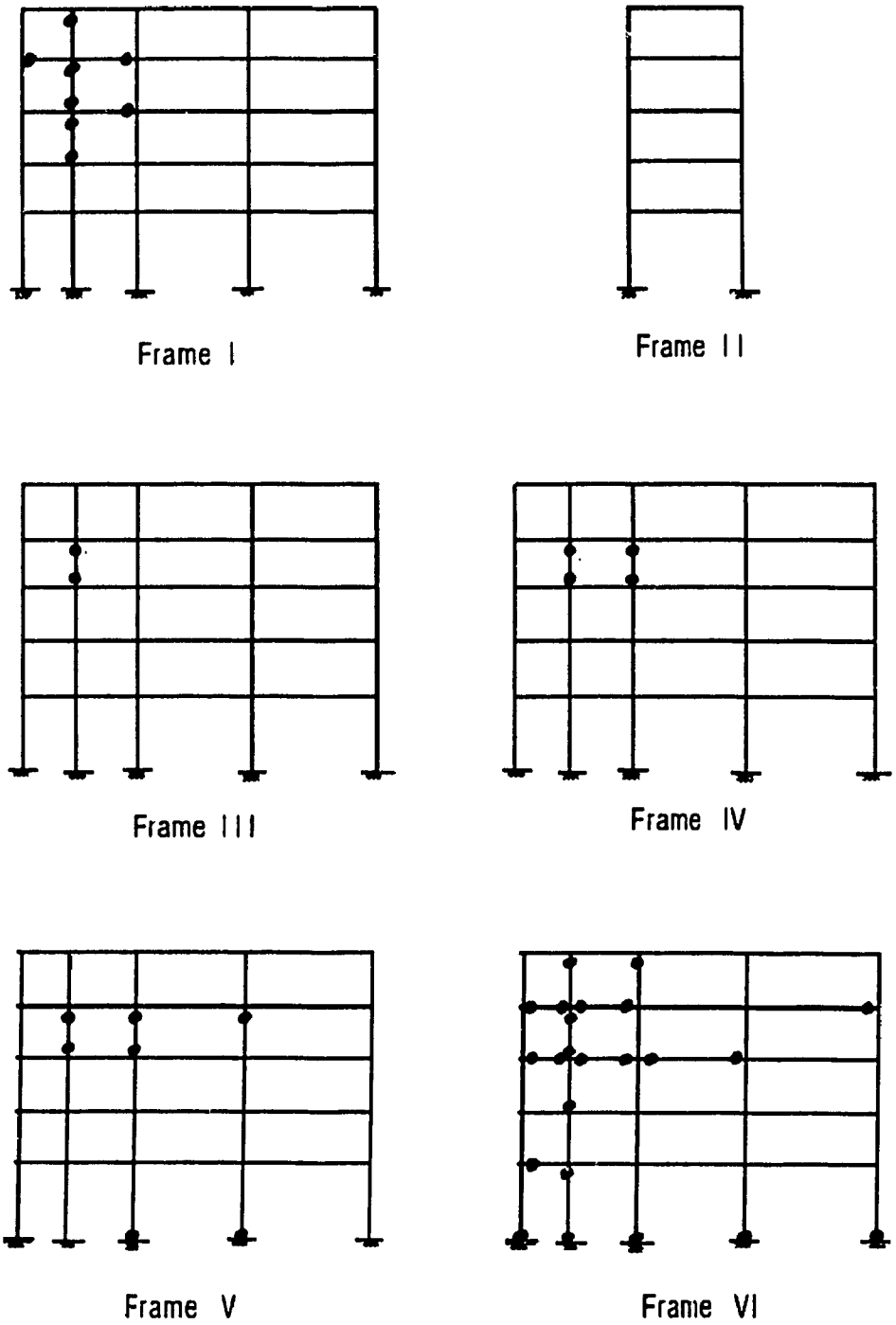

Fig. 6.36a Damage in Frame I to VI , Earthquake in X-Direction, MRF

KB / KF ≈ 0.5 (CM @ Centroid)

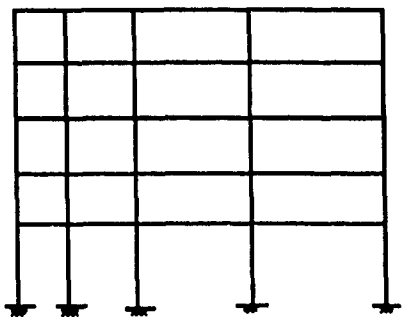

Frame I

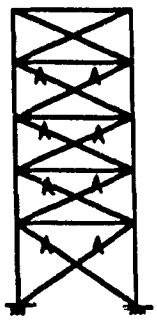

Frame II

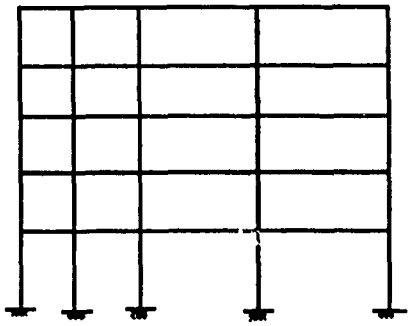

Frame III

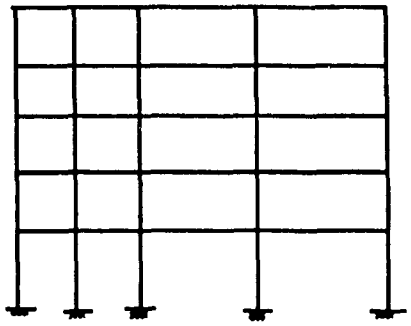

Frame IV

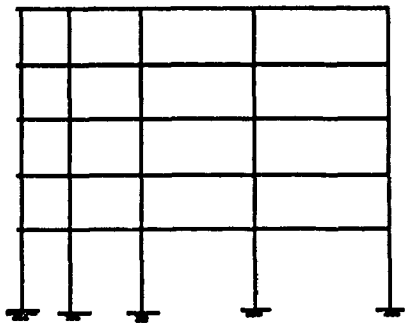

Frame V

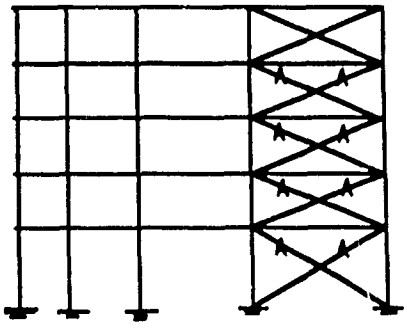

Frame VI

Fig. 6.36b Damage in Frame I to VI , Earthquake in X-Direction, FDBF

KB / KF ≈ 0.5 (CM @ Centroid)

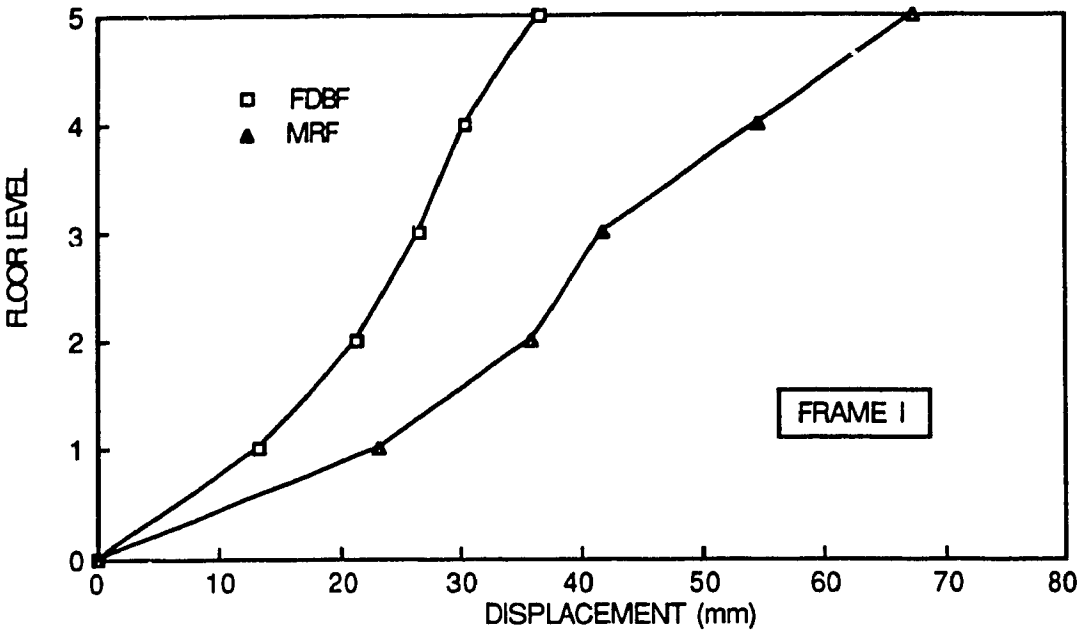

Fig. 6.37a Displacement of Frame I, Earthquake in X-Direction @ 0.18g

(KB / KF≈1.5 and CM @ Centroid)

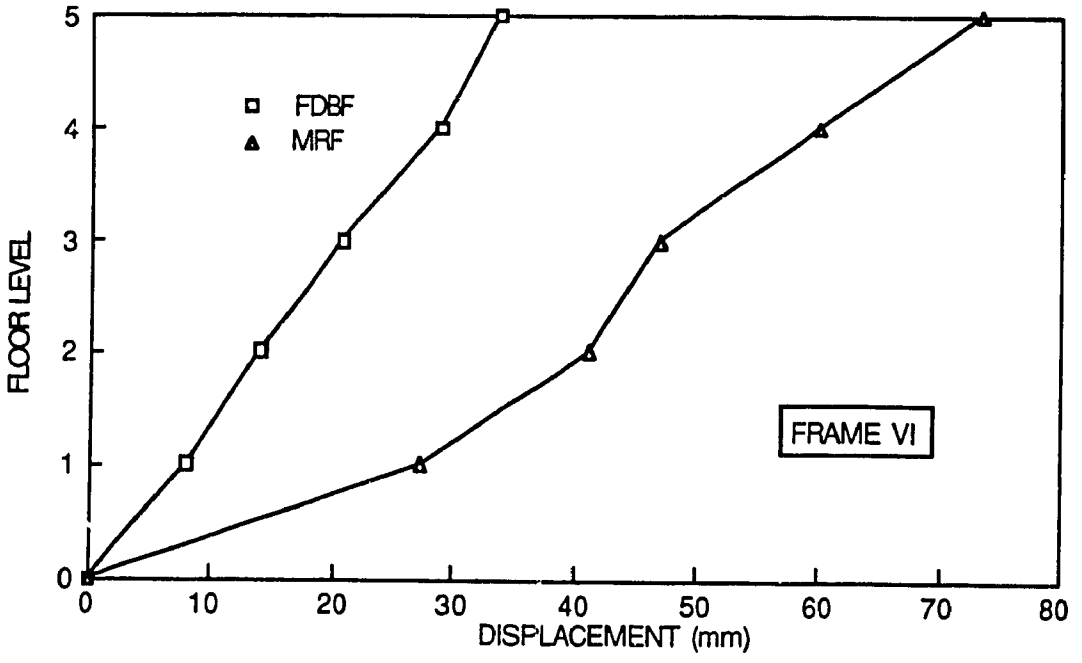

Fig. 6.37b Displacement of Frame VI, Earthquake in X-Direction @ 0.18g

(KB / KF≈1.5 and CM @ Centroid)

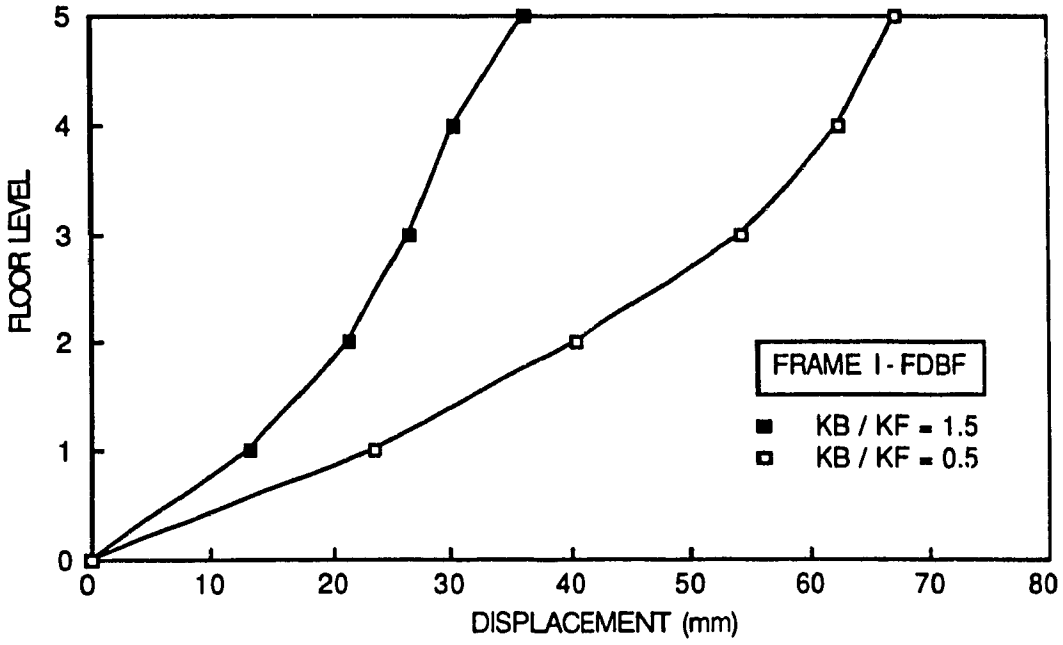

Fig. 6.38 Comparison of Response in Frame I for Different Stiffness Ratio

FDBF, Earthquake in X-Direction @ 0.18g

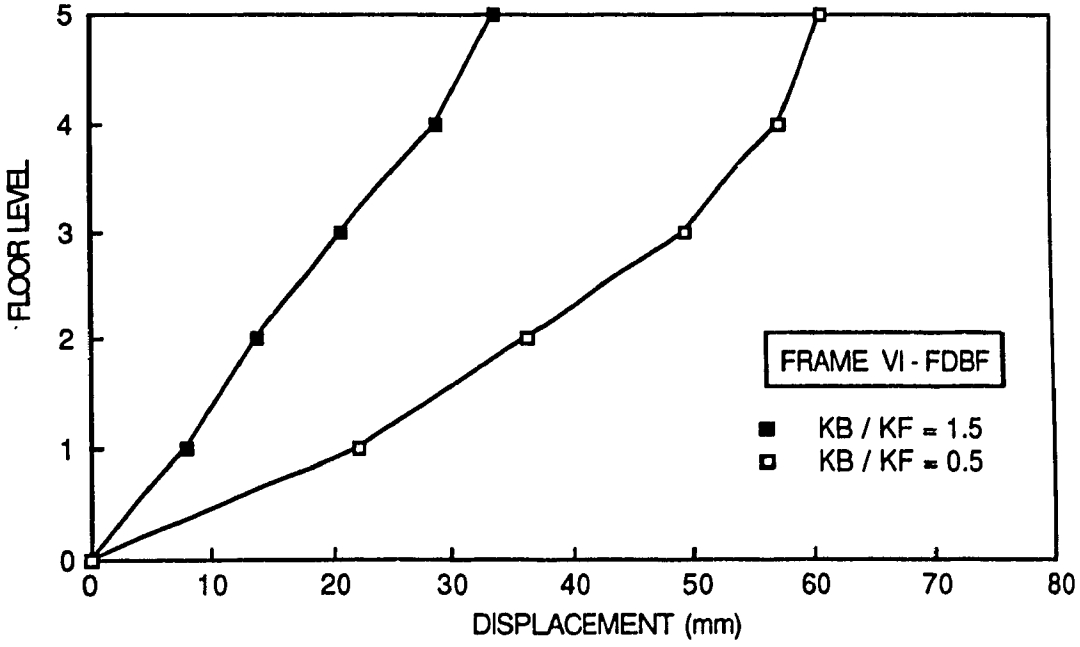

Fig. 6.39 Comparison of Response in Frame VI for Different Stiffness Ratio

FDBF, Earthquake in X-Direction @ 0.18g

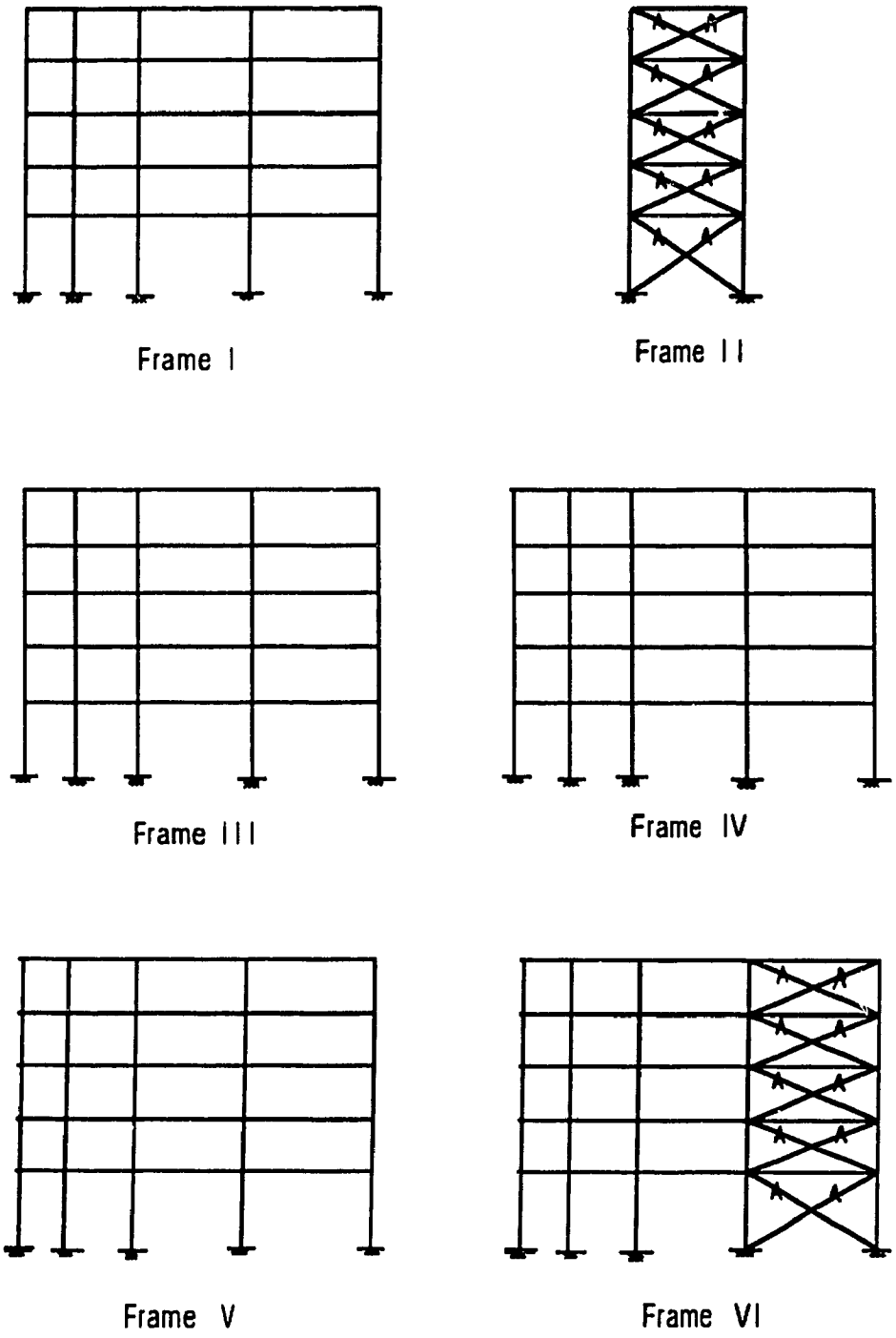

Fig. 6.40 Damage in Frame I to VI , Earthquake in X-Direction, FDBF

KB / KF ≈ 1.5 (CM @ Centroid)

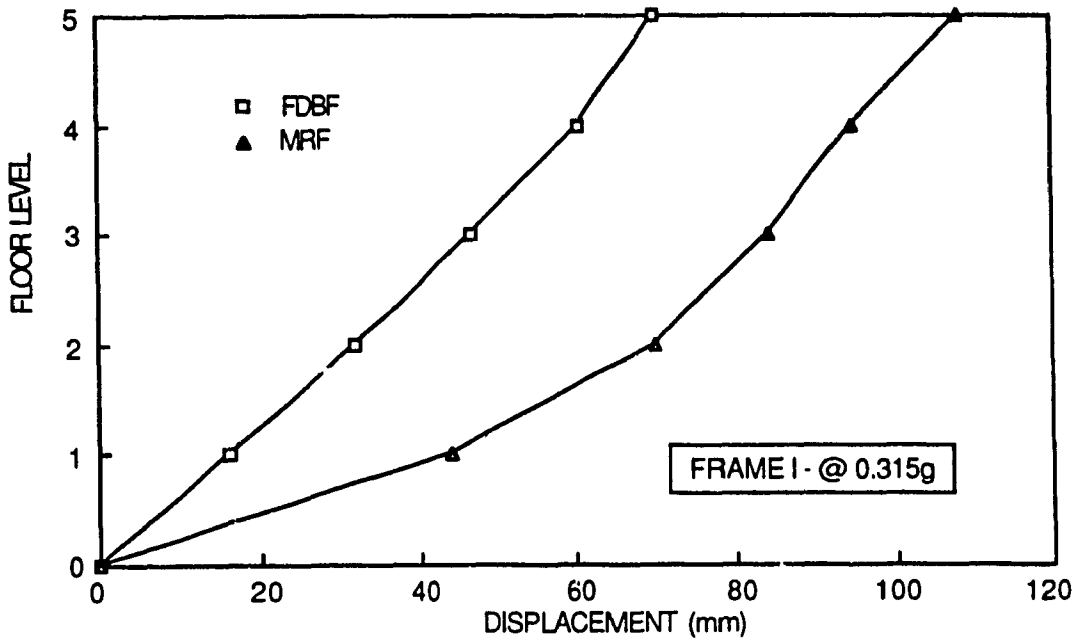

Fig. 6.41a Displacement of Frame I, Earthquake in X-Direction @ 0.315g;
FDBF "Tuned" with respect to Slip Load and Stiffness Ratio

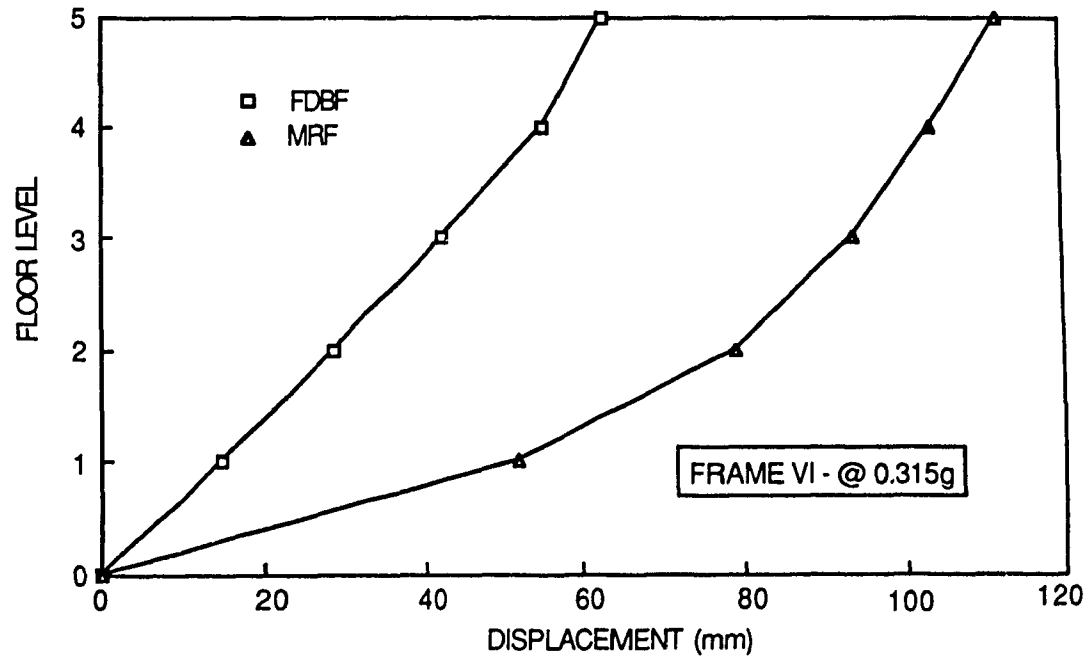

Fig. 6.41b Displacement of Frame VI, Earthquake in X-Direction @ 0.315g;
FDBF "Tuned" with respect to Slip Load and Stiffness Ratio

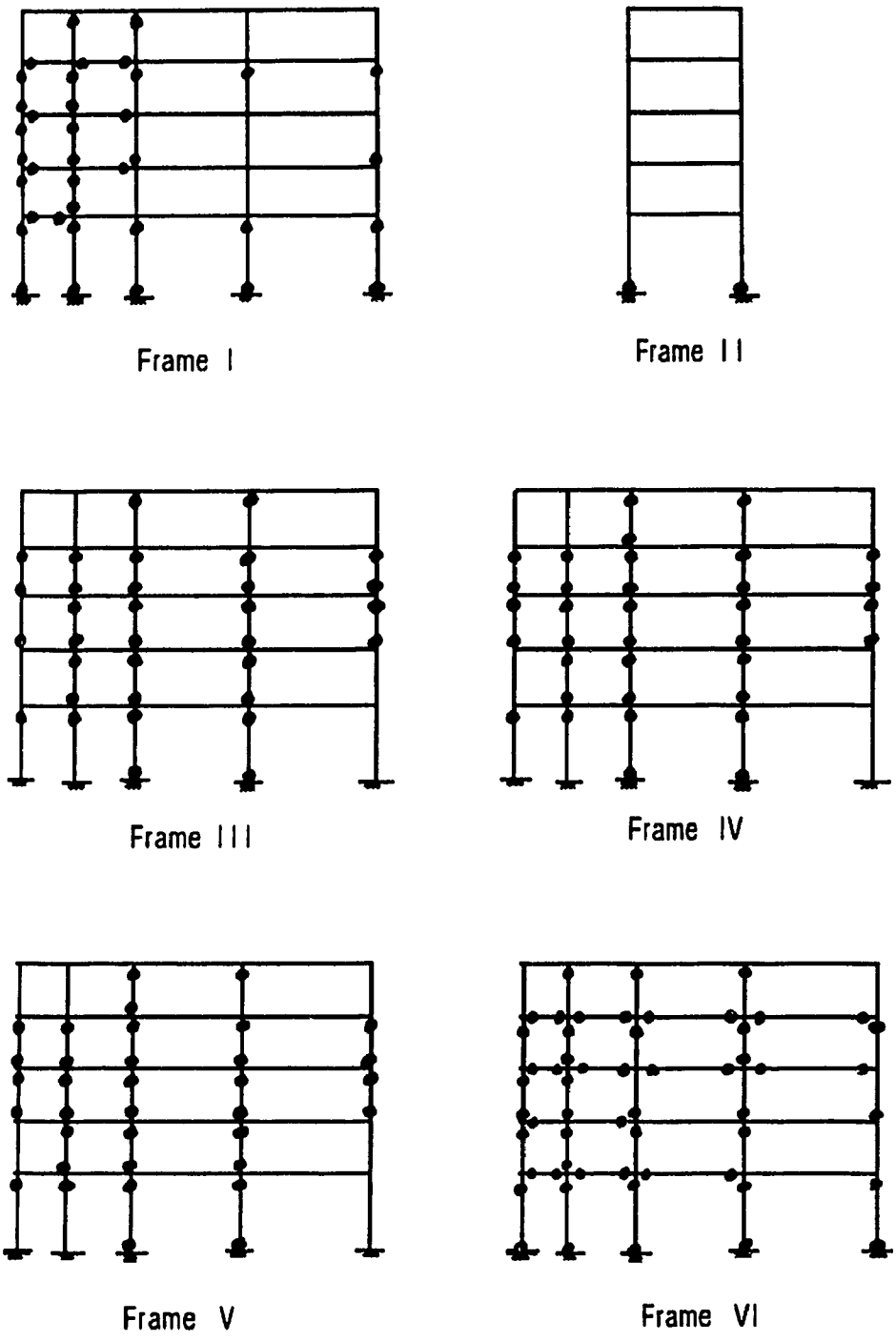

Fig. 6.42a Damage in Frame I to VI , Earthquake in X-Direction,0.315g MRF, (CM @ Centroid)

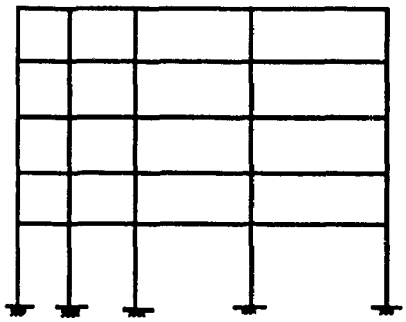

Frame I

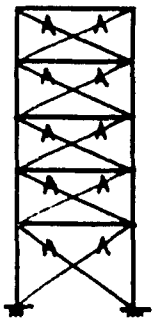

Frame II

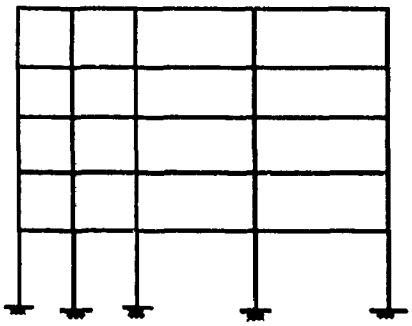

Frame III

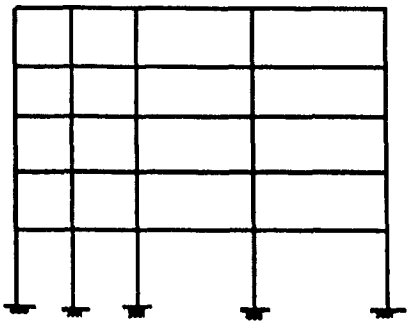

Frame IV

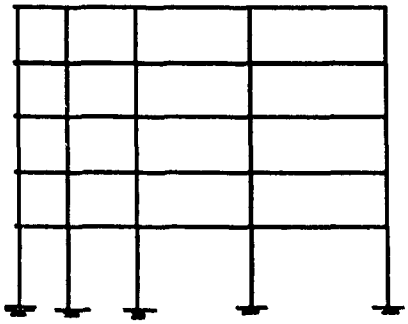

Frame V

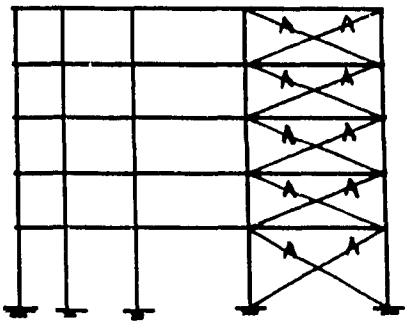

Frame VI

Fig. 6.42b Damage in Frame I to VI , Earthquake in X-Direction,0.315g

FDBF, KB / KF ≈ 1.5 (CM @ Centroid)

CHAPTER VII

CONCLUSIONS

The work presented in this thesis consisted of four main parts; first - a presentation of the causes of accidental eccentricity, in particular those arising from plastic actions such as strength variation and different hysteretic behavior; second- a parametric study of torsional seismic response caused by plastic actions; third- a parametric study of frames with friction dampers, whose benefit more than offsets the increased requirements caused by accidental eccentricity; and fourth- a case study of a five storey reinforced concrete building equipped with friction bracing using the three dimensional non-linear analysis package, Drain-Tabs.

In chapter 2 an equation was derived which gives the expected vatriation in strength λ , for a set safety index β and coefficient of variation of resistance V_R and coefficient of variation of the load V_S . Based on the literature it was determined that a strength variation of $\lambda = 0.3$ corresponds to the maximum expected deviated strength from the mean as envisaged by codes monitoring quality control and for North American construction practice. The derivation of an equation in Chapter 3 permits an evaluation of the probability of occurence for a set strength variation between two structural elements when the coefficient of variation V_R is known. In terms of probability of occurence a strength variation between two individual structural members of $\lambda = 0.3$ has a probability of 6.5 percent for $V_R = 0.14$ and can therefore be considered likely. Note that $\lambda = 0.3$ corresponds approximately to a value of $e_p = 0.18\ \rho$, where e_p is the static plastic eccentricity defined as the distance from the plastic centroid to the center of resistance CR.

Based on the findings of Chapter 4, the variation in strength of lateral load resisting elements may result in considerable accidental torsion. Compared to the symmetric response, this variation may result in sizeable amplification factors for

maximum edge displacement. For a structure relying solely on two lateral load resisting elements the average plus one standard deviation amplification of response is a magnification factor of 1.8 for a strength variation given by $\lambda = 0.40$. In terms of the adequacy of code accidental eccentricity provisions for multi-element systems, the minimum eccentricity of 0.05 D_n becomes inadequate when the static plastic eccentricity e_p exceeds 0.07 ρ; whereas 0.10 D_n is able to account for a static plastic eccentricity less than 0.20 ρ .

For lateral supporting systems consisting of different types of hysteretic behavior on opposite sides of the building, accidental torsion also arises with effects exceeding the 0.05 D_n requirements but within the 0.10 D_n provision of NBCC 1985. Moreover the parametric study indicated that torsionally flexible structures are more susceptible to the effects of accidental eccentricity.

Chapter 5 investigated the ability of friction devices to reduce the response of structures when these are incorporated in simple moment resisting frames. Results corroborate the findings of previous investigators for symmetrical buildings with very substantial improvement of response when the device is proprerly tuned. The parametric study found that tuning with respect to the stiffness ratio KB/KF, which had not been previously investigated, is as important as tuning with respect to the slip load. The study was extended to the more general case of eccentric structures and here also considerable improvement in the response was obtained by the inclusion of friction devices. For these structures it was found that the optimum slip load corresponds to a strength ratio RB/RF = 0.6 which is less than the optimum for symmetric structures RB/RF = 1.0 found in this study as well as by a previous investigator.

The optimum stiffness ratio found lies above KB/KF = 1.0 with little benefit for KB/KF exceeding 2.0. The inclusion of the device reduced the maximum rotation of the structure with greater benefits as the eccentricity is increased and the device also had great influence in reducing the ductility demand. Moreover, it was shown that the device

reduces the energy absorbed by inelastic deformation of the frame by 96 percent for symmetric structures and by 90 percent for structures with low eccentricity; for structures with large eccentricity the reduction is of the order of 70 percent when strucutres are subjected to severe earthquakes.

Finally, the benefit of including the device in a 5 sorey reinforced concrete library building was evaluated. For this case study, it was found that the use of friction bracing reduces the response of structures even if its inclusion causes an eccentricity of $0.10D_n$ and decreases the peak ductility demand considerably. It was found that a fictitious strucutre having similar characteristics as the library building but with a shift in CM by $\pm$ $0.25D_n$ would benefit moderately from the inclusion of friction braces. This was explained by the poor placement of the lone braced bay located at the edge of the structure. Note that such a shift in CM is very unlikely and represents an extreme case with large eccentricity.

An investigation of the effects of friction bracing for seismic excitation parallel to bracing placed near opposite edges of the structure showed reduction in rotation, reduction in peak ductility demand, and good absorption of seismic energy, but small reduction in edge displacement.

Moreover, when the structure was modified with an increase in stiffness ratio to a value of KB/KF $\approx$ 1.5, a significant reduction in edge displacement was also obtained. This implies that the stiffness ratio is an important parameter to consider in the design of friction bracings.

REFERENCES

1. Associate Committee on the National Building Code, National Research Council of Canada, National Building Code of Canada 1985, 2nd Printing 1986.
2. Newmark, N. M., "Torsion in Symmetrical Buildings", Proceedings of the Fourth World Conference on Earthquake Engineering, Santiago, Chile, Jan 13 - 18, 1969, Vol. 2, pp. 19-32.
3. Freudenthal, A. M., "The Safety of Structures", American Society of Civil Engineers, Transactions, Vol. 112, 1947, pp. 125 - 180.
4. Ellingwood, B. R. and A. Ang, "Risk - Based Evaluation of Design Criteria", Journal of the Structural Division, ASCE, Vol. 100, No. ST9, Sept. 1974, pp. 1771 - 1788.
5. MacGregor, J. G., "Safety and Limit States Design for Reinforced Concrete", Canadian Journal of Civil Engineering, Vol. 3, 1976, pp. 484 - 513.
6. Allen, D. E., "Probabilistic Study of Reinforced Concrete in Bending", ACI Journal, Dec. 1970, pp. 989 - 993.
7. Tso, W. K. and I. M. Zelman, "Concrete Strength Variation in Actual Structures", ACI Journal, Dec. 1970, pp. 981 - 988.
8. Galambos, T. V. and M. K. Ravindra, "Properties of Steel for Use in LRFD", Journal of the Structural Division, ASCE, Vol. 104, No. ST9, Sept. 1978, pp. 1459 - 1468.
9. Galambos, T. V. et al, "Probability Based Load Criteria: Assessment of Current Design Practice", Journal of the Structural Division, ASCE, Vol. 108, No. ST5, May 1982, pp. 959 - 977.
10. Yura, J. A. et al, "The Bending Resistance of Steel Beams", Journal of the Structural Division, ASCE, Vol. 104, No. ST9, Sept. 1978, pp. 1355 - 1370.

11. Kennedy, D. J. L. and M. Gad Aly, "Limit States Design of Steel Structures - Performance Factors", Canadian Journal of Civil Engineering, Vol. 7, 1980, pp. 45 - 77.

12. Dumonteil, P., "On the Role of Uncertainty in the Limit States Design of Steel Structures", Canadian Journal of Civil Engineering, Vol. 7, 1980, p. 980 and pp. 588 - 596.

13. Kennedy, D. J. L., chairman, "Guideline for the Development of Limit States Design", CSA Special Publication, S408 - 1981, 34 pp.

14. Freudenthal, A. M., "Safety and the Probability of Structural Failure", American Society of Civil Engineers, Transactions, Vol. 121, 1956, pp. 1337 - 1397.

15. Humar, J. L. and A. M. Awad, "Design for Seismic Torsional Forces", Fourth Canadian Conference on Earthquake Engineering, Proceedings, June 1983, pp. 251 - 260.

16. Kanaan, A. E. and G. H. Powell, "Drain - 2D - A General Purpose Computer Program for Dynamic Analysis of Inelastic Plane Structures", Earthquake Engineering Research Center, University of California, Berkeley, California, April, 1973.

17. Associate Committee on the National Building Code, National Research Council of Canada, National Building Code of Canada 1980, Ottawa 1980.

18. Pall,A.S.,and C. Marsh, "Response of Friction Damped Braced Frames", Journal of the Structural Division,ASCE, Vol. 108, No. ST6, June 1982, pp. 1313-1323.

19. Jennings,P.,"Response of Simple Yielding Structures to Earthquake Excitation", Ph.D.Thesis, California Institute of Technology in Pasadena, 1963, 190 pp.

20. Filiatrault,A., and S. Cherry, "Seismic Tests of Friction Damped Steel Frames", Dynamic Response of Structures, Proceedings of the Third Conference Organized by the Engineering Mechanics Division of the ASCE, March 1986, UCLA, California, pp. 138-145.

21. Aiken I.A., and J.M.Kelly, "Experimental Study of Friction Damping for Steel Frame Structures",unpublished paper, 1988, pp. 1- 17.

22. Pall,A.S., "Energy-Dissipation Devices for Aseismic Design of Buildings", Proceedings of a Seminar on Base Isolation and Passive Energy Dissipation, Applied Technology Council, March 12,1986.

23. Filiatrault,A., and S. Cherry, "Comparative Performance of Friction Damped Systems and Base Isolation Systems For Earthquake Retrofit and Aseismic Design", Earthquake Engineering and Structural Dynamics, Vol.16, 1988, pp.389-416.

24. Pall,A.S., et al., "Friction Dampers for Seismic Control of Concordia University Library Building," Proceedings of the Fifth Canadian Conference on Earthquake Engineering, July 1987, pp. 191-200.

25. Baktash,P., "Friction Damped Braced Frames", PhD Thesis,Concordia University Montreal, Canada, Sept. 1987, 151pp.

26. Guendelman-Israel, R. and G.H. Powell, "Drain-Tabs, A Computer Program for the Inelastic Earthquake Response of Three-Dimensional Buildings," Earthquake Engineering Research Center, EERC-78, March 1977, 125 pages.

27. Associate Committee on the National Building Code, National Research Council of Canada, NBCC 1985, 2nd Edition 1985.

28. Humar, J.L., "Design for Seismic Torsional forces," Canadian Journal of Civil Engineering, Vol. 11, (2), pp. 150-163.

29. Cheung, V.W.-T. and W.K. Tso, "Eccentricity in Irregular Multistorey Buildings," Canadian Journal of Civil Engineering, Vol. 13, Feb. 1986, pp. 46-52.

30. ACI Committee 318, "Building Code Requirements for Reinforced Concrete (ACI 318-83)", American Concrete Institute, 2nd printing, Sept. 1984.

31. Benjamin, J. R. and C. A. Cornell, "Probability, Statistics and Decisions for Civil Engineers", MacGraw Hill, 1970.

32. MacGregor, J. G., S. A. Mirza and B. Ellingwood, "Statistical Analysis of Resistance of Reinforced and Prestressed Concrete Members", ACI Journal, May - June 1983, pp. 167 - 176.

33. MacGregor, J. G., "Load and Resistance Factors for Concrete Design", ACI Journal, July - Aug. 1983, pp. 279 - 287.

34. Galambos, T. V. and M. K. Ravindra, "The Basis for Load and Resistance Factor Design Criteria of Steel Building Structures", Canadian Journal of Civil Engineering, Vol. 4, 1977, pp. 178 - 189.

35. Allen, D. E., "Limit States Design - A Probability Study", Canadian Journal of Civil Engineering, Vol. 2, 1975, pp. 36 - 49.

36. Associate Committee on the National Building Code, National Research Council of Canada. The Supplement to the National Building Code of Canada 1980, Ottawa 1980, 1st Edition 1980.

37. Siu, W. W. C., S. R. Parimi and N. C. Lind, "Practical Approach to Code Calibration", Journal of the Structural Division, ASCE, Vol. 101, No. ST7, July 1975, pp. 1489 - 1480.

38. Canadian Portland Cement Association, "Concrete Design Handbook", CPCA, 1st Printing, Dec. 1985.

39. Tso, W. K., "A Proposal to Improve the Static Torsional Provisions for the National Building Code of Canada", Canadian Journal of Civil Engineering, Vol 10 Dec. 1983, pp. 561 - 565.

40. Rutenberg, A. and O. A. Pekau, "Earthquake Response of Asymmetric Buildings: A Parametric Study", Fourth Canadian Conference on Earthquake Engineering, Proceedings, June 1983, pp. 271 - 281.

41. Tso, W. K., "Seismic Torsional Provisions for Dynamic Eccentricity", Earthquake Engineering and Structural Dynamics, Vol 8, 1980, pp. 275 - 289.

42. Awad, A. M., "Torsional Response of a Single Storey Building Model to Ground Motion", Ph D Thesis, Carlton University, Ottawa, Aug. 1982, 132 pp.

43. Heidebrecht, A. C. and W. K. Tso, "Seismic Loading Provision Changes in National Building Code of Canada 1985", Canadian Journal of Civil Engineering, Vol 12 1985, pp. 653 - 660.

44. Tso, W. K. and V. Meng, "Torsional Provisions in Building Codes", Third Canadian Conference on Earthquake Engineering, Proceedings, Vol. 1, June 1979, pp. 663 - 684.

45. Tso, W. K. and A. W. Sadek, "Inelastic Response of Eccentric Structures", Fourth Canadian Conference on Earthquake Engineering, Proceedings, June 1983, pp. 261 - 269.

46. Kan, C. L. and A. K. Chopra, "Torsional Coupling and Earthquake Response of Simple Elastic and Inelastic Systems", Journal of the Structural Division, ASCE, Vol 107, No. ST8, Aug., 1981, pp. 1569 - 1588.

47. Kan, C. L. and A. K. Chopra, "Simple Model for Earthquake Response Studies of Torsionally Coupled Buildings", Journal of the Engineering Mechanics Division, ASCE, Vol 107, No. EM5, Oct. 1981, pp. 935 - 951.

48. Bozorgnia, Y. and W. K. Tso, "Inelastic Earthquake Response of Asymmetric Structures", Journal of Structural Engineering, Vol 112, No. 2, Feb, 1986, pp. 383 - 400.

49. Tso, W. K. and S. W. Sadek, "Inelastic Seismic Response of Simple Eccentric Structures", Journal of Earthquake Engineering and Structural Dynamics, Vol 13, No. 2, 1985, pp. 255 - 269.

50. Rutenberg, A., and O.A. Pekau, "Seismic Code Provisions for Asymmetric Structures : A Re-evaluation," Engineering Structures, Vol. 9, 1987, pp 255-264.

APPENDIX I

Variation of Strength in Reinforced Concrete Beams

$$M = A_s f_y (d - a/2)$$

$$0.85 f'_c b a = A_s f_y$$

$$a = \frac{A_{s_{des}} f_y}{0.85 f'_c b}$$

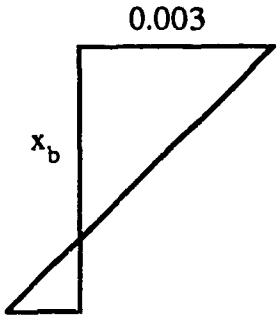

$$x_b = \left(\frac{600}{600 + f_y}\right) d \qquad ; f_y = \text{MPa}$$

$$a_b = \beta_1 x_b \qquad \beta_1 = 0.85 \text{ for } f'_c \leq 30 \text{ MPa}$$

$$a_b = \beta_1 x_b = \beta_1 \left(\frac{600}{600 + f_y}\right) d$$

$$\varepsilon_y = \frac{f_y}{E}$$

$$A_{sb} = \frac{a_b (0.85 f'_c b)}{f_y}$$

$$A_{sb} = 0.85 \beta_1 \left(\frac{600}{600 + f_y}\right) \frac{f'_c}{f_y} bd$$

$$A_{max} = 0.75 A_{sb} = 0.6375 \beta_1 \left(\frac{600}{600 + f_y}\right) \frac{f'_c}{f_y} bd$$

$$A_{des} \approx 0.5 A_{max} = 0.31875 \beta_1 \left(\frac{600}{600 + f_{y_{des}}}\right) \frac{f'_{c_{des}}}{f_{y_{des}}} bd$$

$$a = \frac{A_s f_y}{0.85 f'_c b}$$

$$a = 0.31875\beta_1 \left[\frac{600}{600 + f_{y_{des}}}\right] \frac{f'_{c_{des}}}{f_{y_{des}}} bd \frac{f_y}{0.85 f'_c b}$$

$$M = A_{s_{des}} f_y (d - a/2)$$

$$M = 0.31875\beta_1 \left[\frac{600}{600 + f_{y_{des}}}\right] \frac{f'_{c_{des}}}{f_{y_{des}}} bdf_y \left\{d - 0.159375\beta_1 \left(\frac{600}{600 + f_{y_{des}}}\right) \frac{f'_{c_{des}}}{f_{y_{des}}} \frac{f_y d}{0.85 f'_c}\right\}$$

$$M = 0.31875\beta_1 \left[\frac{600}{600 + f_{y_{des}}}\right] \frac{f'_{c_{des}}}{f_{y_{des}}} bd^2 f_y \left\{1 - 0.1875\beta_1 \left(\frac{600}{600 + f_{y_{des}}}\right) \frac{f'_{c_{des}}}{f_{y_{des}}} \frac{f_y}{f'_c}\right\}$$

usually $\beta_1 = 0.85$ ie. $f'_c \leq 30$ MPa

$$M_n = 0.2709375\left(\frac{600}{600 + f_{y_{des}}}\right) f'_{c_{des}} bd^2 \frac{f_y}{f_{y_{des}}} \left\{1 - 0.159375\left(\frac{600}{600 + f_{y_{des}}}\right) \frac{f'_{c_{des}}}{f'_c} \frac{f_y}{f_{y_{des}}}\right\}$$

$$M_u = \phi M_n = 0.9 M_n$$

$$M_u = 0.2438437\left(\frac{600}{600 + f_{y_{des}}}\right) f'_{c_{des}} bd^2 \frac{f_y}{f_{y_{des}}} \left\{1 - 0.159375\left(\frac{600}{600 + f_{y_{des}}}\right) \frac{f'_{c_{des}}}{f'_c} \frac{f_y}{f_{y_{des}}}\right\}$$

$$M_{u_{des}} = 0.2438437\left(\frac{600}{600 + f_{y_{des}}}\right) f'_{c_{des}} bd^2 \left\{1 - 0.159375\left(\frac{600}{600 + f_{y_{des}}}\right)\right\}$$

Overstrength = OS = $M_u / M_{u_{des}}$

Therefore, $\lambda = (1 - 1/OS)$

APPENDIX II

PROPERTIES OF FRAME VI

Braces	Area of steel mm^2	Slip load KN
E1.1 and E1.2	412.5	75.0
E1.3 and E1.4	825.0	150.0
E1.5 and E1.6	1650.0	300.0
E1.7 and E1.8	2750.0	700.0
E1.9 and E1.10	3850.0	700.0

Columns	I m^4	M_0 KN-m	P_0 KN
E2.1	0.0143	745.0	11150
E2.2	0.0143	745.0	11150
E2.3	0.0143	745.0	11150
E2.4	0.0143	1175.0	12250
E2.5	0.0143	1750.0	13350
E2.6	0.0115	665.0	70500
E2.7	0.0115	905.0	8450
E2.8	0.0115	905.0	8450
E2.9	0.0115	1115.0	8850
E2.10	0.0115	1500.0	9700

E2.11	0.0115	665.0	70500
E2.12	0.0155	905.0	8450
E2.13	0.0115	905.0	8450
E2.14	0.0115	1115.0	8850
E2.15	0.0115	1500.0	9700
E2.16	0.0115	665.0	70500
E2.17	0.0115	905.0	8450
E2.18	0.0115	905.0	8450
E2.19	0.0115	1115.0	8850
E2.20	0.0115	1500.0	9700
E2.21	0.0143	745.0	11150
E2.22	0.0143	745.0	11150
E2.23	0.0143	745.0	11150
E2.24	0.0143	1175.0	12250
E2.25	0.0143	1750.0	13350

Beams	I	M
	m4	KN-m
E5.1	0.0084	660.0
E5.2	0.0084	660.0
E5.3	0.0084	660.0
E5.4	0.0084	660.0
E5.5	0.0084	660.0
E5.6	0.0084	660.0
E5.7	0.0084	660.0
E5.8	0.0084	660.0
E5.9	0.0084	840.0

E5.10	0.0084	660.0
E5.11	0.0084	660.0
E5.12	0.0084	840.0
E5.13	0.0084	840.0
E5.14	0.0084	660.0
E5.15	0.0084	660.0
E5.16	0.0084	840.0
E5.17	0.0084	1156.0
E5.18	0.0084	840.0
E5.19	0.0084	840.0
E5.20	0.0084	1156.0

APPENDIX III

PROPERTIES OF FRAME XI

Braces	Area of steel mm^2	Slip load KN
E1.1 and E1.2	550.0	100.0
E1.3 and E1.4	1100.0	200.0
E1.5 and E1.6	1650.0	300.0
E1.7 and E1.8	2750.0	500.0
E1.9 and E1.10	4125.0	750.0

Columns	I m^4	M_0 KN-m	P_0 KN
E2.1	0.0143	601.0	11150
E2.2	0.0143	801.0	11150
E2.3	0.0143	901.0	11150
E2.4	0.0143	1250.0	12250
E2.5	0.0143	1750.0	13350
E2.6	0.0115	601.0	7010
E2.7	0.0115	801.0	7250
E2.8	0.0115	901.0	8450
E2.9	0.0115	1250.0	8750
E2.10	0.0115	1500.0	9300

E2.11	0.0115	601.0	7010
E2.12	0.0155	801.0	7250
E2.13	0.0115	901.0	8450
E2.14	0.0115	1250.0	8750
E2.15	0.0115	1500.0	9300
E2.16	0.0115	601.0	7010
E2.17	0.0115	801.0	7250
E2.18	0.0115	901.0	8450
E2.19	0.0115	1250.0	8750
E2.20	0.0115	1500.0	9300
E2.21	0.0143	601.0	11150
E2.22	0.0143	801.0	11150
E2.23	0.0143	901.0	11150
E2.24	0.0143	1250.0	12250
E2.25	0.0143	1750.0	13350

Beams	I	M
	m4	KN-m
E5.1	0.0084	660.0
E5.2	0.0084	660.0
E5.3	0.0084	660.0
E5.4	0.0084	660.0
E5.5	0.0084	660.0
E5.6	0.0084	660.0
E5.7	0.0084	660.0
E5.8	0.0084	660.0
E5.9	0.0084	660.0

E5.10	0.0084	660.0
E5.11	0.0084	660.0
E5.12	0.0084	660.0
E5.13	0.0084	660.0
E5.14	0.0084	660.0
E5.15	0.0084	660.0
E5.16	0.0084	660.0
E5.17	0.0084	660.0
E5.18	0.0084	660.0
E5.19	0.0084	660.0
E5.20	0.0084	660.0